SPECIATION OF TECHNETIUM-99 INCORPORATED INTO METAL OXIDE MATRICES: A MOLECULAR LEVEL UNDERSTANDING OF ^{99}Tc REDUCTION AND ITS COMPLEXATION INTO POLYOXOMETALATES

AND

INNOVATION AND ASSESMENT OF GENERAL CHEMISTRY EDUCATION IN A COLLEGE SETTING

By

Donna McGregor

A dissertation submitted to the Graduate Faculty in Chemistry
in partial fulfillment of the requirements for the degree of Doctor of Philosophy,
The City University of New York

2009

This manuscript has been approved and accepted for the
Graduate Faculty in Chemistry in satisfaction of the
Dissertation requirements for the degree of Doctor of Philosophy.

_____	Dr. Lynn C. Francesconi
Date	**Chair of Examining Committee**
_____	Dr. Lakshman
Date	**Executive Officer**

Dr. Michael Mirkin

Dr. Klaus Grohmann

Dr. Charles M. Drain

Dr. Pamela Mills

Dr. Tatyana Polenova

Supervisory Committee

THE CITY UNIVERSITY OF NEW YORK

Abstract

SPECIATION OF TECHNETIUM-99 INCORPORATED INTO METAL OXIDE MATRICES: A MOLECULAR LEVEL UNDERSTANDING OF ^{99}Tc REDUCTION AND ITS COMPLEXATION INTO POLYOXOMETALATES

By

Donna McGregor

Advisor: Professor Lynn Francesconi

Technetium-99 (^{99}Tc) is a long-lived ($T_{1/2}$ = 2.13 x 10^5 years) β-emitting (E_{max} = 294 KeV) radionuclide formed during the fission of ^{235}U and fallout from nuclear weapons testing. It exists in relatively high concentrations in nuclear waste tanks, and the pertechnetate (TcO_4^-) anion has been shown to leach into surrounding subsurface soils and groundwaters. Due to its long half-life and the high mobility of the pertechnetate (TcO_4^-) anion, ^{99}Tc management is an issue for both waste characterization and long-term storage. A better understanding of both its extensive redox chemistry and the parameters that affect the speciation and coordination environment of Tc will promote the development of more appropriate methods for the separation of Tc from nuclear waste tanks as well as more fitting mediums for storage.

Polyoxometalates (POMs) are early transition metal oxide clusters that are chemically robust. They have homogeneous crystalline structures and are known to be good model systems for metal oxide solid-state materials such as the glasses and ceramics used to house nuclear waste. The synthesis of pure ^{99}Tc-POM compounds,

however, is complicated by both the unwanted hydrolysis of the Tc(V) starting material and difficulties with the separation of the free POM ligand from the desired ^{99}Tc-POM complex. We have developed methods for the clean synthesis of the ^{99}Tc - (α_1-$P_2W_{17}O_{61}$)$^{10-}$ and (α_2-$P_2W_{17}O_{61}$)$^{10-}$ Wells-Dawson POM compounds (as both organic and aqueous soluble complexes) and characterized them using various spectroscopic techniques.

POMs also have unique, tunable, electron transfer abilities and can be reduced, both electrochemically and photochemically in the presence of a sacrificial electron donor, by multiple electrons while maintaining their structural integrity. To this end we have investigated a number of POMs; Keggin ions, ($XW_{12}O_{40}^{n-}$, X=P, n=3; Si, n=4; Al, n=5), the Wells-Dawson lacunary isomer (α_2-$P_2W_{17}O_{61}$)$^{10-}$, and a "wheel" POM, $P_8W_{48}O_{184}^{40-}$, for their ability to reduce pertechnetate and sequester low valent ^{99}Tc. The resulting low valent Tc species have been characterized by physical methods including multinuclear NMR and electrochemistry.

Acknowledgements

Thank you, Thank you, Thank you!

To all those people who mean something to me… ***you know who you are***.

I couldn't have done this without you!

Professor Lynn, thank you for you constant support and guidance.

Professor Mills, thank you for teaching me to believe in myself.

My Committee members; *Professor Drain, Professor Polenova, Professor Mirkin and Professor Grohmann*, thank you all for your continued efforts on my part.

Mom and Dad, I love you both…
Thank you for teaching me to fight for what I believe in!

The Rest of you… I love you all!

Table of Contents

Part 1: Speciation of Technetium-99 incorporated into Metal Oxide Matrices: A molecular level understanding of ^{99}Tc reduction and its complexation into Polyoxometalates.

List of Figures

Chapter 1.

Chapter 5

Chapter 6

List of Tables

Chapter 1

Chapter 2

Chapter 6

Chapter 7

List of Schemes

Chapter 2

Chapter 3

Chapter 1: Introduction and Background Information

1.1 Radioactive Waste and its Storage

The colossal surge in the development of nuclear weapons during the Cold War resulted in the production of large quantities of nuclear waste in the United States. Despite strict regulations governing the production and testing of nuclear weapons today, the accumulation of this radioactive waste has endured and it is continuing to persist.

At present the nuclear waste is housed in underground storage tanks at National lab sites such as Hanford in Washington, Savannah River in South Carolina, and Rocky Flats in Colorado. At the Hanford site alone there are 177 of these cylindrical underground storage tanks, and it has been estimated that as of 1998 they contained 54 million gallons of radioactive and chemically hazardous waste. [1]

The first tanks built at Hanford in 1945 were single-shell carbon steel tanks covered by a an outer layer of concrete.[1] These tanks were designed to have a 20 year life-span and boasted capacities ranging from 210 m^3 (55,400 gallons) to 3,800 m^3 (1 million gallons).[2] In 1968 the production of a number of double-shell tanks with capacities ranging from 606 m^3 (160,000 gallons) to 3,800 m^3 (1 million gallons) [2] was begun. These tanks were comprised of two carbon steel liners, a single dome liner, and an outer reinforced concrete encasing. Today Hanford stores 149 single-shell and 28 double-shell underground tanks.

In an attempt to prevent the leakage of waste due to tank corrosion, large amounts of sodium hydroxide or calcium carbonate were added to the waste streams to increase their alkalinity. This however did not prove successful, and there are now 68 single-shell

underground waste tanks at Hanford that are either known to be, or suspected of leaking radioactive chemical waste into the surrounding soils and groundwaters.[2] In addition to the leakage due to corrosion of the waste tanks, there is also evidence of significant leakage from the waste transfer lines. [3]

Among the radioactive nuclides currently leaking from these waste tanks is the long-lived, chemically stable and highly mobile Technetium-99 isotope.

1.2 Technetium

1.2.1 What is Technetium

Technetium (Tc) is a silver-grey second row transition metal that exists as 21 radioactive isotopes and 8 nuclear isomers: ^{93m}Tc, ^{94m}Tc, ^{95m}Tc, ^{96m}Tc, ^{97m}Tc, ^{99m}Tc, ^{102m}Tc and ^{99}Tc. The isotopes have mass numbers that range from ^{90}Tc to ^{111}Tc and half-lives from 0.3 seconds up to 4.2 x 10^6 years. Tc is element number 43 on the periodic table and in group VII positioned between Molybdenum and Ruthenium. In its ground state a neutral Tc atom has 7 valence electrons affording it the flexibility of 8 oxidation states that range from -1 through +7. It is an analog of both manganese (Mn) and rhenium (Re), and exhibits coordination numbers ranging from 4 through 9.

In the ground state Tc atoms have been shown to have one of the following electronic configurations: $[Kr]4s^2 4p^6 4d^6 5s^1$ [4, 5] or $[Kr]4s^2 4p^6 4d^5 5s^2$ [6, 7], with the structure of the electronic cloud in the latter being close to that of both its Mn and Re analogs. Because of the lanthanide contraction however, the ionic radii of Tc^{7+} and Re^{7+} are almost equal, at 0.56Å, while the ionic radius of Mn^{7+} is 0.46Å. This results in the chemical and physical properties of Tc being closer to those of Re than those of Mn. In

fact the tetrahedral structure of the TcO_4^- anion is quite similar to that of the ReO_4^- anion, with the Tc-O and Re-O atomic distances being 1.75Å and 1.97Å respectively. [8]

1.2.2 The discovery of Technetium

Technetium does not readily occur naturally on earth. It was the first man-made element, and although its existence was predicted by Mendeleev in 1869[9], it was not officially discovered until 1937 when E. O Lawrence at the University of California bombarded a plate of natural molybdenum with deutrons in the cyclotron. Lawrence found his sample to exhibit a level of radioactivity that could not be explained by the presence of Molybdenum alone. He presented his finding to E. Segre and C. Perrier of the Royal University of Palermo, Italy, who identified the resulting activity to be that of the missing element of atomic number 43.[10, 11]

In 1946 Perrier and Segre named this missing element technetium, after the Greek word for artificial (being that it was the first element to be artificially produced). And it has since been determined that Lawrence had most likely synthesized the metastable ^{95m}Tc and ^{97m}Tc isomers by the following nuclear reactions:

$$_{42}Mo^{94}(d,n)_{43}Tc^{95m} \qquad t_{1/2} = 61d$$

$$_{42}Mo^{96}(d,n)_{43}Tc^{97m} \qquad t_{1/2} = 91d$$

In 1951 Moore believed he had found lines of ionized $Tc^+(Tc_2)$ to exist in the spectrum of the solar atmosphere,[12] but this discovery was later found to be invalid. The discovery of Tc(I) in the spectra of some S and M stars by Merrill in 1952 and then later in 1956 however proved accurate.[13-16] The first isolation of naturally occurring

technetium on earth however, was not accomplished until 1961, when Kenna and Kuroda successfully separated ^{99}Tc from a sample of Belgian Congo Pitchblende.[17, 18] Because the ^{99}Tc/^{238}U ratio in the pitchblende was found to be close to that of ^{99}Mo/^{238}U it was hypothesized that the ^{99}Tc in the pitchblende must have been formed by the spontaneous fission of ^{238}U.[18]

1.2.3 The Technetium-99 Isotope

Of its 21radioactive isotopes, Tc is most commonly known for its gamma-emitting short lived ^{99m}Tc isotope ($T_{1/2}$ = 6hrs) which is used as a radio imaging agent. The most readily available isotope however, is the ^{99}Tc isotope, which is a long-lived ($T_{1/2}$ = 2.13 x 10^5 years) β-emitting (E_{max} = 294 KeV) [19-21] radionuclide (Figure 1.1) formed during nuclear transformations; specifically the fission of ^{235}U as well as the early stages of plutonium (^{239}Pu and ^{241}Pu) production.

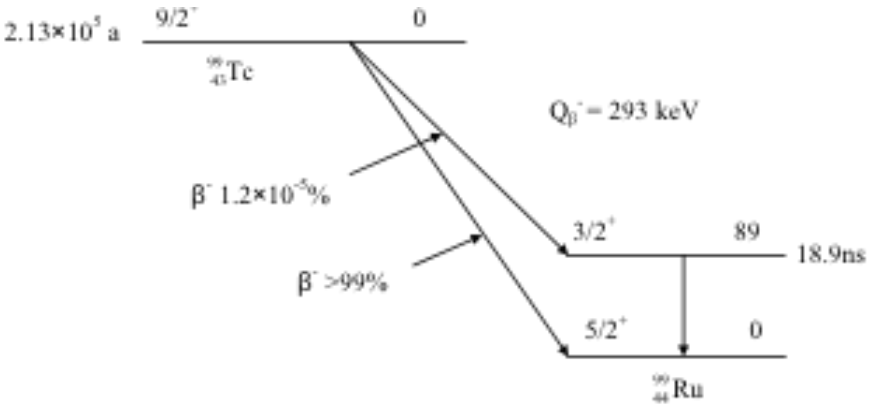

Figure 1.1. The β-decay scheme of ^{99}Tc

Table 1.1. Isotopes of Tc produced during the thermal neutron fission of ^{235}U.

Isotope	^{99}Tc	^{101}Tc	^{102}Tc	^{103}Tc	^{104}Tc	^{105}Tc	^{107}Tc
Yield (%)	6.06	5.6	4.3	3.0	1.8	0.9	0.19

The total cumulative yield of ^{99}Tc from the thermal neutron fission of ^{235}U in a nuclear reactor is estimated to be ~6% (Table 1.1). This results in the production of roughly 1kg of ^{99}Tc per 1 ton of 3% enriched ^{235}U production. [10, 21, 22]

Because of its long half-life ^{99}Tc, along with ^{97}Tc and ^{98}Tc ($T_{1/2} = 2.6 \times 10^6$ years and $T_{1/2} = 4.2 \times 10^6$ years respectively), can be handled in weighable amounts and is thus often used for the study of Tc chemistry. Although the presence of ^{99}Tc in the environment arises primarily due to the above-mentioned nuclear transformations, as well as fallout from nuclear weapons testing (and a small amount from disposal after pharmaceutical use),[23] it can also be synthesized in small quantities (milligram amounts) through the long-term neutron irradiation of very pure natural molybdenum. This is achieved in a nuclear reactor according to the following reaction:

$$^{98}Mo(n,y)^{99}Mo \xrightarrow[67\ hrs]{\beta^-} {}^{99m}Tc \xrightarrow[6.1\ hrs]{i.t.} {}^{99}Tc$$

1.2.4 Some Fundamental Technetium Chemistry

The recognized chemistry of Tc suggests that under aerobic conditions and in a basic environment it exists as the heptavalent pertechnetate anion (TcO_4^-), which is the most thermodynamically stable form of Tc at high pH.[19] A series of thermodynamic data

collected by Torstenfeld in 1981[24] shows that in neutral aqueous solutions the speciation of Tc is highly dependent on the redox potential (Figure 2.1).

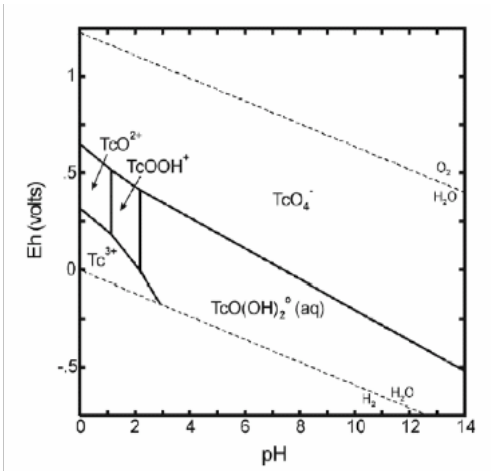

Figure 1.2. Graph of reduction potential (Eh) vs pH showing the speciation of Tc in a non-carbonate aqueous environment.

The TcO_4^- anion is produced when metallic Tc is dissolved in aqueous solutions or nitric acid, as well as when aqueous Tc in any of its oxidation states is treated with oxidizing agents such as H_2O_2, Cl_2, Ce(IV) or HNO_3, etc. TcO_4^- is thus the most prevalent Tc species in non-reducing aqueous solutions [25] as well as one of the most mobile forms of radionuclide species in the environment. Because of its low negative charge (-1) and low hydration energy ($\Delta G° = -251$ kJ/mol) it migrates easily through the environment and does not sorb well onto mineral surfaces, soils or sediments without reduction. [20, 22, 26]

1.3 Environmental Concerns

^{99}Tc, along with isotopes of the actinide elements, comprises a large component of radioactive waste found in waste tanks at Hanford, Savannah River and Melton Valley,

as well as water and soil samples around national laboratory sites such as operating nuclear reactors and fuel reprocessing plants.

When recovering Uranium from spent nuclear fuel, the reprocessing procedure is a chemical technique known as the Purex (plutonium and uranium recovery by extraction) process. During the process a small amount of metallic Tc (along with Mo, Ru, Rh and Pd) remains undissolved and is converted to TcO_4^-. The TcO_4^- is then extracted from the fuel by tributyl phosphate (TBP) and discharged along with the other metals as highly active radioactive waste. This waste is retained in the underground liquid waste tanks for later solidification by either calcination or glassification.

Due to its multiple valencies, long half-life, and the high mobility of the pertechnetate anion in the environment, the ^{99}Tc isotope creates particular concern in these waste tanks, and is an issue for both waste characterization and disposal.[27] The sample matrices associated with aged nuclear waste generally possess complex and varying chemical and radiological composition, and in the case of ^{99}Tc, even the speciation of the analyte may vary depending on the source of the waste material.[28] This means that the chemical composition of Tc in these waste tanks remains unknown. In fact the chemistry and stability of Tc remains unknown in most common storage matrices, such as the above-mentioned glasses and ceramics.

Both the speciation and stability of ^{99}Tc are determined by the interaction between the nuclear waste matrix or the coordination environment of the specific storage material with the particular oxidation state of ^{99}Tc. Because of this, there are presently no obvious storage materials for ^{99}Tc. In Hanford for example, the radioactive waste was initially treated with NaOH (decreasing acidity to pH = 10), for storage in single-shell low-carbon

steel-lined concrete tanks. Over time however, this waste has undergone reprocessing, which leads to the formation of residual sludges, saltcake and supernatant; consequently resulting in substantial leakage.[29]

For example, ^{99}Tc was found to be present in surface water samples at Argonne National Lab in Illinois as early as 1965,[30] and recently it has been noted that radioactive wastes have begun leaking into ground water supplies. Once present in the water supply the long lived ^{99}Tc isotope can be taken up into the food chain as an analog of sulfate[22], thus contaminating regions in the mid-western United States. It has also been shown that $^{99}TcO_4^-$ ions in soil may compete with nutrient ions for uptake by plant roots and some plants. Subsequently animals can take-up and metabolize ^{99}Tc, thus being exposed to a radiation dose.[31]

Although the physiological effects of Tc have not been studied extensively there is evidence that upon ingestion Tc is retained in the stomach, blood and saliva, and can accumulate in the thyroid gland in concentrations of up to 24%. Although not lethal, these concentrations of ^{99}Tc are potentially very dangerous as they have the ability to cause lesion of body tissue due to ß-radiation. [32]

1.4 Waste remediation and disposition

Removal of pertechnetate from the nuclear waste tanks was initially accomplished through ion exchange of the pertechnetate species[19], but both extraction and reduction methods have also proved successful.

1.4.1 Ion-Exchange Methods

Work by Burgeson[33] and King[34] has shown that the Superlig® 639 ion exchange resin exhibits high efficiency (99% removal) as well as selectivity (over competition for high NO^- concentrations) for TcO_4^- from waste tank supernate. Gut *et al.* have developed novel bifunctional anion-exchange resins by using two quaternary ammonium groups of long chain trihexylamines to improve the selectivity, and short chain triethylamines to enhance both the kinetics and the exchange capacity.[35]

Although the ion exchange resins are advantageous due to their high selectivity and capacity, the method suffers from the interference of competing ions, high cost, regeneration, desorption and second contamination of the resins.

1.4.2 Extraction Methods

Extraction of heptavalent Tc(VII) from both water and NaOH solutions with 2-nitrophenyl octyl ether (NPOE) has been reported to occur from alkaline solutions. This is surprising since NPOE has no donating atoms for cation association and thus does not fall into the class of typical complexation molecules such as crown ethers. Similarly extraction of the perrhenate, ReO_4^- occurred in a 1:1 stoichiometry with the hypothesis being that the co-extracted cation is expected to play an important role in the extraction mechanism. [25]

Like most solvents used for Tc extraction, NPOE is toxic to the environment. In an attempt to find a non-toxic alternative, supercritical CO_2 modified with a polar organic solvent has been used to extract ion pairs of perrhenate, the nonradioactive congener of pertechnetate. Temperature, pressure, solvent modification and ion-pairing agents were

examined in order to maximize the extraction, and tetrabutyl ammonium cation was found to form the most efficient ion pair for perrhenate extraction using methanol-modified $SFCO_2$ at 70ºC and 477atm.[31]

1.4.3 Reduction of Pertechnetate

More often, the focus seems to be on pertechnetate reduction, where Fe(II) appears to be the most common reductant. The mobile pertechnetate ion can be removed from solution by reduction to insoluble, lower-valence Tc(IV) species (such as $^{99}TcO_2 \bullet nH_2O$ or $^{99}TcS_2$), which can then be physically adsorbed to a solid surface or physically mixed with glass, cement or ceramic. This reduction results in the immobilization of the radionuclide in sediments and is accomplished under anoxic conditions using a variety of bacteria, zerovalent iron or Fe(II)-containing minerals. [22]

In 2004, Wildung et al, studied the reduction of pertechnetate in core samples from sediments that exhibited dissimilatory iron reduction potentials. In all sediments the dominant electron donor proved to be Fe(II): [36]

$$TcO_4^-{}_{(aq)} + 3Fe^{2+} + (7+n)\ H_2O = 5H^+ + TcO_2 \bullet nH_2O_{(s)} + 3Fe(OH)_3$$

A group from Stockholm, Sweden studied the reduction of TcO_4^- to $TcO_2 \bullet nH_2O$ by Fe(II) in slightly acidic to basic media, and reported that the reduction was very slow to proceed. They found that Fe(II) in solution did not act to reduce Tc(VII), but rather that it was only after precipitation of the Fe(II) species as $Fe(OH)_2(s)$ or $FeCO_3(s)$ with NaOH, that pertechnetate reduction occurred. They proposed a mechanism for the

disappearance of technetium from the solution to be sorption of TcO_4^- on precipitated Fe(II), followed by surface mediated three-electron reduction of TcO_4^- to $TcO_2 \bullet nH_2O$, where the rate of reduction was observed to be proportional to the amount of precipitated Fe(II). [37]

$$TcO_4^- \rightarrow TcO_4^{2-} \rightarrow TcO_4^{3-} \rightarrow TcO_2 \bullet nH_2O$$

In an analogous study by this same group, the surface mediated reduction of pertechnetate in solution by Fe(II)-bearing fracture filling material from granite, hornblende, and magnetite was studied. They found that the three-electron reduction of TcO_4^- to the low solubility $TcO_2 \bullet nH_2O(s)$, although thermodynamically possible is kinetically hindered. The rate constant of the pertechnetate disappearance from solution is dependent on the specific surface area of the Fe(II) content of the solid, which is in agreement with their earlier findings. [37]

In 2000 Lloyd et. al. studied the direct and indirect Fe(II) mediated reduction of technetium by Fe(III) reducing bacteria. They found that the bacteria may play an important role in the immobilization of Tc in soil sediments by directly coupling the oxidation of hydrogen to the enzymatic reduction of Tc(VII) to Tc(IV), which appeared as a black precipitate in the bacterial cell culture. Alternatively, they postulated an indirect mechanism, where acetate aided in the reduction of Fe(III), and the Fe(II) formed was able to abiotically transfer electrons to Tc(VII).[22]

Later, a study examining the behavior of Tc at low concentrations as microbial anoxia develops established similar findings. TcO_4^- removal from solution was found to occur while Fe(III) reducing conditions develop in association with the active

accumulation of microbially generated Fe(II) in sediments, once again confirming that it was Fe(II) that acted to reduce the pertechnetate. [26]

1.4.4 The Prevalent Problem

Unfortunately, the reduced ^{99}Tc(IV) in the form of all the aforementioned amorphous oxides has been shown to be prone to re-oxidation. Upon re-oxidation all ^{99}Tc (IV) species hydrolyze back to the mobile ^{99}Tc(VII) ($^{99}TcO_4^-$). An example of this can be seen in a recent study by Lukens.[20] In this study it was found that the ^{99}Tc(IV) oxides and sulfides that had formed upon the reduction of $^{99}TcO_4^-$ with grout-containing reductants, began to slowly re-oxidize back to $^{99}TcO_4^-$ over time. In fact, it was shown as early as 1985 that in the presence of any aqueous solutions the TcO_2 formed in the glassification of high-level waste begins to undergo hydrolysis. In the presence of oxygen and water, TcO_2 was found to easily undergo oxidation to the soluble TcO_4^-, and the process was shown to be enhanced radiolytically.[38, 39]

1.5 Our Approach

Because minerals and colloids in the environment as well as common storage matrices, including glass and ceramics, are comprised of metal oxides, it is important to try and develop an understanding of the speciation and mobility of ^{99}Tc in metal oxides, as well as characterize the reactions involving labile technetium and its available anions.

Understanding the extensive redox chemistry (including the parameters that will effect the speciation, coordination environment and oxidation states) of Tc incorporated into metal oxide matrices will promote a better understanding of how to identify and

develop more appropriate methods for both the separation of Tc from nuclear waste tanks as well as more fitting storage matrices. In an effort to help advance the development of an appropriately stable waste-form for ^{99}Tc we will be probing its redox chemistry by studying the interaction of ^{99}Tc with Polyoxometalates, that are essentially soluble metal oxide matrices.

1.6 Polyoxometalates

1.6.1 What are Polyoxometalates?

Polyoxometalates (POMs) are nanometer-sized transition metal-oxide clusters with the general formula $[X_xM_mO_p]^{n-}$; where X is termed the heteroatom and can be a variety of p- or d-block elements, M represents the principal metal (or addenda atom) and is usually a high valent early transition metal such as Mo^{VI} or W^{VI}, and O is oxygen. POMs are always anionic in nature and are known to be chemically robust. They have homogeneous crystalline structures, and can easily be modified with respect to incorporation of transition metal ions, charge, size, redox potential, and solubility. [40]

The first POM compounds were reported over 150 years ago, and today there are more than 70 different elements that have been reportedly incorporated into POM structures.[41] When incorporated into the POM framework, metals exist in their highest valent state (no d electrons). This allows for the POM oxygen atoms to donate electrons to the metal unfilled orbitals to form a strong bond between the POM and the metal.

1.6.2 Why Polyoxometalates

The choice of polyoxometalates for this study is due to their similarity to solid metal oxide structures. POMs possess closely packed oxygen atoms in their frameworks that render them good model systems to simulate solid oxide structures such as metal oxide ceramics and minerals.[42-46] Their structures are also comprised of metal to oxygen bond order differences that alternate in length resulting in the formation of rings with alternating short-long Oxygen-Metal-Oxygen bonds.[43, 44] These properties of POMs permit synthesis and examination of the structure and speciation chemistry of incorporated ^{99}Tc on the molecular level, thus allowing specific studies of the oxidation states of Tc under varying experimental conditions. [47, 48]

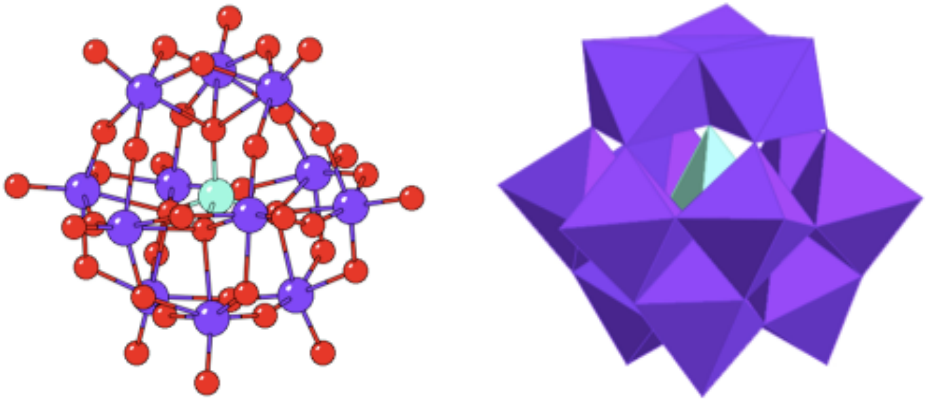

Figure 1.3. The KEGGIN $[XW_{12}O_{40}]^{n-}$ (X = Al, Si or P and n = 5, 4,3) structure shown in Ball and Stick (on the left) and Polyhedral (on the right) Representations.

Figure 1.3 shows two common and complementary representations of a Keggin POM, $[XW_{12}O_{40}]^{n-}$ (X = Al, Si or P and n = 5, 4, 3). The Keggin POM consists of a central XO_4^{3-} core, where X (the heteroatom) may be one of most p or d block elements,

surrounded by a cage of 12 MO_3 units, where M (the principal metal) is one of the early to mid transition metals such as W(VI), Mo(VI), V(V), Nb(V) or Ti(IV). The structure on the left in Figure 1.3 represents the Ball-and-Stick representation of a Keggin. In this representation each individual atom is depicted as a ball and each bond as an adjoining stick. In the case above the central heteroatom is shown in aqua, the 12 tungsten principal metals in purple and the adjacent oxygen atoms in red.

POMs can also be depicted using a Polyhedral representation (shown on the right in Figure 1.3). In the polyhedral representation the central XO_4^{3-} core is represented as a central tetrahedron (shown in aqua) surrounded by 12 MO_6 octahedrons (shown in purple). In this representation the adjoining corners of each octahedron share an oxygen atom; to accurately depict the 12 MO_3 units.

Simple modifications to the basic POM structure afford a variety of possible binding environments in which to perform speciation studies. If we consider the Keggin structure as an example, replacement of one of the principal metals with an early transition metal ion of lower valency decreases the metal-oxygen bond strength. This causes an increase in the surface basicity of the POM, thereby creating a soft binding site for surface binding of soft lower valent ^{99}Tc species. This phenomenon is depicted in Figure 1.4, where the dark blue octahedra represent WO_3 units and the aqua octahedra represent MO_3 units where the W have been replaced by a metal ion in a lower valent state.

Figure 1.5 illustrates the formation of a lacunary POM structure that offers an alternative site for binding of transition metals. By removing one or more of the WO^{4+} units a vacancy can be fashioned within the POM skeleton, thus giving rise to hard

binding sites. Higher valent ^{99}Tc species can then be incorporated into these defects to become chemically bound within the POM framework.

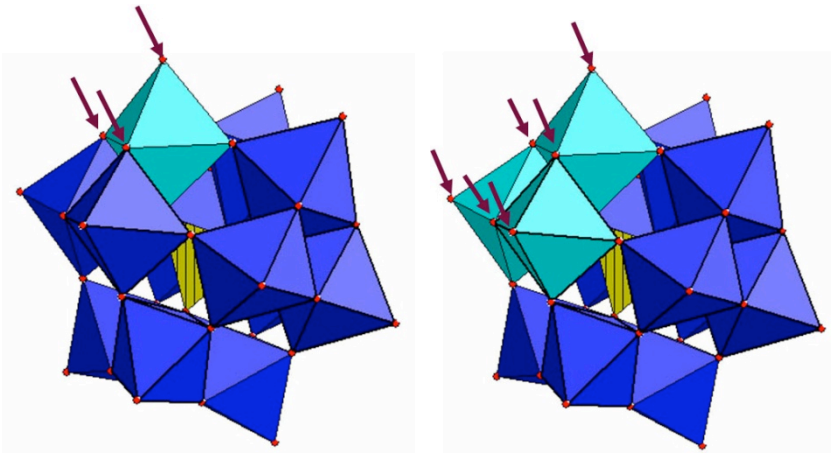

Figure 1.4. The KEGGIN $[XW_{12}O_{40}]^{n-}$ structure showing the replacement of high valent W atoms (depicted by dark blue octahedron) with metals in a lower valent state (shown in aqua octahedron) to create soft binding sites.

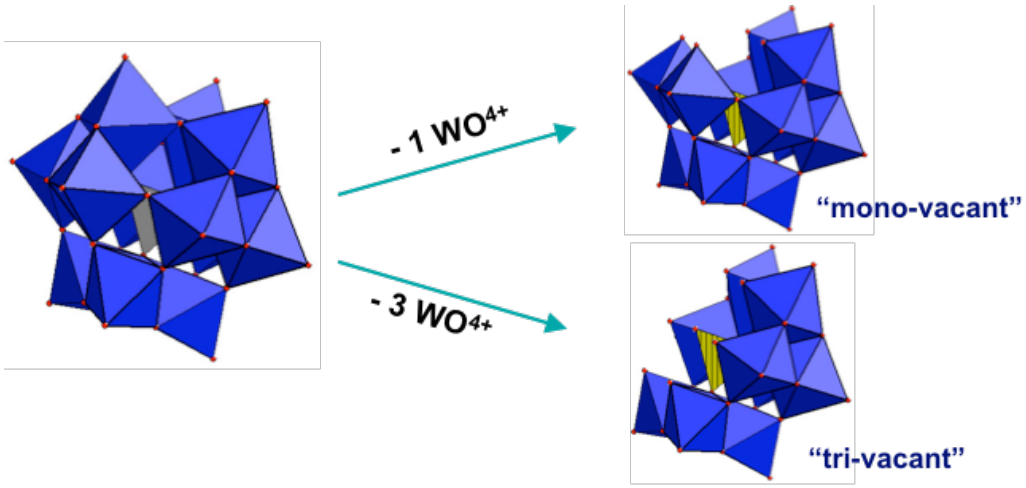

Figure 1.5. The KEGGIN $[XW_{12}O_{40}]^{n-}$ structure showing the removal of WO4+ units to create hard binding sites.

1.6.3 The Wells-Dawson Lacunary $[P_2W_{17}O_{61}]^{10-}$ Polyoxometalate

The complexation of lanthanides and transition metals to polyoxometalates can thus occur in multiple positions; either into the defect site of "lacunary" polyoxometalates, or directly to the surface oxygen atoms. A prime example of a lacunary POM is the monovacant lacunary polyoxometalate $[P_2W_{17}O_{61}]^{10-}$, of which two isomers, α-1 and α-2 (Figure 1.6) can be prepared. [49-51]

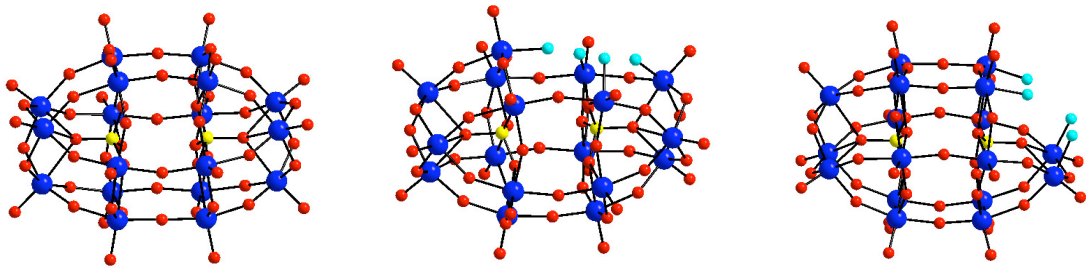

Figure 1.6. The Wells-Dawson family of Polyoxometalates. A) The Parent $[\alpha\text{-}P_2W_{18}O_{62}]^{6-}$, a plenary POM. B) The lacunary $[\alpha_1\text{-}P_2W_{17}O_{61}]^{10-}$ isomer and C) The $[\alpha_2\text{-}P_2W_{17}O_{61}]^{10-}$ isomer. The dark blue circles represent tungsten atoms, the red circles represent oxygen atoms, and the cyan circles represent oxygen atoms available for bonding to lanthanide and transition metal ions.

The polyoxoanion $[P_2W_{17}O_{61}]^{10-}$ is prepared from the Wells-Dawson heteropolyanion $\alpha\text{-}[P_2W_{18}O_{62}]^{6-}$, (a spheroid of ca. 20 Å by 10 Å with 18 peripheral oxygen atoms).[47] Removal of one $[W(VI)=O]^{4+}$ group from the plenary $\alpha\text{-}[P_2W_{18}O_{62}]^{6-}$ anion gives rise to the monovacant, lacunary Wells-Dawson polyoxoanion $[P_2W_{17}O_{61}]^{10-}$. Removal of a $[WO]^{4+}$ unit from a "cap" WO_6 polyhedron of the parent $\alpha\text{-}[P_2W_{18}O_{62}]^{6-}$ results in the defect or lacunary structure of Cs symmetry, forming the α-2 isomer, while removal of a $[WO]^{4+}$ unit from a "belt" region results in the lacunary structure of C_1 symmetry, forming the α-1 isomer.[51]

These isomers are known to function as tetradentate ligands with four strongly basic O donor atoms directed at the vacant site left by the removal of $[WO]^{4+}$. It is this defect site that provides the primary binding site for cationic complexation. [50, 51]

Importantly, the defects of POMs possess distinct features that impact both the redox properties and binding strengths to the bound transition metals. The mono-vacant $(\alpha_2\text{-}P_2W_{17}O_{61})^{10-}$ and $(\alpha_1\text{-}P_2W_{17}O_{61})^{10-}$ Wells-Dawson POMs (Figure 1.3) possess defects with distinct and different steric and electronic properties that have been exploited to study the coordination environment and speciation of ^{99}Tc as well as its third row congener Re.

Earlier work in our lab and that of others has shown that the α_1 site is sterically larger and less flexible than the α_2 site (3.7 Å separation between adjacent corner-shared metal ions in the α_1 site as compared to 3.4 Å in the α_2 site). The α_1 site thus provides a sterically inflexible environment as compared to the adaptable environment of the α_2 site. The α_1 site is also comparatively basic, described by Contant to be due to the orientation of the PO_4^{3-} tetrahedron within the cavity of the W-O framework, positioning a basic oxygen atom near the α_1 site.[52] This basicity requires cations of high charge/size ratio in order to stabilize it.[52-56 57-64]

The α_1 and α_2 sites also differ in their redox properties. It has been shown in the literature that electrons added to the Wells-Dawson anion are mostly delocalized over only the 12 equatorial tungsten atoms located in the belt (α_1) site. [65-69] A series of DFT calculations by Poblet have shown that reduction occurs preferentially in the LUMO and LUMO +1 orbitals, which are comprised mainly of the d_{xy}-orbitals centered on the belt (α_1) metals. This occurs because they are at lower energy than the LUMO +2 orbital

(Figure 1.7) which is mainly delocalized over the cap region.[65] This means that the first reduction in a Wells-Dawson anion always takes place at the equatorial position [66, 67, 70, 71] and transition metals substituted into the belt (α_1) position will be more readily reduced than those substituted in the cap (α_2). [55-57, 66, 72]

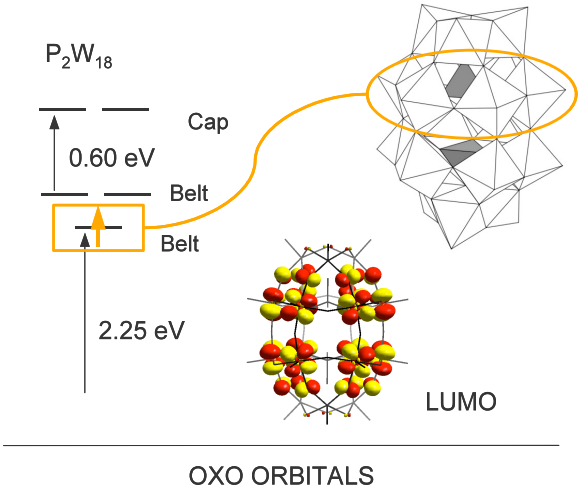

Figure 1.7. Molecular Orbital diagram of the Wells-Dawson ion, $P_2W_{18}O_{62}^{6-}$ showing that the LUMO and LUMO +1 (comprised of metal dxy orbitals from the belt) are at lower energy than the LUMO +2.

1.6.4 The Keggin Polyoxometalate

POMs may also act as electron reservoirs and some, such as Keggin ions, have been shown to undergo stepwise multi-electron redox processes while maintaining their structural integrity.[73] The basic structure of a Keggin POM $[XM_{12}O_{40}]^{n-}$ is shown in Figure 1.3.

Due to their facile delivery of multiple electrons, Keggin POMs have been used as electron transfer agents in the clean formation of metal nanoparticles from high-valent metal ion salts.[74-76] The metal nanoparticles are monodispersed and easily formed via

transfer of electrons from a gold surface (for example) through POM's to the high valent metal salts. The use of POMs for reduction of metal ions is versatile. The reduction potentials of Keggin POMs can be "tuned" by incorporation of elements into many positions of the POM or by simply varying the central heteroatom (which dictates the overall charge on the POM). As the negative charge on the anion increases, the reduction potential of the POM becomes more negative (Figure 1.6)[74-76], rendering them better reducing agents.

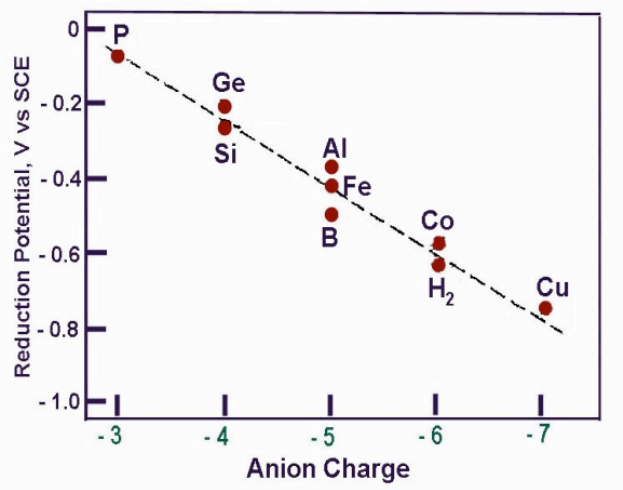

X	-n / -(n+1)	# e- red.	pH range	E, mV (vs. NHE)
P	-3/-4	1 e-	1.0 – 2.0	255 (228)
P	-4/-5	2 e-	1	-15 (29)
Si	-4/-5	1 e-	1.0 – 4.5	55 (23)
Si	-5/-6	2 e-	1.0 – 4.5	-205 (-182)
Al	-5/-6	1 e-	1.8 – 7.5	-130
Al	-6/-7	2 e-	2.05	-330
Al	-6/-7	2 e-	3	-350
Al	-6/-7	2 e-	7.2	-360
Co	-6/-8	2 e-	1.0- 2.0	(-36)

Figure 1.8. The graph on top illustrates the reduction potentials of Keggin polyoxometalates (α-$XW_{12}O_{40}^{n-}$) as a function of the central heteroatom (X). As the negative charge on the anion increases the reduction potential becomes more negative. (Reduction potentials are shown vs. SCE, 0.241 V should be added to reference NHE as shown in the table to the right).

Comparing the reduction potentials in Figure 1.8 with the standard reduction potentials for the reduction of TcO_4^- to the metallic Tc^0 or Tc(IV) (shown below at pH=0 vs NHE) it can be seen that the POM reduction potentials are favorable for the reduction of Tc(VII).

$$TcO_4^- + 8H^+ + 7e^- \longleftrightarrow Tc_{(s)} + 4H_2O \qquad E^o = 0.472\ V$$
$$TcO_4^- + 5H^+ + 3e^- \longleftrightarrow Tc(OH)_2^{2+}{}_{(aq)} + 2H_2O \qquad E^o = 0.620\ V$$
$$TcO_4^- + 4H^+ + 3e^- \longleftrightarrow TcO_{2(s)} + 2H_2O \qquad E^o = 0.738\ V$$

1.6.5 Reduction of Polyoxometalates

Reduced POMs can be generated electrochemically by using bulk electrolysis, by incorporation of reduced transition metal ions or by photochemistry with a sacrificial organic molecule such as propan-2-ol (Isopropyl Alcohol, IPA) as an electron donor. IPA has been used in the literature to aid in the reduction of $(PW_{12}O_{40})^{3-}$ and $(SiW_{12}O_{40})^{4-}$ when exposed to aqueous metal ions, such as Ag^+, $AuCl_4^-$, Pd^{2+}, $PtCl_6^{2-}$ and Hg^2 .[77, 78, 79]

There are several postulated mechanisms by which the photolytic reduction of POMs may occur. Figure 1.9 outlines one such mechanism. In figure 1.9 HPA indicates the parent Heteropolyacid (or oxidized form of the POM), and HPB indicates the Heteroplyblue (or reduced form of the POM). When sunlight hits the sample the HPA becomes promoted to an excited state where it is able to pick up an electron to generate the electron rich HPB.

$$HPA + Solvent \longleftrightarrow HPA^* \longleftrightarrow HPB + Solvent$$

The reduced POM (HPB) is then able to transfer electrons to TcO_4^- (for its reduction to Tc^V, Tc^0 or TcO_2) while regenerating the parent HPA.

$$HPB + TcO_4^- \longleftrightarrow HPA + \text{reduced Tc } (Tc^V, Tc^0, TcO_2)$$

By this mechanism the POM is regenerated with each new reduction cycle to act as a catalyst for the continued reduction of TcO_4^-.

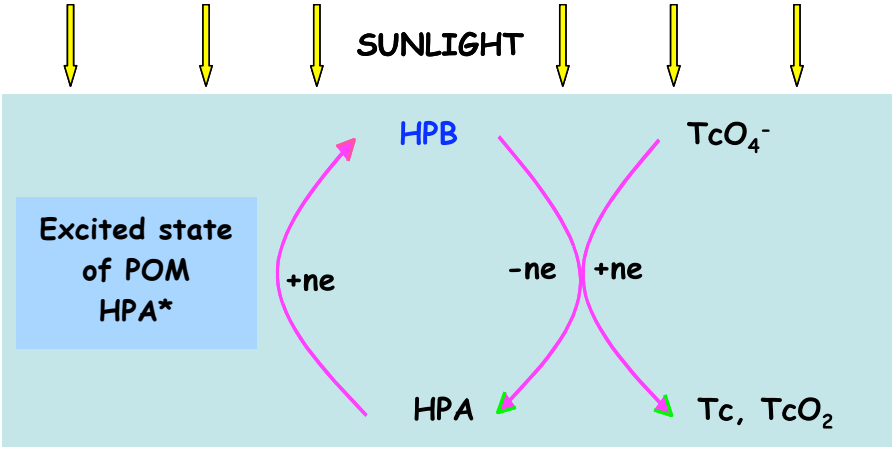

Figure 1.9. Proposed mechanism for the photolytic reduction of POMs; Sunlight irradiates the oxidized form of the POM (HPA) causing its promotion to an excited state where it is able to pick up electrons for its reduction to the electron rich reduced POM (Heteroplyblue, HPB). The HPB is then able to transfer electrons to TcO_4^- (for its reduction to a lower valent state) while regenerating the parent HPA.

Upon reduction of pertechnetate the oxidized form of the POM is regenerated and may act to stabilize the resulting low valent Tc species. Figure 1.10 illustrates schematically a strategy for the use of reduced POMs for the reduction and stabilization of pertechnetate. By this method the oxidized POM is reduced (either electrochemically or irradiated under UV light in the presence of a sacrificial organic compound) to yield a 1 or 2 electron reduced POM. TcO_4^- is then added and subsequently gains electrons from the reduced POM to yield either Tc^0, or Tc^{IV}. Upon re-oxidation the POM can act to

stabilize the resulting low valent Tc species. The reduction to Tc^{IV} will be accompanied by incorporation of the Tc into the bonds of the polyoxometalate, while if the Tc^{0} metal is formed the POM should adhere to the outer edges of the Tc^{0} particle, thereby passivating it. POMs then, may be an excellent addition to present strategies that seek to reduce pertechnetate to lower valent immobile states.

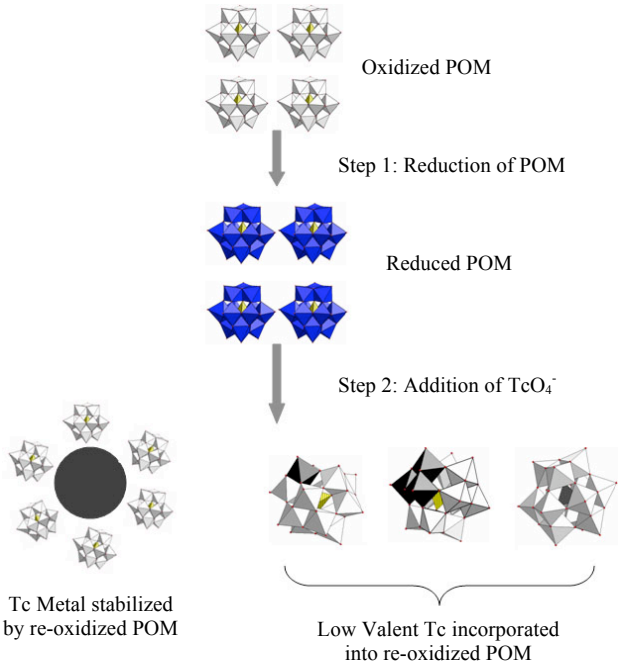

Figure 1.10. Proposed use of POMs as reducing agents for the reduction of TcO_4^-.

1.7 Objectives of this Thesis

1. A study of the chemical principles that contribute to the stability of low valent technetium on the molecular level. Chapters 2 and 3 will focus on the study of the explicit parameters (speciation, coordination environment and oxidation chemistry) that influence the oxidation state stability of ^{99}Tc as incorporated into polyoxometalates

(specifically the α_1-$[P_2W_{17}O_{61}]^{10-}$ and α_2-$[P_2W_{17}O_{61}]^{10-}$ lacunary Wells-Dawson POMs) acting as models for minerals and metal oxide storage matrices.

2. Development of new methodologies for the clean and efficient reduction of Tc^{VII} to a lower valent Tc species. Chapter 4 will present a new and efficient means for the reduction and stabilization of Tc. Taking advantage of the strong and highly tunable electron transfer capabilities of reduced Polyoxometalates, they have been employed to transfer electrons to the mobile Tc^{VII} (pertechnetate) anion for reduction, and possible passivation of the reduced species (either a non-mobile Tc^{IV} species or to the metallic Tc^0 state) by incorporation firmly into the POM matrix (as opposed to surface or physical adsorption).

1.8 References

1. Jurisson, S. S.; Lydon, J. D., *Chem. Rev.* **1999,** *99*, 2205-2218.

2. Committee on the Review of the Hanford Sites environmental Remediation Science and Technology Plan. Board on radioactive waste Management, National Research Council.Sciene and Technology for Environmental Cleanup at Hanford. National Acedemy Press, Washington D.C. : 2001.

3. *Summary of the Hanford Site Environmental Report for the Calender year 2007.*; PNNL-17603-SUM; Pacific Northwest National Laboratory, Richland, washington: Sept 2008.

4. Van Ostenberg, D. O.; Trapp, H. D.; Lam, D. J., *Phys. Rev.* **1962,** *126*.

5. Kessler, K. G.; Trees, R. E., *Phys. Rev.* **1953,** *92*.

6. Schwochau, K., *Angew. Chem.* **1964,** *76*.

7. Boyd, G., *J. Chem. Educ.* **1959,** *36*, 3.

8. Cobble, J. W., *J. Chem. Phys.* **1953,** *21*.

9. Mendeleev, D. I., *Liebigs Ann. Chem, Suppl.* **1872,** *8*, 133-229.

10. Perrier, C.; Segre, E., *J. Chem. Phys.* **1937,** *5*, 712 - 716.

11. Perrier, C.; Segre, E., *Nature (London)* **1937,** *140*, 193 - 194.

12. Moore, C. E., *Science* **1951,** *114*, 59 - 61.

13. Miller, F. J.; Zittel, H. E., *Analyt. Chem.* **1963,** *35*.

14. Merrill, P. W., *Astrophys. J.* **1952,** *116*, 21 - 26.

15. Merrill, P. W., *Science* **1952,** *115*, 484.

16. Merrill, P. W., *Publ. Astron. Soc. Pac.* **1956,** *68*, 70 - 71.

17. Kenna, B. T.; Kuroda, P. K., *J. Inorg. Nucl. Chem.* **1961,** *23*, 142 - 144.

18. Kenna, B. T.; Kuroda, P. K., *J. Inorg. Nucl. Chem.* **1964,** *26*, 493 - 499.

19. Lukens, W. W.; Shuh, D. K.; Schroeder, N. C.; Ashley, K. R., *Environ. Sci. Technol.* **2004,** *38*, 229-233.

20. Lukens, W. W.; Bucher, J. J.; Shuh, D. K.; Edelstein, N. M., *Environ. Sci. Technol.* **2005,** *39*, 8064-8070.

21. French, M. A.; Hao, Z.; Pates, J. M.; Bryan, S. E.; Wilson, R. C., *Anal. Chem.* **2005,** *77*, 135.

22. Lloyd, J. R.; Sole, V. A.; Van Praagh, C. V. G.; Lovley, D. R., *Appl. Environ. Microbiol.* **2000,** *66*, 3743-3749.

23. Wildung, R. E.; Gorby, Y. A.; Krupka, K. M.; Hess, N. J.; Li, S. W.; Plymale, A. E.; McKinley, J. P.; Fredrickson, J. K., *Appl. Environ. Microbiol.* **2000,** *66* (6), 2451-2460.

24. Torstenfeld, B., *Technetium in the Geological Environment, A literature survey*. 1981.

25. Chen, J.; Boerrigter, H.; Veldkamp, A., *Radiochim. Acta* **2001,** *89*.

26. Burke, I. T.; Boothman, C.; Lloyd, J. R.; Mortimer, R. J. G.; Livens, F. R.; Morris, K., *Environ. Sci. Technol.* **2005,** *39*, 4109-4116.

27. DiPrete, D. P.; DiPrete, C. C.; Sigg, A., *Journal of radioanal. and nuclear chemistry* **2005,** *263*.

28. Egorov, O., B.; O'Hara, M., J.; Grate, J., W., *Anal. Chem. 76*.

29. Wakoff, B.; Nagy, K., L., *Environ. Sci. Technol.* **2004,** *38*.

30. Golchert, N. W.; Sedlet, J., *Anal. Chem.* **1969,** *41*, 669 - 671.

31. Gawenis, J., A.; Kauffman, J., F.; Jurisson, S., S, *Anal. Chem.* **2001,** *73* (9).

32. Cobble, J. W.; Boyd, G. E.; Smith, W. T.; Nelson, C. M.; Parker, G. W., *J. Amer. Chem. Soc.* **1952,** *74*, 1852.

33. Burgeson, I. E.; Deschane, J. R.; Blanchard, J. D. L., *Separation Science and Technology* **2005,** *40*, 201 - 223.

34. King, W. D.; Hassan, N. M.; McCabe, D. J.; Hamm, L. L.; Johnson, M. E., *Separation Science and Technology* **2003,** *38*, 3093 - 3114.

35. Gu, B. H.; Brown, G. M.; Bonnesen, P. V.; Liang, L. Y.; Moyer, B. A.; Ober, R.; Alexandratos, S. D., *Environ. Sci. Technol.* **2000,** *34*, 1075 - 1080.

36. Wildung, R. E.; Li, S. W.; Murray, C. J.; Krupka, K. M.; Xie, Y.; Hess, N. J.; Roden, E. E., *FEMS Microbiology Ecology* **2004,** *49*, 151-162.

37. Daqing, C.; Eriksen, T. E., *Environ. Sci. Technol.* **1996,** *30*.

38. Magirius, S.; Carnall, W. T.; Kim, J. I., *Radiochim. Acta* **1985,** *38*, 29-32.

39. Lieser, K. H.; Coetzee, P. P.; Foerster, M., *Radiochim. Acta* **1985,** *38*, 33-35.

40. Hill, C., *Chem. Rev.* **1998,** *98*, 1-3.

41. Gouzerh, P.; Proust, A., *Chem Rev* **1998,** *98*, 327 - 357.

42. Day, V. W.; Klemperer, W. G., *Science* **1985,** *228*, 533-541.

43. Leclerc-Laronze, N., M. ; Haouas, M.; Marrot, J.; Taulelle, F.; Herve, G., *Angew. Chem. Int. Ed.* **2006,** *45* (1), 139-142.

44. Fang, X.; Hill, C. L., *Angew. Chem. Int. Ed.* **2007,** *46*, 3877-3880.

45. Day, V. W.; Klemperer, W. G.; Schwartz, C.; Wang, R.-C., Molecular Models of early transition metal oxides: polyoxoanions as organic functional groups. In *Surface Organometallic Chemistry: Molecular Approaches to Surface Catalysis*, Kluwer Academic Publishers: New York, 1988; p 173.

46. Long, D.-L.; Burkholder, E.; Cronin, L., *Chem. Soc. Rev.* **2007,** *36*, 105-121.

47. Saito, A.; Choppin, G. R., *Inorg. Chem.* **1991,** *30* (24), 4563-4566.

48. Saito, A.; Tomari, H.; Choppin, G. R., *Inorganica Chimica Acta* **1997,** *258*, 145-153.

49. Luo, Q.; Howell, R. C.; Bartis, J.; Dankova, M.; Horrocks, W. D., Jr.; Rheingold, A. L.; Francesconi, L. C., *Inorg. Chem.* **2002,** *41*, 6112-6117.

50. Luo, Q.; Howell, R. C.; Dankova, M.; Bartis, J.; Williams, C. W.; Horrocks, W. D., Jr.; Young, J., V.G.; Rheingold, A. L.; Francesconi, L. C.; Antonio, M. R., *Inorg. Chem.* **2001,** *40*, 1894-1901.

51. Bartis, J.; Dankova, M.; Lessmann, J. J.; Luo, Q.-H.; Horrocks, W. D., Jr.; Francesconi, L. C., *Inorganic Chemistry* **1999,** *38*, 1042-1053.

52. Ciabrini, J.-P.; Contant, R., *J. Chem. Research (S) 1993, 391* **1993**, 2720-2744.

53. Contant, R.; Ciabrini, J.-P., *J. Chem. Research (S) 1982, 50-51* **1982,** *1982*, 641-660.

54. Contant, R.; Rocchiccioli-Deltcheff, C.; Fournier, M.; Thouvenot, R., *Calloids and Surfaces A: Physicochemical and Engineering Aspects* **1993,** *72*, 301-306.

55. Contant, R.; Abbessi, M.; Canny, J.; Belhouari, A.; Keita, B.; Nadjo, L., *Inorg. Chem.* **1997,** *36*, 4961-4967.

56. Contant, R.; Herve, G., *Reviews in Inorganic Chemistry* **2002,** *22* (2), 63-111.

57. Keita, B.; Girard, F.; Nadjo, L.; Contant, R.; Canny, J.; Richet, M., *Journ. of Electroanal. Chem.* **1999,** *478*, 76-82.

58. Harmalker, S. P.; Leparulo, M. A.; Pope, M. T., *J. Amer. Chem. Soc.* **1983,** *105*, 4286-4292.

59. Leparulo-Loftus, M. A.; Pope, M. T., *Inorg. Chem.* **1987,** *26*, 2112-2120.

60. Sadakane, M.; Dickman, M. H.; Pope, M. T., *Inorg. Chem.* **2001,** *40* (12), 2715-2719.

61. Sadakane, M.; Ostuni, A.; Pope, M. T., *J. Chem. Soc. Dalton Trans.* **2002**, 63-67.

62. Abbessi, M.; Contant, R.; Thouvenot, R.; Herve, G., *Inorg. Chem.* **1991,** *30*, 1695-1702.

63. Zhang, C.; Howell, R. C.; Fieselmann, H. L.; Todaro, L.; Francesconi, L. C., *Inorg. Chem.* **2005,** *44*, 3569-3578.

64. Boglio, C.; Lenoble, G.; Duhayon, C.; Hasenknopf, B.; Thouvenot, R.; Zhang, C.; Howell, R.; Burton-Pye, B.; Francesconi, L. C.; Lacote, E.; Thorimbert, S.; Malacria, M.; Afonso, C.; Tabet, J.-C., *Inorg Chem* **2006,** *45* (3), 1389-1398.

65. Keita, B.; Lu, Y. W.; Nadjo, L.; Contant, R., *Electrochemistry Communications* **2000,** *2*, 720-726.

66. Kozik, M.; Hammer, C. F.; Baker, L. C. W., *J. Am. Chem. Soc.* **1986,** *108*, 2748-2749.

67. Kozik, M.; Baker, L. C. W., *J. Am. Chem. Soc.* **1990,** *112*, 7604-7611.

68. Acerete, R.; Hammer, C. F.; Baker, L. C. W., *Journ. Amer. Chem. Soc.* **1982,** *104*, 5384-5390.

69. Ciabrini, J. P.; Contant, R.; Fruchart, J. M., *Polyhedron* **1983,** *2* (11), 1229-33.

70. Lopez, X.; Bo, C.; Poblet, J. M., *J. Am. Chem. Soc.* **2002,** *124*, 12574-12582.

71. Keita, B.; Levy, B.; Nadjo, L.; Contant, R., *New. J. Chem.* **2002,** *26*, 1314-1319.

72. Contant, R.; Richet, M.; Lu, Y. W.; Keita, B.; Nadjo, L., *Eur. J. Inorg. Chem.* **2002**, 2587-2593.

73. Mandal, S.; Selvakannan, P. R.; Pasricha, R.; Sastry, M., *J. Amer. Chem. Soc.* **2003,** *125*, 8440-8441.

74. Geletii, Y. V.; Hill, C. L.; Bailey, A. J. H., K.I.; Atalla, R. H.; Weinstock, I. A., *Inorg. Chem.* **2005,** *44*, 8955-8966.

75. Altenau, J. J.; Pope, M. T.; Prados, R. A.; So, H., *Inorg. Chem.* **1977,** *14* (2), 417-421.

76. Pope, M. T.; Varga, G. M., *Inorg. Chem.* **1966,** *5* (7), 1249-1254.

77. Mandal, S.; Mandale, A. B.; Sastry, M., *J. Mater. Chem.* **2004,** *14*, 2868-2871.

78. Troupis, A.; Hiskia, A.; Papaconstantinou, E., *New J. Chem.* **2001,** *25*, 361-363.

79. Hiskia, A.; Troupis, A.; Papaconstantinou, E., *International Journal of Photoenergy* **2002,** *4*, 35-40.

80. Grika, E.; Troupis, A.; Hiskia, A.; Papaconstantinou, E., *Environ. Sci. Technol.* **2005,** *39*, 4242-4248.

Chapter 2: Aqueous Soluble ^{99}Tc (V) complexes of the $(\alpha_1\text{-}P_2W_{17}O_{61})^{10-}$ and $(\alpha_1\text{-}P_2W_{17}O_{61})^{10-}$ Well-Dawson Lacunary POMs.

2.1 Introduction

One of the key obstacles faced by researchers when trying to identify and develop separation strategies for the removal of ^{99}Tc from nuclear waste tanks and to design and develop storage matrices involves the ability to control the extensive redox chemistry of ^{99}Tc. Because minerals and colloids in the environment as well as common storage matrices (such as glass and ceramics) are comprised of metal oxides, it is important to develop a fundamental understanding of both the speciation and stability of ^{99}Tc when incorporated into metal-oxide systems.

POM's provide a stable framework within which to study both the coordination environment and oxidation state stability of transition metals, such as ^{99}Tc. The defects of POMs possess distinct features that impact the redox properties as well as binding strengths of the metals bound within the vacancies**.** The mono-vacant $(\alpha_2\text{-}P_2W_{17}O_{61})^{10-}$ and $(\alpha_1\text{-}P_2W_{17}O_{61})^{10-}$ Wells-Dawson POMs (Figure 2.1) possess defects with distinct and different steric and electronic properties that can be exploited to study the coordination environment and speciation of ^{99}Tc and its third row congener Re. Earlier work in our lab and that of others has shown that the α_1 site is sterically larger and less flexible than the α_2 site (3.7 Å separation between adjacent corner shared metal ions in the α_1 site as compared to 3.4 Å in the α_2 site).[1] The α_1 site thus provides a sterically inflexible environment as compared to the adaptable environment of the α_2 site. The α_1 site is also

comparatively basic and this basicity requires cations of high charge/size ratio in order to stabilize it. [2]

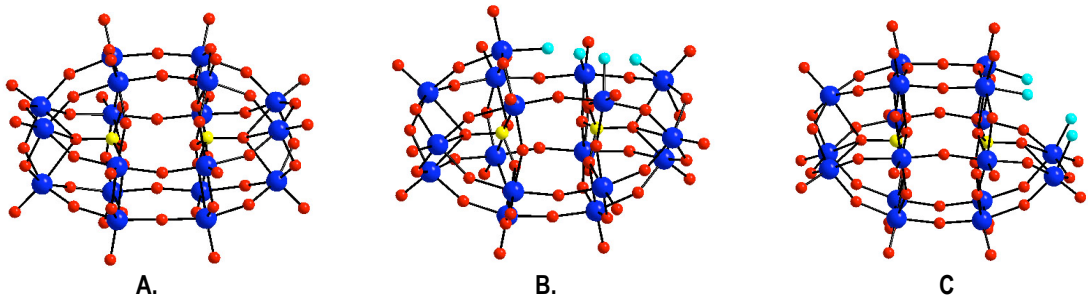

Figure 2.1. The Wells-Dawson family of Polyoxometalates. A) The Parent $[\alpha\text{-}P_2W_{18}O_{62}]^{6-}$, a plenary POM. B) The lacunary $[\alpha_1\text{-}P_2W_{17}O_{61}]^{10-}$ isomer and C) The $[\alpha_2\text{-}P_2W_{17}O_{61}]^{10-}$ isomer. The dark blue circles represent tungsten atoms, the red circles represent oxygen atoms, and the cyan circles represent oxygen atoms available for bonding to lanthanide and transition metal ions.

In this chapter we attempt to develop insight into the explicit parameters (speciation, coordination environment and oxidation state chemistry) that influence the stability of ^{99}Tc incorporated into aqueous soluble mono-vacant Wells-Dawson Polyoxometalates (POMs). POMs are used as model systems to mimic metal oxide matrices. We have adapted methods that we developed for the study of lanthanide polyoxometalate speciation in order to study the molecular level chemistry of multi oxidation state ^{99}Tc as incorporated into the $(\alpha_1\text{-}P_2W_{17}O_{61})^{10-}$ and $(\alpha_2\text{-}P_2W_{17}O_{61})^{10-}$ Wells-Dawson metal oxide bonds.

2.2 Experimental

2.2.1 General

^{99}Tc is a weak β- emitter with a half-life of 2×10^5 years. All reported Tc syntheses were performed in an appropriately equipped lab approved for the use of low-

level radioactivity. Correct and suitable radioactive material handling procedures were employed. All materials were purchased as reagent grade and used without further purification. Water was obtained using a Millipore Direct Q5 system (conductivity =18 μΩ). Solid ammonium pertechnetate (NH_4TcO_4) was purchased from Oak Ridge National Laboratory. This NH_4TcO_4 is contaminated with TcO_2 due to radiolytic autoreduction and is black in color. Pure NH_4TcO_4 is a white crystalline solid. To regenerate pure pertechnetate the raw NH_4TcO_4 was dissolved in water and heated with hydrogen peroxide until the volume had decreased by half. The resulting aqueous solution was standardized using a well-established UV-vis protocol. [3] $(NBu_4)TcOCl_4$ was prepared from NH_4TcO_4 according to a published procedure.[3] The aqueous soluble α_1-$P_2W_{17}O_{61}^{10-}$ and α_2-$P_2W_{17}O_{61}^{10-}$ ligands were prepared as described in the literature.[4-6] The α_1-$[Fe(H_2O)P_2W_{17}O_{61}]^{7-}$ for electrochemistry was prepared as previously described.[5] Infrared analyses were performed on a Perkin Elmer 1625 FTIR Spectrometer using a KBr pellet.

2.2.2. Collection of NMR Data.

NMR data were collected on a JEOL GX-400 spectrometer using 5 or 10 mm NMR tubes fitted with a Teflon insert (purchased from Wilmad Glass). Resonance frequencies are 161.8 MHz for ^{31}P and 16.7 for ^{183}W. Chemical shifts are given with respect to external 85% H_3PO_4 for ^{31}P and 2.0 M Na_2WO_4 for ^{183}W. Typical acquisition parameters for ^{31}P spectra included the following: spectral width, 10000 Hz; acquisition time, 0.8 s; pulse delay, 1 s; pulse width, 15 μs (50° tip angle). From 200 to 1000 scans were required. For ^{183}W spectra, typical conditions included the following: spectral

width, 10000 Hz; acquisition time, 1.6 s; pulse delay, 0.5 s; pulse width, 50 μs (45° tip angle). From 1000 to 30000 scans were acquired. For all spectra, the temperature was controlled to ± 0.2 deg. For the ^{31}P and ^{183}W chemical shifts, the convention used is that the more negative chemical shifts denote more upfield resonances. Because of the low abundance (14%) of the ^{183}W nucleus in natural W, ^{183}W NMR spectroscopy requires sample sizes of approximately 30 mM. The samples used for ^{183}W NMR experiments were thus scaled up and prepared *in situ*.

2.2.3 Collection of Electrochemical Data.

Electrochemical data were obtained using a BAS Voltammetric Analyzer System controlled by BAS CV-50W software (for PC). The cell used for cyclic voltammetry (CV) contained a glassy-carbon working electrode (BAS standard disk electrode, 3 mm OD), a Pt wire auxiliary electrode (0.5 mm), and a BAS Ag/AgCl (3 M NaCl) reference electrode. Prior to obtaining electrochemical data, solutions were de-aerated for at least 30 minutes with high purity Argon (Ar). Fine polishing of the glassy-carbon working electrode was adapted from the procedure of Keita and co-workers.[7] Unless otherwise noted, scan rates were 10 mV/s^{-1}, and all experiments were carried out at ambient temperature under an Ar atmosphere.

2.2.4 Preparation of Buffer Solutions.

The aqueous electrolyte solution used for the electrochemical pH study was a constant 0.5 M Na_2SO_4 solution prepared at a variety of pH values as follows:

pH 0: To a 0.5 M solution of Na_2SO_4 (7.1 g Na_2SO_4 in 100 mL 0.5 M H_2SO_4) was added concentrated H_2SO_4 to adjust the pH to **0.03**.

pH 1: To a 0.5 M solution of Na_2SO_4 (7.1 g Na_2SO_4 in 100 mL 0.5 M H_2SO_4) was added concentrated H_2SO_4 to adjust the pH to **1.01**.

pH 3: To a 0.5 M solution of Na_2SO_4 (7.1 g Na_2SO_4 in 100 mL 0.5 M H_2SO_4) was added concentrated H_2SO_4 to adjust the pH to **2.98.**

pH 5: To a 0.5 M solution of Na_2SO_4 (7.1 g Na_2SO_4 in 0.01 M Sodium Acetate buffer prepared by mixing 24 mL 0.01 M NaOAc with 76 mL 0.01 M NaOAc) was added 1 M KOH to adjust the pH to **5.04**.

pH 7: To a 0.5 M solution of Na_2SO_4 (8.5 g Na_2SO_4 in 0.1 M Phosphate buffer prepared by mixing 50 mL 0.1 M Na_2HPO_4 with 70 mL 0.1 M NaH_2PO_4) was added 1 M KOH to adjust the pH to **6.98**.

pH 8: To a 0.5 M solution of Na_2SO_4 (7.1 g Na_2SO_4 in 100 mL H_2O) was added 1 M KOH to adjust the pH to **8.02.**

2.2.5 Synthesis of Tc(V) Compounds.

$K_{7-n}H_n[Tc^VO(\alpha_1\text{-}P_2W_{17}O_{61})]$: To a 20 mL scintillation vial containing a yellow-green solution of $(NBu)_4TcOCl_4$ (100 mg, 0.2 mmol) dissolved in 1 mL MeOH was added 60 uL (0.98 mmol) of ethylene glycol $(CH_2OH)_2$ to produce a blue-green $TcO(eg)_2^-$ complex. To this was added in one portion a clear, colorless solution of $[K_{10}(\alpha_1\text{-}P_2W_{17}O_{61})]$ (447 mg, 0.099 mmol) dissolved in 5 mL H_2O (to which was added a small amount of $LiCl_3$ to aid the dissolution of the POM). The vial containing the resulting dark red/brown suspension was immediately capped and vigorously shaken for

3 – 5 minutes. The suspension was centrifuged to yield a brown solid and a dark red-brown supernatant. The supernatant was allowed to sit at room temperature for up to 48 hours to allow any unreacted α_1-$P_2W_{17}O_{61}^{10-}$ ligand (as monitored by ^{31}P NMR) to seed out of the solution. 20 mL of ethanol was added to the supernatant to precipitate a dark red/brown solid, which was collected by vacuum filtration.

Yield: 40 - 60% based on $(NBu)_4TcOCl_4$. IR (KBr, cm^{-1}) ν_{max}: 790 cm^{-1} (strong, broad), 953 cm^{-1} (weak), 1086 cm^{-1} (strong). ^{31}P NMR: (160 MHz, D_2O, 300 K, ppm) δP: -11.60 (1P), -12.722 (1P). ^{183}W NMR: (16.7 MHz, D_2O, 300 K, ppm) δW: -37.457 (1W), -118.123 (1W), -121.023 (1W), -132.912 (1W), -148.997 (1W), -174.527 (3W), -187.921 (1W), -191.110 (3W), -206.705 (2W), -233.418 (1W)

$K_{7-n}H_n[Tc^VO(\alpha_2$-$P_2W_{17}O_{61})]$: To a 20 mL scintillation vial containing a yellow-green solution of $(NBu)_4TcOCl_4$ (100 mg, 0.2 mmol) dissolved in 1 mL MeOH was added 60 uL (0.98 mmol) of ethylene glycol $(CH_2OH)_2$ to produce a blue-green $TcO(eg)_2^-$ complex. To this was added in one portion a clear, colorless solution of $[K_{10}(\alpha_2$-$P_2W_{17}O_{61})]$ (447 mg, 0.099 mmol) dissolved in 5 mL H_2O at 90 °C. The vial containing the resulting dark brown suspension was immediately capped and vigorously shaken for 3 – 5 minutes. While still warm the suspension was centrifuged to yield a brown solid and a dark brown supernatant. The supernatant was allowed to sit at room temperature for up to 72 hours to allow any unreacted a_2-$P_2W_{17}O_{61}^{10-}$ ligand (as monitored by ^{31}P NMR) to seed out of the solution. 10 mL of ethanol was added to the supernatant to precipitate a dark brown solid, which was collected by vacuum filtration.

Yield: 40 - 60% based on $(NBu)_4TcOCl_4$. IR (KBr, cm^{-1}) ν_{max}: 790 cm^{-1} (strong,

broad), 953 cm^{-1} (weak), 1086 cm^{-1} (strong). ^{31}P NMR: (160 MHz, D_2O, 300 K, ppm) δP: -11.60 (1P), -13.16(1P). ^{183}W NMR (16.7 MHz, D_2O, 300 K, ppm) δW: -131.059 (2W), -161.506 (1W), -179.912 (2W), -181.720 (2W), -192.189 (2W), -195.228 (2W), -199.685 (2W), -214.819 (2W), -228.776 (2W)

2.3 Results and Discussion

2.3.1 Synthesis of compounds

Because ^{99}Tc is radioactive, synthesis of ^{99}Tc-POM compounds can only be achieved using mg quantities of reagents. Performing such small-scale syntheses with POMs is inherently dfficult, but even more so with Tc compounds. The Tc(V) starting material, $TcOCl_4^-$, hydrolyses readily to $TcO_2 \bullet H_2O$ in the presence of both water and methanol and separation of any free POM ligand from the desired ^{99}Tc-POM complex is complicated by the similarities in their respective solubilities. Generally, separation of transition metal POM complexes is achieved by fractional crystallizations, but the small sample size required for these syntheses make fractional crystallization difficult. Herein is reported a method by which ethylene glycol ($(CH_2OH)_2$, eg) is used as a "transfer ligand" in the synthesis; both to eliminate or reduce hydrolysis of $TcOCl_4^-$ as well as to facilitate the transfer of Tc to the POM framework. This has been summarized in Scheme 2.1.

$$K_{10}(\alpha_{1/2}\text{-}P_2W_{17}O_{61})^{10-} + TBATcOCl_4 \xrightarrow[\text{Ethylene Glycol}]{H_2O,\ MeOH} K_7\text{-}nH_n[TcO(\alpha_{1/2}\text{-}P_2W_{17}O_{61})]$$

Scheme 2.1. Simplified schematic representation of the synthesis of K_7-$nH_n[TcO(\alpha_{1/2}\text{-}P_2W_{17}O_{61})]$

Hydrolysis of the $TcOCl_4^-$ starting material to $TcO_2 \bullet H_2O$ resulted in inconsistencies with the ^{31}P NMR data used to monitor the progress of the reaction. The NMR signals are often broad or not visible with the presence of $TcO_2 \bullet H_2O$ due to paramagnetic broadening of the ^{31}P resonances caused by the unpaired elecrons on the Tc (Tc(IV), d^3). $TcO_2 \bullet H_2O$ is also colloidal and cannot be filtered from the reaction solution. To accurately monitor the species over the course of the reaction it became necessary to take ^{31}P NMR at each step of the synthesis. The resulting NMR shifts that were observed during the synthesis of the $K_{7-n}H_n[Tc^VO(\alpha_2\text{-}P_2W_{17}O_{61})]$ compound are summarized in Table 2.1

In summary, the crude reaction mix showed no peaks in the ^{31}P NMR (due to the presence of the paramagnetic $TcO_2 \bullet xH_2O$ species). The colloidal $TcO_2 \bullet xH_2O$ was removed from the crude reaction mixture by centrifugation. After centrifugation the supernatant showed peaks of the desired product as well as excess $K_{10}(\alpha_1/\alpha_2\text{-}P_2W_{17}O_{61})$ starting material. Allowing the supernatant to sit at room temperature in a vial overnight resulted in the precipitation of a mixed white and brown solid material. The white solid was idetified to be $K_{10}(\alpha_1/\alpha_2\text{-}P_2W_{17}O_{61})$ and the black solid $TcO_2 \bullet xH_2O$. While the black-brown solid proved insoluble in aqueous solution, a significant amount of it was subsequently found to be soluble in acetonitrile. ^{31}P NMR of this soluble solid revealed that it contained almost pure TBA Tc(V) $(\alpha_{1/2}\text{-}P_2W_{17}O_{61})^{10-}$ compound. These compounds will be discussed in detail in Chapter 3 of this dissertation.

The mixture was filtered to remove the solids, upon which the dark brown filtrate showed ^{31}P NMR peaks of pure product (Table 2.1 shows this for the $K_{7-n}H_n[Tc^VO(\alpha_2\text{-}P_2W_{17}O_{61})]$ complex), further affirming that the white solid was indeed excess ligand. If

the original supernatant was allowed to stand for periods of time greater than one week α-$P_2W_{18}O_{62}^{6-}$ (the parent Wells-Dawson POM) was seen to form in solution. This α-$P_2W_{18}O_{62}^{6-}$ proved to be inseparable from the desired product.

Compound or step in synthesis	^{31}P NMR shift (ppm)
Pure K_7-$nH_n[Tc^VO(\alpha_2$-$P_2W_{17}O_{61})]$	**-11.60, -13.11**
Crude Rxn mix	No Peaks
Brown Supernatant	**-11.60, -13.11** (-7.75)
Brown Filtrate	**-11.60**, **-13.11**

Table 2.1. ^{31}P NMR data showing chemical shifts at various stages of the synthesis of K_7-$nH_n[TcO(\alpha_2$-$P_2W_{17}O_{61})]$.

Isolation of solid product was initially attempted by adding an excess of KCl. Although this did result in the formation of a dark brown solid, this solid showed no peaks in the ^{31}P NMR. In subsequent reactions it was discovered that the use of an excess of ethanol resulted in the precipitation of pure K_7-$nH_n[TcO((\alpha_1/\alpha_2$-$P_2W_{17}O_{61})]$ as shown by ^{31}P NMR. The yields obtained for these reactions were never more than 60%. The low yields can be attributed to the formation of $TcO_2 \bullet xH_2O$ coupled with the manipulations required to isolate pure solid product. It was found that maintaining a 1:1 ratio of Tc to α_2-$P_2W_{17}O_{61}^{10-}$ ligand is important for optimizing the yield of product (albeit at ~ 50 %).

Even a small excess of Tc (>1 eq.) results in the formation of a large amount of dark brown to black precipitate (presumed to be $TcO_2 \bullet xH_2O$). Using an excess of α_2/α_1-$P_2W_{17}O_{61}^{10-}$ ligand to compensate for this does not prevent formation of this $TcO_2 \bullet xH_2O$; rather, the result is always an excess of α_2/α_1-$P_2W_{17}O_6^{10-}$ being present in the crude

product (as determined by ^{31}P NMR). This phenomenon would indicate that the formation kinetics of the K_7-$nH_n[TcO((\alpha_1/\alpha_2\text{-}P_2W_{17}O_{61})]$ product are slower than that of the disproportionation of Tc(V) to $TcO_2 \bullet xH_2O$. This can be affected by counterion composition. The excess TBA (introduced with the $TcOCl_4^-$ starting material) might adhere to the surface of the highly charged POM, rendering it less reactive while allowing for more Tc(V) to further disproportionate to $TcO_2 \bullet xH_2O$.

The use of ethylene glycol (eg), as a transfer ligand to mediate the hydrolysis of $TcOCl_4^-$ and facilitate transfer of Tc for isolation of $K_{7\text{-}n}H_n[Tc^VO(\alpha_2/\alpha_1\text{-}P_2W_{17}O_{61})]$ proved successful. The $TcO(eg)_2^-$ complex[10] was not isolated during the procedure, but rather formed *in situ.* When the α_1/α_2 POM is added to this $TcO(eg)_2^-$ complex, the ethylene glycol ligands are replaced by the tetradentate $\alpha_{1/2}\text{-}P_2W_{17}O_{61}^{10-}$ ligand to form the Tc^V K_7-$nH_n[TcO(\alpha_{1/2}\text{-}P_2W_{17}O_{61})]$ product.

In addition to the 1:1 Tc: $\alpha_{1/2}\text{-}P_2W_{17}O_{61}^{10-}$ stoichiometry, we found that a Tc : eg ratio of between a 1:3.5 and 1:6 was required to obtain an optimal yield and purity. A ratio of less than 1:3.5 resulted in the formation of an increased amount of both the $TcO_2 \bullet H_2O$ containing dark solid and free $\alpha_{1/2}\text{-}P_2W_{17}O_{61}^{10-}$ ligand, while a ratio of more than 1:6 resulted in a low yield and increased difficulty when isolating a pure product as a solid. Regardless of the Tc: $\alpha_{1/2}\text{-}P_2W_{17}O_{61}^{10-}$ stoichiometry, the formation of the TBA Tc(V) $(\alpha_{1/2}\text{-}P_2W_{17}O_{61})^{10-}$compound could not be procluded.

2.3.2 Infrared Spectroscopy.

Figures 2.2 and 2.3 show the infrared spectra of the resulting $K_{7\text{-}n}H_n[Tc^VO(\alpha_1P_2W_{17}O_{61})]$ and $K_{7\text{-}n}H_n[Tc^VO(\alpha_2P_2W_{17}O_{61})]$ complexes, respectively. In

each case the characteristic W=O POM stretches at 790 cm^{-1} (strong, broad), 953 cm^{-1} (weak), 1086 cm^{-1} (strong) are visible.

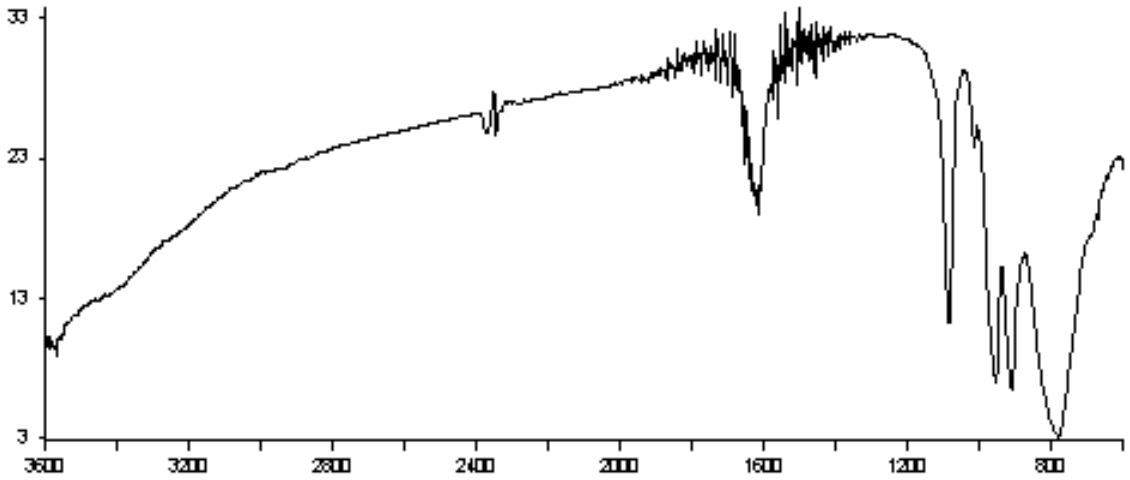

Figure 2.2 : Infrared Spectrum of $K_{7-n}H_n[Tc^{V}O(\alpha_1P_2W_{17}O_{61})]$

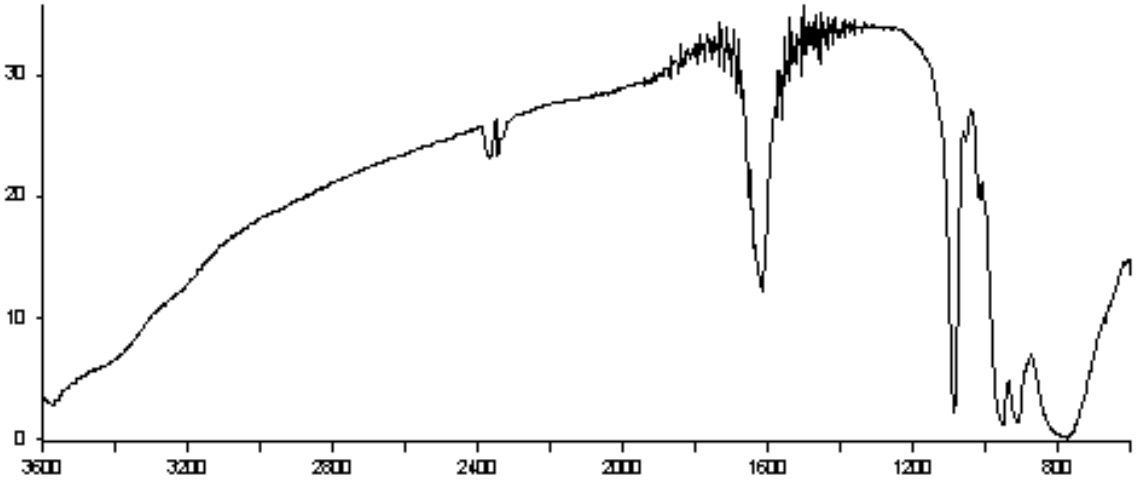

Figure 2.3 : Infrared Spectrum of $K_{7-n}H_n[Tc^{V}O(\alpha_2P_2W_{17}O_{61})]$

Not surprisingly, the IR of our Tc compounds are very similar to that of the parent $[P_2W_{18}O_{62}]^{6-}$ POM. This behavior is identical to what we have observed in our lab for

Re. The IR spectra for Re^{V}, Re^{VI}, Re^{VII} substituted into the α_2-$P_2W_{17}O_{61}$ framework are similar to the parent $[P_2W_{18}O_{62}]^{6-}$.[11] This is also what Ortega and Pope observed for Re substituted into a variety of Keggin POMS[12]; the IR spectra for Re^{V}, Re^{VI}, Re^{VII} substituted into the $XW_{11}O_{39}^{n-}$ framework are similar to the parent $XW_{12}O_{40}^{(n+2)-}$ POM. The characteristic Tc=O stretch is expected to occur at 900 – 960 cm^{-1}. This is superimposed by the bands from the W=O framework.

2.3.3 ^{31}P NMR Spectroscopy.

Figures 2.4 and 2.5 show ^{31}P NMR spectra for the aqueous soluble $K_{7-n}H_n[Tc^{V}O(\alpha_1P_2W_{17}O_{61})]$ and $K_{7-n}H_n[Tc^{V}O(\alpha_2P_2W_{17}O_{61})]$) complexes, respectively. As has been observed for transition metals[13-17] and lanthanide ions, [18-27] two resonances are found for the Tc^{V} α_1-$P_2W_{17}O_{61}^{10-}$ and α_2-$P_2W_{17}O_{61}^{10-}$ species. The upfield resonance in each case is assigned to P1, the phosphorous atom close to the Tc^{V} center and the remote phosphorous, P2, is assigned to the downfield resonance. A summary of the NMR shifts is given in Table 2.2.

Compound	^{31}P NMR, ppm	^{183}W NMR, ppm
$K_{7-n}H_n[Tc^{V}O(\alpha_2$-$P_2W_{17}O_{61})]$	-11.60, -13.16	-131.059 (2), -161.506 (1), -179.912 (2), -181.720 (2), -192.189 (2), -195.228 (2), -199.685 (2), -214.819 (2), -228.776 (2)
$K_{7-n}H_n[Tc^{V}O(\alpha_1$-$P_2W_{17}O_{61})]$	-11.60, -12.722	-37.457 (1), -118.123 (1), -121.023 (1), -132.912 (1), -148.997 (1), -174.527 (3), -187.921 (1), -191.110 (3), -206.705 (2), -233.418 (1)

Table 2.2. Multinuclear NMR Data for Tc^{V} substituted into the α_1-$[P_2W_{17}O_{61}]^{10-}$ and α_2-$[P_2W_{17}O_{61}]^{10-}$ Wells-Dawson POMs

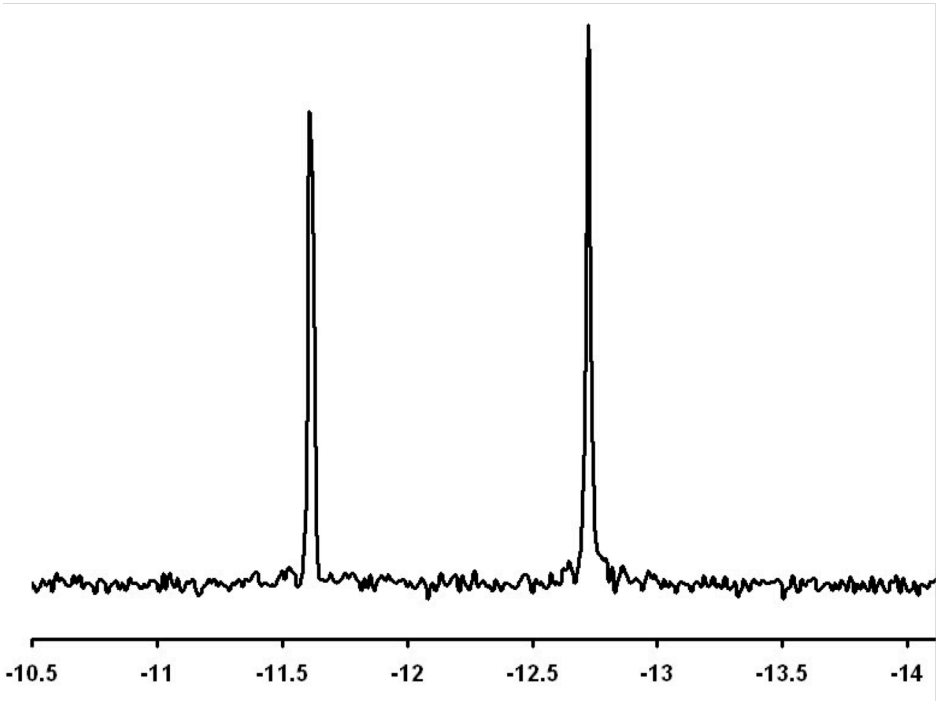

Figure 2.4 ^{31}P NMR Spectrum of $K_{7-n}H_n[Tc^{V}O(\alpha_1P_2W_{17}O_{61})]$

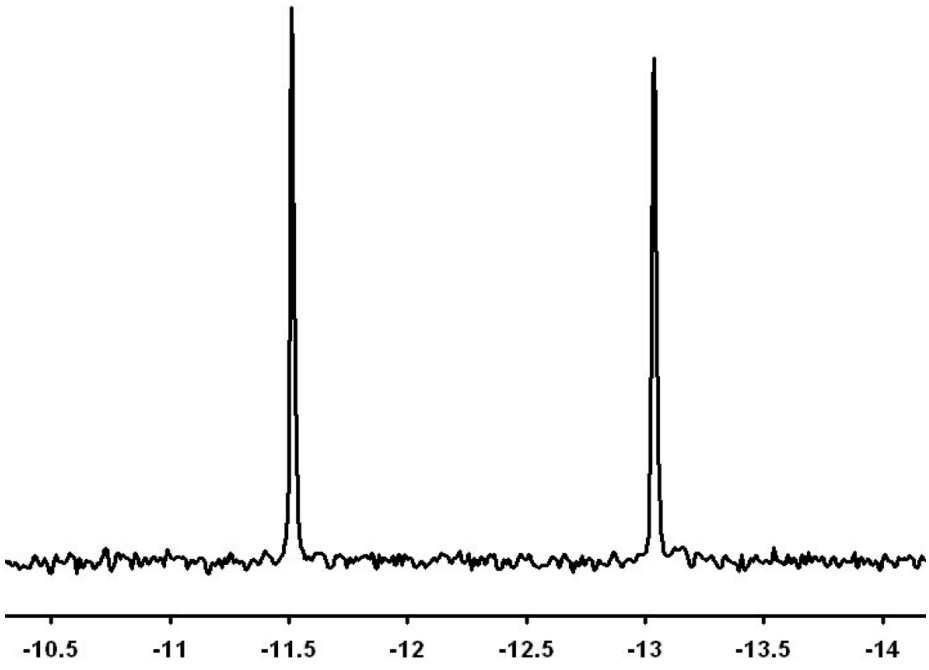

Figure 2.5. ^{31}P NMR Spectrum of $K_{7-n}H_n[Tc^{V}O(\alpha_2P_2W_{17}O_{61})]$

^{31}P NMR is a well-established technique to assess for polyoxometalate impurities down to the 2% level.[13-15] It has been used extensively in the literature to identify pure Wells-Dawson complexes of both transition metals[13-17] and lanthanides. [18-27] The ^{31}P NMR spectra in Figures 2.4 and 2.5 establish that the purity of the Tc^{V} complexes of α_1-$P_2W_{17}O_{61}^{10-}$ and α_2-$P_2W_{17}O_{61}^{10-}$ are both greater than 98%.

2.3.4 ^{183}W NMR Spectroscopy.

Figures 2.6 and 2.8 show ^{183}W NMR spectra for the aqueous soluble $K_{7-n}H_n[Tc^{V}O(\alpha_2P_2W_{17}O_{61})]$ and $K_{7-n}H_n[Tc^{V}O(\alpha_1P_2W_{17}O_{61})]$) complexes respectively. A summary of the NMR shifts is given in Table 2.2. As can be seen in Figure 2.6, the aqueous soluble $Tc^{V}O$ complex of the α_2-$P_2W_{17}O_{61}^{10-}$ isomer clearly shows 9 well-resolved resonances, which is what is expected for a molecule of C_s symmetry (see Figure 2.7). This spectrum is different from the free α_2-$P_2W_{17}O_{61}^{10-}$ ligand[16, 28] and the resonances display appropriate integrations for incorporation of the $Tc^{V}O$ center into the cap region of the α_2-$P_2W_{17}O_{61}^{10-}$ lacunary POM (Figure 2.1).

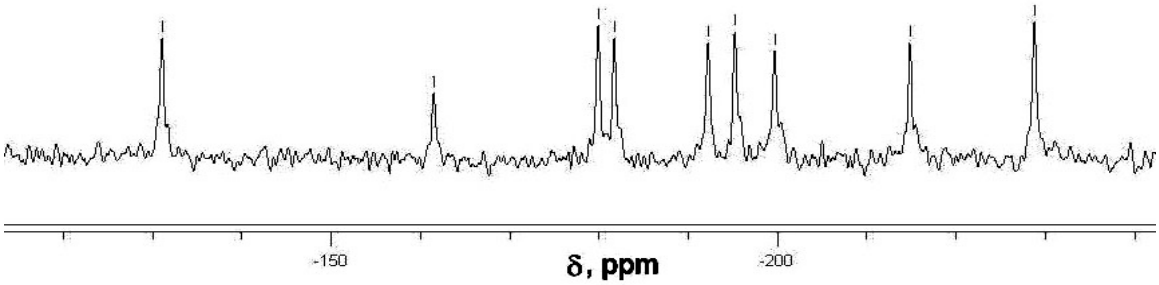

Figure 2.6. ^{183}W NMR Spectrum of $K_{7-n}H_n[Tc^{V}O(\alpha_2P_2W_{17}O_{61})$

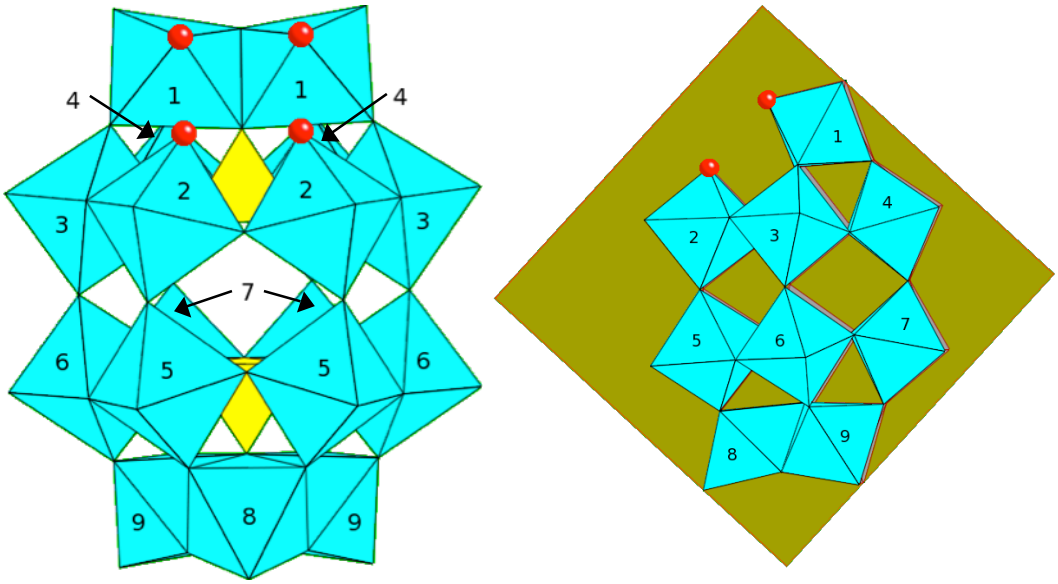

Figure 2.7 Polyhedral Representation of $K_{7-n}H_n[Tc^{V}O(\alpha_2P_2W_{17}O_{61})$ highlighting its Cs symmetry shown from the front (left) and side (right), in which there are 9 in-equivalent W atoms.

Incorporation of the $Tc^{V}O$ core is also observed in the α_1-$P_1W_{17}O_{61}^{10-}$ isomer, which is of C1 symmetry (see Figure 2.9). The pattern observed in Figure 2.8 is clearly different from the $Tc^{V}O\alpha_2$-$P_2W_{17}O_{61}^{7-}$ species and from both the α_2-$P_2W_{17}O_{61}^{10-}$ and α_1-$P_2W_{17}O_{61}^{10-}$ ligands.[16] In Figure 2.8 the aqueous soluble $Tc^{V}O$ complex of the α_1-$P_1W_{17}O_{61}^{10-}$ isomer is clearly approaching the 17 resonances expected for incorporation of the $Tc^{V}O$ center into the belt region of the α_1-$P_2W_{17}O_{61}^{10-}$ lacunary POM (Figure 2.1). Many of the resonances overlap as is often seen at 400 MHz. Although the resonances have not been assigned to specific tungsten atoms, the upfield resonance is likely attributed to a W atom close to the vacancy. Assignment of peaks to specific W atoms (using correlation spectroscopy) requires molar sample concentrations. These concentrations are not possible whilst working with Tc.

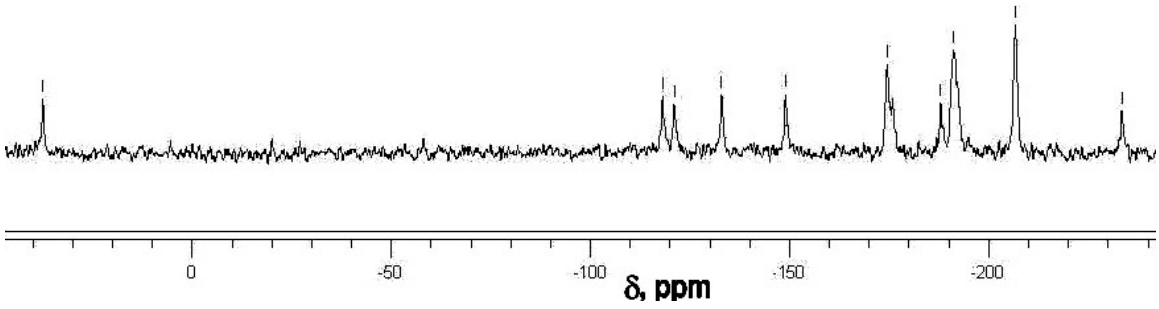

Figure 2.8. ^{183}W NMR Spectrum of $K_{7-n}H_n[Tc^{V}O(\alpha_1P_2W_{17}O_{61})$

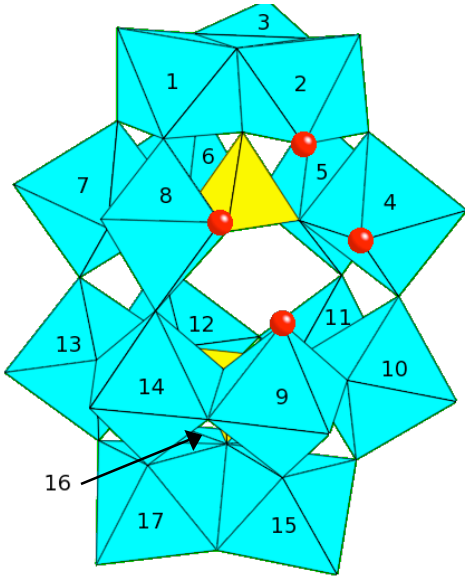

Figure 2.9 Polyhedral Representation of $K_{7-n}H_n[Tc^{V}O(\alpha_1P_2W_{17}O_{61})$ highlighting its C_1 symmetry, in which there are 17 in-equivalent W atoms. (atom 16 lies behind atoms 15 and 17).

2.3.5 Electrochemistry.

As reported by Nadjo and co-workers[29] cyclic voltammetry is a powerful method that can be used to identify the α_1 and α_2- $[P_2W_{17}O_{61}]^{10-}$ Wells-Dawson POM isomers. It is often employed as a means to characterize transition metal complexes of these isomers and to assess their purity.

An initial characterization of the $K_{7-n}H_n[Tc^VO(\alpha_2P_2W_{17}O_{61})]$ and $K_{7-n}H_n[Tc^VO(\alpha_1P_2W_{17}O_{61})]$ complexes was carried out in a 0.5 M Na_2SO_4 dissolved in a sodium acetate buffer (0.01 M CH_3COONa and 0.01 M CH_3COOH,) at pH 5.00. This buffer system was chosen because it has been shown in the literature that most of the transition metal-substituted α_1/α_2-$P_2W_{17}O_{61}$ complexes and the α_1/α_2-$P_2W_{17}O_{61}$ ligands are stable in a sodium acetate buffer at pH 5. [28-30]

Figures 2.10 and 2.11 compare the CVs of the α_1-$[P_2W_{17}O_{61}]^{10-}$ and α_2-$[P_2W_{17}O_{61}]^{10-}$ ligands (solid line) with the CVs of the $K_{7-n}H_n[Tc^VO(\alpha_1P_2W_{17}O_{61})]$ and $K_{7-n}H_n[Tc^VO(\alpha_2P_2W_{17}O_{61})]$ complexes (dotted line) respectively. For both figures, the scans have been restricted to the domain where no derivatization of the working electrode is observed. Proceeding to more negative potentials could lead to adsorption of the reduced species onto the electrode surface.

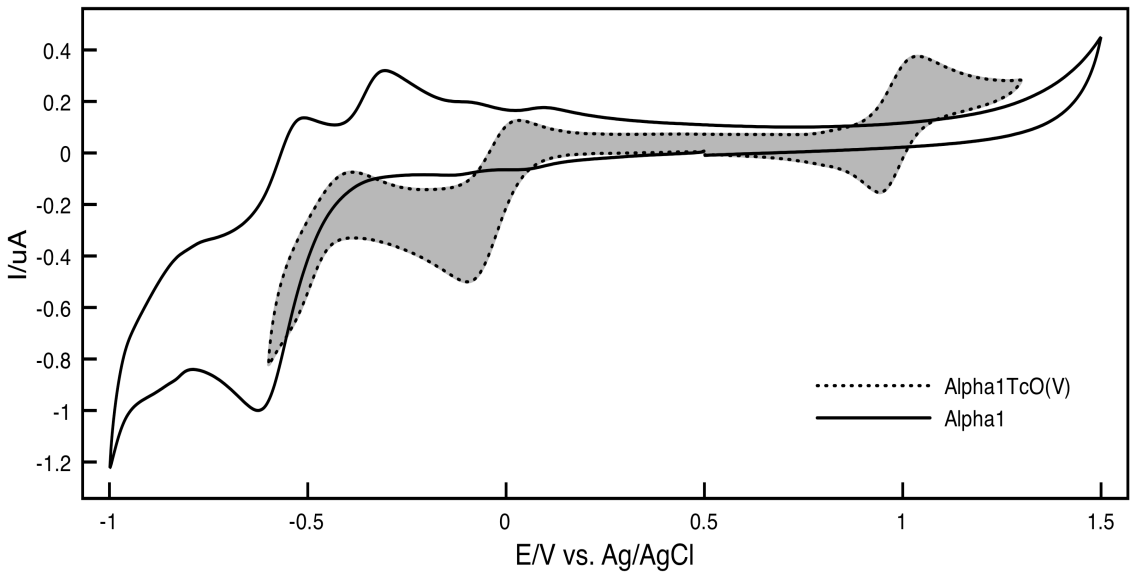

Figure 2.10. CV of α_1-$[P_2W_{17}O_{61}]^{10-}$ (solid line) and $K_{7-n}H_n[Tc^VO(\alpha_1P_2W_{17}O_{61})]$ (dotted line) in 0.5 M Na_2SO_4 dissolved in a sodium acetate buffer (0.01 M CH_3COONa and 0.01 M CH_3COOH,) at pH 5.00. Working electrode, glassy carbon, auxiliary electrode platinum wire and reference electrode, Ag/AgCl. Scan rate 10 mV/s.

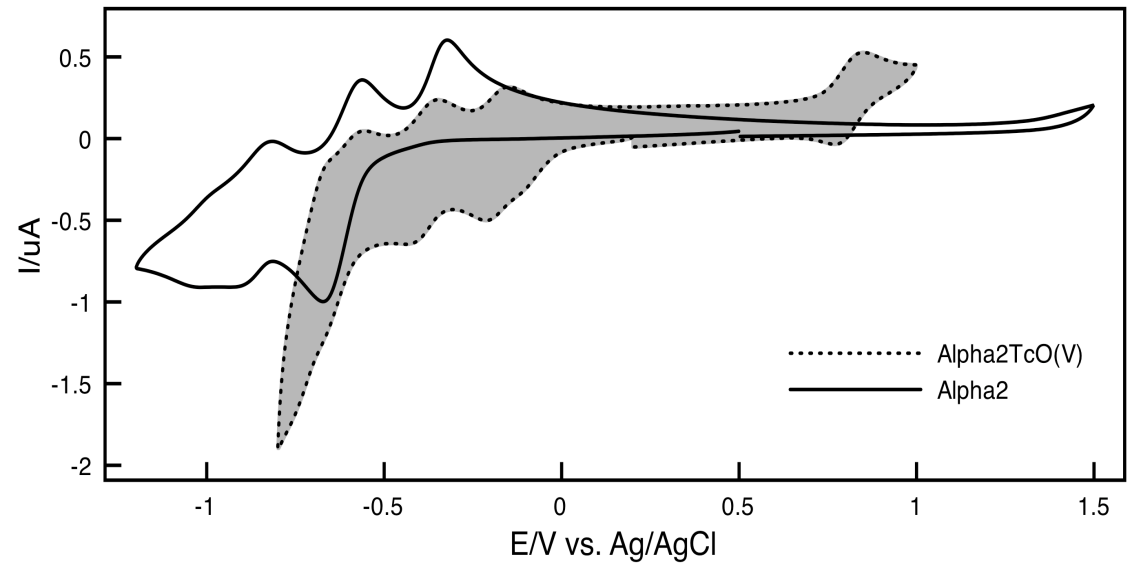

Figure 2.11. CV of α_2-$[P_2W_{17}O_{61}]^{10-}$ (solid line) and $K_{7-n}H_n[Tc^VO(\alpha_2P_2W_{17}O_{61})]$ (dotted line) in 0.5 M Na_2SO_4 dissolved in a sodium acetate buffer (0.01 M CH_3COONa and 0.01 M CH_3COOH,) at pH 5.00. Working electrode, glassy carbon, auxiliary electrode platinum wire and reference electrode, Ag/AgCl. Scan rate 10 mV/s.

The CVs of the Tc^{V} α_1- and the α_2- substituted compounds clearly show a new reversible couple in the positive (oxidative) potential region that does not occur in the lacunary parents. For both the $K_{7-n}H_n[Tc^{V}O(\alpha_1P_2W_{17}O_{61})]$ (Figure 2.10) and the $K_{7-n}H_n[Tc^{V}O(\alpha_2P_2W_{17}O_{61})]$ complexes (Figure 2.9) this reversible couple ($E_{1/2}$ occurring at +990 mV and +809 mV respectively) can be attributed to the Tc^{V}/Tc^{VI} redox process.

The CVs also show a new reversible couple in the negative region that does not exist in the lacunary parents. In the case of the $K_{7-n}H_n[Tc^{V}O(\alpha_1P_2W_{17}O_{61})]$ compound (Figure 2.10) this wave ($E_{1/2}$ = -33 mV) can clearly be accredited to the Tc^{V}/Tc^{IV} redox process within the substituted complex. In the case of the $K_{7-n}H_n[Tc^{V}O(\alpha_2P_2W_{17}O_{61})]$ compound (Figure 2.11) the Tc^{V}/Tc^{IV} redox process is attributed to the first reduction wave ($E_{1/2}$ = -175 mV). The other redox waves present in the negative potential region are attributed to the reduction of the tungsten framework of the POM. This behavior has been observed by Keita et al. for both Fe^{III} and Cu^{II} substituted α_1 and α_2 complexes; where the reduction of the iron and copper centers occur at more positive potentials compared to the reduction of the tungsten framework.[31, 32]

By examining the position of the rest potential in each case, the electrochemical studies above clearly confirm that technetium center present within the structure of the compounds $K_{7-n}H_n[Tc^{V}O(\alpha_1P_2W_{17}O_{61}$and $K_{7-n}H_n[Tc^{V}O(\alpha_2P_2W_{17}O_{61})]$ is in the +5 oxidation state. As can be seen from the CV data the ^{99}Tc(V) center can either be reduced to Tc(IV) or oxidized to Tc(VI).

Due to the highly contaminative nature of the ^{99}Tc isotope it was not possible to conduct bulk electrolysis experiments directly on the $K_{7-n}H_n[Tc^{V}O(\alpha_1/\alpha_2P_2W_{17}O_{61})]$ compounds. The number of electrons consumed during the Tc^{V}/Tc^{IV} redox process was

determined by comparison of the $K_{7-n}H_n[Tc^VO(\alpha_1P_2W_{17}O_{61})]$ CV with that of the Fe^{III}/Fe^{II} wave in the compound α_1-$[P_2W_{17}O_{61}Fe^{III}(H_2O)]^{7-}$ for solutions with the same 10^{-4} M concentration of Tc and Fe ($\alpha_1P_2W_{17}O_{61}$) compounds. This comparison revealed that the redox couple consumes one electron per molecule (Figure 2.12).

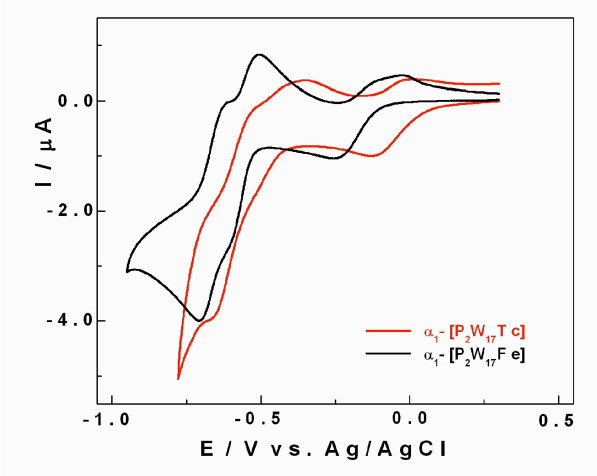

Figure 2.12. CV of $K_{7-n}H_n[Tc^VO(\alpha_1P_2W_{17}O_{61})]$ (red line) and α_1-$K_7[P_2W_{17}O_{61}Fe^{(III)}(H_2O)]$ (black line) in 1M CH_3COONa/CH_3COOH, pH = 5.00. Working electrode, glassy carbon, auxiliary electrode, platinum wire and reference electrode, Ag/AgCl. Scan rate 10 mV/s. Credit for data collection and interpretation to Dr. Israel M. Mbomekalle, Institut Lavoisier, Université de Versailles St. Quentin

Figure 2.13 and Table 2.3 allow for a comparison of the Tc^V/Tc^{IV} and Tc^V/Tc^{VI} reduction couples between the two compounds $K_{7-n}H_n[Tc^VO(\alpha_1P_2W_{17}O_{61})]$ (solid line) and $K_{7-n}H_n[Tc^VO(\alpha_2P_2W_{17}O_{61})]$ (dotted line). The CV data shows that both the Tc^V/Tc^{IV} and Tc^V/Tc^{VI} redox processes occur at more positive potentials (+142 mV and +181 mV respectively) when the ^{99}Tc has been incorporated into the α_1- vacancy as compared to substitution into the α_2- vacancy. This confirms that the reduction of Tc(V) to Tc(IV) is facilitated in the α_1- isomer compared to the α_2- isomer, while the oxidation of Tc(V) to Tc(VI) is more difficult in the α_1- isomer than in the α_2- isomer. This ease of reduction

for substitution into the α_1-$[P_2W_{17}O_{61}]^{10-}$ POM as compared to the α_2-$[P_2W_{17}O_{61}]^{10-}$ POM is consistent with literature results found for first row transition metals, where it has been shown that transition metal cations substituted into the α_1 position are more readily reduced than when substituted in the α_2 position. [29, 30, 33, 34]

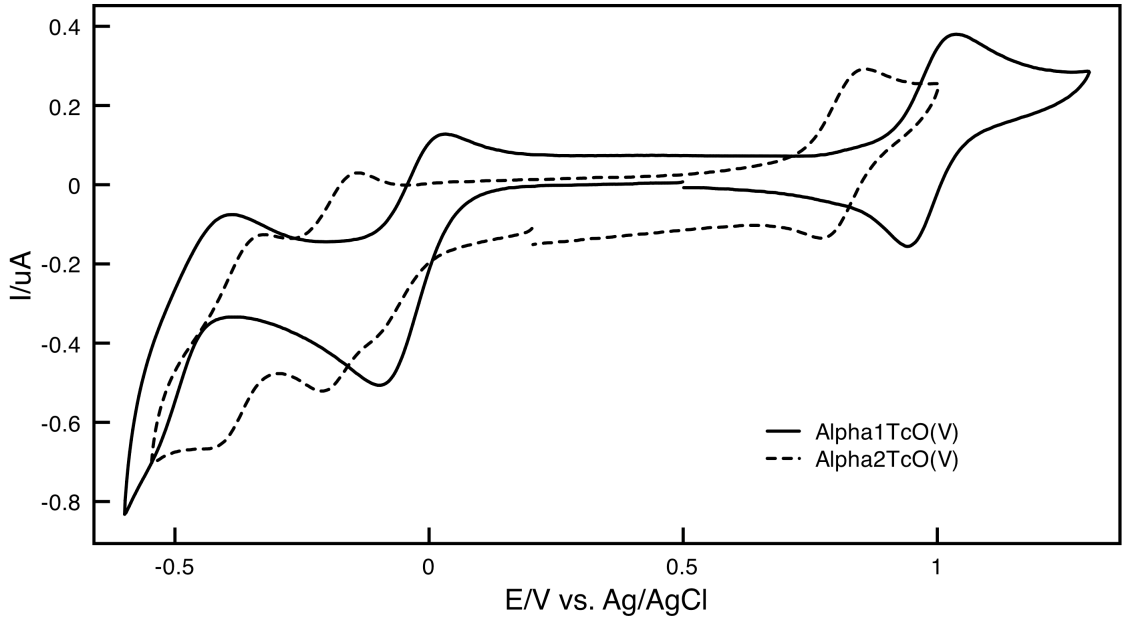

Figure 2.13 CV of $K_{7-n}H_n[Tc^VO(\alpha_1P_2W_{17}O_{61})]$ (solid line) and $K_{7-n}H_n[Tc^VO(\alpha_2P_2W_{17}O_{61})]$ (dotted line) in 0.5 M Na_2SO_4 dissolved in a sodium acetate buffer (0.01 M CH_3COONa and 0.01 M CH_3COOH,) at pH 5.00. Working electrode, glassy carbon, auxiliary electrode platinum wire and reference electrode, Ag/AgCl. Scan rate 10 mV/s.

$E_{1/2}$ (mV)	$Tc^{5/4}$	$Tc^{5/6}$
$K_{7-n}H_n[Tc^VO(\alpha_1\text{-}P_2W_{17}O_{61})]$	-33 (E_c= -98, E_a= 32)	+990 (E_c= 942, E_a= 1037)
$K_{7-n}H_n[Tc^VO(\alpha_2\text{-}P_2W_{17}O_{61})]$	-175 (E_c= -212, E_a=-139)	+809 (E_c= 771, E_a= 847)
$\Delta(\alpha_1\text{-}\alpha_2)$	+142	+181

Table 2.3. Half-wave peak potentials for the Tc^V substituted into the α_1-$[P_2W_{17}O_{61}]^{10-}$ and α_2-$[P_2W_{17}O_{61}]^{10-}$ Wells-Dawson POMs. at pH = 5; scan rate 10 $mV.s^{-1}$.

This phenomenon may be attributed to the fact that electrons added to the Wells-Dawson anion are mostly delocalized over only the 12 equatorial tungsten atoms located in the belt (α_1) site[28, 35-38] and is illustrated in Figure 2.14. A series of DFT calculations by Poblet have shown that reduction occurs preferentially in the LUMO and LUMO +1 orbitals. These orbitals are comprised mainly of the d_{xy}-orbitals centered on the belt (α_1) metals, which are at lower energy than the LUMO +2 orbital which is mainly delocalized over the cap region.[35] This means that the first reduction in a Wells-Dawson anion always takes place at the equatorial position and transition metals substituted into the belt (α_1) position will be more readily reduced than those substituted in the cap (α_2).

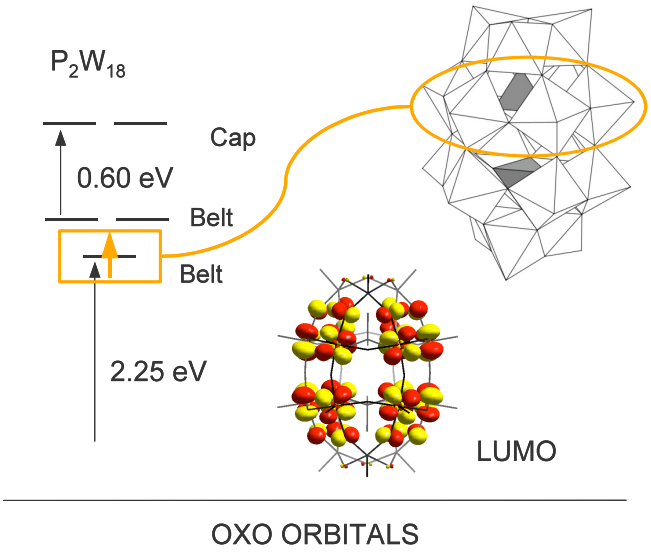

Figure 2.14 Molecualr Orbital diagram of the Wells-Dawson ion, $P_2W_{18}O_{62}^{6-}$ showing that the LUMO and LUMO +1 (comprised of metal dxy orbitals from the belt) are at lower energy than the LUMO +2. Figure kindly provided by Professor Josep Poblet,Universitat Rovira Virgili, Departament de Quimica Fisica & Inorganica

The ease of reduction for metal ions coordinated in the α_1 position may also be attributed to the orientation of the PO_4^{3-} tetrahedron; this has been postulated by Nadjo and co-workers.[33] Figure 2.15 illustrates this orientation. In the α_1-$[P_2W_{17}O_{61}]^{10-}$ POM a

basic oxygen atom is positioned near the vacancy. The basic oxygen of the α_1 defect (gray in Figure 2.15) is bound to the adjacent phosphorous atom and one tungsten atom. In the corresponding oxygen of the α_2 defect, binding occurs to one phosphorous atom and two tungsten atoms. The oxygen atom in the α_1 site would thus favor stronger coupling of the transition metal with the W atoms in the belt. This in turn may aid in protonation events that would facilitate reduction. Theoretical treatments are consistent with these findings; the LUMO in the frontier orbitals of the parent α-$P_2W_{18}O_{61}^{6-}$ (a"$_1$) consists of 96% α1 character.[39]

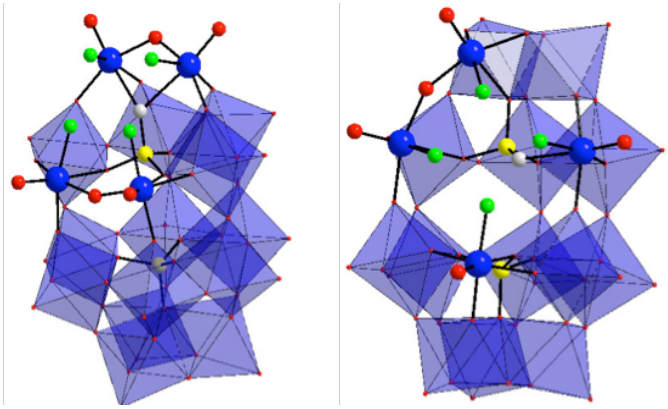

α_2- $P_2W_{17}O_{61}^{10-}$ α_1- $P_2W_{17}O_{61}^{10-}$

Figure 2.15. Representations of the defect sites of the α_2- $P_2W_{17}O_{61}^{10-}$ and α_1- $P_2W_{17}O_{61}^{10-}$ Wells-Dawson POMS. The tungsten atoms that create the defect are shown as balls. The tungsten atoms not involved in the defect are represented as octahedra. The oxygen atoms bound to the W atoms of the defect are shown in green. All other oxygen atoms bound to W atoms are shown in red. The P atoms are yellow. The oxygen atom bound to the phosphorous of the defect is shown in off white.

2.3.6 pH Study

In an attempt to understand the effect of protonation on the Tc^V speciation and compare the energies of the α_1- and α_2-$[Tc^VOP_2W_{17}O_{61}]^{7-}$ complexes an electrochemical

study as a function of pH was conducted on both the free $(\alpha_1\text{-}P_2W_{17}O_{61})^{10-}$ and $(\alpha_1\text{-}P_2W_{17}O_{61})^{10-}$ ligands as well as the α_1- and α_2-$[Tc^{V}OP_2W_{17}O_{61}]^{7-}$ complexes.

2.3.6.1 $(\alpha_1\text{-}P_2W_{17}O_{61})^{10-}$ and $(\alpha_2\text{-}P_2W_{17}O_{61})^{10-}$

Figures 2.16, 2.17, 2.18, 2.19 and 2.20 show a comparison of the CV data for the $(\alpha_1\text{-}P_2W_{17}O_{61})^{10-}$ and $(\alpha_2\text{-}P_2W_{17}O_{61})^{10-}$ ligands at pH values of 0, 1, 3, 5 and 7 respectively. At pH values of 0, 1 and 3 (shown in Figures 2.16, 2.17 and 2.18 respectively) the two well-resolved (reversible) redox processes in the negative potential region are attributed to tungsten (W) reduction/oxidation processes within the α_1 and α_2 ligands. Specifically these waves can be accredited to two successive two-electron redox couples. At pH values of 5 and 7 (shown in Figures 2.19 and 2.20) this first W reduction for both α_1 and α_2 transpires as a single two-electron reduction wave coupled to two one-electron oxidation waves, while the second W reduction occurs at values that are too negative to be observed in the electrochemical window of this experiment.

The CV data for the $(\alpha_1\text{-}P_2W_{17}O_{61})^{10-}$ ligand at low pH exhibit trace amounts of an impurity which manifests as an irreversible oxidation wave at +127 mV for pH = 0 and a reversible redox process centered at +40 mV for both pH = 1 and pH = 3. This is not unexpected and may be attributed to a number of things, one of which is the isomerization of the α- form of the POM to the β. It is also plausible that the high sensitivity of electrochemistry as (an analytical tool) coupled with the sensitive $(\alpha_1\text{-}P_2W_{17}O_{61})^{10-}$ synthesis allow for trace amounts of the parent heteropolyanion α-$[P_2W_{18}O_{62}]^{6-}$ (not detected by ^{31}P NMR) to be detected as an impurity by this method. The known instability of $(\alpha_1\text{-}P_2W_{17}O_{61})^{10-}$ in a highly acidic or basic environment may

also lead to degradation of the compound to the parent heteropolyanion under these acidic conditions.

As the pH is further increased the redox process attributed to this impurity becomes better defined, and the two successive reversible waves become more pronounced. These redox couples are centered at – 100 mV and +40 mV and can now be assigned to the parent α-$[P_2W_{18}O_{62}]^{6-}$ heteropolyanion. This behavior indicates that as the solvent environment becomes more basic the $(\alpha_1\text{-}P_2W_{17}O_{61})^{10-}$ ligand undergoes more decomposition to the parent α-$[P_2W_{18}O_{62}]^{6-}$.

The $(\alpha_2\text{-}P_2W_{17}O_{61})^{10-}$ ligand is known to be stable over a larger pH range and shows traces of the parent heteropolyanion α-$[P_2W_{18}O_{62}]^{6-}$ (as an irreversible reduction at +40 mV) only under highly acidic conditions, with no decomposition at pH values above 1.

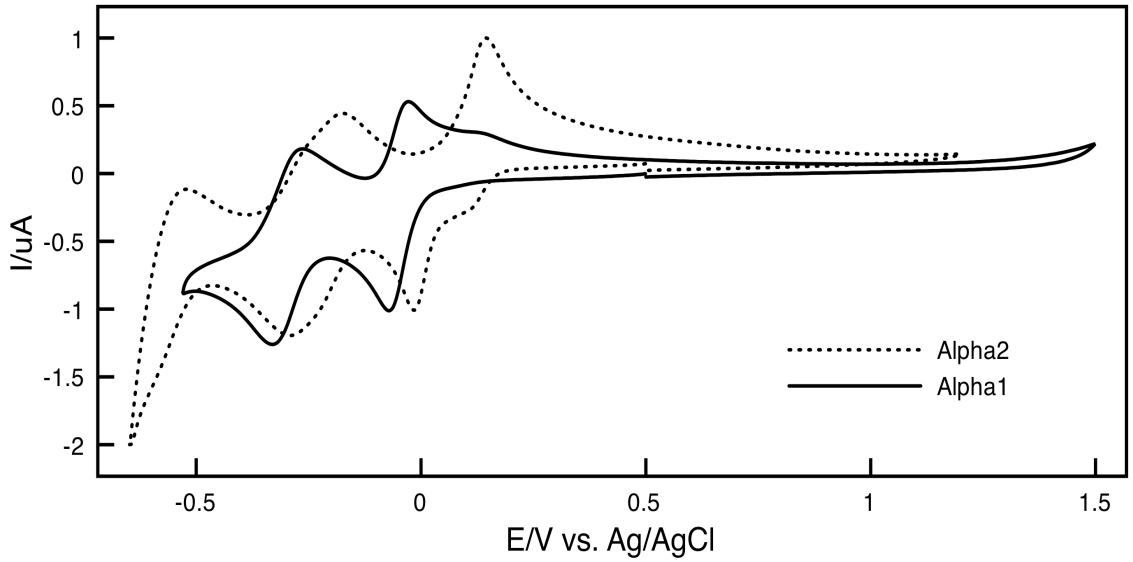

Figure 2.16 CV for 10^{-3} M $(\alpha_1\text{-}P_2W_{17}O_{61})^{10-}$ and $(\alpha_2\text{-}P_2W_{17}O_{61})^{10-}$ ligands at pH = 0. Electrolyte, 0.5 M Na_2SO_4. Working electrode, glassy carbon, auxiliary electrode, platinum wire and reference electrode, Ag/AgCl. Scan rate 10 mV/s.

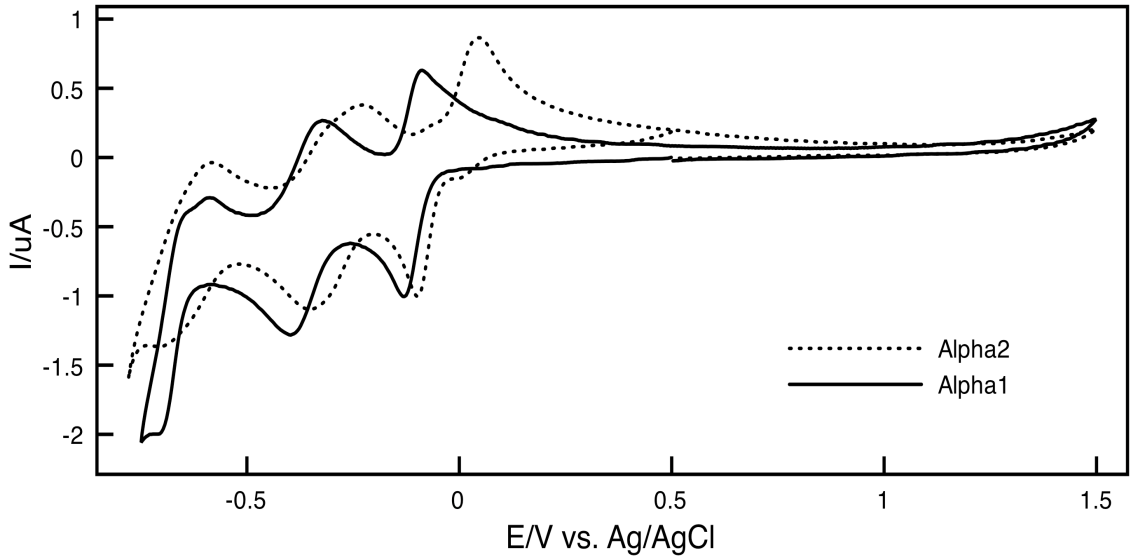

Figure 2.17 CV for 10^{-3} M $(\alpha_1\text{-}P_2W_{17}O_{61})^{10-}$ and $(\alpha_2\text{-}P_2W_{17}O_{61})^{10-}$ ligands at pH = 1. Electrolyte, 0.5 M Na_2SO_4. Working electrode, glassy carbon, auxiliary electrode, platinum wire and reference electrode, Ag/AgCl. Scan rate 10 mV/s.

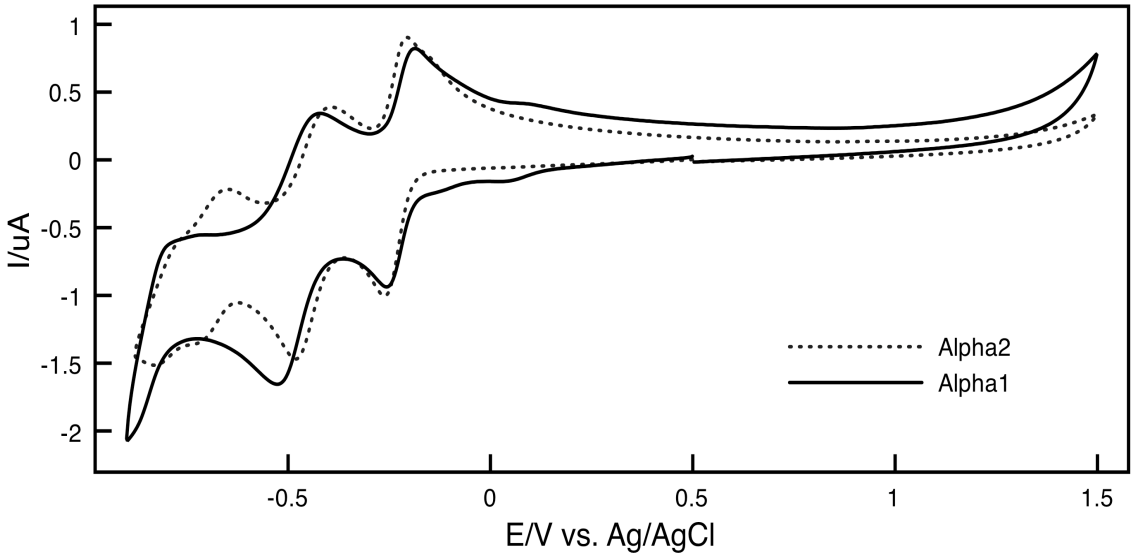

Figure 2.18 CV for 10^{-3} M $(\alpha_1\text{-}P_2W_{17}O_{61})^{10-}$ and $(\alpha_2\text{-}P_2W_{17}O_{61})^{10-}$ ligands at pH = 3. Electrolyte, 0.5 M Na_2SO_4. Working electrode, glassy carbon, auxiliary electrode, platinum wire and reference electrode, Ag/AgCl. Scan rate 10 mV/s.

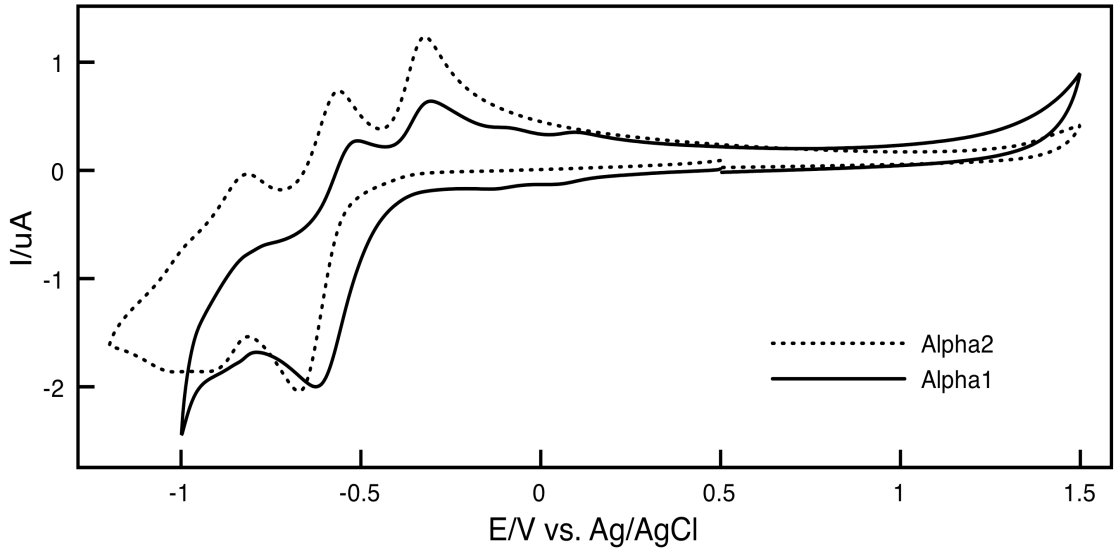

Figure 2.19 CV for 10^{-3} M $(\alpha_1\text{-}P_2W_{17}O_{61})^{10-}$ and $(\alpha_2\text{-}P_2W_{17}O_{61})^{10-}$ ligands at pH = 5. Electrolyte, 0.5 M Na_2SO_4. Working electrode, glassy carbon, auxiliary electrode, platinum wire and reference electrode, Ag/AgCl. Scan rate 10 mV/s.

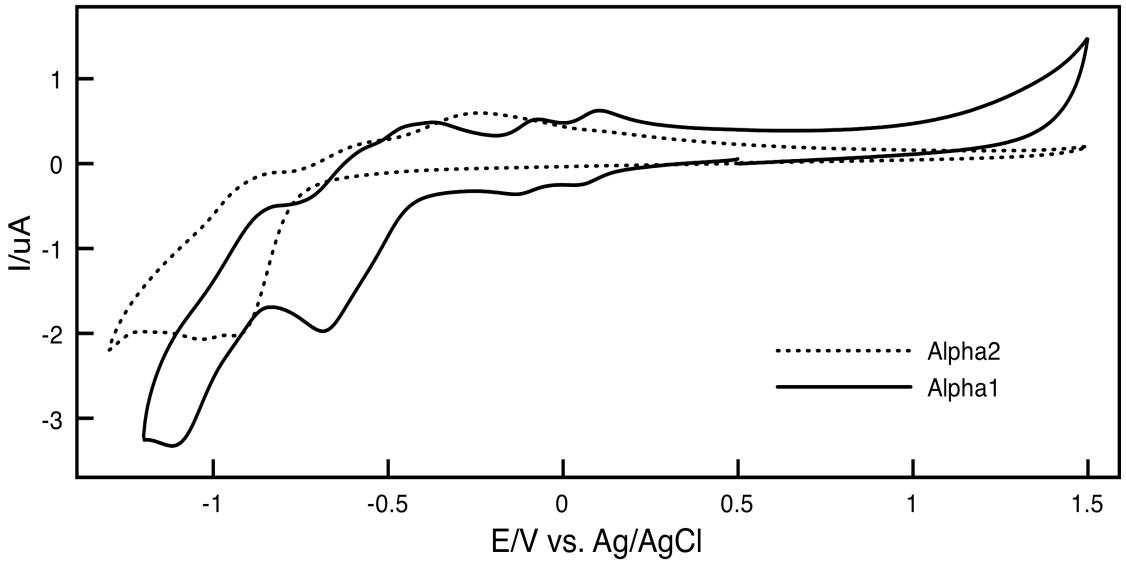

Figure 2.20 CV for 10^{-3} M $(\alpha_1\text{-}P_2W_{17}O_{61})^{10-}$ and $(\alpha_2\text{-}P_2W_{17}O_{61})^{10-}$ ligands at pH = 7. Electrolyte, 0.5 M Na_2SO_4. Working electrode, glassy carbon, auxiliary electrode, platinum wire and reference electrode, Ag/AgCl. Scan rate 10 mV/s.

Table 2.4 summarizes the reduction potentials for the $(\alpha_1\text{-}P_2W_{17}O_{61})^{10-}$ and $(\alpha_2\text{-}P_2W_{17}O_{61})^{10-}$ ligands. A general shift of all reduction peak potentials (for both α_1 and α_2) towards more negative values with increasing pH is observed. This means that reduction is favored at lower pH values, and can be attributed to the increase in the number of available protons that would aid in the transfer of electrons. At pH values above 7 the redox couples of the tungsten framework are not visible in the available electrochemical window. These redox processes become largely undefined with increasing pH, and are eclipsed by the sharp reduction peak observed due to the evolution of hydrogen under the given set of experimental conditions.

E (mV)	α_1- $P_2W_{17}O_{61}^{10-}$			α_2- $P_2W_{17}O_{61}^{10-}$		
	E_{c1}	E_{c2}	E_{c1} -E_{c2}	E_{c1}	E_{c2}	E_{c1} -E_{c2}
pH = 0	-72	-331	+259	-16	-292	+276
pH = 1	-129	-398	+269	-98	-354	+252
pH = 3	-257	-526	+269	-262	-481	+219
pH = 5	-682	-	-	-670	-	-
pH = 7	-687	-	-	-939	-	-

Table 2.4. Reduction potentials (E_c) for the first two reductions in the α_1-$[P_2W_{17}O_{61}]^{10-}$ and α_2-$[P_2W_{17}O_{61}]^{10-}$ Wells-Dawson POMs at pH values 0 through 7. Electrolyte, 0.5 M Na_2SO_4. Working electrode, glassy carbon, auxiliary electrode, platinum wire and reference electrode, Ag/AgCl. Scan rate 10 $mV.s^{-1}$.

The difference between the first two redox processes has also been calculated in the available pH range. For the $(\alpha_1\text{-}P_2W_{17}O_{61})^{10-}$ ligand this gap remains an almost constant + 260 mV. For $(\alpha_2\text{-}P_2W_{17}O_{61})^{10-}$ however, a slight closing of the gap with an increase in pH is observed (from + 276 mV at pH = 0 to + 219 mV at pH =3). At pH

values above 3 the reduction of the second W wave occurs outside the electrochemical window of this experiment.

Figure 2.21 shows a plot of the first reduction potentials for $(\alpha_1\text{-}P_2W_{17}O_{61})^{10-}$ and $(\alpha_2\text{-}P_2W_{17}O_{61})^{10-}$ as a function of pH. Under all available pH conditions the second reduction in the $(\alpha_1\text{-}P_2W_{17}O_{61})^{10-}$ ligand always occurs at a more negative potential (by -41 mV on average) than the corresponding reduction in the $(\alpha_2\text{-}P_2W_{17}O_{61})^{10-}$ ligand. This reduction is thus easier to achieve in the slightly more acidic $(\alpha_2\text{-}P_2W_{17}O_{61})^{10-}$ ligand under these conditions. At pH values above 3 the redox processes associated with this reduction occur at values outside the electrochemical window of this experiment.

For the first reduction however, the shift toward more negative potentials (with increasing pH) is clearly more pronounced in the $(\alpha_2\text{-}P_2W_{17}O_{61})^{10-}$ ligand than in the $(\alpha_1\text{-}P_2W_{17}O_{61})^{10-}$. This phenomenon results in a convergence of the first tungsten reduction observed for α_1 and α_2 at pH = 3, and then a crossing over of the waves. This ultimately gives rise to a switch in the ease with which this reduction is achieved for these ligands. Table 2.5 summarizes the differences in reduction potentials for this process. At pH values of 0 and 1 the first W reduction waves for $(\alpha_1\text{-}P_2W_{17}O_{61})^{10-}$ occur at more negative values than those for $(\alpha_2\text{-}P_2W_{17}O_{61})^{10-}$; by - 56 mV and - 31 mV respectively. At pH = 3 these reduction waves are similar (+ 5 mV difference) and at pH values of 5 and 7 the first W reduction of the $(\alpha_1\text{-}P_2W_{17}O_{61})^{10-}$ ligand occurs at a more positive potential than that of the $(\alpha_2\text{-}P_2W_{17}O_{61})^{10-}$ ligand; by + 42 mV and + 252 mV respectively.

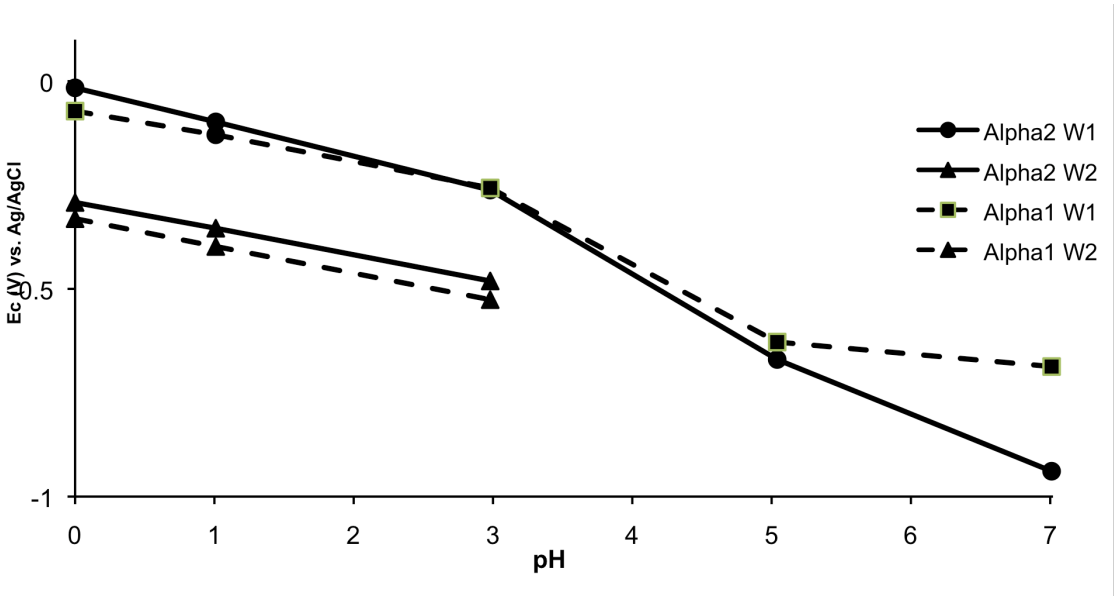

Figure 2.21 Reduction potentials of α_1-$[P_2W_{17}O_{61}]^{10-}$ and α_2-$[P_2W_{17}O_{61}]^{10-}$ as a function of pH.

E_{c1} (mV)	pH = 0	pH = 1	pH = 3	pH = 5	pH = 7
α_1- $P_2W_{17}O_{61}^{10-}$	-72	-129	-257	-682	-687
α_2- $P_2W_{17}O_{61}^{10-}$	-16	-98	-262	-670	-939
$\Delta(\alpha_1-\alpha_2)$	-56	-31	+5	+42	+252

Table 2.5. Reduction potentials for the first reduction process in the α_1-$[P_2W_{17}O_{61}]^{10-}$ and α_2-$[P_2W_{17}O_{61}]^{10-}$ Wells Dawson POMs.

These results indicate that (under the given set of experimental conditions) at pH values below 3 the α_2 ligand is more easily reduced than the α_1 ligand, while at pH values of 3 and above, the reduction of the α_1 ligand is more easily achieved than the corresponding reduction for the α_2 ligand.

2.3.6.2 $K_{7-n}H_n[Tc^{V}O(\alpha_1P_2W_{17}O_{61})]$

Figures 2.22, 2.23 and 2.24 show the CV data for the $K_{7-n}H_n[Tc^{V}O(\alpha_1P_2W_{17}O_{61})]$ compound at pH values 0 through 8. These CVs show the characteristic $(\alpha_1\text{-}P_2W_{17}O_{61})^{10-}$ Wells-Dawson W redox couples in the negative potential region, as well as two well-resolved (reversible) redox processes at more positive potentials. Based on a comparison to the free $(\alpha_1\text{-}P_2W_{17}O_{61})^{10-}$ ligand, these couples are attributed to the two one-electron Tc^{V}/Tc^{IV} and Tc^{V}/Tc^{VI} redox processes. Despite changes in pH the complete reversibility of both Tc waves is seen to persist, thereby speaking to the fundamental stability of the compound in both highly acidic and slightly basic media. CV data showing a comparison between the free ligand and the $K_{7-n}H_n[Tc^{V}O(\alpha_1P_2W_{17}O_{61})]$ complex can be found in the appendix.

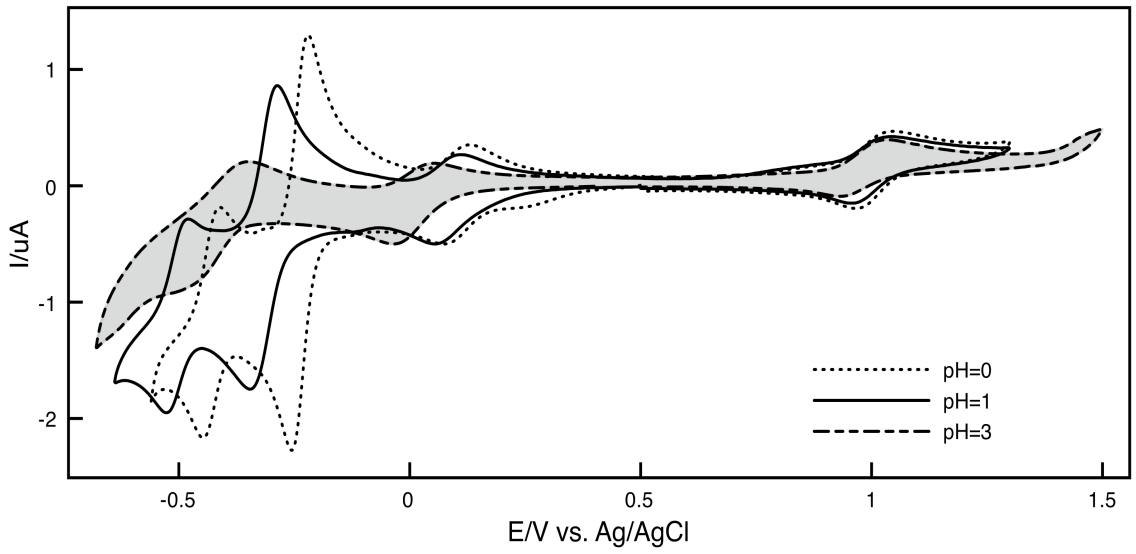

Figure 2.22 CV data of $K_{7-n}H_n[Tc^{V}O(\alpha_1P_2W_{17}O_{61})]$ as a function of pH (pH values = 0, 1, 3). Electrolyte, 0.5 M Na_2SO_4. Working electrode, glassy carbon, auxiliary electrode, platinum wire and reference electrode, Ag/AgCl. Scan rate 10 mV/s.

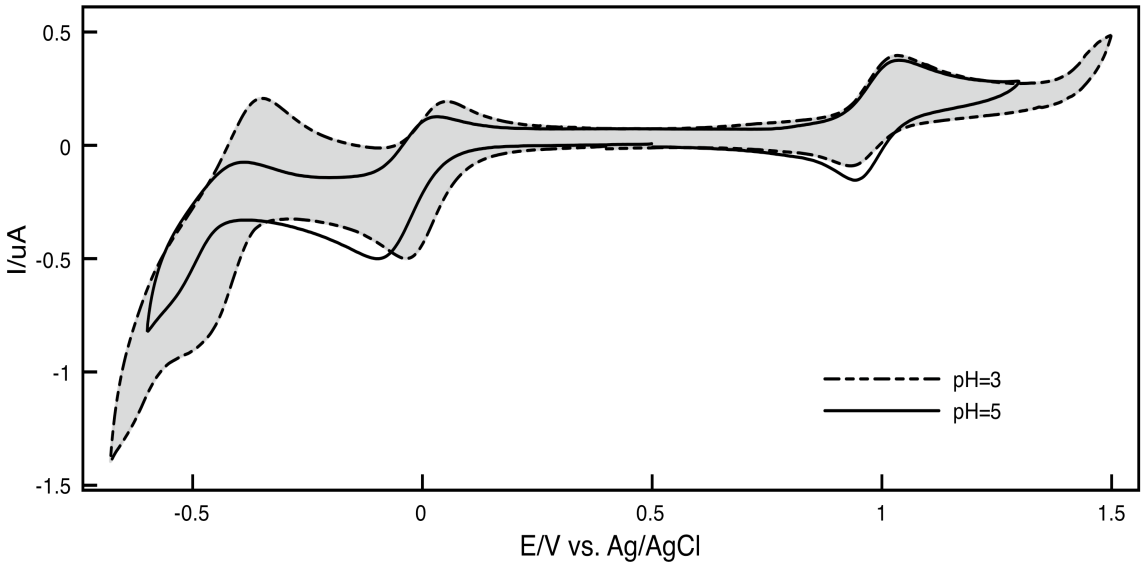

Figure 2.23 CV data of $K_{7-n}H_n[Tc^{V}O(\alpha_1P_2W_{17}O_{61})]$ as a function of pH (pH values = 3, 5). Electrolyte, 0.5 M Na_2SO_4. Working electrode, glassy carbon, auxiliary electrode, platinum wire and reference electrode, Ag/AgCl. Scan rate 10 mV/s.

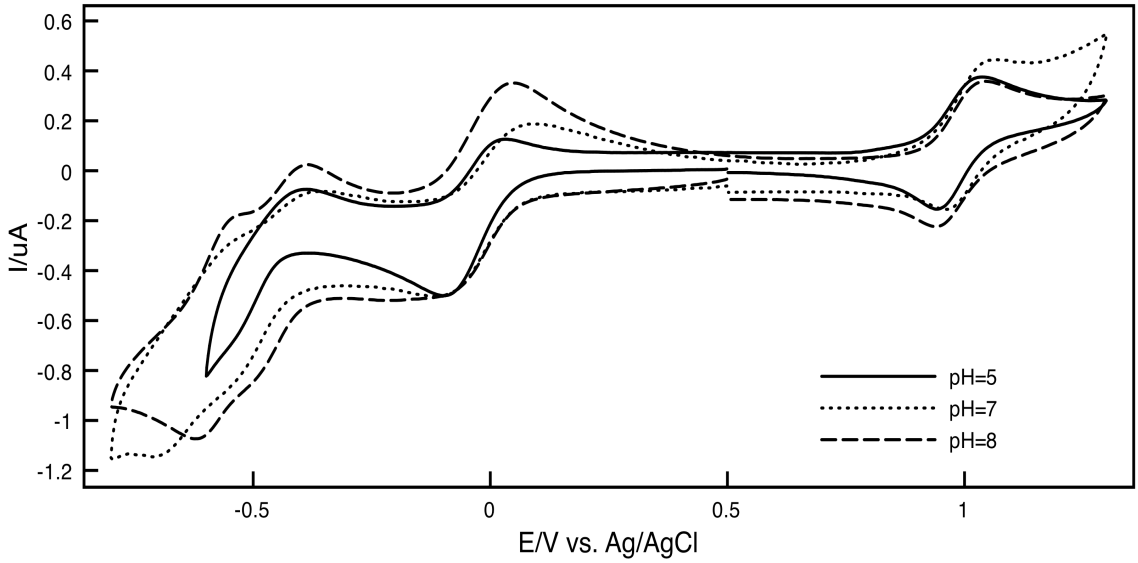

Figure 2.24 CV data of $K_{7-n}H_n[Tc^{V}O(\alpha_1P_2W_{17}O_{61})]$ as a function of pH (pH values = 5, 7, 8). Electrolyte, 0.5 M Na_2SO_4. Working electrode, glassy carbon, auxiliary electrode, platinum wire and reference electrode, Ag/AgCl. Scan rate 10 mV/s.

Half-wave potentials ($E_{1/2}$, where $E_{1/2} = (E_c + E_a)/2$) for all redox processes have been summarized in Table 2.6, and Figure 2.25 shows a plot of half wave potentials as a function of pH. There is a general shift of all redox couples present in the negative potential region toward more negative potential values as the pH increases, i.e., both the Tc^{V}/Tc^{IV} redox process as well as those waves attributed to the W framework of the POM are observed to move toward more negative potentials with increasing pH values. Specifically, the redox couples of the tungsten framework are observed to shift from $E_{1/2}$ = -139 mV at pH = 0 to $E_{1/2}$ = -490 mV at pH = 3, while at pH values above 3 they move out of the available electrochemical window and become largely undefined.

pH	W (1st wave) $E_{1/2}$ (mV)	$Tc^{5/4}$ $E_{1/2}$ (mV)	$Tc^{5/6}$ $E_{1/2}$ (mV)
0	-139	102	1006
1	-315	85	998
3	-424	6	984
5	(-493)[a]	-32	990
7	(-472)[a]	-14	1013
8	(-490)[a]	-25	993

Table 2.6. Half wave peak potentials for the Tc^{V} substituted into the α_1-$[P_2W_{17}O_{61}]^{10-}$ Wells-Dawson POM. At pH values of 0 through 8. Scan rate 10 $mV.s^{-1}$. $E_{1/2} = (E_c + E_a)/2$

[a] Estimated values based on the de-convolution of the raw CV data.

The half-wave potentials for the Tc^{V}/Tc^{IV} redox process change from $E_{1/2}$ = +102 mV at pH = 0 to $E_{1/2}$ = -32 mV at pH = 5 (see Table 2.5). At pH values above 5 the Tc^{V}/Tc^{IV} redox couple is found to be largely insensitive to changes in pH (at an average $E_{1/2}$ = -20 mV), and becomes less defined as the reduction wave begins to flatten. The corresponding reoxidation wave however, remains unaffected. The redox waves assigned

to the Tc^{V}/Tc^{VI} process (centered around $E_{1/2}$ = + 1000 mV) are observed to remain consistently impervious to changes in pH. The general shift observed for the Tc^{V}/Tc^{IV} reduction couples toward more negative reduction potentials with increasing pH means that the reduction of Tc(V) to Tc(IV) in the α_1- vacancy is more easily achieved in an acidic medium. The ease of reduction at low pH can be attributed to an increase in the number of protons. The protons may in turn aid in the transfer of electrons to the Tc center, possibly by stabilizing the $Tc\text{-}O^{-}$ ion that forms upon reduction.

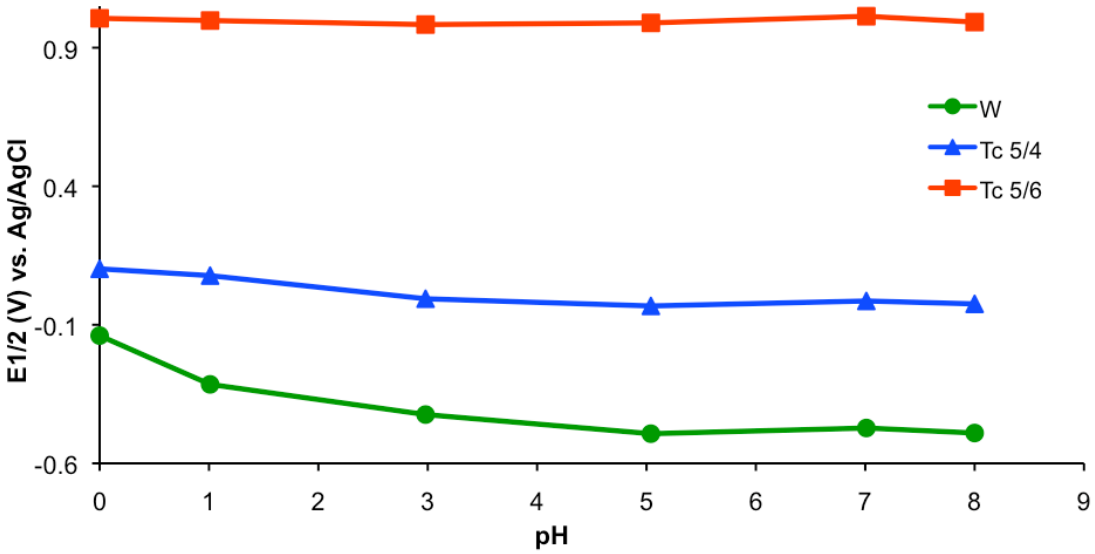

Figure 2.25. Reduction potentials of 10^{-3} M α_1-$[Tc^{V}OP_2W_{17}O_{61}]^{5-}$ as a function of pH.

2.3.6.3 $K_{7-n}H_n[Tc^{V}O(\alpha_2P_2W_{17}O_{61})]$

Figures 2.26, 2.27 and 2.28 show the CV data for the $K_{7-n}H_n[Tc^{V}O(\alpha_2P_2W_{17}O_{61})]$ compound at pH values 0 through 8. These CVs once again show the characteristic (α_2-$P_2W_{17}O_{61})^{10-}$ Wells-Dawson W redox couples in the negative potential region as well as a

single well resolved reversible redox processes at positive potential. This reversible wave centered at $E_{1/2}$ = +800 mV is accredited to the 1 electron Tc^{V}/Tc^{VI} redox process. In the negative potential region however, we now see two reversible redox couples that occur at a more positive potentials than those of the W framework. By comparison to the free $(\alpha_2\text{-}P_2W_{17}O_{61})^{10-}$ ligand, these couples have been attributed to the 2 successive one-electron Tc^{V}/Tc^{IV} and Tc^{IV}/Tc^{III} redox processes. While these waves are difficult to discern under highly acidic conditions, they become better resolved as the pH is increased. CV data showing a comparison between the free ligand and the $K_{7-n}H_n[Tc^{V}O(\alpha_2P_2W_{17}O_{61})]$ complex can be found in the appendix.

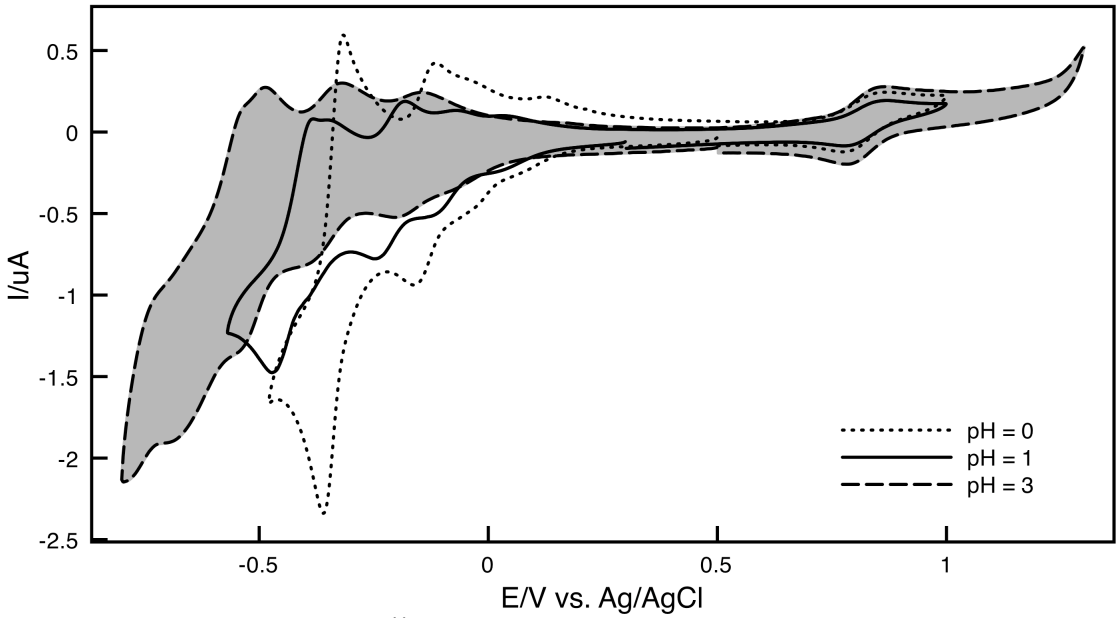

Figure 2.26 CV data of $K_{7-n}H_n[Tc^{V}O(\alpha_2P_2W_{17}O_{61})]$ as a function of pH (pH values = 0, 1, 3). Electrolyte, 0.5 M Na_2SO_4. Working electrode, glassy carbon, auxiliary electrode, platinum wire and reference electrode, Ag/AgCl. Scan rate 10 mV/s.

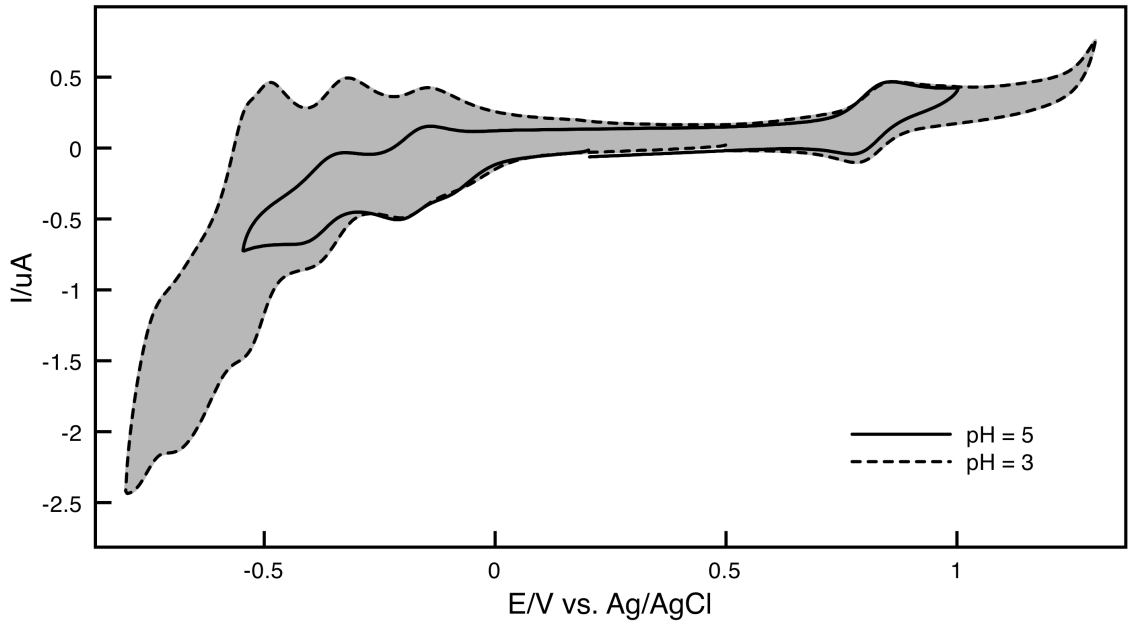

Figure 2.27 CV data of $K_{7-n}H_n[Tc^{V}O(\alpha_1P_2W_{17}O_{61})]$ as a function of pH (pH values = 3, 5). Electrolyte, 0.5 M Na_2SO_4. Working electrode, glassy carbon, auxiliary electrode, platinum wire and reference electrode, Ag/AgCl. Scan rate 10 mV/s.

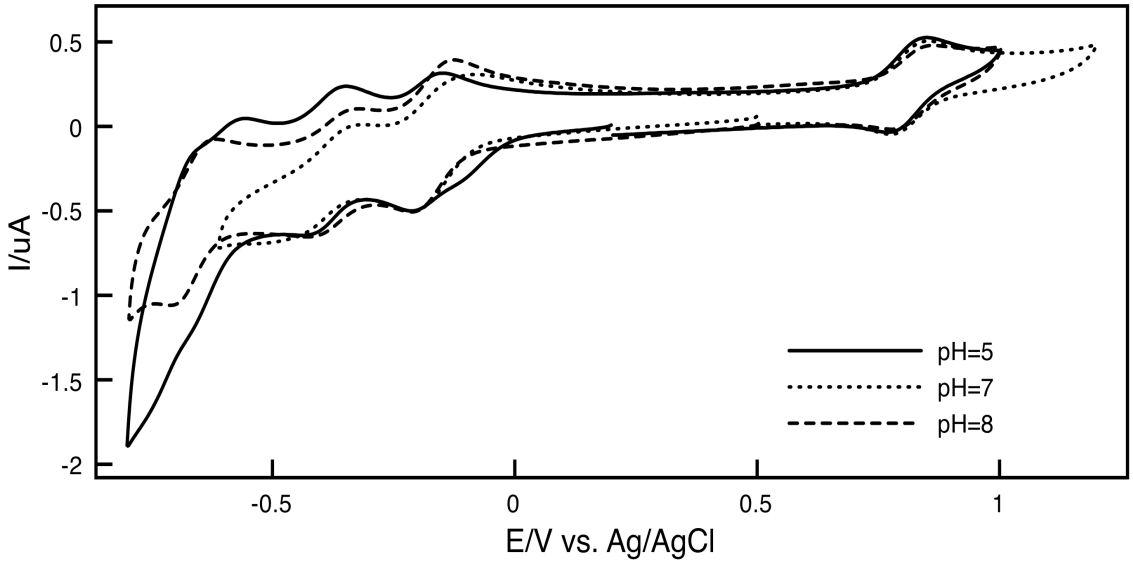

Figure 2.28 CV data of $K_{7-n}H_n[Tc^{V}O(\alpha_2P_2W_{17}O_{61})]$ as a function of pH (pH values = 5, 7, 8). Electrolyte, 0.5 M Na_2SO_4. Working electrode, glassy carbon, auxiliary electrode, platinum wire and reference electrode, Ag/AgCl. Scan rate 10 mV/s.

Half-wave potentials for $K_{7-n}H_n[Tc^{V}O(\alpha_2P_2W_{17}O_{61})]$ have been summarized in Table 2.7. Once again, both the reduction and oxidation waves for the Tc^{V}/Tc^{VI} couple ($E_{1/2}$ = +800 mV) remain largely unaffected by changes in pH, while the redox couples in the negative potential region show a general shift toward more negative potential values with increasing pH. The redox couples of the tungsten framework are observed to move from $E_{1/2}$ = -339 mV at pH = 0 to $E_{1/2}$ = -521 mV at pH = 3, while at pH values above 3 they occur outside the available electrochemical window and become indeterminate. For the Tc^{V}/Tc^{IV} and Tc^{IV}/Tc^{III} couples, there is a change from $E_{1/2}$ = -37 mV and -135 mV at pH = 0 to $E_{1/2}$ = -165 mV and -359 mV at pH = 3 respectively. At pH values of 3 and above for the Tc^{V}/Tc^{IV} and 5 and above for the Tc^{IV}/Tc^{III} these couples becomes largely insensitive to changes in pH.

pH	W (1st wave) $E_{1/2}$ (mV)	$Tc^{4/3}$ $E_{1/2}$ (mV)	$Tc^{5/4}$ $E_{1/2}$ (mV)	$Tc^{5/6}$ $E_{1/2}$ (mV)
0	-339	-135	(-37)[a]	+822
1	-427	-212	(-93)[a]	+823
3	-521	-359	-165	+821
5	-	-393	-178	+809
7	-	-411	-164	+814
8	-	-397	-167	+811

Table 2.7. Half wave peak potentials for the Tc^{V} substituted into the α_2-$[P_2W_{17}O_{61}]^{10-}$ Wells-Dawson POM at pH values of 0 through 8. Scan rate 10 $mV.s^{-1}$.

[a] Estimated values based on the de-convolution of the raw CV data.

Because the Tc^{V}/Tc^{IV} redox couple shoulders that of the Tc^{IV}/Tc^{III} under acidic conditions, the reduction potentials for the Tc^{V}/Tc^{IV} couple at pH values of 0 and 1 were calculated from a de-convolution of the original CV data. This data can be found in the

appendix. At pH values of 3 and above the redox processes for the Tc^{V}/Tc^{IV} and Tc^{IV}/Tc^{III} become more defined as 2 distinct and separate 1 electron processes. Figure 2.29 shows a plot of the half-wave potentials as a function of pH and better illustrates the increased splitting between the Tc^{V}/Tc^{IV} and Tc^{IV}/Tc^{III} redox couples with increasing pH. This general trend of more negative reduction potentials with increasing pH for the Tc metal center within the $(\alpha_2\text{-}P_2W_{17}O_{61})^{10-}$ ligand means that the reduction of Tc in the α_2-vacancy is more easily achieved in an acidic medium, with the $Tc^{IV/III}$ couple showing a greater sensitivity toward changes in pH than the $Tc^{V/IV}$ couple. The ease of reduction at low pH may once again be attributed to an increase in the number of protons in an acidic medium, which may in turn aid in the transfer of electrons to the Tc center.

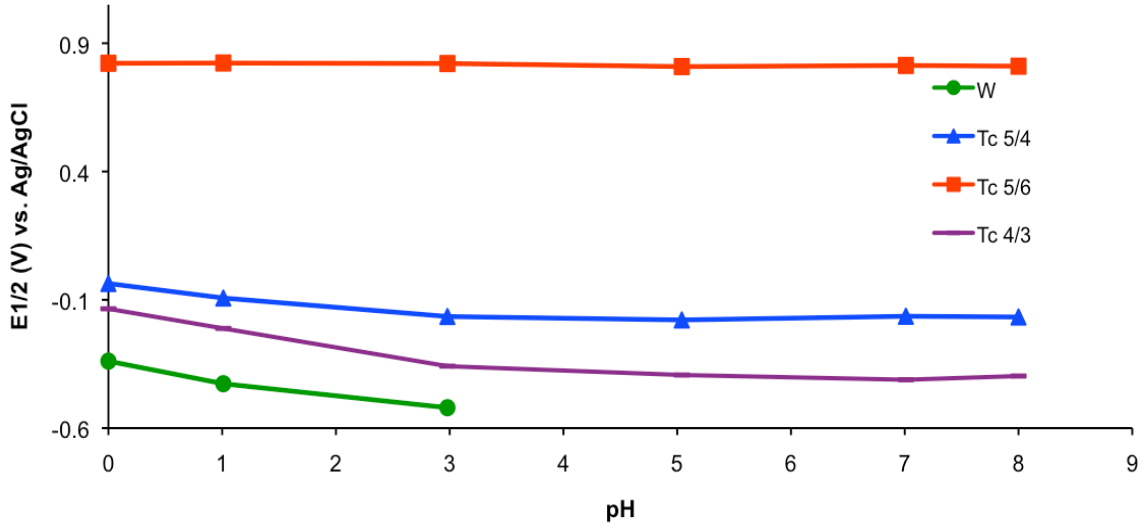

Figure 2.29. Reduction potentials of 10^{-3} M α_2-$[Tc^{V}OP_2W_{17}O_{61}]^{5-}$ as a function of pH.

This behavior (both the movement of the reduction potentials with pH as well as the increased splitting in the $Tc^{IV/III}$ and $Tc^{V/IV}$ couples) corroborates work done in our lab

by Dr. Israel Mbomekalle with rhenium substituted into the α_2-$[P_2W_{17}O_{61}]^{10-}$ POM (Figure 2.30), as well as what has been found in the literature. Ortega *et. al.,* for example, have observed a similar trend for $[SiW_{11}ReO_{40}]^{5-}$ POM. In both cases the metal substitued into the lacunry POM showed a shift in reduction potentials for both the V/IV and IV/III redx processes toward more negative values with increasing pH.

In the case of the Rhenium-substituted α_2-$[P_2W_{17}O_{61}]^{10-}$ POM, under highly acidic conditions the V/IV and IV/III couples are completely eclipsed and exhibit a single two-electron redox process rather than two successive one-electron processes. Above pH 1 however, this single two-electron process splits into two well defined single-electron reductions.

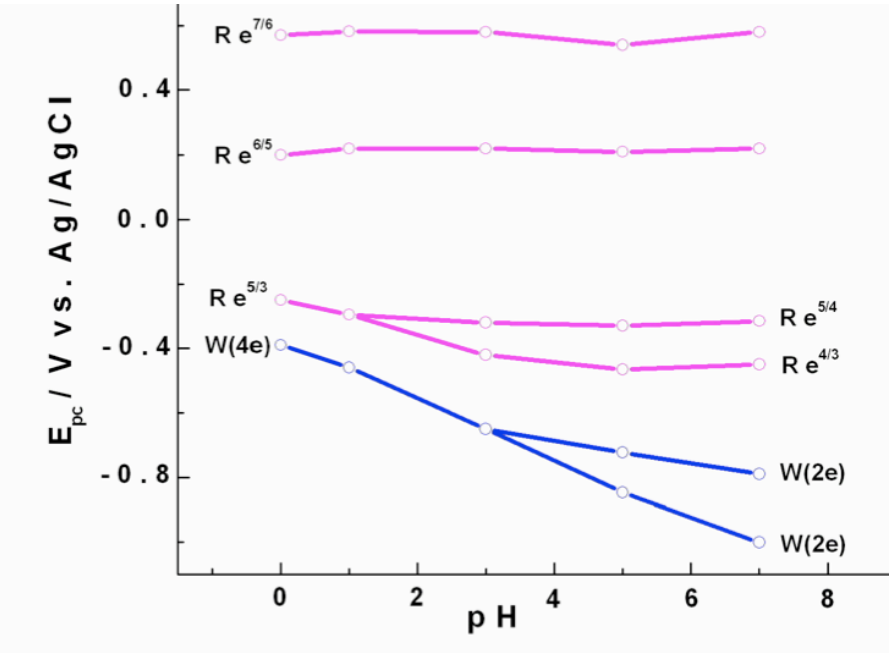

Figure 2.30. Reduction potentials of 10^{-3} M α_2-$[Re^{V}OP_2W_{17}O_{61}]^{5-}$ as a function of pH. The $Re^{VII/VI}$ and $Re^{VI/V}$ waves remain relatively unchanged with changing pH. The $Re^{V/III}$ wave splits into two waves: $Re^{V/IV}$ and $Re^{IV/III}$ at pH values of 3 and above. The $4e^-$ W reduction splits into two $2e^-$ processes at pH values of 5 and above.
Graph courtesy of Dr. Israel Mbomekalle (unpublished results).

2.3.6.4 $K_{7-n}H_n[Tc^VO(\alpha_1P_2W_{17}O_{61})]$ and $K_{7-n}H_n[Tc^VO(\alpha_2P_2W_{17}O_{61})]$ comparison

Table 2.8 shows a comparison of the $Tc^{V/IV}$ reduction in the $K_{7-n}H_n[Tc^VO(\alpha_1P_2W_{17}O_{61})]$ and $K_{7-n}H_n[Tc^VO(\alpha_2P_2W_{17}O_{61})]$ compounds. At all pH values (0 through 8) the $Tc^{V/IV}$ redox couple occurs at a more positive potential of ~150 mV. This means that irrespective of protonation effects, Tc in the α_1-$[P_2W_{17}O_{61}]^{10-}$ vacancy is always more easily reduced than the Tc in the α_2-$[P_2W_{17}O_{61}]^{10-}$ vacancy.

$E_{1/2}$ (mV)	pH = 0	pH = 1	pH = 3	pH = 5	pH = 7	pH = 8
α_1-$[Tc^VOP_2W_{17}O_{61}]^{5-}$	+102	+81	+6	-32	-14	-25
α_2-$[Tc^VOP_2W_{17}O_{61}]^{5-}$	-37	-93	-165	-178	-164	-167
$\Delta(\alpha_1-\alpha_2)$	+139	+174	+159	+146	+141	+142

Table 2.8 Comparison of the half wave peak potentials for the $Tc^{V/IV}$ reduction in $K_{7-n}H_n[Tc^VO(\alpha_1P_2W_{17}O_{61})]$ and $K_{7-n}H_n[Tc^VO(\alpha_2P_2W_{17}O_{61})]$ at pH values of 0 through 8. Scan rate 10 $mV.s^{-1}$.

This phenomenon is explained by the delocalization of electrons added to the Wells-Dawson anion, (Figure 2.14), where these electrons are mostly delocalized over only the 12 equatorial tungsten atoms located in the belt (α_1) site.[28, 35-38] This means that the first reduction in a Wells-Dawson anion always takes place at the equatorial position[30, 36, 37, 40] and transition metals substituted into the belt (α_1) position will be more readily reduced than those substituted in the cap (α_2).[29, 30, 33, 34, 37]

Table 2.9 shows the Free Energy (ΔG) associated with the $Tc^{V/IV}$ reduction reaction for the α_1-$[Tc^{V}OP_2W_{17}O_{61}]^{5-}$ and α_2-$[Tc^{V}OP_2W_{17}O_{61}]^{5-}$ complexes.

$$Tc^{V} + 1e^{-} \longrightarrow Tc^{IV}$$

ΔG is calculated as ΔG = -nFE, where n = the charge per 1 electron, F = 96 500 C/mol and E is the potential for the $Tc^{V/IV}$ reduction reaction, E_c in V (E_c and E_a values corresponding to the $Tc^{V/IV}$ redox couple for both α_1-$[Tc^{V}OP_2W_{17}O_{61}]^{5-}$ and α_2-$[Tc^{V}OP_2W_{17}O_{61}]^{5-}$ can be found in the appendix).

There is an observable increase in the free energy associated with the $Tc^{V/IV}$ reduction with increasing pH until a pH value of 5 for both α_1-$[Tc^{V}OP_2W_{17}O_{61}]^{5-}$ and α_2-$[Tc^{V}OP_2W_{17}O_{61}]^{5-}$. At higher pH values the free energy associated with this transition stabilizes at an average of 9.7 kJ for the α_1-$[Tc^{V}OP_2W_{17}O_{61}]^{5-}$ complex and 20 kJ for the α_2-$[Tc^{V}OP_2W_{17}O_{61}]^{5-}$ complex. These free energy values remain constant from pH 5 to pH 8. This would imply a difference in the behavior of the complexes under acidic conditions, where protonation events may aid in the reduction of the Tc metal, as compared to more basic conditions.

pH	α_1-$[Tc^{V}OP_2W_{17}O_{61}]^{5-}$ ΔG (kJ)	α_2-$[Tc^{V}OP_2W_{17}O_{61}]^{5-}$ ΔG (kJ)	$\Delta G(\alpha_2 - \alpha_1)$ (kJ)
0	-7.1	4.15	11.2
1	-5.6	11.4	17
3	6.3	18.8	12.5
5	9.5	20.7	10.8
7	10	20.4	10.4
8	9.4	20.5	11.1

Table 2.9 Free Energy values for the $Tc^{V/IV}$ transition in the α_1-$[Tc^{V}OP_2W_{17}O_{61}]^{5-}$ and α_2-$[Tc^{V}OP_2W_{17}O_{61}]^{5-}$ complexes.

Because this free energy is associated with the spontenaity of a reduction reaction to occur, the increasingly positive free energy with increasing pH corroborates the assertion that the $Tc^{V/IV}$ reduction is easier to achieve in an acidic medium; i. e. the addition of an electron to Tc(V) for its subsequent reduction to Tc(IV) is more favorable under acidic conditions. Clearly the free energy requirement associated with the reduction of Tc in the α_2-$[Tc^{V}OP_2W_{17}O_{61}]^{5-}$ complex is greater than in the α_1-$[Tc^{V}OP_2W_{17}O_{61}]^{5-}$ (by an average of 12.2 kJ), once again corroborating the ease of reduction observed for transition metals substituted into the α_1 POM vacancy.

Tabulated values of the HOMO-LUMO energy gap for the α_1-$[Tc^{V}OP_2W_{17}O_{61}]^{5-}$ and α_2-$[Tc^{V}OP_2W_{17}O_{61}]^{5-}$ compounds can be found in table 2.10. The HOMO-LUMO energy gap can be extracted from electrochemical data by calculating the difference between the half-wave peak potentials of the HOMO (defined to be the couple that exists in the oxidative potential region of the CV) and the LUMO (defined to be the first redox couple to exist in the reductive potential region of the CV). This energy gap is calculated in electronvolts (eV). According to the CV data, these orbital assignments for both the α_1-$[Tc^{V}OP_2W_{17}O_{61}]^{5-}$ and α_2-$[Tc^{V}OP_2W_{17}O_{61}]^{5-}$ complexes are the $Tc^{5/6}$ and $Tc^{5/4}$ couples.

There is a noteworthy increase in the size of this energy gap with increasing pH; up to and including pH = 5 for α_1-$[Tc^{V}OP_2W_{17}O_{61}]^{5-}$) and pH = 3 for α_2-$[Tc^{V}OP_2W_{17}O_{61}]^{5-}$. At higher pH values the size of this energy gap remains unchanged. This phenomenon substantiates the earlier claim that the reduction of Tc becomes more difficult until a certain pH value is reached, at which point protonation effects become negligible. This would further imply that the α_1-$[Tc^{V}OP_2W_{17}O_{61}]^{5-}$ and α_2-$[Tc^{V}OP_2W_{17}O_{61}]^{5-}$ complexes behave slightly differently under acidic and basic

conditions. This can be attributed to the different solvent environments which likely lead to the formation of protonated species under acidic conditions. This experimental observation is consistent with DFT calculations by Joseph Poblet where the reduction energy (RE) for the protonated HTc^{V}/HTc^{IV} reduction reactions are at greater negative ΔG values than the unprotonated Tc^{V}/Tc^{IV} reduction reactions.

pH	α_1-$[Tc^{V}OP_2W_{17}O_{61}]^{5-}$ HOMO-LUMO Gap (eV)	α_2-$[Tc^{V}OP_2W_{17}O_{61}]^{5}$ HOMO-LUMO Gap (eV)	Δ ($\alpha_1 - \alpha_2$) (eV)
0	0.898	0.853	0.045
1	0.911	0.910	0.0015
3	0.968	0.988	0.02
5	1.015	0.971	0.034
7	1.021	0.971	0.05
8	1.011	0.972	0.04

Table 2.10 HOMO-LUMO energy Gap values for α_1-$[Tc^{V}OP_2W_{17}O_{61}]^{5-}$ and α_2-$[Tc^{V}OP_2W_{17}O_{61}]^{5-}$.

A comparison between the α_1 and α_2 isomeric forms of the $[Tc^{V}OP_2W_{17}O_{61}]^{5-}$ complex reveals that the HOMO-LUMO energy gap is consistently larger in α_1-$[Tc^{V}OP_2W_{17}O_{61}]^{5-}$ than in the α_2-$[Tc^{V}OP_2W_{17}O_{61}]^{5-}$. Although this feels counter-intuitive, it might be explained by examining the HOMO-LUMO energy transitions for these molecules. Poblet and co., for example, have (by extensive DFT calculations) characterized the energy transitions for Tc^{VII} substituted into the lacunary Wells-Dawson POMS. Their calculations reveal that the HOMO in both the α_1 and α_2 isomers is always the Tc d_{xy} orbital and that this orbital lies at a slightly higher energy in the α_2 POM. Further, they have shown that while an electron excited in the α_1 isomer undergoes an exclusively Tc to Tc transition (from the Tc d_{xy} ground state orbital to the Tc=O π^*

orbital), in the α_2 isomer there is a rearrangement of the orbital energy levels and the W d_{xy} orbital drops to a lower energy than that of the Tc=O π^*. This rearrangement, coupled to the ground state energies of the Tc d_{xy} orbital in the α_1 and α_2 POMs, results in a smaller HOMO-LUMO energy gap for the α_2 isomer. It is feasible then that a similar situation mmight exist for Tc(V) substituted into the lacunary Wells-Dawson POMs. a similar effect α_2-$[Tc^{V}OP_2W_{17}O_{61}]^{5-}$.

2.4 Conclusions

$Tc^{V}O$ complexes of the α_1-$[P_2W_{17}O_{61}]^{10-}$ and α_2-$[P_2W_{17}O_{61}]^{10-}$ lacunary Wells-Dawson polyoxometalates have successfully been synthesized as aqueous soluble K salts. The syntheses rely on the use of ethylene glycol as a "transfer ligand" to facilitiate the stabilization of the $Tc^{V}O$ core as the complexes are formed. The complexes have been characterized by IR, multinuclear NMR spectroscopy and electrochemical methods. The combination of these characterization techniques provides definitive evidence that the ^{99}Tc has been incorporated into the vacancy of the α_1 and α_2 frameworks in the +5 oxidation state.

We find that, in aqueous solution, Tc^{V} is reduced more readily in the lacunary α_1-site as compared to the α_2-site, and that this reduction is favorable under acidic conditions. Free Energy and HOMO-LUMO energy gap calculations match well with theoretical DFT calculations and corroborate this assertion.

2.5 References

1. Zhang, C.; Howell, R. C.; Luo, Q.; Fieselmann, H. L.; Todaro, L.; Francesconi, L. C., *Inorg. Chem.* **2005,** *44*, 3569-3578.

2. Boglio, C.; Lenoble, G.; Duhayon, C.; Hasenknopf, B.; Thouvenot, R.; Zhang, C.; Howell, R.; Burton-Pye, B. P.; Francesconi, L. C.; Lacote, E.; Thorimbert, S.; Malacria, M.; Afonso, C.; Tabet, J.-C., *Inorg Chem* **2006,** *45* (3), 1389-1398.

3. Davison, A.; Trop, H.; DePamphilis, B.; Jones, A., *Inorganic Synthesis* **1982,** *21*, 160.

4. Ciabrini, J.-P.; Contant, R., *J. Chem. Research (S) 1993, 391* **1993**, 2720-2744.

5. Contant, R., *Inorg. Synth.* **1990,** *27*, 71-111.

6. Bartis, J.; Dankova, M.; Blumenstein, M.; Francesconi, L. C., *Journal of Alloys and Compunds* **1997,** *249*, 56-68.

7. Keita, B.; Girard, F.; Nadjo, L.; Contant, R.; Belghiche, R.; Abessi, M., *J. Electroanal. Chem.* **2001,** *508* (1-2), 70-80.

8. Contant, R.; Ciabrini, J.-P., *J. Chem. Res. (S) 1977, 222* **1977,** *M*, 2601-2617.

9. Contant, R.; Ciabrini, J.-P., *J. Chem. Research (S) 1982, 50-51* **1982,** *1982*, 641-660.

10. Davison, A.; DePamphilis, B. V.; Jones, A. G.; Franklin, K. L.; Lock, C. J. L., *Inorg. Chim. Acta* **1987,** *128* (2), 161-167.

11. Venturelli, A.; Nilges, M. J.; Smirnov, A.; Belford, R. L.; Francesconi, L. C., *J. Chem. Soc., Dalton Trans.* **1999**, 301-310.

12. Ortega, F.; Pope, M. T., *Inorg. Chem.* **1984,** *23*, 3292-3297.

13. Finke, R. G.; Rapko, B.; Saxton, R. J.; Domaille, P. J., *J. Am. Chem. Soc.* **1986,** *108*, 2947-2960.

14. Finke, R. G.; Droege, M. W.; Domaille, P. J., *Inorg. Chem.* **1987,** *26*, 3886-3896.

15. Finke, R. G.; Lyon, D. K.; Nomiya, K.; Sur, S.; Mizuno, N., *Inorg. Chem.* **1990,** *29* (10), 1784-1787.

16. Bartis, J.; Kunina, Y.; Blumenstein, M.; Francesconi, L. C., *Inorg. Chem.* **1996,** *35* (5), 1497-1501.

17. Jorris, T. L.; Kozik, M.; Casan-Pastor, N.; Domaille, P. J.; Finke, R. G.; Miller, W. K.; Baker, L. C. W., *J. Am. Chem. Soc.* **1987,** *109*, 7402-7408.

18. Sadakane, M.; Dickman, M. H.; Pope, M. T., *Inorg. Chem.* **2001,** *40* (12), 2715-2719.

19. Sadakane, M.; Ostuni, A.; Pope, M. T., *J. Chem. Soc. Dalton Trans.* **2002**, 63-67.

20. Zhang, C.; Howell, R. C.; Fieselmann, H. L.; Todaro, L.; Francesconi, L. C., *Inorg. Chem.* **2005,** *44*, 3569-3578.

21. Boglio, C.; Lenoble, G.; Duhayon, C.; Hasenknopf, B.; Thouvenot, R.; Zhang, C.; Howell, R. C.; Burton-Pye, B. P.; Francesconi, L. C.; Lacote, E.; Thorimbert, S.; Malacria, M.; Afonso, C.; Tabet, J.-C., *Inorg. Chem.* **2006,** *45* (3), 1389-1398.

22. Bartis, J.; Sukal, s.; Dankova, M.; Kraft, E.; Kronzon, R.; Blumenstein, M.; Francesconi, L. C., *J. Chem. Soc., Dalton Trans* **1997**, 1937-1944.

23. Bartis, J.; Dankova, M.; Lessmann, J. J.; Luo, Q.-H.; Horrocks, W. D., Jr.; Francesconi, L. C., *Inorganic Chemistry* **1999,** *38*, 1042-1053.

24. Salmonte, J. L.; Pope, M. T., *Canadian Journal of Chemistry* **2001,** *79* (5/6), 802-808.

25. Howell, R. C.; Perez, F. G.; Jain, S.; Horrocks, W. D., Jr.; Rheingold, A. L.; Francesconi, L. C., *Angew. Chem. Int. Ed.* **2001,** *40*, 4301-4304.

26. Zhang, C.; Howell, R.; Scotland, K. B.; Perez, F. G.; Todaro, L.; Francesconi, L. C., *Inorg Chem* **2004,** *43*, 7691-7701.

27. Zhang, C.; Bensaid, L.; McGregor, D.; Fang, X.; Howell, R. C.; Burton-Pye, B.; Luo, Q.; Todaro, L.; Francesconi, L. C., *J. Cluster Sci.* **2006,** *17*, 389-426.

28. Acerete, R.; Hammer, C. F.; Baker, L. C. W., *Journ. Amer. Chem. Soc.* **1982,** *104*, 5384-5390.

29. Keita, B.; Girard, F.; Nadjo, L.; Contant, R.; Canny, J.; Richet, M., *Journ. of Electroanal. Chem.* **1999,** *478*, 76-82.

30. Contant, R.; Richet, M.; Lu, Y. W.; Keita, B.; Nadjo, L., *Eur. J. Inorg. Chem.* **2002**, 2587-2593.

31. Keita, B.; Levy, B.; Nadjo, L.; Contant, R., *New. J. Chem.* **2002,** *26*, 1314-1319.

32. Keita, B.; Belhouari, A.; Nadjo, L.; Contant, R., *J. Electroanal. Chem.* **1998,** *442*, 49-57.

33. Contant, R.; Abbessi, M.; Canny, J.; Belhouari, A.; Keita, B.; Nadjo, L., *Inorg. Chem.* **1997,** *36*, 4961-4967.

34. Contant, R.; Herve, G., *Reviews in Inorganic Chemistry* **2002,** *22* (2), 63-111.

35. Keita, B.; Lu, Y. W.; Nadjo, L.; Contant, R., *Electrochemistry Communications* **2000,** *2*, 720-726.

36. Kozik, M.; Baker, L. C. W., *J. Am. Chem. Soc.* **1990,** *112*, 7604-7611.

37. Kozik, M.; Hammer, C. F.; Baker, L. C. W., *J. Am. Chem. Soc.* **1986,** *108*, 2748-2749.

38. Ciabrini, J. P.; Contant, R.; Fruchart, J. M., *Polyhedron* **1983,** *2* (11), 1229-33.

39. Lopez, X.; Bo, C.; Poblet, J. M., *J. Amer. Chem. Soc.* **2002,** *124*, 12574-12582.

40. Lopez, X.; Bo, C.; Poblet, J. M., *J. Am. Chem. Soc.* **2002,** *124*, 12574-12582.

Chapter 3: Organic Soluble ^{99}Tc (V and VI) complexes of the (α_1-$P_2W_{17}O_{61}$)$^{10-}$ and (α_2-$P_2W_{17}O_{61}$)$^{10-}$ Well-Dawson Lacunary POMs.

3.1 Introduction

An understanding of the extensive redox and chemical speciation of technetium is necessary to address issues of separation from radioactive waste streams as well as for development of matrices for immobilization of ^{99}Tc. We have extensively investigated the aqueous speciation of Tc(V) incorporated into the lacunary (α_1-$P_2W_{17}O_{61}$)$^{10-}$ and (α_2-$P_2W_{17}O_{61}$)$^{10-}$ Wells-Dawson isomers (Chapter 2). Here we extend this chemistry into organic solvents. It has been noted in the literature that the organic soluble (tetrabutylammonium (NBu_4)) metal substituted Wells-Dawson POMs ((NBu_4)$_{10-x}H_x$[α_1/α_2-$P_2W_{17}O_{61}$]) are often more stable than their aqueous soluble counterparts.[1] In addition, employment of organic solvents should expand the electrochemical range of the ^{99}Tc complexes. By migrating the chemistry into organic solvents the rich redox chemistry of Tc can be explored in situations where the stability of different oxidation states is more pronounced. Organic solvents allow for an extension of the electrochemical polarization range and as such metal reductions that occur at low potential values (and would be eclipsed by the evolution of hydrogen in aqueous solution) can be observed.

The synthesis and characterization of organic soluble ^{99}Tc complexes of the (α_1-$P_2W_{17}O_{61}$)$^{10-}$ and (α_2-$P_2W_{17}O_{61}$)$^{10-}$ Well-Dawson Lacunary POMs then, allow an opportunity to build upon the chemistry of the aqueous soluble complexes and advance the understanding of the redox and chemical speciation and stability of Tc incorporated into POMs.

3.2 Experimental

3.2.1 General

^{99}Tc is a weak β- emitter with a half-life of 2 x 10^5 years. All reported Tc syntheses were performed in an appropriately equipped lab approved for the use of low-level radioactivity. Correct and suitable radioactive material handling procedures were employed. All materials were purchased as reagent grade and used without further purification. Water was obtained using a Millipore Direct Q5 system (conductivity =18 μΩ). Solid ammonium pertechnetate (NH_4TcO_4) was purchased from Oak Ridge National Laboratory. This NH_4TcO_4 is contaminated with TcO_2 due to radiolytic autoreduction and is black in color. Pure NH_4TcO_4 is a white crystalline solid. To regenerate pure pertechnetate the raw NH_4TcO_4 was dissolved in water and heated with hydrogen peroxide until the volume had decreased by half. The resulting aqueous solution was standardized using a well-established UV-vis protocol. [2] $(NBu_4)TcOCl_4$ was prepared from NH_4TcO_4 according to a published procedure.[2] The organic soluble α_1-$P_2W_{17}O_{61}^{10-}$ and α_2-$P_2W_{17}O_{61}^{10-}$ ligands were prepared as described in the literature.[3-5]

3.2.2. Collection of NMR Data.

NMR data were collected on a JEOL GX-400 spectrometer using 5 or 10 mm NMR tubes fitted with a Teflon insert (purchased from Wilmad Glass). Resonance frequencies are 161.83 MHz for ^{31}P, 16.7 for ^{183}W and 161.83 MHz for ^{99}Tc. Chemical shifts are given with respect to external 85% H_3PO_4 for ^{31}P , 2.0 M Na_2WO_4 for ^{183}W and 2.0 M NH_4TcO_4 for ^{99}Tc.

Typical acquisition parameters for ^{31}P spectra included the following: spectral

width, 10000 Hz; acquisition time, 0.8 s; pulse delay, 1 s; pulse width, 15 μs (50° tip angle). From 200 to 1000 scans were required. For ^{183}W spectra, typical conditions included the following: spectral width, 10000 Hz; acquisition time, 1.6 s; pulse delay, 0.5 s; pulse width, 50 μs (45° tip angle). From 1000 to 30000 scans were acquired. For ^{99}Tc spectra, the acquisition parameters included the following: spectral width, 10000 Hz; acquisition time, 0.9 s; pulse delay, 1 s; pulse width, 50 μs (45° tip angle)

For all spectra, the temperature was controlled to ± 0.2 deg. For the ^{31}P and ^{183}W chemical shifts, the convention used is that the more negative chemical shifts denote more upfield resonances.

3.2.3 Collection of Electrochemical Data.

Electrochemical data were obtained using a BAS Voltammetric Analyzer System controlled by BAS CV-50W software (for PC). The cell used for cyclic voltammetry (CV) contained a glassy-carbon working electrode (BAS standard disk electrode, 3 mm OD), a Pt wire auxiliary electrode (0.5 mm), and a Ag/Ag^+ reference electrode (Ag wire in 0.1mM $AgNO_3$ in MeCN). Prior to obtaining electrochemical data, solutions were de-aerated for at least 30 minutes with high purity Argon (Ar). Fine polishing of the glassy-carbon working electrode was adapted from the procedure of Keita and co-workers. [6] Unless otherwise noted, scan rates were 10 mV/s, and all experiments were carried out in a 0.1M tetrabutylammonium hexafluorophosphate in dry acetonitrile electrolyte at ambient temperature under an Argon (Ar) atmosphere.

3.2.4 Synthesis of Tc(V) and Tc(VI) Compounds via a Metathesis reaction.

$(NBu_4)_{7-x}H_x[Tc^VO(\alpha_2\text{-}P_2W_{17}O_{61})]$: To a solution of $K_{7-n}H_n[Tc^VO(\alpha_2\text{-}P_2W_{17}O_{61})]$ (500 mg, 0.1 mmol) dissolved in 5 ml 0.5 M H_2SO_4 was added a 10 molar equivalent of solid $(NBu_4)Br$ (322 mg, 1 mmol) to immediately precipitate out a dark brown solid. This solid was isolated by vacuum filtration to yield the desired $(NBu_4)_{7-n}H_n[Tc^VO(\alpha_1\text{-}P_2W_{17}O_{61}]$ product and a small amount of $[\alpha\text{-}P_2W_{18}O_{62}]^{6-}$ as identified by ^{31}P NMR. Yield: 80 – 90 % based on $(NBu_4)TcOCl_4$. ^{31}P NMR: (160 MHz, CD_3CN, 300 K, ppm) δP: -12.07 (1), -12.37 (1).

$(NBu_4)_{7-n}H_n[Tc^VO(\alpha_1\text{-}P_2W_{17}O_{61})]$: To a solution of $K_{7-n}H_n[Tc^VO(\alpha_2\text{-}P_2W_{17}O_{61})]$ (500 mg, 0.1 mmol) in 5 mL water was added a 10 molar equivalent of $(NBu_4)Br$ (322 mg, 1 mmol) dissolved in 5 mL 0.5 M H_2SO_4. Immediately upon addition of $(NBu_4)Br$ a dark red-brown precipitate was observed. This solid was isolated by vacuum filtration to yield the desired $(NBu_4)_{7-n}H_n[Tc^VO(\alpha_1\text{-}P_2W_{17}O_{61}]$ product and a small amount of $[\alpha\text{-}P_2W_{18}O_{62}]^{6-}$ as identified by ^{31}P NMR. Yield: 80 – 90 % based on $(NBu_4)TcOCl_4$. ^{31}P NMR: (160 MHz, CD_3CN, 300 K, ppm) δP: -12.44 (1), -12.8 (1).

$(NBu_4)_{6-n}H_n[Tc^{VI}O(\alpha_1\text{-}P_2W_{17}O_{61})]$: To a solution of $(NBu_4)_{7-n}H_n[Tc^VO(\alpha_1\text{-}P_2W_{17}O_{61})]$ (100 mg, mmol) in 2 mL acetonitrile was added a drop of concentrated bromine (Br_2) and allowed to stir overnight. ^{31}P NMR: (160 MHz, CD_3CN, 300 K, ppm) δP: +38.96 (1), -12.23 (1)

3.2.5 Attempts at a Direct Organic Synthesis of Tc(V) Compounds by reaction of $(NBu_4)Tc^{V}OCl_4$ with the tetrabutylammonium salt of $(\alpha_1/\alpha_2\text{-}P_2W_{17}O_{61})^{10-}$

3.2.5.1. $(NBu_4)_{7-x}H_x[Tc^{V}O(\alpha_2\text{-}P_2W_{17}O_{61})]$.

Method 1.1: To a stirring suspension of $(NBu_4)_{10-x}H_x(\alpha_2\text{-}P_2W_{17}O_{61})$ (460 mg, 0.073 mmol) in CH_2Cl_2 (4 ml) was added drop-wise a solution of $(NBu_4)TcOCl_4$ (36.5 mg, 0.073 mmol) in CH_2Cl_2 (1 ml). The resulting blue-violet solution was stirred for 1 hour during which time a lavender precipitate evolved. The solution was decanted and the solid was washed repeatedly with portions of CH_2Cl_2. The solid is a mixture of starting ligand and a minimal amount of the desired product.

Method 1.2: To a stirring solution of $(NBu_4)_{10-x}H_x$ $(\alpha_2\text{-}P_2W_{17}O_{61})]$ (375 mg, 0.06 mmol) in 1 mL CD_3CN was added a solution of $(NBu_4)TcOCl_4$ (30 mg, 0.06 mmol) in 1mL CD_3CN, to immediately produce a dark blue color. 2 hours of stirring resulted in a blue-purple solution. 2 mL of water was added to precipitate a dark brown-purple oil which was re-dissolved in 2 mL acetone. The addition of an excess of toluene resulted in the formation of a lavender-purple solid, isolated by vacuum filtration. This solid is a mixture of the starting ligand and a minimal amount of the desired product.

Method 1.3: To a stirring solution of $[(NBu_4)_{10-x}H_x(\alpha_2\text{-}P_2W_{17}O_{61})]$ (375 mg, 0.06 mmol) in 1 mL CD_3CN was added a solution of $(NBu_4)TcOCl_4$ (30 mg, 0.06 mmol) in 1mL CD_3CN and 22 μL (0.18 mmol) ethylene glycol (eg) to immediately produce a red-purple color. 4 hours of stirring resulted in a blue-purple solution. 2 mL of water was

added to precipitate a dark brown oil which was re-dissolved in 2 mL acetone. The addition of an excess of toluene resulted in the formation of a lavender-purple solid, isolated by vacuum filtration. This solid is a mixture of the starting ligand and a minimal amount of the desired product.

Method 1.4: To a stirring solution of $[(NBu_4)_{10-x}H_x(\alpha_2\text{-}P_2W_{17}O_{61})]$ (375 mg, 0.06 mmol) in 1 mL CH_3CN/CH_2Cl_2 was added a solution of $(NBu_4)TcOCl_4$ (30 mg, 0.06 mmol) in 1 mL CD_3CN under a variety of conditions, to immediately produce a bright blue-purple solution. The reaction solution was allowed to stir for up to 12 hours while monitoring by ^{31}P NMR. In all cases the reaction solution proves to be a mixture of the starting ligand and a minimal amount of the desired product. The reaction conditions have been summarized in table 3.1

Starting materials (S.M.)	Method	Solvent	Ratio of S.M.	Added reagents/Reaction conditions
$(NBu_4)_{10-x}H_x(\alpha_2\text{-}P_2W_{17}O_{61})]$ and $(NBu_4)TcOCl_4$	1.4a	CH_3CN	1:1	1.6 eq. Triethylamine (NEt_3)
	1.4b		1:1	3.2 eq. Triethylamine (NEt_3)
	1.4c		1:2	-
	1.4d		1:4	-
	1.4e		1:1	Reflux
	1.4f	CH_2Cl_2	1:1	Reflux
	1.4g		1:3	-

Table 3.1. Summary of the various reaction conditions attempted for the direct synthesis of $(NBu_4)_{7-n}H_n[Tc^VO(\alpha_2\text{-}P_2W_{17}O_{61})]$ from the reaction of $(NBu_4)TcOCl_4$ with $[(NBu_4)_9H(\alpha_2\text{-}P_2W_{17}O_{61})]$

3.2.5.2. $(NBu_4)_{7-n}H_n[Tc^VO(\alpha_1\text{-}P_2W_{17}O_{61})]$.

Method 2.1: To a stirring slurry of $[(NBu_4)_{10-x}H_x(\alpha_1\text{-}P_2W_{17}O_{61})]$ (267.5 mg, 0.043 mmol) in CH_2Cl_2 (3 ml) was added drop-wise a solution of $(NBu_4)TcOCl_4$ (21.4 mg, 0.043 mmol) in CH_2Cl_2 (0.5 ml). The solution immediately changed color to red-purple and was allowed to stir for 1 hour, after which a red-brown precipitate separated from the solution. The supernatant was decanted and the resulting solid washed repeatedly with portions of CH_2Cl_2 to give yield a red-brown solid. This solid is a mixture of the starting ligand and a small amount of the desired product.

Method 2.2: To a stirring solution of $[(NBu_4)_{10-x}H_x(\alpha_1\text{-}P_2W_{17}O_{61})]$ (375 mg, 0.06 mmol) in 1 mL CD_3CN was added dropwise a solution of $(NBu_4)TcOCl_4$ (30 mg, 0.06 mmol) in 1 mL CD_3CN, to immediately produce a bright orange-red color that became dark red over the course of the addition. 1.5 hours of stirring resulted in a bright red-purple solution. 2 mL of water was added to precipitate a dark red-brown oil which was re-dissolved in 2 mL acetone. The addition of an excess of toluene resulted in the formation of a red-brown solid, isolated by vacuum filtration. This solid is a mixture of the starting ligand and a small amount of the desired product.

Method 2.3: To a stirring solution of $[(NBu_4)_{10-x}H_x(\alpha_1\text{-}P_2W_{17}O_{61})]$ (382 mg, 0.062 mmol) in 1 mL CD_3CN was added dropwise a solution of $(NBu_4)TcOCl_4$ (38 mg, 0.07 mmol) in 1 mL CD_3CN and 30 uL (0.42 mmol) ethylene glycol (eg), to immediately produce a bright blue-green color that became dark red over the course of the addition. 3 hours of stirring resulted in a bright red solution. 2mL of water was added to precipitate a

dark red-brown oil which was re-dissolved in 2 mL acetone. The addition of an excess of toluene resulted in the formation of a red-brown solid, isolated by vacuum filtration. This solid is a mixture of the starting ligand and a small amount of the desired product.

3.2.6. Attempts at Oxidation of $(NBu_4)_{7-n}H_n[Tc^VO(\alpha_1/\alpha_2\text{-}P_2W_{17}O_{61})]$.

Method 3.1: To a red/brown solution of $(NBu_4)_{7-n}H_n[Tc^VO(\alpha_1/\alpha_2\text{-}P_2W_{17}O_{61})]$ prepared by Metathesis (30 mg, 0.005 mmol) in 2 mL CD_3CN was added an appropriate amount of oxidizing agent (summarized in table 3.2) and allowed to stir for up to 48 hours as monitored by ^{31}P NMR.

Starting Material	Method	Oxidizing agent	Amount	Color change
$(NBu_4)_{10-x}H_x$ (α_1-$P_2W_{17}O_{61}$)	3.1a	H_2O_2	2 drops	Light Yellow
	3.1b	Ag^+ (Triflate)	10 mg	-
	3.1c	Solution in Air	-	-
	3.1d	Solid in Air	-	-
$(NBu_4)_{10-x}H_x$ (α_2-$P_2W_{17}O_{61}$)	3.1e	Br_2	1 drop	Dark orange
	3.1f	H_2O_2	2 drops	Light yellow
	3.1g	Ag^+ (Triflate)	10 mg	-
	3.1h	Solution in Air	-	-
	3.1i	Solid in Air	-	-

Table 3.2. Summary of the various oxidizing agents employed for the oxidation of $(NBu_4)_{7-n}H_n[Tc^VO(\alpha_1/\alpha_2\text{-}P_2W_{17}O_{61})]$ to $(NBu_4)_{6-n}H_n[Tc^{VI}O(\alpha_1/\alpha_2\text{-}P_2W_{17}O_{61})]$

3.2.7 Ligand Stability Studies

Method 4.1: To a solution of $(NBu_4)_{10-x}H_x[(\alpha_1\text{-}P_2W_{17}O_{61})]$, $(NBu_4)_{10-x}H_x[(\alpha_2\text{-}P_2W_{17}O_{61})]$ or $(NBu_4)_6[P_2W_{18}O_{62}]$ (100 mg) in 1 mL CH_3CN was added the appropriate amount of oxidizing agent. The solution was allowed to stir for up to 7 days and tracked with ^{31}P NMR. Experimental conditions are summarized in Table 3.3.

POM	Oxidizing agent	Amount
$(NBu_4)_{10-x}H_x[(\alpha_1\text{-}P_2W_{17}O_{61})]$	H_2O_2	2 drops
	Ag^+ (Triflate)	10 mg
	Br_2	1 drop
$(NBu_4)_{10-x}H_x[(\alpha_1\text{-}P_2W_{17}O_{61})]$	H_2O_2	2 drops
	Ag^+ (Triflate)	10 mg
	Br_2	1 drop
$(NBu_4)_6[P_2W_{18}O_{62}]$	H_2O_2	2 drops
	Ag^+ (Triflate)	10 mg
	Br_2	1 drop

Table 3.3. Summary of the various oxidizing agents employed for the stability studies. In general, the procedure consisted of dissolving the POM in 1mL CD_3CN followed by the addition of oxidizing agent. The resulting solution was monitored by ^{31}P NMR for up to 7 days.

3.3 Results and Discussion

3.3.1 Synthesis of Tc(V) and Tc(VI) Compounds via Metathesis

$(NBu_4)_{7-n}H_n[Tc^VO(\alpha_1/\alpha_2\text{-}P_2W_{17}O_{61})]$. Although the synthesis of organic soluble metal substituted Keggin POMs is easily achieved through the extraction of the TBA salts from an aqueous reaction solution, the direct synthesis of metal substituted organic

soluble Wells-Dawson POMs has continued to prove difficult. Numerous metal substituted (NBu_4) salts of Wells-Dawson POMs have been prepared, but the synthetic route to such compounds is almost exclusively achieved through the metathesis of aqueous soluble (for example, potassium (K) or lithium (Li)) salts under controlled pH conditions.[1, 7] Finke et. al. for example, have successfully prepared a multitude of metal substituted tetra-n-butylammonium salts of α_2-$P_2W_{17}O_{61}(M^{n+}\ Br)(^{n-11})$, where M = Mn^{3+}, Fe^{3+}, Co^{2+}, Ni^{2+} and Cu^{2+}. In all cases a metathesis reaction from the potassium (K) salt was required, and they observed the need for stringent control of both the reaction pH as well as the correct stoichiometric ratios between reactants. [1] We have prepared organic soluble lanthanide α_1-$P_2W_{17}O_{61}$ and α_2-$P_2W_{17}O_{61}$ complexes also through Metathesis reactions.

For the synthesis of the $(NBu_4)_{7-n}H_n[Tc^{V}O(\alpha_1/\alpha_2\text{-}P_2W_{17}O_{61})]$ complexes, we have observed similar behavior to Finke. Despite attempts under a variety of experimental conditions, including a range of solvent systems (CH_2Cl_2 or Acetonitrile), pH conditions and reaction stoichiometries we found the synthesis of the $(NBu_4)_{7-n}H_n[Tc^{V}O(\alpha_1/\alpha_2\text{-}P_2W_{17}O_{61})]$ complex directly from the $(NBu_4)_{10-x}H_x[\alpha_1/\alpha_2\text{-}P_2W_{17}O_{61}]$ ligand unsuccessful, yielding only minimal amounts of the desired complex and primarily unreacted free $(NBu_4)_{10-x}H_x[\alpha_1/\alpha_2\text{-}P_2W_{17}O_{61}]$ ligand.

The most expeditious method to form the $(NBu_4)_{7-n}H_n[Tc^{V}O(\alpha_1/\alpha_2\text{-}P_2W_{17}O_{61})]$ compounds was found to be via a metathesis reaction from the aqueous soluble potassium salts. This was achieved using methods developed by Finke *et. al*. for transition metal substituted tetra-n-butylammonium salts of the α_2-$P_2W_{17}O_{61}$ POM, [1] and by our lab for the isolation of $Re^{V,VI,VII}$ α_2-$P_2W_{17}O_{61}$ complexes.[8]

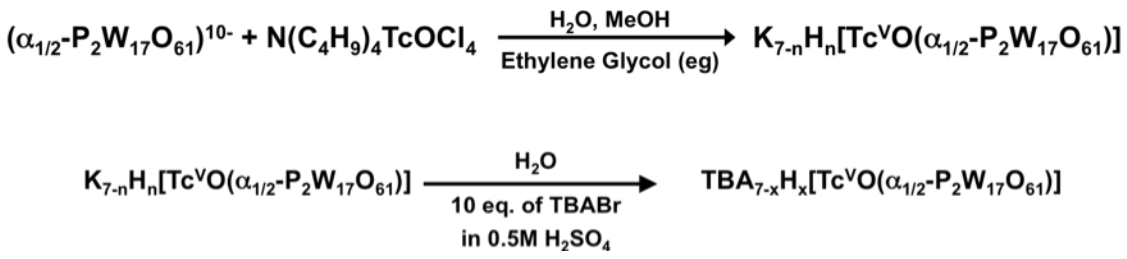

Scheme 3.1. Simplified schematic representation of the synthesis of $TBA_{7-x}H_x[Tc^VO(\alpha_{1/2}\text{-}P_2W_{17}O_{61})]$ via a metathesis reaction.

Scheme 3.1 illustrates the metathesis reaction pathway. The complete metathesis of the K salts for both $(NBu_4)_{7-x}H_x[Tc^VO(\alpha_1/\alpha_2\text{-}P_2W_{17}O_{61})]$ compounds was found to require 10 molar equivalents of tetrabutylammonium bromide ($(NBu_4)Br$) and highly acidic conditions (pH = 0.33). We find that pure $(NBu_4)_{7-x}H_x[Tc^VO(\alpha_1/\alpha_2\text{-}P_2W_{17}O_{61})]$ complex cannot be extracted directly from the *in situ* aqueous reaction mixture. The reaction solution of $K_{7-n}H_n[Tc^VO(\alpha_1/\alpha_2\text{-}P_2W_{17}O_{61})]$ possesses a number of by-products (TcO_2, unreacted ligand) that preclude isolation of the metathesized TBA product. A pure tetrabutylammonium (NBu_4) complex can only be achieved from the direct metathesis of an isolated $K_{7-n}H_n[Tc^VO(\alpha_1/\alpha_2\text{-}P_2W_{17}O_{61})]$ solid. The resulting $(NBu_4)_{7-n}H_n[Tc^VO(\alpha_1/\alpha_2\text{-}P_2W_{17}O_{61})]$ products were characterized using ^{31}P NMR and cyclic voltammetry.

$(NBu_4)_{6-n}H_n[Tc^{VI}O(\alpha_1\text{-}P_2W_{17}O_{61})]$. Oxidation of Tc^V to Tc^{VI} in the $\alpha_1\text{-}P_2W_{17}O_{61}$ structure was accomplished through the addition of a small amount of Br_2. Attempts to achieve this oxidation directly in air, with H_2O_2 and silver triflate ($AgCF_3SO_3$) proved unsuccessful. The addition of H_2O_2 resulted in decomposition of the complex to $(NBu_4)_6[P_2W_{18}O_{62}]$ (according to ^{31}P NMR and ^{183}W NMR), while the addition of Ag^+

and stirring in air had no observable effect. These results make sense in light of the theoretical reduction potentials of H_2O_2, Br and Ag where H_2O_2 is the strongest of the oxidizing agents and Ag^+ the weakest.

$H_2O_2 + 2\ H^+ + 2\ e^- \longrightarrow 2\ H_2O$	+1.77 V
$Br_2 + 2e^- \longrightarrow 2Br^-$	+1.07 V
$Ag^+ + e^- \longrightarrow Ag$	+0.80 V

The Tc^{VI} product was characterized using ^{31}P NMR, where the presence of a highly downfield shifted resonance is likely due to influence of the paramagnetic Tc^{VI} center. This is similar to what we observed in our lab for the rhenium analog.[8] EPR studies are currently underway. Unfortunately, we have been unable to successfully isolate a solid of this compound. Although the addition of an excess of EtOH/Ether results in the formation of a dark brown solid, ^{31}P NMR characterization of this solid indicate that it has undergone reduction back to the Tc(V) compound.

3.3.2 Characterization by ^{31}P NMR Spectroscopy

^{31}P NMR is a well-established technique to assess impurities of polyoxometalates at the 2% level [9-11] and has been used to identify pure Wells-Dawson complexes of transition metals[9-13] and lanthanides.[14-23] Because of the low abundance (14%) of the ^{183}W nucleus in natural W, ^{183}W NMR spectroscopy requires sample sizes of approximately 30 mM. Due to the low solubility of the tetrabutylammonium salts, we were unable to obtain ^{183}W NMR spectra to characterize these compounds. Table 3.4

contains a summary of the ^{31}P NMR resonances for the $Tc^{V}O$ and $Tc^{VI}O$ $(\alpha_1\text{-}P_2W_{17}O_{61})^{7-}$ and $(\alpha_2\text{-}P_2W_{17}O_{61})^{7-}$ complexes.

Compound	Synthetic Route	^{31}P NMR, ppm
$(NBu_4)_{7-n}H_n[Tc^{V}O(\alpha_2\text{-}P_2W_{17}O_{61})]$	Metathesis	-12.07, -12.37
$(NBu_4)_{7-n}H_n[Tc^{V}O(\alpha_1\text{-}P_2W_{17}O_{61})]^{7-}$	Metathesis	-12.44, -12.80
$(NBu_4)_{6-n}H_n[Tc^{VI}O(\alpha_1\text{-}P_2W_{17}O_{61})]^{7-}$	Oxidation with Br_2	+38.96, -12.23

Table 3.4. ^{31}P NMR Data for Tc^{V} and Tc^{VI} substituted into the $\alpha_1\text{-}[P_2W_{17}O_{61}]^{10-}$ and $\alpha_2\text{-}[P_2W_{17}O_{61}]^{10-}$ Wells-Dawson POMs. Solvent, CD_3CN.

$(NBu_4)_{7-n}H_n[Tc^{V}O(\alpha_1/\alpha_2\text{-}P_2W_{17}O_{61})]$. Figure 3.1. shows the ^{31}P NMR of the tetrabutylamonium Br_2 salts of $Tc^{V}O(\alpha_1\text{-}P_2W_{17}O_{61})^{7-}$ (green spectrum shown on the top) and $Tc^{V}O(\alpha_2\text{-}P_2W_{17}O_{61})^{7-}$ (blue spectrum shown on the bottom), respectively. In each case two distinct resonances are observed. This is expected for the two inequivalent P atoms in these molecules. The upfield resonance in each case is assigned to P1, the phosphorous atom close to the Tc^{V} center and the remote phosphorous, P2, is assigned to the downfield resonance. These resonances are different from both the $(\alpha_1\text{-}P_2W_{17}O_{61})^{7-}$ and $(\alpha_2\text{-}P_2W_{17}O_{61})^{7-}$ ligands, as well as the aqueous soluble K salts of $Tc^{V}O(\alpha_1\text{-}P_2W_{17}O_{61})^{7-}$ and $Tc^{V}O(\alpha_2\text{-}P_2W_{17}O_{61})^{7-}$.

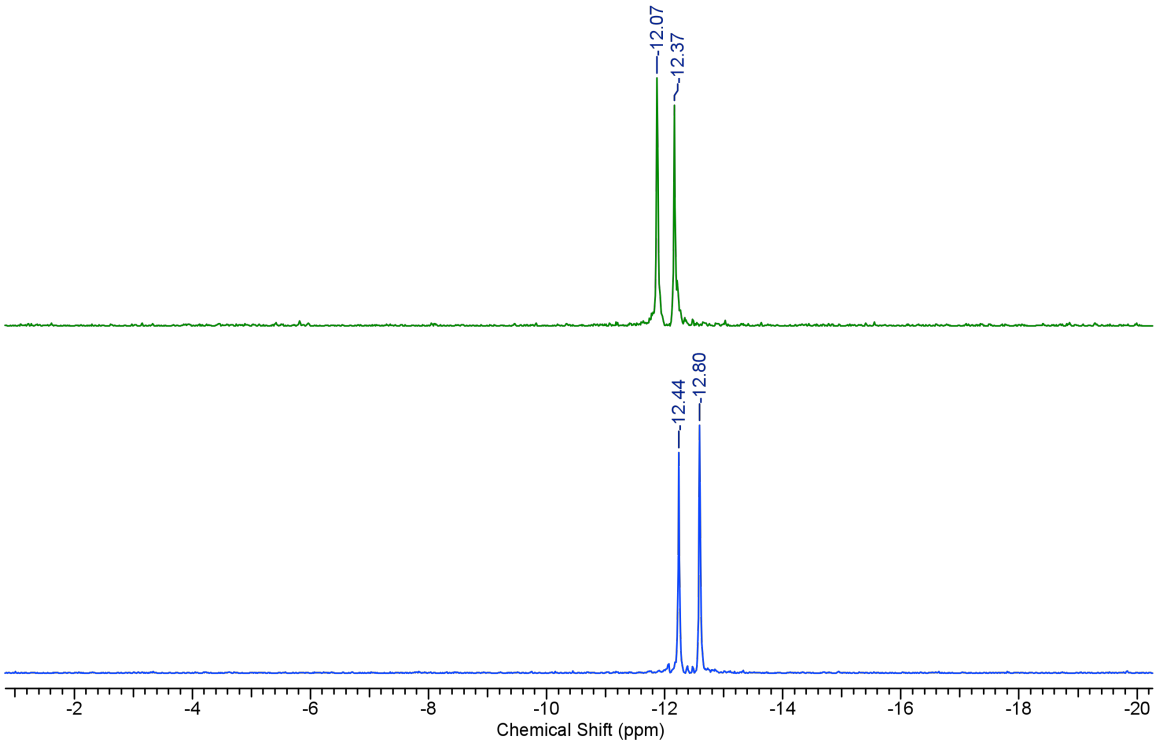

Figure 3.1. ^{31}P NMR data for $(NBu_4)_{7-n}H_n[Tc^{V}O(\alpha_2\text{-}P_2W_{17}O_{61})]$ (top) and $(NBu_4)_{7-n}H_n[Tc^{V}O(\alpha_2\text{-}P_2W_{17}O_{61})]$ (bottom) as prepared by a metathesis reaction. Solvent: CD_3CN.

$(NBu_4)_{7-n}H_n[Tc^{VI}O(\alpha_1\text{-}P_2W_{17}O_{61})]$. Figure 3.2 shows the ^{31}P NMR of the tetrabutylammonium (NBu_4) salt of $Tc^{VI}O(\alpha_1\text{-}P_2W_{17}O_{61})^{7-}$. Two resonances are observed, as expected for the two inequivalent P atoms in this molecule. This paramagnetic (d^1) $Tc^{VI}O$ $\alpha_1\text{-}P_2W_{17}O_{61}^{6-}$ species exhibits a broad highly upfield shifted resonance at + 38.95 ppm; this is consistent with the proximal P1 phosphorous atom close to the paramagnetic center. The analogous $Re^{VI}(\alpha_2\text{-}P_2W_{17}O_{61})^{6-}$ species exhibits similar behavior.[8]

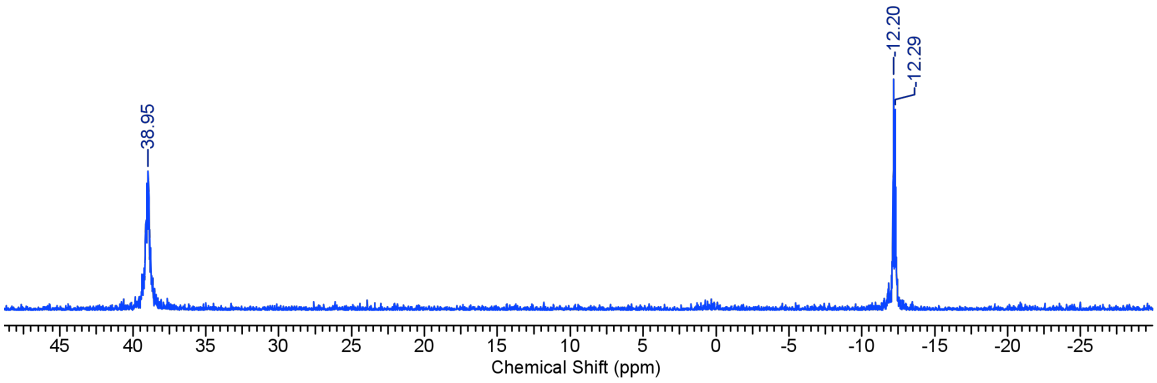

Figure 3.2. ^{31}P NMR data for $(NBu_4)_{7-n}H_n[Tc^{VI}O(\alpha_1\text{-}P_2W_{17}O_{61})]$ as prepared by the oxidation of the $(NBu_4)_{7-n}H_n[Tc^{V}O(\alpha_1\text{-}P_2W_{17}O_{61})]$ using bromine. Solvent, CD_3CN

3.3.3 Electrochemistry.

As reported by Nadjo and co-workers cyclic voltammetry is a powerful method that can be used to identify the α_1 and α_2- $[P_2W_{17}O_{61}]^{10-}$ isomers. [24] It is often employed as a means to characterize transition metal complexes of these isomers and to assess their purity. [24, 25]

Figure 3.3 shows CV data for both the $(NBu_4)_{7-n}H_n[Tc^{V}O(\alpha_1\text{-}P_2W_{17}O_{61})]$ and $(NBu_4)_{7-n}H_n[Tc^{V}O(\alpha_2\text{-}P_2W_{17}O_{61})]$ complexes and reduction potentials have been summarized in Table 3.5. The CVs of both the Tc^{V} α_1- and the α_2- substituted compounds show two reversible redox couples in the positive potential region, confirming the presence of Tc in these complexes. Redox waves in the positive potential region are characteristic of metal substituted POMs and are always attributed to the chemistry of the metal. The rest potential for both compounds is c.a. +0 mV, which allows for the assignment of these positive redox couples to the two successive 1 electron $Tc^{V/VI}$ and Tc

$^{VI/VII}$ redox processes. Notably, in organic solvent we are able to access the $Tc^{VI/VII}$ couple that proved unattainable in an aqueous medium.

Both compounds also exhibit several reversible redox processes in the negative potential region. These can be attributed to mostly tungsten (W) redox chemistry. The first of these might be attributed to the $Tc^{V/IV}$ redox process but this cannot be claimed with certainty.

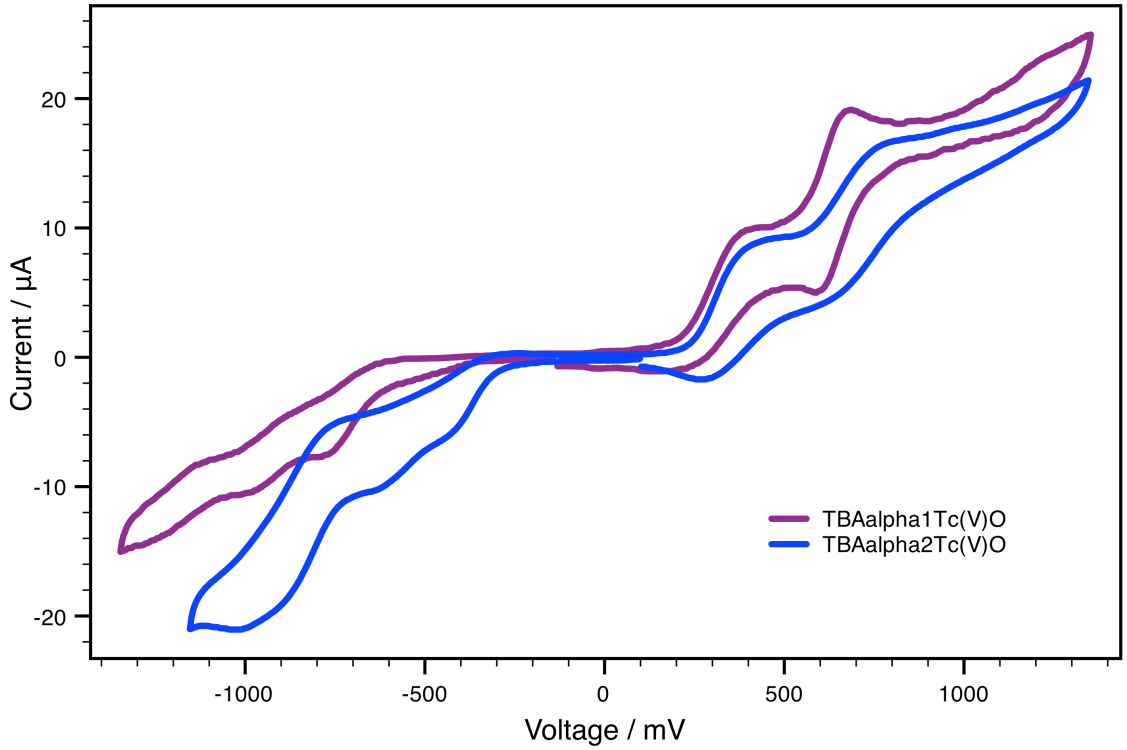

Figure 3.3 CV data $(NBu_4)_{7-n}H_n[Tc^{V}O(\alpha_1\text{-}P_2W_{17}O_{61})]$ and $(NBu_4)_{7-n}H_n[Tc^{V}O(\alpha_2\text{-}P_2W_{17}O_{61})]$. Electrolyte, 0.1M tetrabutylammonium hexafluorophosphate. Working electrode, glassy carbon, auxiliary electrode, platinum wire and reference electrode, Ag/Ag+. Scan rate 10 mV/s.

E (mV)	α_1-$[Tc^{V}OP_2W_{17}O_{61}]^{5-}$			α_2-$[Tc^{V}OP_2W_{17}O_{61}]^{5--}$		
	1st W?	$Tc^{5/6}$	$Tc^{6/7}$	1st W?	$Tc^{5/6}$	$Tc^{6/7}$
E_c	-773	216	589	-438	274	655
E_a	-620	405	685	-319	421	770
$E_{1/2}$	-697	311	637	-379	348	713

Table 3.5 Reduction Potentials for $(NBu_4)_{7-n}H_n[Tc^{V}O(\alpha_1\text{-}P_2W_{17}O_{61})]$ and $(NBu_4)_{7-n}H_n[Tc^{V}O(\alpha_2\text{-}P_2W_{17}O_{61})]$.

Table 3.6 highlights the differences between the half-wave reduction potentials for both the $Tc^{V/VI}$ and $Tc^{VI/VII}$ redox processes in $(NBu_4)_{7-n}H_n[Tc^{V}O(\alpha_1\text{-}P_2W_{17}O_{61})]$ and $(NBu_4)_{7-n}H_n[Tc^{V}O(\alpha_2\text{-}P_2W_{17}O_{61})]$. Reduction of the Tc metal center is observed to occur at more positive potentials in the $Tc^{V}O(\alpha_2\text{-}P_2W_{17}O_{61})$ complex ($E_{1/2}$ = 348 mV for $Tc^{V/VI}$ and $E_{1/2}$ = 713 mV for $Tc^{VI/VII}$) as compared to the $Tc^{V}O(\alpha_1\text{-}P_2W_{17}O_{61})$ ($E_{1/2}$ = 311 mV for $Tc^{V/VI}$ and $E_{1/2}$ = 637 mV for $Tc^{VI/VII}$). This means that in organic solvent the reduction of Tc is easier to achieve in the more rigid and slightly more acidic α_2 vacancy than in the α_1. Although in direct contrast to what is observed for the reduction of Tc in aqueous solution, where reduction of Tc is always favored in the $\alpha_1$vacancy, this is most likely due to the effect of the counterion or protonation effects that are more pronounced in organic solvents.

Further, this illustrates that the oxidation of the Tc^{V} metal center to Tc^{VI} will be more difficult in the $(NBu_4)_{7-n}H_n[Tc^{V}O(\alpha_2\text{-}P_2W_{17}O_{61})]$ complex. This corroborates our findings, where oxidation of the Tc in this complex proved beyond our reach by the chemical addition of oxidizing agents.

$E_{1/2}$ (mV)	$Tc^{5/6}$	$Tc^{6/7}$
α_1-$[Tc^{V}OP_2W_{17}O_{61}]^{5-}$	311	637
α_2-$[Tc^{V}OP_2W_{17}O_{61}]^{5-}$	348	713
Δ (α_2 –α_1)	+37	+76

Table 3.6 Summary of half-wave reduction potentials comparing the $(NBu_4)_{7-n}H_n[Tc^{V}O(\alpha_1\text{-}P_2W_{17}O_{61})]$ and $(NBu_4)_{7-n}H_n[Tc^{V}O(\alpha_2\text{-}P_2W_{17}O_{61})]$.

The transition from aqueous to organic solvents allows for an extension of the Tc redox chemistry to include the $Tc^{V/VI}$ and $Tc^{VI/VII}$ transitions. Table 3.7 shows the free energy (ΔG) associated with the $Tc^{VI/V}$ and $Tc^{VII/VI}$ reduction reactions in the $(NBu_4)_{7-n}H_n[Tc^{V}O(\alpha_1\text{-}P_2W_{17}O_{61})]$ and $TBA_{7-n}H_n[Tc^{V}O(\alpha_2\text{-}P_2W_{17}O_{61})]$ complexes.

$$Tc^{VI} + 1e^- \longrightarrow Tc^{V}$$

$$Tc^{VII} + 1e^- \longrightarrow Tc^{VI}$$

ΔG is calculated as $\Delta G = -nFE$, where n = number of moles of electron, F = 96 500 C/mol and E is potential for reduction of the $Tc^{VI/V}$ and $Tc^{VI/VII}$ redox couples, E_c in V. There is an observable difference between the free energy values for the $(NBu_4)_{7-n}H_n[Tc^{V}O(\alpha_1\text{-}P_2W_{17}O_{61})]$ and $(NBu_4)_{7-n}H_n[Tc^{V}O(\alpha_2\text{-}P_2W_{17}O_{61})]$ complexes; of 5.6 kJ and 6.4 kJ for the $Tc^{VI/V}$ and $Tc^{VI/VII}$ reductions respectively.

Free energy is a measure of the spontaneity of a reaction. More negative free energy values indicate preferentially favored reactions. Both $(NBu_4)_{7-n}H_n[Tc^{V}O(\alpha_1\text{-}P_2W_{17}O_{61})]$ and $(NBu_4)_{7-n}H_n[Tc^{V}O(\alpha_2\text{-}P_2W_{17}O_{61})]$ complexes exhibit negative free energy values, with those for the $(NBu_4)_{7-n}H_n[Tc^{V}O(\alpha_2\text{-}P_2W_{17}O_{61})]$ complex being more negative

for both Tc reductions. This means that in both cases the reduction of the Tc center is favored in the $(NBu_4)_{7-n}H_n[Tc^{V}O(\alpha_2\text{-}P_2W_{17}O_{61})]$ complex, which in turn indicates that the oxidation of Tc in the $(NBu_4)_{-n}H_n[Tc^{V}O(\alpha_2\text{-}P_2W_{17}O_{61})]$ complex is more difficult. This confirms our earlier findings; we are unable to chemically oxidize the Tc(V) metal to Tc(VI) in the α_2-vacancy.

Compound	ΔG for $Tc^{V/VI}$ (kJ)	ΔG for $Tc^{VI/VII}$ (kJ)
$\alpha_1\text{-}[Tc^{V}OP_2W_{17}O_{61}]^{5-}$	-20.8	– 56.8
$\alpha_2\text{-}[Tc^{V}OP_2W_{17}O_{61}]^{5-}$	-26.4	-63.2
$\Delta (\alpha_2 - \alpha_1)$	-5.6	-6.4

Table 3.7 Free Energy values for the $Tc^{V/VI}$ and $Tc^{VI/VII}$ transitions in $\alpha_1\text{-}[Tc^{V}OP_2W_{17}O_{61}]^{5-}$ and $\alpha_2\text{-}[Tc^{V}OP_2W_{17}O_{61}]^{5-}$.

Tabulated values of the HOMO-LUMO energy gap for the $(NBu_4)_{7-n}H_n[Tc^{V}O(\alpha_1\text{-}P_2W_{17}O_{61})]$ and $(NBu_4)_{7-n}H_n[Tc^{V}O(\alpha_2\text{-}P_2W_{17}O_{61})]$ complexes can be found in table 3.8. The HOMO-LUMO energy gap can be extracted from electrochemical data by calculating the difference between the half-wave peak potentials of the HOMO (defined to be the first redox couple that exists in the oxidative potential region of the CV) and the LUMO (defined to be the first redox couple to exist in the reductive potential region of the CV). This energy gap is calculated in electronvolts (eV). According to the CV data these orbital assignments for both the $\alpha_1\text{-}[Tc^{V}OP_2W_{17}O_{61}]^{5-}$ and $\alpha_2\text{-}[Tc^{V}OP_2W_{17}O_{61}]^{5-}$ complexes are the $Tc^{V/VI}$ redox couple for the HOMO, and the first reduction wave (at -697 mV for the α_1 complex and -379 mV for the α_2 complex) for the LUMO. The exact

nature of the LUMO remains unknown in these systems and may be either due to a W or due to the $Tc^{V/IV}$.

Compound	HOMO-LUMO Gap (eV)
α_1-$[Tc^{V}OP_2W_{17}O_{61}]^{5-}$	1.00
α_2-$[Tc^{V}OP_2W_{17}O_{61}]^{5-}$	0.72
Δ (α_1 -α_2)	0.28

Table 3.8 HOMO-LUMO energy Gap values for α_1-$[Tc^{V}OP_2W_{17}O_{61}]^{5-}$ and α_2-$[Tc^{V}OP_2W_{17}O_{61}]^{5-}$.

A comparison between the α_1 and α_2 isomeric forms of the $[Tc^{V}OP_2W_{17}O_{61}]^{5-}$ complex reveals that the HOMO-LUMO energy gap is larger by 0.28 eV in α_1-$[Tc^{V}OP_2W_{17}O_{61}]^{5-}$ as compared to that in α_2-$[Tc^{V}OP_2W_{17}O_{61}]^{5-}$. This finding is consistent with our observations in aqueous solvent.

3.3.4 Direct Synthesis of Tc(V) Compounds.

In an attempt to circumvent the complicated synthesis of $K_{7-n}H_n[Tc^{V}O(\alpha_1/\alpha_2\text{-}P_2W_{17}O_{61})]$ en route to the tetrabutylammonium (NBu_4) salts we attempted to synthesize the $(NBu_4)_{-n}H_n[Tc^{V}O(\alpha_1/\alpha_2\text{-}P_2W_{17}O_{61})]$ complexes directly from the $(NBu_4)_{10-x}H_x[\alpha_1/\alpha_2\text{-}P_2W_{17}O_{61}]$ ligands. This method is outlined in scheme 3.2. Although these syntheses resulted in both vibrant color changes (from clear and colorless to various shades of red, blue and purple) as well as notable shifts in the ^{31}P NMR, this synthetic route proved unsuccessful in all cases, yielding only minimal amounts of the desired $(NBu_4)_{7-n}H_n[Tc^{V}O(\alpha_1/\alpha_2\text{-}P_2W_{17}O_{61})]$ complex (if any) and primarily unreacted free $(NBu_4)_{10-}$

$_xH_x[\alpha_1/\alpha_2\text{-}P_2W_{17}O_{61}]$ ligand (as identified by ^{31}P NMR and electrochemistry).

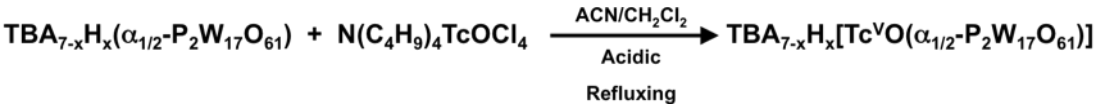

Scheme 3.2. Simplified schematic representation of the attempted direct synthesis of $(NBu_4)_{7-x}H_x[Tc^VO(\alpha_{1/2}\text{-}P_2W_{17}O_{61})$

It is worth noting here that the true protonation state of the $(NBu_4)_{10-x}H_x[\alpha_1/\alpha_2\text{-}P_2W_{17}O_{61}]$ ligands remains unknown for our starting materials and that this is a common occurence for these POMs in nonaqueous solvents.[7] This phenomenon makes the ^{31}P NMR characterizations of these compounds complex. Different degrees of protonation in a single batch of ligand may result in multiple ^{31}P NMR resonances for a pure compound, instead of the expected two resonances for the two inequivalent P atoms. For the free ligand these protonation issues may be circumvented by the addition of a small amount of water to the NMR samples, but in the non-aqueous reaction mixtures the addition of water was found to cause precipitation, thus making *in situ* ^{31}P NMR characterizations difficult.

Our initial attempts at the direct synthesis of $(NBu_4)_{7-n}H_n[Tc^VO(\alpha1/\alpha2\text{-}P_2W_{17}O_{61})]$ resulted in the isolation of a lavender/purple solid for $(NBu_4)_{7-n}H_n[Tc^VO(\alpha_2\text{-}P_2W_{17}O_{61})]$ (methods 1.1, 1.2 and 1.3), and a red/brown solid for $(NBu_4)_{7-n}H_n[Tc^VO(\alpha_1\text{-}P_2W_{17}O_{61})]$ (methods 2.1, 2.2 and 2.3). The ^{31}P NMR for these solids showed multiple resonances, which were initially attributed to protonation effects (the existence of more than one protonation state within the same sample) and upon the addition of water two distinct resonances resulted that were different from those of the $(NBu_4)_{10-x}H_x[\alpha_1/\alpha_2\text{-}P_2W_{17}O_{61}]$

starting materials (see table 3.9). It was subsequently established however (by ^{31}P NMR), that these NMR shifts were still due to protonation effects (specifically the formation of a $(NBu_4)_{10-x}H_x[\alpha_1/\alpha_2\text{-}P_2W_{17}O_{61}]$ ligand with a different formal degree of protonation), rather than the formation of a Tc-POM complex.

Compound	^{31}P NMR, ppm
$(NBu_4)_{10-n}H_n[\ (\alpha_2\text{-}P_2W_{17}O_{61})]$	-9.37, -12.47
$(NBu_4)_{7-n}H_n[Tc^VO(\alpha_2\text{-}P_2W_{17}O_{61})]$	-9.43, -12.2
$(NBu_4)_{10-n}H_n[\ (\alpha_1\text{-}P_2W_{17}O_{61})]$	-11.5, -13.03
$(NBu_4)_{7-n}H_n[Tc^VO(\alpha_1\text{-}P_2W_{17}O_{61})]^{7-}$	-10.59, -12.21

Table 3.9. ^{31}P NMR Data comparing the free $\alpha_1\text{-}[P_2W_{17}O_{61}]^{10-}$ and $\alpha_2\text{-}[P_2W_{17}O_{61}]^{10-}$ ligands with the Tc^V substituted $\alpha_1\text{-}[P_2W_{17}O_{61}]^{10-}$ and $\alpha_2\text{-}[P_2W_{17}O_{61}]^{10-}$ complexes as prepared by the direct method. Solvent, CD_3CN with the addition of a small amount of water.

In early 2009 Finke et. al. attempted to establish the true nature (protonation state) of the $(NBu_4)_{10-x}H_x[\alpha_2\text{-}P_2W_{17}O_{61}]$ ligand.[7] They began with the synthesis of $(NBu_4)_{8.4}H_{1.6}[\alpha_2\text{-}P_2W_{17}O_{61}]$, which was characterized by ^{31}P NMR and confirmed by elemental analysis to contain between 8 and 9 (NBu_4) groups. This species was deprotonated using $(NBu_4)OH$ and monitored by ^{31}P NMR to give the monoprotonated $(NBu_4)_9H_1[\alpha_2\text{-}P_2W_{17}O_{61}]$. Comparison of the NMR data revealed that the ^{31}P NMR resonances are noticably different for the two formulations, with the $(NBu_4)_9H[\alpha_2\text{-}P_2W_{17}O_{61}]$ compound exhibiting resonances that are markedly further apart than those for the more protonated species. This is illustrated in Figure 3.4[7] which reproduces the NMR results of Finke, et. al.

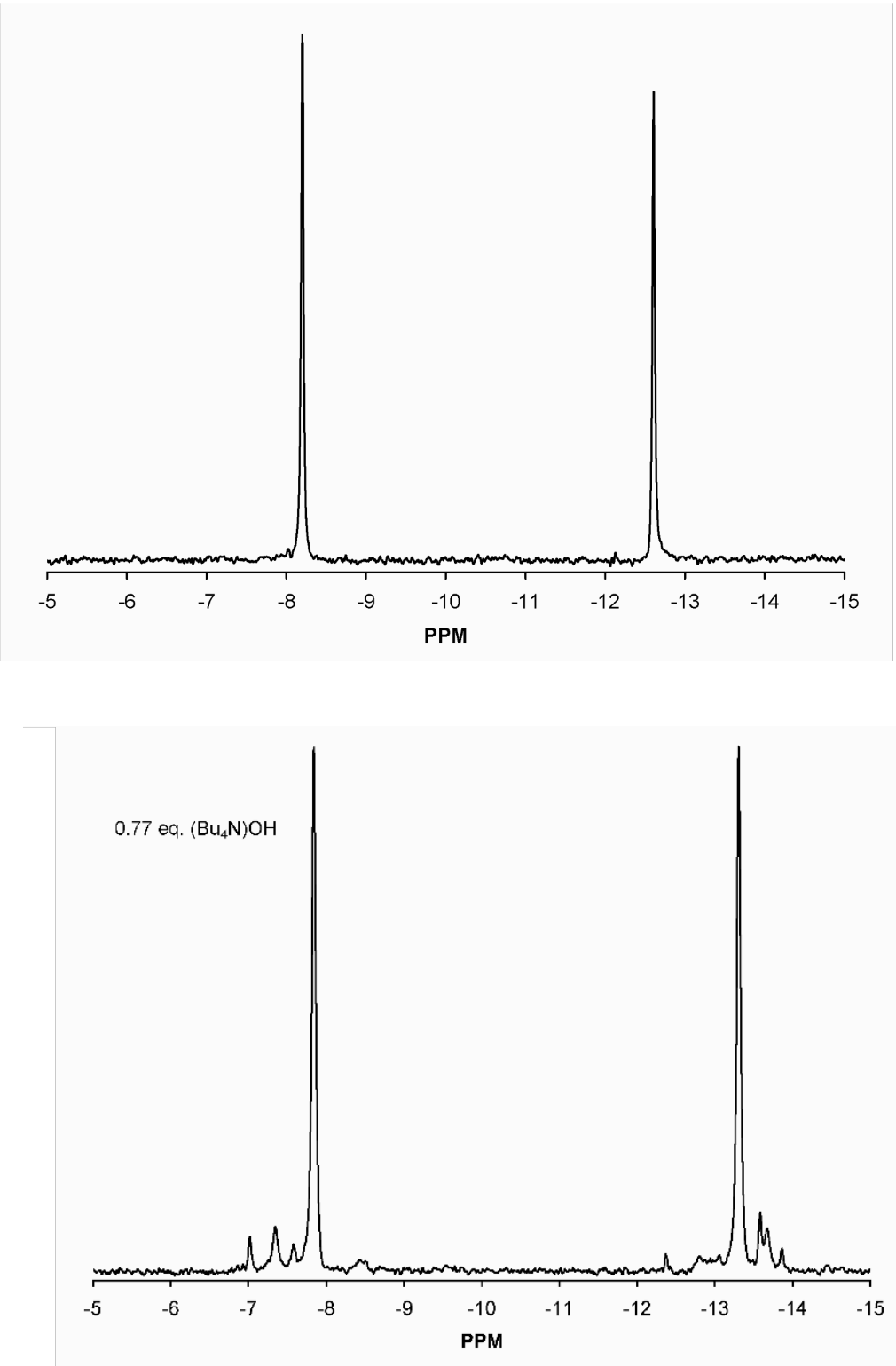

Figure 3.4. ^{31}P NMR of $(Bu_4N)_{8.4}(H_{1.6}[\alpha_2\text{-}P_2W_{17}O_{61}])\bullet 1.4H_2O$ (top) and $(Bu_4N)_9(H[\alpha_2\text{-}P_2W_{17}O_{61}])\bullet 1.4H_2O$ (bottom) in CD_3CN (taken from Finke et. al.) [7]

To examine this behavior in our compounds, the $(NBu_4)_{10-x}H_x[\alpha_2\text{-}P_2W_{17}O_{61}]$ ligand (exhibiting multitple protonation peaks, indicating a heavily protonated POM species) was titrated with a 1 M solution of $(NBu_4)OH$ in methanol (MeOH) and tracked by ^{31}P NMR. This experiment provides compelling evidence that the ^{31}P NMR resonaces observed for the direct synthesis of $(NBu_4)_{6-n}H_n$ $[Tc^{VI}O(\alpha_1/\alpha_2\text{-}P_2W_{17}O_{61})]$ are in fact due to a heavily protonated ligand species. The resulting ^{31}P NMR shifts are shown in Table 3.10.

Compound	Eq. of $(Bu_4N)OH$	^{31}P NMR, ppm
$TBA_{10-x}H_x[\alpha_2\text{-}P_2W_{17}O_{61}]$	0	-8.8[a], -9.7[a], -9.8, -10.2, -11.9 -12.0, 12.1, 12.2[a], -12.5[a]
	1	-8.9[a], -9.4 -9.9[a], -12.2, -12.7[a], -12.9[a]
	2	-8.6, -8.7[a], -2.7, -13.1[a]

Table 3.10. ^{31}P NMR Data for $(NBu_4)_{10-x}H_x[\alpha_2\text{-}P_2W_{17}O_{61}]$ when titrated with $(NBu_4)OH$. Solvent:CD_3CN (No addition of water).
[a] indicates dominant peaks

There is an observable shift in the dominating resonances of both the proximal (near the vacancy) and remote (opposite the vacancy) P atoms; from -8.8 and -12.5 to -8.7 and -13.1 ppm respectively. As observed by Finke the less protonated species has ^{31}P NMR resonances that are farther apart that those for the more protonated species. Notably the shift for the remote P resonance is significantly larger than that for the proximal P. This implies that although the deprotonation of the POM directly impacts the ^{31}P NMR resonances, it does not necessarily induce a large effect on the properties inherent to the POM vacancy (which is the primary binding site for transition metal complexes).

Figure 3.5 shows representative ^{31}P NMR spectra illustrating the multiple

resonances (protonation effects) for the lavender-purple and red-brown solids isolated by this direct method. Upon the addition of a small amount of water these effects become significantly reduced yielding only two ^{31}P NMR resonances, those matching a more protonated $(NBu_4)_{10-x}H_x[\alpha_1/\alpha_2\text{-}P_2W_{17}O_{61}]$ ligand species. Figure 3.6 illustrates the effect of the sequential addition of water to the ^{31}P NMR sample of $(NBu_4)_{7-n}H_n[Tc^VO(\alpha_2\text{-}P_2W_{17}O_{61})]$. The multiple resonances observed for this species converge at -9.43 and -12.20 ppm. As compared to Table 3.10 these resonances match those for the more protonated $(NBu_4)_{10-x}H_x[\alpha_2\text{-}P_2W_{17}O_{61}]$ ligand species.

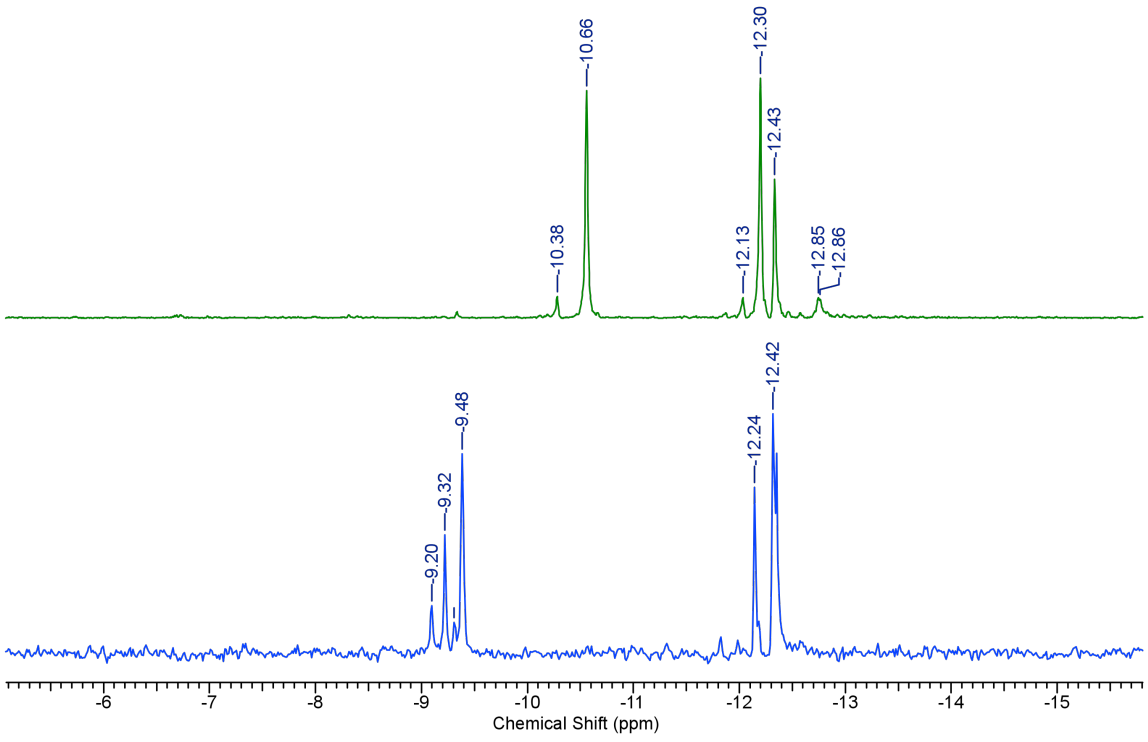

Figure 3.5. ^{31}P NMR data for $(NBu_4)_{7-n}H_n[Tc^VO(\alpha_1\text{-}P_2W_{17}O_{61})]$ (top) and $(NBu_4)_{7-n}H_n[Tc^VO(\alpha_2\text{-}P_2W_{17}O_{61})]$ (bottom) as prepared by a the direct reaction of $(NBu_4)_{10-x}H_x[\alpha_2\text{-}P_2W_{17}O_{61}]$ and Tc(V) . Solvent, CD_3CN (No addition of water).

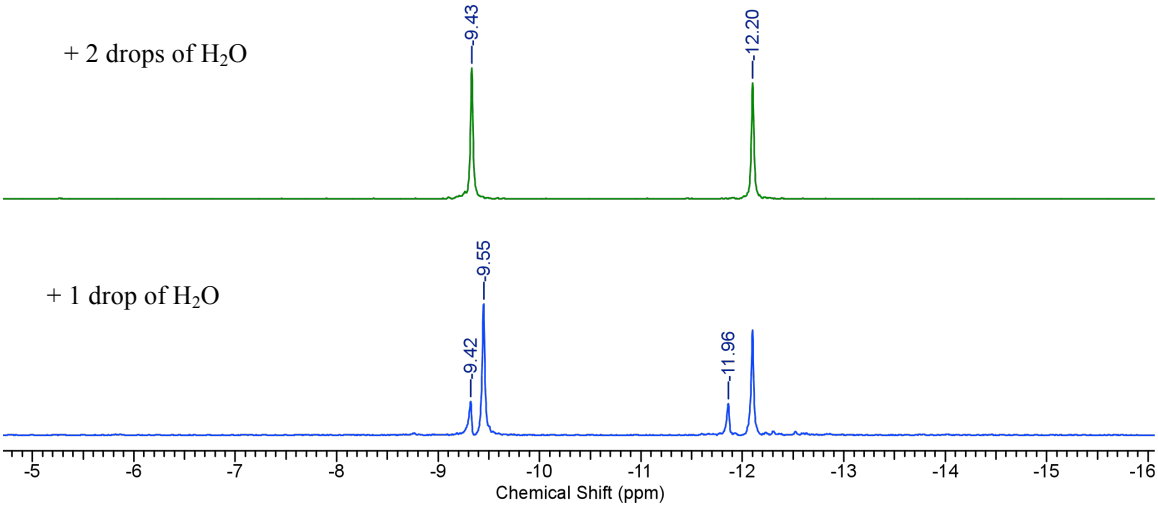

Figure 3.6. ^{31}P NMR data for $(NBu_4)_{7-n}H_n[Tc^{V}O(\alpha_2\text{-}P_2W_{17}O_{61})]$ showing the effect of the addition of water to a sample prepared by a the direct reaction of $(NBu_4)_{10-x}H_x[\alpha_2\text{-}P_2W_{17}O_{61}]$ and Tc(V). Solvent, CD_3CN.

Despite the compelling NMR data refuting the formation of a Tc-POM complex, the vibrant color changes observed for these reactions provide empirical evidence for the formation of a transition metal POM species, possibly in such small quantities as to be undetectable by ^{31}P NMR. To explore this hypothesis the lavender-purple and red-brown solids were crystallized from acetone/toluene to yield ellipsoidal dark purple and dark red crystals for the (α_2-$P_2W_{17}O_{61}$) and (α_1 -$P_2W_{17}O_{61}$) species respectively. Unfortunately these crystals were not of good enough quality to obtain crystal structures, but were characterized electrochemically (an analytical tool known to be more sensitive than ^{31}P NMR).

Figure 3.7 shows the CV of the ellipsoidal dark purple crystals obtained for the (α_2-$P_2W_{17}O_{61}$) species. This CV is very similar to that obtained for the $(NBu_4)_{7-n}H_n[Tc^VO(\alpha_2\text{-}P_2W_{17}O_{61})]$ complex as prepared via a metathesis reaction (Figure 3.8), and shows the two reversible $Tc^{V/VI}$ and $Tc^{VI/VII}$ couples in the positive potential region c.a. + 350 mV and + 700 mV respectively.

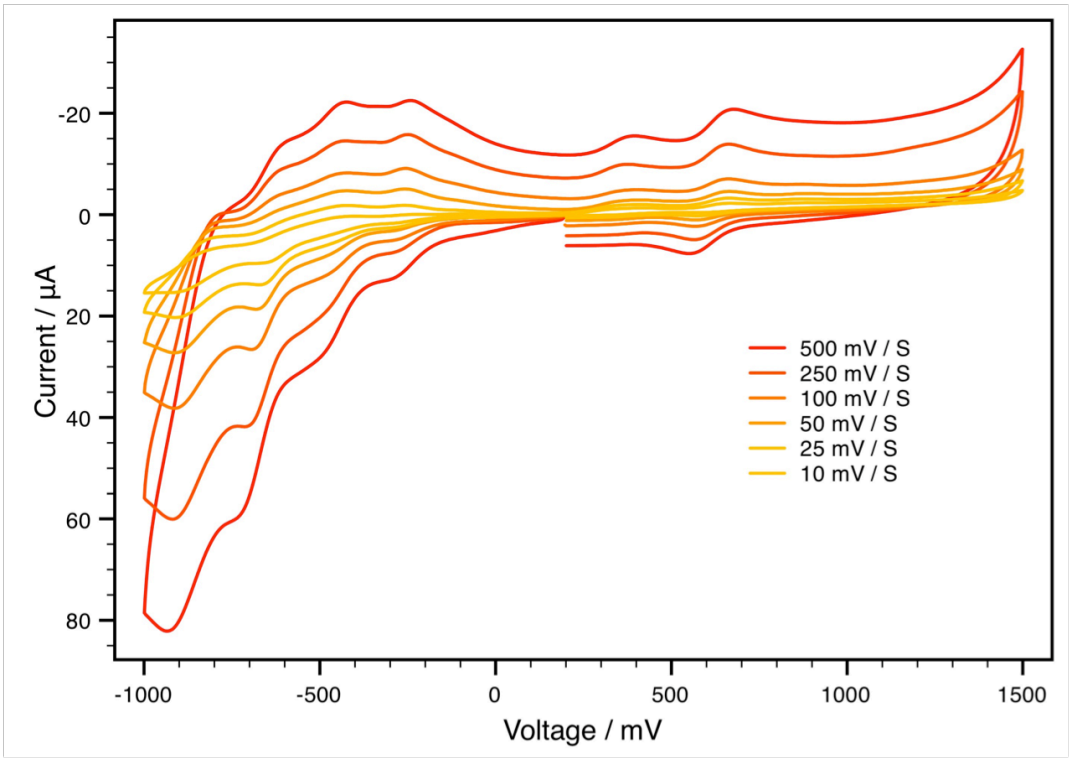

Figure 3.7 CV data for the dark purple crystals of $(NBu_4)_{7-n}H_n[Tc^VO(\alpha_2\text{-}P_2W_{17}O_{61})]$ (prepared via the direct method) at various scan rates. Electrolyte, 0.1M tetrabutylammonium hexafluorophosphate. Working electrode, glassy carbon, auxiliary electrode, platinum wire and reference electrode.

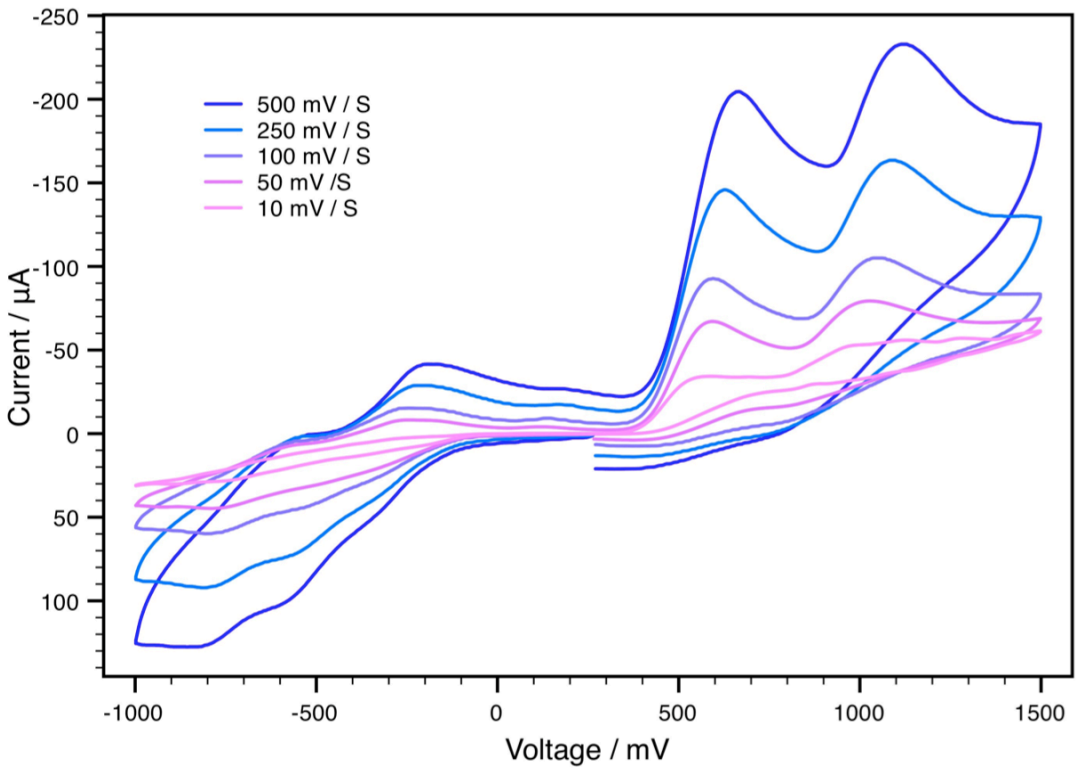

Figure 3.8 CV data of $(NBu_4)_{7-n}H_n[Tc^{V}O(\alpha_2\text{-}P_2W_{17}O_{61})]$ (prepared via a Metathesis reaction) at various scan rates. Electrolyte, 0.1M tetrabutylammonium hexafluorophosphate. Working electrode, glassy carbon, auxiliary electrode, platinum wire and reference electrode.

Although these couples are very small as compared to those attributed to the W framework (in the negative potential region), they are diagnostic for the Tc^{V} (α_2-$P_2W_{17}O_{61}$) complex and confirm the presence of Tc in the purple crystals. The presence of these Tc couples corroborate the formation of a very small amount of the $(NBu_4)_{6-n}H_n[Tc^{VI}O(\alpha_1/\alpha_2\text{-}P_2W_{17}O_{61})]$ complex via the direct synthetic method, albeit being too small to be detected by ^{31}P NMR.

In an attempt to explore the seemingly low reactivity of the $TBA_{10-x}H_x[\alpha_1/\alpha_2\text{-}P_2W_{17}O_{61}]$ ligands a series of solution experiments (Method 1.4) were conducted to examine the reaction between $(NBu_4)_{10-x}H_x[\alpha_2\text{-}P_2W_{17}O_{61}]$ and $(NBu_4)TcOCl_4$ directly. The $(NBu_4)_{10-x}H_x[\alpha_2\text{-}P_2W_{17}O_{61}]$ ligand was chosen for this study becasue of its increased

stability as compared to the $(NBu_4)_{10-x}H_x[\alpha_1\text{-}P_2W_{17}O_{61}]$ ligand. The experimental conditions are summarized in Table 3.1. The synthesis was attempted in two solvent systems (CH_2Cl_2 and acetonitrile) to probe the solubility of the $(NBu_4)_{10-x}H_x[\alpha_2\text{-}P_2W_{17}O_{61}]$ starting material. To overcome any thermodynamic parameters the reaction was heated under reflux conditions, and an attempt to circumvent any kinetic issues was achieved by sequentially increasing the Tc to POM mole ratio (in an effort to force the reaction equilibrium toward the formation of the desired product).

It was further postulated that the ligand binding site may be inaccessible to the Tc(V) starting material due to steric effects. The vacancy in the $(NBu_4)_{10-x}H_x[\alpha_2\text{-}P_2W_{17}O_{61}]$ POM structure exhibits four negatively charged oxygen atoms that allow for tetradentate chelation. If this site is inundated with protons these oxygens become unavailable for further binding. To ensure access to these oxygen atoms, triethylamine (Et_3N) was added to deprotonate the $(NBu_4)_{10-x}H_x[\alpha_2\text{-}P_2W_{17}O_{61}]$ ligand before the addition of the Tc(V) starting material.

Despite the above-mentioned attempts under a variety of experimental conditions, we found that in all cases using $(NBu_4)_{10-x}H_x[\alpha_2\text{-}P_2W_{17}O_{61}]$ and $(NBu_4)TcOCl_4$ directly, resulted in ^{31}P NMR resonances indicative of mostly unreacted $(NBu_4)_{10-x}H_x[\alpha_2\text{-}P_2W_{17}O_{61}]$ starting material. We postulate then, that the low reactivity of the $(NBu_4)_{10-x}H_x[\alpha_1/\alpha_2\text{-}P_2W_{17}O_{61}]$ ligands must be due to the inherent nature of the lacunary binding site in organic solvent.

3.3.5 Oxidation of Tc(V) Compounds.

Attempts at oxidation of Tc^{V} to Tc^{VI} in the $\alpha_2\text{-}P_2W_{17}O_{61}$ structure proved

unsuccessful in all cases. The resulting multinuclear NMR resonances are shown in Table 3.11. Attempts to achieve this oxidation were attempted in air, with Br_2, H_2O_2 and Ag^+ ($AgCF_3SO_3$). The addition of H_2O_2 resulted in decomposition of the complex to $(NBu_4)_6[P_2W_{18}O_{62}]$ (according to ^{31}P NMR, ^{99}Tc NMR and ^{183}WNMR) while stirring in air and the addition of both Br_2 and Ag^+ produced no noticeable effect.

Oxidation of Tc^V to Tc^{VI} in the α_1-$P_2W_{17}O_{61}$ was accomplished through the addition of a small amount of Br_2. Attempts to achieve this oxidation with both H_2O_2 and Ag Triflate proved unsuccessful. The addition of H_2O_2 resulted in decomposition of the complex to $(NBu_4)_6[P_2W_{18}O_{62}]$ (according to ^{31}P NMR, ^{99}Tc NMR and ^{183}W NMR) while the addition of Ag^+ had no observable effect.

The decomposition of the Tc-POM complexes to $(NBu_4)_6[P_2W_{18}O_{62}]$ was affirmed by multinuclear NMR spectroscopy. The plenary $P_2W_{18}O_{62}$ POM has a symmetrical structure with a plane of symmetry that cuts the molecule directly down the center. This results in only one type of P atom resonance and two types of W. This is depicted in Figure 3.9.

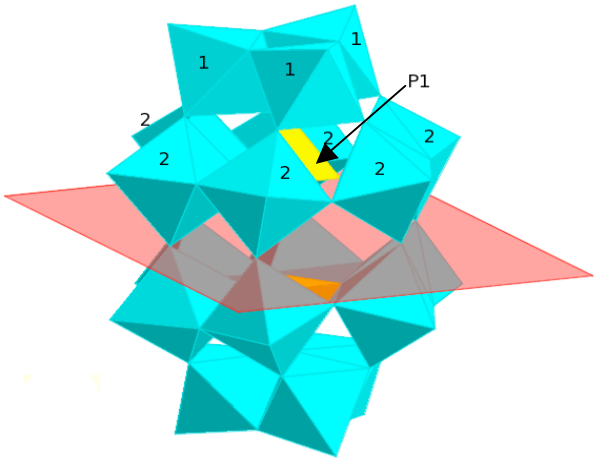

Figure 3.9. Polyhedral Representation of TBA6P2W1862 highlighting its plane of symmetry, resulting in only 1 type of P atom and 2 types of W atoms.

For both the α_1 and α_2 Tc complexes the ^{31}P NMR (after the addition of H_2O_2) shows only one resonance, representative of the two equivalent P atoms in the symmetrical $(NBu_4)_6[P_2W_{18}O_{62}]$ structure. This was further affirmed by ^{183}W NMR, where only 2 NMR resonances are seen. ^{99}Tc NMR run on these samples shows a resonance at -716 ppm. This resonance is indicative of TcO_4^-, suggesting that the Tc(V) has been fully oxidized to Tc(VII) and is no longer bound within the POM vacancy.

Starting Material and ^{31}P NMR shifts	Method	^{31}P NMR ppm	^{183}W NMR ppm	^{99}Tc NMR ppm
$(NBu_4)_{7-n}H_n[Tc^VO(\alpha_2\text{-}P_2W_{17}O_{61})]$ (-12.07, -12.37)	H_2O_2	-12.68	-120.9, -160.5	-716
	Br_2	-12.07, -12.37	-	-
	Ag^+	-12.07, -12.37	-	-
$(NBu_4)_{7-n}H_n[Tc^VO(\alpha_1\text{-}P_2W_{17}O_{61})]^{7-}$ (-12.44, -12.8)	H_2O_2	-12.68	-120.9, -160.5	-716
	Br_2	+ 38.96, -12.23	-	-
	Ag^+	-12.44, - 12.8	-	-

Table 3.11. Multinuclear NMR Data for the attempted oxidation of Tc(V) substitued α_1-$[P_2W_{17}O_{61}]^{10-}$ and α_2-$[P_2W_{17}O_{61}]^{10-}$ Wells-Dawson POMs. Solvent CD_3CN

These results can be explained by examining the theoretical reduction potentials of H_2O_2, Br_2 and Ag^+. These values (as measured in aqueous solution under standard conditions) confirm that H_2O_2 is the strongest oxidizing agent and Ag^+ the weakest.

$$H_2O_2 + 2\,H^+ + 2\,e^- \longrightarrow 2\,H_2O \qquad +1.77\ V$$

$$Br_2 + 2e^- \longrightarrow 2Br^- \qquad +1.07\ V$$

$$Ag^+ + e^- \longrightarrow Ag \qquad +0.80\ V$$

3.3.6 Ligand stability studies

To ensure that the multinuclear NMR resonances observed for the oxidation of the Tc(V) within the α_1-$[P_2W_{17}O_{61}]^{10-}$ and α_2-$[P_2W_{17}O_{61}]^{10-}$ vacancies were in fact due to the oxidation of the Tc, rather than a reaction between the ligand and the oxidizing agent, the stability of the α_1-$[P_2W_{17}O_{61}]^{10-}$ and α_2-$[P_2W_{17}O_{61}]^{10-}$ POMs was examined upon exposure to H_2O_2, Br_2 and Ag^+. The results are summarized in Table 3.12. Both (NBu_4) ligands proved stable to the effects of Br_2 and Ag^+ for up to 7 days, but showed complete decomposition to the parent $(NBu_4)_6[P_2W_{18}O_{62}]$ POM (within a few hours) upon the addition of H_2O_2. These results further corroborate that the ^{31}P NMR resonances observed for the addition of Br_2 to the $(NBu_4)_{7-n}H_n[Tc^VO(\alpha_1\text{-}P_2W_{17}O_{61})]^{7-}$ complex are due to the oxidation of the Tc(V) to Tc(VI) within the POM vacancy.

Starting Material and ^{31}P NMR shifts	Method	^{31}P NMR ppm
$TBA_{10-x}H_x[\alpha_2\text{-}P_2W_{17}O_{61}]$ (-9.48, -12.42)	H_2O_2	-12.68
	Br_2	-9.48, -12.42
	Ag^+	-9.48, -12.42
$TBA_{10-x}H_x[\alpha_1\text{-}P_2W_{17}O_{61}]$ (-10.66, -12.3)	H_2O_2	-12.68
	Br_2	-10.66, -12.3
	Ag^+	-10.66, -12.3

Table 3.12. Multinuclear NMR Data for the α_1-$[P_2W_{17}O_{61}]^{10-}$ and α_2-$[P_2W_{17}O_{61}]^{10-}$ Wells-Dawson POMs upon exposure to a variety of oxidizing agents. Solvent: CD_3CN; this set of experiments shows that both POMs are decomposed to α-$[P_2W_{18}O_{62}]^{6-}$ upon treatment with H_2O_2.

3.4 Conclusion

$Tc^{V}O$ complexes of the α_1-$[P_2W_{17}O_{61}]^{10-}$ and α_2-$[P_2W_{17}O_{61}]^{10-}$ lacunary Wells-Dawson polyoxometalates have successfully been synthesized as organic soluble tetrabutylammonium (NBu_4) salts by the direct metathesis of the aqueous soluble K salts. The syntheses are largely dependent on the purity of the $K_{7-n}H_n[Tc^{V}O(\alpha_1/\alpha_2P_2W_{17}O_{61})]$ starting materials. The $Tc^{VI}O$ complex of the α_1-$[P_2W_{17}O_{61}]^{10-}$ lacunary Wells-Dawson POM has been prepared by the oxidation of the Tc^{V} complex with bromine. The resulting complexes have been characterized by multinuclear NMR spectroscopy and electrochemical methods.

Despite attempts under a variety of experimental conditions, including a range of solvent systems (CH_2Cl_2 or Acetonitrile), pH conditions and reaction stoichiometries we found the synthesis of the $(NBu_4)_{7-n}H_n[Tc^{V}O(\alpha_1/\alpha_2\text{-}P_2W_{17}O_{61})]$ complex directly from the $(NBu_4)_{10-x}H_x[\alpha_1/\alpha_2\text{-}P_2W_{17}O_{61}]$ ligand unsuccessful, yielding only minimal amounts of the desired complex and primarily unreacted free $(NBu_4)_{10-x}H_x[\alpha_1/\alpha_2\text{-}P_2W_{17}O_{61}]$ ligand. Studies to probe the low reactivity of the α_1 and α_2 tetrabutylammonium (NBu_4) salts proved inconclusive.

We find that, in organic solution, the Tc metal center is more readily reduced in the lacunary α_2-site as compared to the α_1-site, which is in direct contrast to what was observed in aqueous solution. Experimentally determined free energy and HOMO-LUMO energy gap calculations corroborate this assertion.

3.5 References

1. Lyon, D. K.; Miller, W. K.; Novet, T.; Domaille, P. J.; Evitt, E.; Johnson, D. C.; Finke, R. G., *J. Amer. Chem. Soc.* **1991,** *113*, 7209-7221.

2. Davison, A.; Trop, H.; DePamphilis, B.; Jones, A., *Inorganic Synthesis* **1982,** *21*, 160.

3. Ciabrini, J.-P.; Contant, R., *J. Chem. Research (S) 1993, 391* **1993**, 2720-2744.

4. Contant, R., *Inorg. Synth.* **1990,** *27*, 71-111.

5. Bartis, J.; Dankova, M.; Blumenstein, M.; Francesconi, L. C., *Journal of Alloys and Compunds* **1997,** *249*, 56-68.

6. Keita, B.; Girard, F.; Nadjo, L.; Contant, R.; Belghiche, R.; Albessi, M., *J. Electroanal. Chem.* **2001,** *508* (1-2), 70 - 80.

7. Graham, C. R.; Ott, L. S.; Finke, R. G., *Langmuir* **2009,** *25*, 1327 - 1336.

8. Venturelli, A.; Nilges, M. J.; Smirnov, A.; Belford, R. L.; Francesconi, L. C., *J. Chem. Soc., Dalton Trans.* **1999**, 301-310.

9. Finke, R. G.; Rapko, B.; Saxton, R. J.; Domaille, P. J., *J. Am. Chem. Soc.* **1986,** *108*, 2947-2960.

10. Finke, R. G.; Droege, M. W.; Domaille, P. J., *Inorg. Chem.* **1987,** *26*, 3886-3896.

11. Finke, R. G.; Lyon, D. K.; Nomiya, K.; Sur, S.; Mizuno, N., *Inorg. Chem.* **1990,** *29* (10), 1784-1787.

12. Jorris, T. L.; Kozik, M.; Casan-Pastor, N.; Domaille, P. J.; Finke, R. G.; Miller, W. K.; Baker, L. C. W., *J. Am. Chem. Soc.* **1987,** *109*, 7402-7408.

13. Bartis, J.; Kunina, Y.; Blumenstein, M.; Francesconi, L. C., *Inorg. Chem.* **1996,** *35* (5), 1497-1501.

14. Sadakane, M.; Dickman, M. H.; Pope, M. T., *Inorg. Chem.* **2001,** *40* (12), 2715-2719.

15. Sadakane, M.; Ostuni, A.; Pope, M. T., *J. Chem. Soc. Dalton Trans.* **2002**, 63-67.

16. Salmonte, J. L.; Pope, M. T., *Canadian Journal of Chemistry* **2001,** *79* (5/6), 802-808.

17. Bartis, J.; Sukal, s.; Dankova, M.; Kraft, E.; Kronzon, R.; Blumenstein, M.; Francesconi, L. C., *J. Chem. Soc., Dalton Trans* **1997**, 1937-1944.

18. Bartis, J.; Dankova, M.; Lessmann, J. J.; Luo, Q.-H.; Horrocks, W. D., Jr.; Francesconi, L. C., *Inorganic Chemistry* **1999,** *38*, 1042-1053.

19. Boglio, C.; Lenoble, G.; Duhayon, C.; Hasenknopf, B.; Thouvenot, R.; Zhang, C.; Howell, R. C.; Burton-Pye, B. P.; Francesconi, L. C.; Lacote, E.; Thorimbert, S.; Malacria, M.; Afonso, C.; Tabet, J.-C., *Inorg. Chem.* **2006,** *45* (3), 1389-1398.

20. Howell, R. C.; Perez, F. G.; Jain, S.; Horrocks, W. D., Jr.; Rheingold, A. L.; Francesconi, L. C., *Angew. Chem. Int. Ed.* **2001,** *40*, 4301-4304.

21. Zhang, C.; Howell, R. C.; Scotland, K. B.; Perez, F. G.; Todaro, L.; Francesconi, L. C., *Inorg. Chem.* **2004,** *43*, 7691-7701.

22. Zhang, C.; Howell, R. C.; Luo, Q.; Fieselmann, H. L.; Todaro, L.; Francesconi, L. C., *Inorg. Chem.* **2005,** *44*, 3569-3578.

23. Zhang, C.; Bensaid, L.; McGregor, D.; Fang, X.; Howell, R. C.; Burton-Pye, B.; Q., L.; Todaro, L.; Francesconi, L. C., *Journal of Cluster Science* **2006,** *17*, 389-426.

24. Keita, B.; Girard, F.; Nadjo, L.; Contant, R.; Canny, J.; Richet, M., *Journ. of Electroanal. Chem.* **1999,** *478*, 76-82.

25. Contant, R.; Richet, M.; Lu, Y. W.; Keita, B.; Nadjo, L., *Eur. J. Inorg. Chem.* **2002**, 2587-2593.

Chapter 4: Reduction of the pertechnetate (TcO_4^-, Tc^{VII}) using POMs

4.1 Introduction

^{99}Tc comprises a large component of radioactive waste found in waste tanks at Hanford, Savannah River and Melton Valley, as well as water and soil samples around national laboratory sites. The recognized chemistry of Tc suggests that under aerobic conditions and in a basic environment, the thermodynamically stable heptavalent pertechnetate anion (TcO_4^-) exists. This oxyanion it exists as the heptavalent pertechnetate anion (TcO_4^-), which is the most thermodynamically stable form of Tc at high pH 17[1], migrates easily through the environment and does not sorb well onto mineral surfaces, soils or sediments.[2-4] The long half-life, and the high mobility of the pertechnetate anion in the environment create a particular concern and the need for remediation strategies.

One of the most commonly considered potential strategies for ^{99}Tc remediation is focused on pertechnetate reduction. The idea is that the mobile pertechnetate ion can be removed from solution by reduction to insoluble, lower-valence Tc(IV) species (such as $^{99}TcO_2 \bullet nH_2O$), which can then be physically adsorbed to a solid surface, or mixed with glass, cement or ceramic. Unfortunately, it has been found that the reduced $^{99}Tc(IV)$ in the form of all the aforementioned amorphous oxides is prone to re-oxidation. Upon re-oxidation all ^{99}Tc (IV) species hydrolyze back to the mobile $^{99}Tc(VII)$ ($^{99}TcO_4^-$) anion.[2]

In radiopharmaceutical chemistry the focus has been on not merely physical absorption to a solid surface, but rather chemical incorporation into the bonds of another molecule. ^{99m}Tc, as pertechnetate, is reduced by stannous ion in the presence of ligands,

which act to form a complex with the resulting low-valent Tc species. Herein we have developed a new strategy for the reduction and complexation of ^{99}Tc using a single material (Polyoxometalates) both to reduce pertechnetate as well as sequester the resulting low valent ^{99}Tc species.

Because POMs can undergo stepwise, multi-electron redox reactions, while maintaining their structural integrity[5], they have been used in the literature for the reduction of metal ions to their metallic state.[6-9] In this chapter a variety of POMs (See figure 4.1) will be explored for the reduction of the mobile Tc^{VII} anion, pertechnetate, to either a non mobile Tc^{IV} species or to the metallic Tc^{0} state. Among them the α_2-$[P_2W_{17}O_{61}]^{10-}$ Wells Dawson POM, the highly reducing and stable $(AlW_{12}O_{40})^{5-}$ Keggin POM, and non-Keggin wheel shaped $(P_8W_{48}O_{184})^{40-}$.

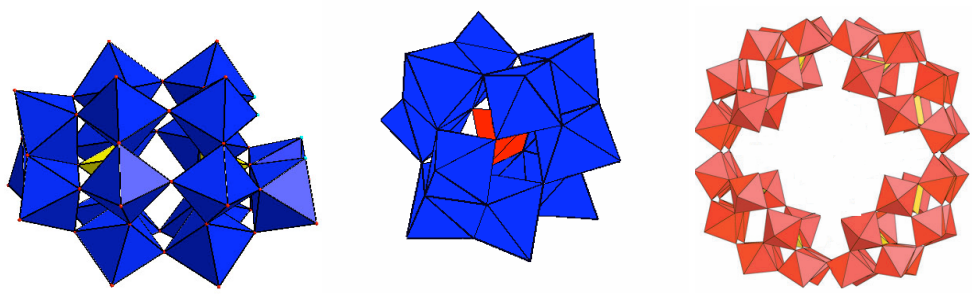

Figure 4.1. a) The α_2-$[P_2W_{17}O_{61}]^{10-}$ Wells Dawson structure. b) The KEGGIN $[AlW_{12}O_{40}]^{5-}$ c) The wheel shape non-Keggin $[P_8W_{48}O_{184}]^{40-}$ structure.

Two simple methods were chosen for reduction; the first is the electrochemical reduction using bulk electrolysis (electrolysis experiment performed by Dr. Israel Mbomekalle), and the second the reduction of each POM using visible light in the presence of a sacrificial organic ligand, which would act as an electron donor. Propan-2-

ol (Isopropyl Alcohol, IPA) was chosen as the sacrificial electron donor because it has been used in the literature to aid in the reduction of $(PW_{12}O_{40})^{3-}$ and $(SiW_{12}O_{40})^{4-}$ when exposed to aqueous metal ions, such as Ag^{+}, $AuCl_4^{-}$, Pd^{2+}, $PtCl_6^{2-}$ and Hg^{2+}.[10-12]

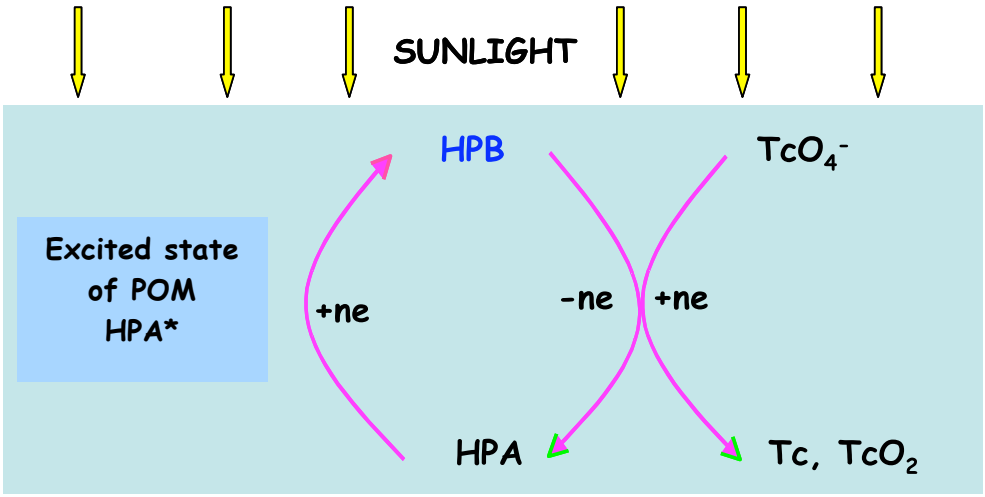

Figure 4.2. Proposed mechanism for the photolytic reduction of POMs; Sunlight irradiates the oxidized form of the POM (HPA) causing its promotion to an excited state where it is able to pick up electrons for its reduction to the electron rich reduced POM (Heteroplyblue, HPB). The HPB is then able to transfer electrons to TcO_4^- (for its reduction to a lower valent state) while regenerating the parent HPA.

There are several postulated mechanisms by which the photolytic reduction of POMs may occur. Figure 4.2 outlines one such mechanism. In figure 4.2 HPA indicates the parent Heteropolyacid (or oxidized form of the POM), and HPB indicates the Heteroplyblue (or reduced form of the POM). When the sample is irradiated by sunlight the HPA becomes promoted to an excited state where it is able to pick up an electron, to generate the reduced HPB.

$$HPA + Solvent \longleftrightarrow HPA^* \longleftrightarrow HPB + Solvent$$

The reduced POM (HPB) is then able to transfer electrons to TcO_4^- (for its reduction to Tc^V, Tc^0 or TcO_2) while regenerating the parent HPA.

$$HPB + TcO_4^- \longleftrightarrow HPA + \text{reduced Tc } (Tc^V, Tc^0, TcO_2)$$

By this mechanism the POM is regenerated with each new reduction cycle to act as a catalyst for the continued reduction of TcO_4^-.

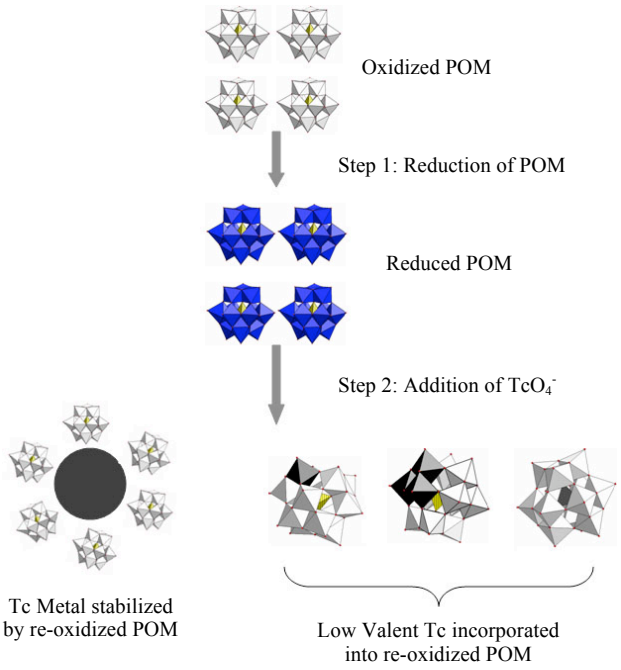

Figure 4.3. Proposed use of POMs as UV-switchable reducing agents in the reduction of TcO_4^-.

Upon reduction of pertechnetate, the oxidized form of the POM is regenerated and will likely stabilize the resulting low valent Tc species. Figure 4.3 illustrates this schematically. The oxidized POM is reduced to yield a 1 or 2 electron reduced POM. TcO_4^- is then added and subsequently gains electrons from the reduced POM to yield either Tc^0, or Tc^{IV}. The reduction to Tc^{IV} is accompanied by incorporation of the Tc into

the bonds of the polyoxometalate, while reduction to the Tc^0 metal should result in the adherence of the POM to the of the Tc^0 particle, thereby passivating it.

4.2 Experimental

4.2.1 General

^{99}Tc is a weak β- emitter with a half-life of 2 x 10^5 years. All reported Tc manipulations were performed in an appropriately equipped lab approved for the use of low-level radioactivity. Correct and suitable radioactive material handling procedures were employed. All materials were purchased as reagent grade and used without further purification. Pure water was used throughout, and was obtained using a Millipore Direct Q5 system (conductivity =18 μΩ).

Solid ammonium pertechnetate (NH_4TcO_4) was purchased from Oak Ridge National Laboratory. Pure NH_4TcO_4 is a white crystalline solid, but appears black in color upon radiolytic autoreduction to TcO_2. To regenerate pure pertechnetate the raw NH_4TcO_4 was dissolved in water and heated with hydrogen peroxide until the volume had decreased by half. The resulting aqueous solution was standardized using a well-established UV-Vis protocol.[13] All POMs were prepared as described in the literature; the aqueous soluble α_2-$P_2W_{17}O_{61}^{10-}$, $(P_8W_{48}O_{184})^{40-}$ and $(AlW_{12}O_{40})^{5-}$ were prepared as described in Inorganic Synthesis.[14] UV-Vis data was collected on a Varian Cary 50 UV-Visible Spectrophotometer at 300K.

4.2.2. Collection of NMR Data.

NMR data were collected on a JEOL GX-400 spectrometer using 5 or 10 mm NMR tubes fitted with a Teflon insert (purchased from Wilmad Glass). ^{31}P NMR data were collected at 161.8 MHz. Chemical shifts are given with respect to external 85% H_3PO_4. Typical acquisition parameters for ^{31}P spectra included the following: spectral width, 10000 Hz; acquisition time, 0.8 s; pulse delay, 1 s; pulse width, 15 μs (50° tip angle). From 200 to 1000 scans were required. From 1000 to 3000 scans were acquired. For all spectra, the temperature was controlled to ± 0.2 deg. For the chemical shifts, the convention used is that the more negative chemical shifts denote more upfield resonances.

4.2.3 Collection of Electrochemical Data.

Electrochemical data were obtained using a BAS Voltammetric Analyzer System controlled by BAS CV-50W software (for PC).

The cell used for cyclic voltammetry (CV) contained a glassy-carbon working electrode (BAS standard disk electrode, 3 mm OD), a Pt wire auxiliary electrode (0.5 mm), and a BAS Ag/AgCl (3M NaCl) reference electrode. Prior to obtaining electrochemical data, solutions were de-aerated for at least 30 min with high purity argon (Ar). Fine polishing of the glassy-carbon working electrode was adapted from the procedure of Keita and co-workers.[15] Unless otherwise noted, scan rates were 10 mV/s, and all experiments were carried out at ambient temperature under an Ar atmosphere.

Electrochemical reduction was achieved using Bulk Electrolysis in a BAS Bulk Electrolysis cell. The working electrode was a reticulated glassy carbon cage, the

auxiliary electrode was a platinum wire placed in a separated compartment and the reference electrode was Ag/AgCl in 3 M NaCl.

4.2.4 Samples for Characterization at pH=0.33

TcO_4^-: A 10^{-4} M clear colorless solution of TcO_4^- was characterized electrochemically in 0.5 M H_2SO_4 at pH = 0.33. The cyclic voltammetry experiment was performed with a scan rate of 10 mV/s, a glassy carbon working electrode, a platinum wire auxiliary electrode and a Ag/AgCl (in 3 M NaCl) reference electrode.

POMs: 10^{-3} M solutions of all POMs ($[\alpha_2\text{-}P_2W_{17}O_{61}]^{10-}$, $[P_8W_{48}O_{184}]^{40-}$ and $[AlW_{12}O_{40}]^{5-}$) in a 0.5 M H_2SO_4 solution at pH = 0.33 were characterized electrochemically as well as by ^{31}P NMR for P containing compounds. For α_2-$P_2W_{17}O_{61}^{10-}$, ^{31}P characterizations were completed on 5 mM and 30 mM samples. The experiments were performed immediately upon making the solutions and then again 26 hours later for CV and monitored by ^{31}P NMR for up to 7 days. The POMs were stable to degradation under these conditions.

4.2.5 Electrochemical Reduction of α_2-$[P_2W_{17}O_{61}]^{10-}$

A clear colorless 10^{-3} M solution of pure α_2-$[P_2W_{17}O_{61}]^{10-}$ (245 mg) in 0.5 M H_2SO_4 (50 mL) was placed in an electrolysis cell and purged with nitrogen for about 30 min, after which a potential of -200 mV was applied to the working electrode. Immediately upon applying the potential the clear colorless solution became a deep blue (which is characteristic of reduced POMs). This blue solution re-oxidizes and becomes clear when exposed to air and so must be kept in an inert atmosphere.

4.2.6 Photolytic Reduction of α_2-$P_2W_{17}O_{61}^{10-}$, $(P_8W_{48}O_{184})^{40}$ and $(AlW_{12}O_{40})^{5-}$.

^{31}P NMR Samples: 10 mL of 30 mM POM solution (α_2-$[P_2W_{17}O_{61}]^{10-}$ and $[P_8W_{48}O_{184}]^{40-}$) was prepared in 50% D_2O:H_2SO_4 and isopropyl alcohol (33 % by volume, 1 mL) was added. 2 mL of the stock solution was place in a 10 mL NMR tube under Argon and sealed with parafilm. The samples were exposed to sunlight and after 1 to 3 days of exposure a color change from clear and colorless to blue/purple was observed, which is indicative of POM reduction.

Electrochemistry and UV-Vis Samples: 10^{-3} M solutions of all POMS (α_2-$[P_2W_{17}O_{61}]^{10-}$, $[P_8W_{48}O_{184}]^{40-}$ and $[AlW_{12}O_{40}]^{5-}$) were prepared in 0.5 M H_2SO_4 containing 30% IPA and sealed in a 20 mL glass vial under argon. The samples were placed on the window ledge for exposure to sunlight. Initially all solutions were clear and colorless but over the course of one week all solutions produced a blue color that is indicative of POM reduction.

4.2.7 Preparation of TcO_4^- Samples

4.2.7.1 For reduction by electrochemically reduced α_2-$[P_2W_{17}O_{61}]^{12-}$

A slight excess of 0.2 M TcO_4^- solution was added to an already prepared 10^{-3} M solution of the electrochemically reduced α_2-$[P_2W_{17}O_{61}]^{12-}$ and an immediate change from blue to orange was observed.

4.2.5.2 For reduction by photolytically reduced POMs

^{31}P NMR Samples: 30 mM solutions of POM (α_2-$[P_2W_{17}O_{61}]^{10-}$, and $[P_8W_{48}O_{184}]^{40-}$) in 50% D_2O:H_2SO_4 containing 30 % IPA (by volume, 1 mL) were prepared directly in a 5 mL NMR tube (without a Teflon liner). A slight excess of ~ 0.2 M TcO_4^- solution was added and the tube sealed with parafilm under argon. The samples were exposed to sunlight and after 1 to 7 days of exposure a color change from clear and colorless to orange or red was observed.

Electrochemistry and UV-Vis Samples: A slight excess of ~ 0.2 M TcO_4^- solution was added to a 10^{-3} M solution of POM (α_2-$[P_2W_{17}O_{61}]^{10-}$, $[P_8W_{48}O_{184}]^{40-}$ and $[AlW_{12}O_{40}]^{5-}$) prepared in 0.5 M H_2SO_4 containing 30% IPA . The vials were sealed under Argon, sealed with parafilm and exposed to sunlight. Within 24 hours a color change from blue to orange was observed.

4.3 Results and Discussion

4.3.1 Characterization of TcO_4^-

Figure 4.4 shows the CV profile of a 10^{-4} M solution of TcO_4^-. From the CV the reduction of TcO_4^- occurs at -500 mV vs. Ag/AgCl. The crossing of the current observed a -300 mV indicates deposition of a solid material (possibly TcO_2 or Tc^0) on the working electrode. The symetrical gaussian wave located at +650 mV indicated the dissolution of the adsorbed compound during the re-oxidation process.

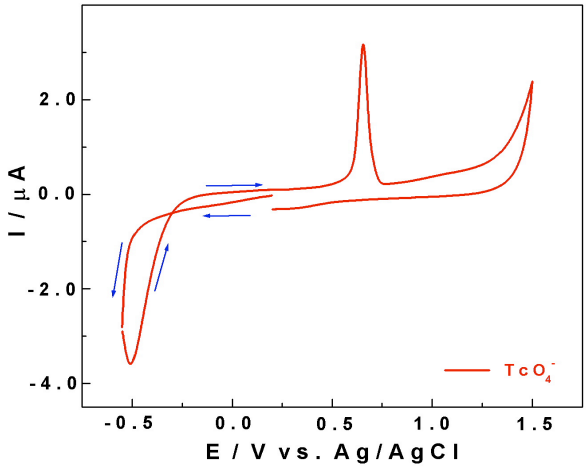

Figure 4.4. CV profile of 10^{-4} M TcO_4^- in 0.5 M H_2SO_4 at pH = 0.33. Glassy carbon working electrode, platinum wire auxillary electrode, Ag/AgCl working electrode and scan rate of 10 $mV.s^{-1}$

4.3.2 Reduction of TcO_4^- using electrochemically reduced α_2-$[P_2W_{17}O_{61}]^{10-}$

Figure 4.5 shows the standard reduction potentials for the reduction of Tc(VII) to either Tc(0) or Tc(IV) as a function of pH. This figure clearly illustrates that the reduction of TcO_4^- is favored at low pH. Because lacunary POMs such as α_2-$[P_2W_{17}O_{61}]^{10-}$ are known to decompose to their plenary parent POMs in acidic media (under pH = 3), the compound had to be fully characterized at pH 0.33 before its redox properties could be exploited for the reduction of pertechnetate. The compound was found to be fairly stable at pH 0.33.

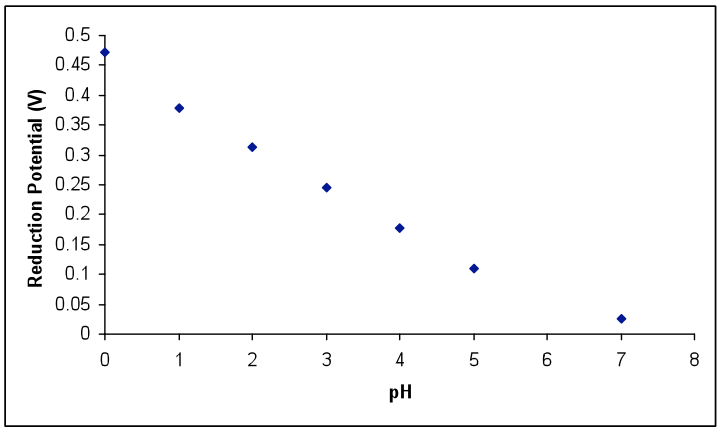

$TcO_4^- + 8H^+ + 7e^-$ $Tc_{(s)} + 4H_2O$

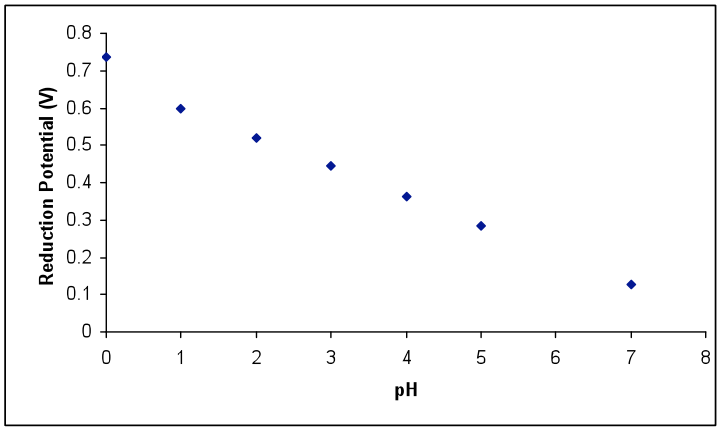

$TcO_4^- + 4H^+ + 3e^-$ $TcO_{2(s)} + 2H_2O$

Figure 4.5. Reduction potentials of Tc(VII) reduction as a function of pH. Reduction Potentials (vs. NHE) become more negative with increasing pH thus indicating that reduction of TcO_4^- is favored at lower pHs.

Figures 4.6 and 4.7 show the ^{31}P NMR for 2 concentrations of α_2-$[P_2W_{17}O_{61}]^{10-}$ (5 mM and 30 mM respectively) at pH = 0.33. Over the course of 1 week there is only a minimal amount of decomposition to the parent α-$[P_2W_{18}O_{62}]^{6-}$ for the low concentration

samples (see Figure 4.6), while a significant amount of decomposition is observed for the higher concentration (see Figure 4.7).

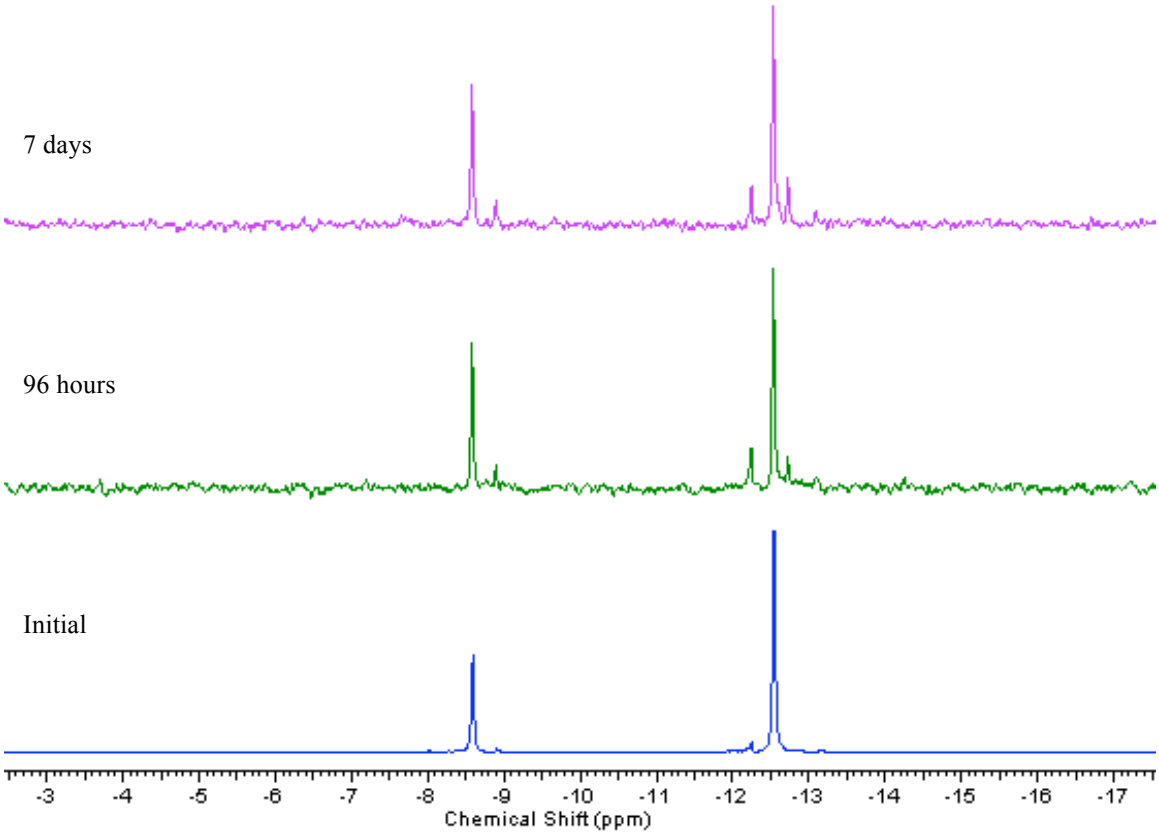

Figure 4.6. ^{31}PNMR spectrum of 5 mM α_2-$[P_2W_{17}O_{61}]^{10-}$ at pH 0.33 as monitored over the course of 1 week.

In Figure 4.6 two distinct resonances at -8.7 and -12.64 ppm persist for up to 1 week. These resonances are indicative of pure α_2-$[P_2W_{17}O_{61}]^{10-}$. Decomposition of α_2-$[P_2W_{17}O_{61}]^{10-}$ to the parent α-$[P_2W_{18}O_{62}]^{6-}$ is not observed until 96 hours in solution, as indicated by the appearance of the minor resonances at -9.09, -12.34 and -12.83 ppm. The resonance at -12.83 ppm is indicative of α-$[P_2W_{18}O_{62}]^{6-}$. Notably this resonance remains small in comparison to the α_2-$[P_2W_{17}O_{61}]^{10-}$ ligand peaks for up to 7 days. This means

there is only a minimal breakdown in the α_2-$[P_2W_{17}O_{61}]^{10-}$ POM structure, indicating the relative stability of this POM under these experimental conditions and at low concentration.

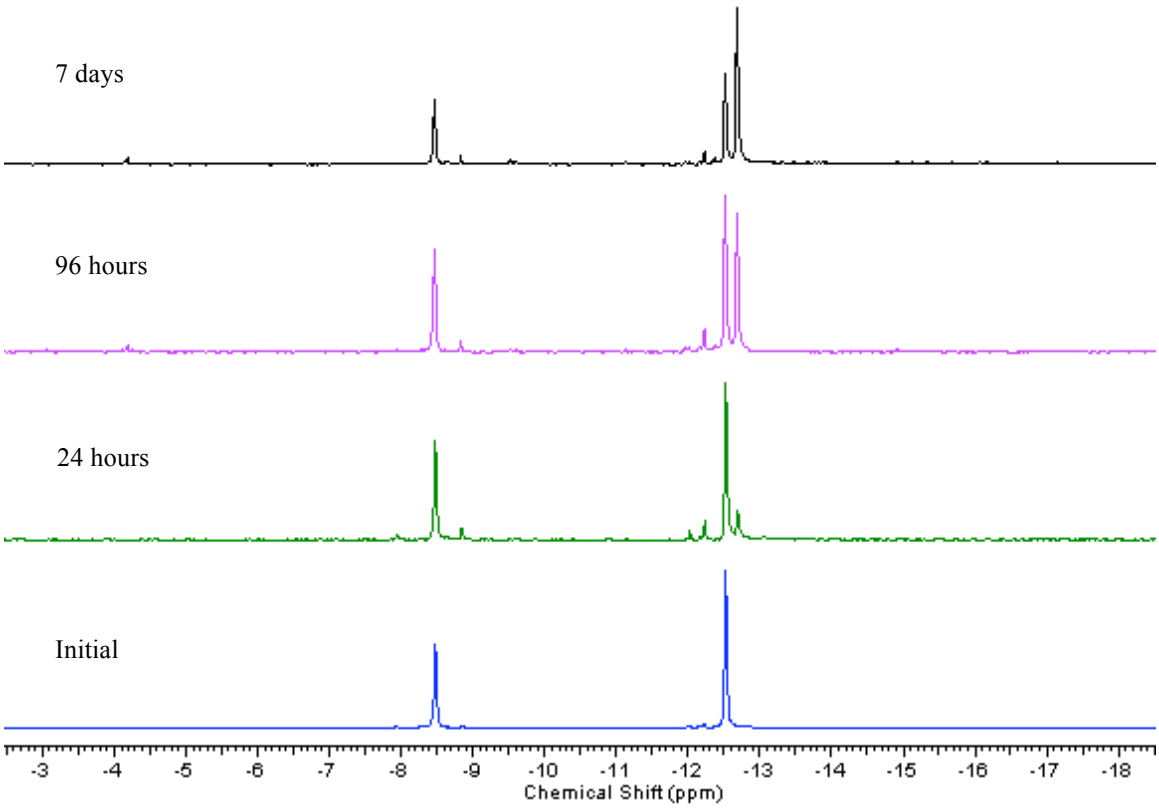

Figure 4.7. ^{31}PNMR spectrum of 30 mM α_2-$[P_2W_{17}O_{61}]^{10-}$ at pH 0.33 as monitored over the course of 1 week.

In Figure 4.7 the decomposition of α_2-$[P_2W_{17}O_{61}]^{10-}$ to the parent α-$[P_2W_{18}O_{62}]^{6-}$ is observed after 24 hours in solution (as indicated by the appearance of the minor resonances at -9.09, -12.34 and -12.83 ppm). The resonance at -12.83 ppm is indicative of α-$[P_2W_{18}O_{62}]^{6-}$ and continues to grow in over time. After 1 week the resonance for α-$[P_2W_{18}O_{62}]^{6-}$ is larger than those that represent the α_2-$[P_2W_{17}O_{61}]^{10-}$ ligand. This means

that at higher concentrations there is a significant breakdown in the α_2-$[P_2W_{17}O_{61}]^{10-}$ POM structure after 1 week.

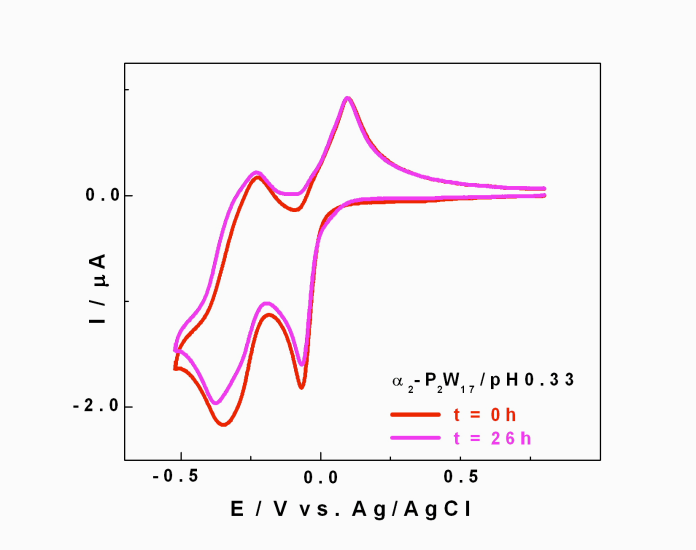

Figure 4.8 CV of 10^{-3} M α_2-$[P_2W_{17}O_{61}]^{10-}$ at pH=0.33. The red trace represents the first two reduction waves of the compound as soon as it is dissolved in the medium and the pink trace is this same solution 26 hours later.

Figure 4.8 shows the CV of α_2-$[P_2W_{17}O_{61}]^{10-}$ at pH = 0.33. The CV data is collected on a 10^{-3} M sample and is restricted to the 2 first reduction waves; both of which are 2 electron reversible redox processes (as determined by Bulk Electrolysis). These waves represent the reduction of the tungsten framework. Comparison of these waves to those of a 10^{-3} M solution of α-$[P_2W_{18}O_{62}]^{6-}$ (The parent Wells-Dawson POM) under the same experimental conditions can be seen in Table 4.1.

Even though lacunary POMs such as α_2-$[P_2W_{17}O_{61}]^{10-}$ are known to decompose to their plenary parent POMS in acidic media (under pH = 3), these results (both ^{31}P NMR and CV) clearly show that even after 24 hours, no substantial amount of α-

$[P_2W_{18}O_{62}]^{6-}$ can be seen at low concentrations, confirming the stability of the compound in this medium and at low pH.

	1st wave		2nd wave		3rd wave	
	E_c (mV)	$E_{1/2}$(mV)	E_c (mV)	$E_{1/2}$(mV)	E_c (mV)	$E_{1/2}$(mV)
α_2-$[P_2W_{17}O_{61}]^{10-}$	-60 (2e)	+21	-340 (2e)	-285	-650(2e)	-610
α-$[P_2W_{18}O_{62}]^{6-}$	-5 (1e)	+28	-140 (1e)	-108	-390 (2e)	-363

Table 4.1. α_2-$[P_2W_{17}O_{61}]^{10-}$ and $[P_2W_{18}O_{62}]^{6-}$ W-reduction peak potentials, E_{pc}, and half-wave potentials, $E_{1/2}$ (defined as $E_c + E_a$) /2). All potentials are measured in 0.5 M H_2SO_4 pH = 0.33.

Following its characterization at low pH the α_2-$[P_2W_{17}O_{61}]^{10-}$ POM was electrochemically reduced by 2 electrons using Bulk Electrolysis:

$$\alpha_2\text{-}[P_2W_{17}O_{61}]^{10-} + 2e^- \longrightarrow \alpha_2\text{-}[P_2W_{17}O_{61}]^{12-}$$

Figure 4.9 shows a comparison of the CV's for both the oxidized α_2-$[P_2W_{17}O_{61}]^{10-}$ and reduced α_2-$[P_2W_{17}O_{61}]^{12-}$ forms of this POM. The changes in the first reduction wave of the α_2-$[P_2W_{17}O_{61}]^{12-}$ (Figure 4.9b) clearly show the formation of a new compound. The single 2 e^- reduction wave present at -60 mV for the oxidized species splits into two 1 e^- reduction waves for the reduced species (Figure 4.9, Table 4.2). It is conceivable that upon reduction this wave becomes more resolved due to the delocalization of added electrons around the belt W's which cause a change in the symmetry.

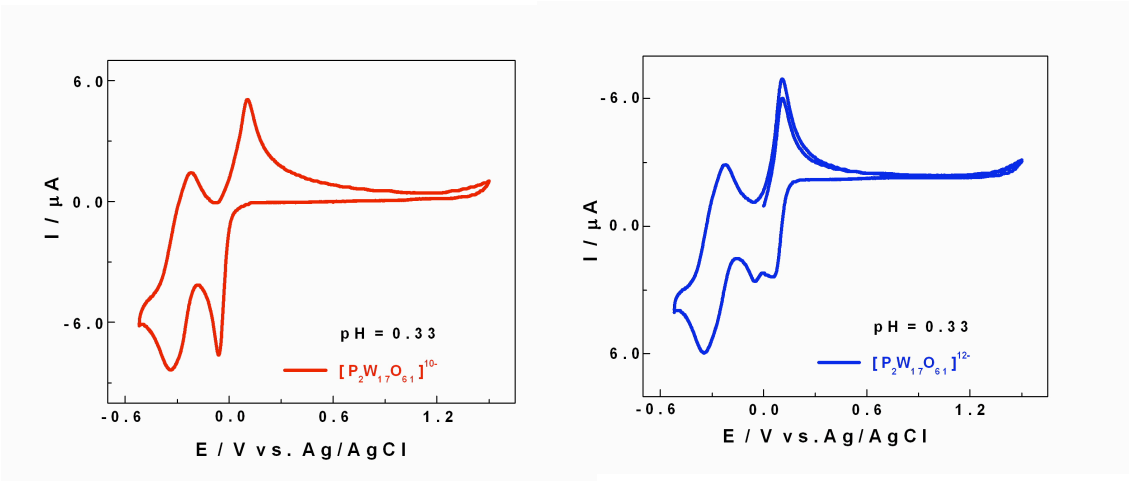

a) b)

Figure 4.9. Cyclic voltammograms of a) 10^{-3} M α_2-$[P_2W_{17}O_{61}]^{10-}$ and b) 10^{-3} M α_2-$[P_2W_{17}O_{61}]^{12-}$ in 0.5 M H_2SO_4 pH = 0.33. The scan rate was 10 $mV.s^{-1}$, the working electrode was glassy carbon, the auxiliary electrode was a platinum wire and the reference electrode was Ag/AgCl in 3 M NaCl.

When a slight excess of 0.2 M TcO_4^- solution is added to the 10^{-3} M blue solution of two-electron reduced α_2-$[P_2W_{17}O_{61}]^{10-}$ an immediate color change from blue to orange is observed. Figure 4.10 shows the CV data for the two-electron reduced α_2-$[P_2W_{17}O_{61}]^{12-}$ (blue trace) and the two-electron reduced α_2-$[P_2W_{17}O_{61}]^{12-}$ plus TcO_4^- (orange trace). The CV profile of this orange solution shows two new redox couples in the positive potential region, and does not match that of either the unreduced α_2-$[P_2W_{17}O_{61}]^{10-}$ or the two-electron reduced α_2-$[P_2W_{17}O_{61}]^{12-}$ (shown in Figure 4.9). These redox couples are attributed to Tc reduction processes and the CV is identical to tha obtained for the chemically synthesised $K_{7-n}H_n[Tc^{V}O(\alpha_2P_2W_{17}O_{61})]$ compound (at pH = 0) from chapter 2. This clearly indicates the formation of a new species upon addition of the TcO_4^-, implying that the Tc^{VII} is in fact being reduced and possibly sequestered by the reduced α_2-$[P_2W_{17}O_{61}]^{12-}$. This finding proved significant as it encouraged the

continuation of this study to include the photolytic reduction of POMs for the reduction of TcO_4^-.

pH = 0.33	E_{a1} (mV)	E_{a2} (mV)
α_2-$[P_2W_{17}O_{61}]^{10-}$	+102	-60
α_2-$[P_2W_{17}O_{61}]^{12-}$	+106	+60 (-48)

Table 4.2. First wave reduction (E_{c1}) and oxidation (E_{a1}) potentials for 10^{-3} M α_2-$[P_2W_{17}O_{61}]^{10-}$ (shown in red) and 10^{-3} M α_2-$[P_2W_{17}O_{61}]^{12-}$ (shown in blue) in 0.5 M H_2SO_4 pH = 0.33.

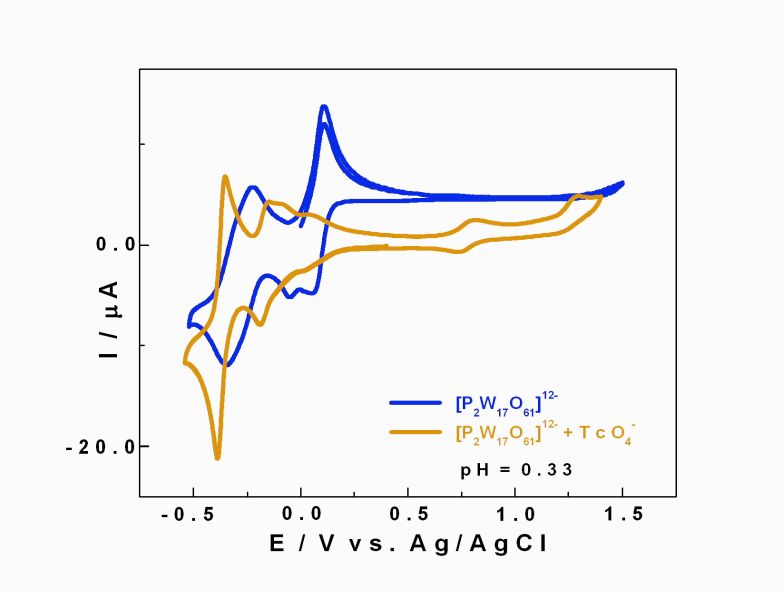

Figure 4.10. CV data for α_2-$[P_2W_{17}O_{61}]^{12-}$ (blue trace) and α_2-$[P_2W_{17}O_{61}]^{12-}$ plus TcO_4^- (orange trace) in 0.5 M H_2SO_4 pH = 0.33. Glassy carbon working electrode, platinum wire auxillary electrode, Ag/AgCl working electrode and scan rate of 10 mV.s$^-$

Figure 4.11 shows a comparison of the reduction of TcO_4^- by α_2-$[P_2W_{17}O_{61}]^{12-}$ to that of ReO_4^- under the same experimental conditions. This comparison reveals that the

reductions due to Tc occur at more possitive potentials than those of Re. This indicates that Tc^{VII} is more easily reduced than Re^{VII} under these conditions. This finding is consistent with the theoretical reduction potentials of Tc and Re, which indicate the ease of reduction for Tc as compared to Re.

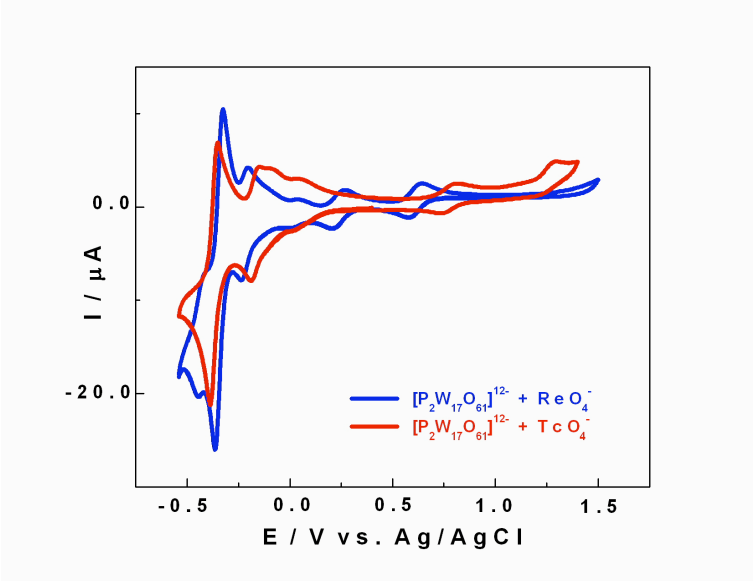

Figure 4.11. CV data for TcO_4^- and α_2-$[P_2W_{17}O_{61}]^{12-}$ (red trace) and ReO_4^- and α_2-$[P_2W_{17}O_{61}]^{12--}$ (blue trace) in 0.5 M H_2SO_4 at pH = 0.33. Glassy carbon working electrode and scan rate 10 mV.s-1 (Figure courtesy of Dr. Israel Mbomekalle)

4.3.5 Reduction of TcO_4^- using photolytically reduced α_2-$[P_2W_{17}O_{61}]^{10-}$

Following the successful reduction of TcO_4^- by an electrochemically reduced sample of α_2-$[P_2W_{17}O_{61}]^{10-}$ the study was expanded and a 10^{-3} M solution of α_2-$[P_2W_{17}O_{61}]^{10-}$ (prepared in 0.5 M H_2SO_4 containing 30% IPA) was photolytically reduced using sunlight. Upon reduction of the POM a slight excess of TcO_4^- was added to the already reduced sample of α_2-$[P_2W_{17}O_{61}]^{10-}$.

Figure 4.12 shows the color changes Visible when a slight excess of clear colorless TcO_4^- is added to an already reduced blue sample of α_2-$[P_2W_{17}O_{61}]^{10-}$. A clear

colorless solution of α_2-$[P_2W_{17}O_{61}]^{10-}$ (Figure 4.12A) turns blue upon exposure to sunlight in the presence of IPA (Figure 4.12B). Upon addition of a slight excess of a clear colorless solution of TcO_4^- (Figure 4.12 C) the solution changes color from blue to dark orange (Figure 4.12D). The formation of the dark orange color provides evidence of TcO_4^- reduction, and the loss of blue color indicates re-oxidation of the POM. The resulting orange solution was characterized by both CV and UV-Vis. For ^{31}P NMR a new sample was prepared and characterized *in situ* (directly in a 5 mL NMR tube).

A B C D

Figure 4.12. The color changes incurred during the photolytic reduction of TcO_4^- using α_2-$[P_2W_{17}O_{61}]^{10-}$. Upon expose to sunlight in the presence of IPA the clear colorless α_2-$[P_2W_{17}O_{61}]^{10-}$ (A) becomes reduced and exhibits the characteristic blue solution (B) Upon addition of a clear colorless solution of TcO_4^- (C) the solution changes from blue to dark orange (D).

Figure 4.13 compares the CV profiles of reduced α_2-$[P_2W_{17}O_{61}]^{10-}$ and the orange solution of reduced α_2-$[P_2W_{17}O_{61}]^{10-}$ plus TcO_4^-. The CV profile of the orange solution clearly shows the existence of two new redox couples, a semi/quasi reversible wave located at +1300 mV and a well resolved reversible couple at + 800 mV. Comparison of this data to that obtained for the chemically synthesised $K_{7-n}H_n[Tc^VO(\alpha_2P_2W_{17}O_{61})]$ compound (at pH = 0) from chapter 2 allows for the accreditation of these waves to the $Tc^{V/VI}$ (+800 mV) and $Tc^{VI/VII}$ (+1300 mV) redox processes. The $Tc^{V/IV}$ couple appears as an unresolved shoulder on the first W reduction centred around 0 mV. Observation of the

rest potential at +300 mV indicates that the resulting Tc species is in the +5 oxidation state in this new compound.

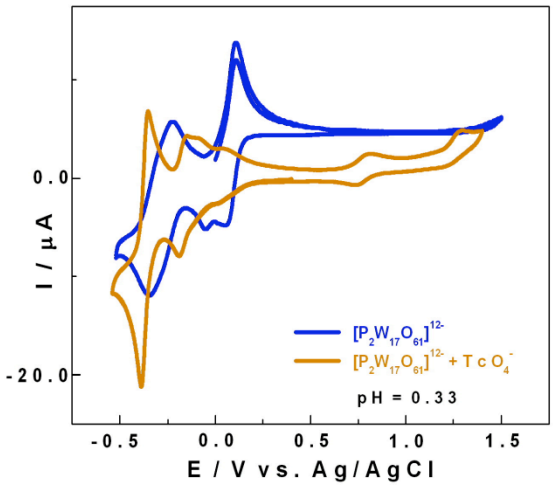

Figure 4.13. CV profiles of reduced α_2-$[P_2W_{17}O_{61}]^{10-}$ (blue trace) and reduced α_2-$[P_2W_{17}O_{61}]^{10-}$ plus TcO_4^- (orange trace). In 0.5 M H_2SO_4 at pH = 0.33 with a glassy carbon working electrode, a platinum wire auxillary electrode, a Ag/AgCl working electrode and scan rate of 10 $mV.s^{-1}$

Figure 4.14 shows the UV data comparing α_2-$[P_2W_{17}O_{61}]^{10-}$, reduced α_2-$[P_2W_{17}O_{61}]^{10-}$, and reduced α_2-$[P_2W_{17}O_{61}]^{10-}$ plus TcO_4^-. This data shows that the orange solution resulting from addition of TcO_4^- to the blue solution of reduced α_2-$[P_2W_{17}O_{61}]^{10-}$ (orange trace) results in the appearance of a new absorption band at 494 nm, accompanied by the loss of the absorption band around 900 nm which is present in the UV profile of the reduced α_2-$[P_2W_{17}O_{61}]^{10-}$ (blue trace). The absorption band at 494 nm is accredited to the resulting Tc(V) species. The position of this band is consistent with other Tc(V) species in the literature. This data once again supports the suggestion that the reduced POM donates electrons to Tc^{VII} for its reduction to a lower valent species.

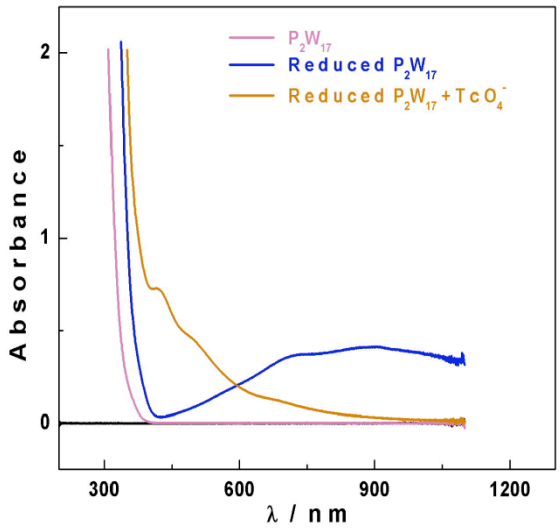

Figure 4.14 UV-Vis data comparing α_2-$[P_2W_{17}O_{61}]^{10-}$ (pink trace), reduced α_2-$[P_2W_{17}O_{61}]^{10-}$ (blue trace) and reduced α_2-$[P_2W_{17}O_{61}]^{10-}$ plus TcO_4^- (orange trace).

Figure 4.15 shows the ^{31}P NMR of the resulting orange solution (reduced α_2-$[P_2W_{17}O_{61}]^{10-}$ plus TcO_4^-). This spectrum shows 3 distinct peaks of almost equal intensity, at -11.17 ppm, -12.62 ppm and -13.26 ppm. The peaks at -11.17 and -13.26 ppm exactly match to those of the chemically synthesized $K_{7-n}H_n[Tc^VO(\alpha_2P_2W_{17}O_{61})]$ compound from Chapter 2. This result corroborates both the assertion that the resulting low valent Tc species is in the +5 oxidation state, and the hypothesis that the reoxidized POM can act to chemically incorporate the resulting low valent Tc species. The resonance at -12.62 ppm is indicative of the parent α-$[P_2W_{18}O_{62}]^{6-}$ molecule and is not unexpected under these highly acidic conditions for a saturated solution (as was observed in the α_2-$[P_2W_{17}O_{61}]^{10-}$ stability study).

This finding has a significant impact on the possibility for the development of metal-oxide storage matrices that would not succumb to reoxidation of Tc to Tc(VII) and encouraged us to look for other POMs that might exhibit similar behavior.

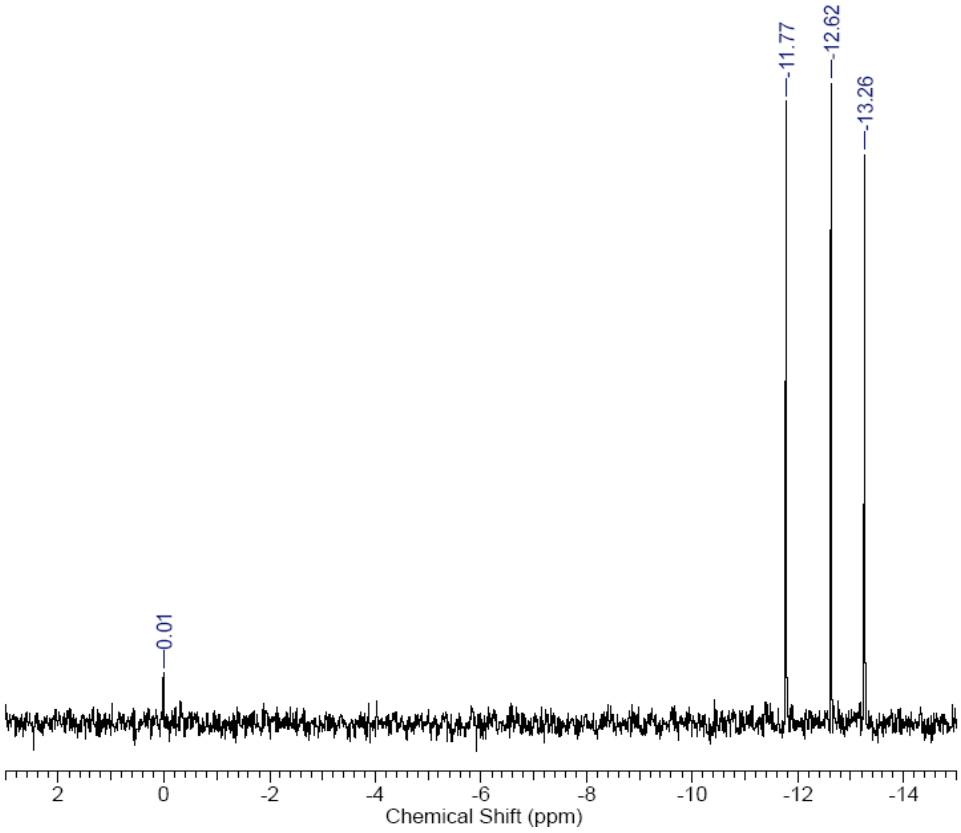

Figure 4.15. ^{31}P NMR Spectra of reduced α_2-$[P_2W_{17}O_{61}]^{10-}$ plus TcO_4^-

4.3.6 Reduction of TcO_4^- using other photolytically reduced POMs

In addition to the α_2-$[P_2W_{17}O_{61}]^{10-}$ Wells-Dawson anion, a variety of other POMs were chosen for the photolytic reduction of pertechnetate; among then the Keggin $(AlW_{12}O_{40})^{5-}$ $(SiW_{12}O_{40})^{5-}$ and $(PW_{12}O_{40})^{3-}$ POMs, as well as the non-Keggin $(P_8W_{48}O_{184})^{40-}$ wheel structure. This dissertation will focus only on the $(AlW_{12}O_{40})^{5-}$ and

$(P_8W_{48}O_{184})^{40-}$. Based on the experimentally determined reduction potentials these hold the most promise for the reduction of TcO_4^-.

Before reduction of these POMs could be achieved their reduction potentials were determined experimentally under the highly acidic conditions (pH 0.33) necessary for the reduction of TcO_4^- to occur. This is important both to characterize the stability of the POMs and to verify their suitability for facilitating the reduction of TcO_4^- (which was found to occur at -500 mV, see Figure 4.3). The stability of $[P_8W_{48}O_{184}]^{40-}$ at pH = 0.33 was further verified by ^{31}P NMR.

	1st wave	2nd wave	3rd Wave
	E_{pc} (mV)	E_{pc} (mV)	E_{pc} (mV)
$[AlW_{12}O_{40}]^{5-}$	-410 (2e)	-540 (2e)	-720 (8e)
$[P_8W_{48}O_{184}]^{40-}$	-182 (8e)	-455 (8e)	-

Table 4.3. W-Reduction potentials for $[AlW_{12}O_{40}]^{5-}$, [and $[P_8W_{48}O_{184}]^{40-}$ in 0.5 M H_2SO_4 at pH = 0.33. Scan rate was 10 $mV.s^{-1}$, the working electrode was glassy carbon, the auxiliary electrode was a platinum wire and the reference electrode was Ag/AgCl in 3 M NaCl.

Table 4.3 shows the reduction potentials of $[AlW_{12}O_{40}]^{5-}$, and $[P_8W_{48}O_{184}]^{40-}$ measured in 0.5 M H_2SO_4 at pH = 0.33 by cyclic voltammetry. This data shows that both can acquire multiple electrons at potentials less negative than that of Tc^{VII} reduction. $[AlW_{12}O_{40}]^{5-}$ can gain 4 electrons and $[P_8W_{48}O_{184}]^{40-}$ can gain 16 electrons; both without incurring any changes to the POM framework.

Figure 4.16 shows the ^{31}P NMR for $[P_8W_{48}O_{184}]^{40-}$. The spectrum exhibits a single peak at -7.31 ppm. The presence of this single peak confirms the symmetrical structure of the wheel shaped $[P_8W_{48}O_{184}]^{40-}$ POM, where all the P atoms are chemically equivalent, and shows no decomposition of the POM structure, thereby confirming the stability of the

compound under these conditions. Figures 4.17 shows the CV profile of $[AlW_{12}O_{40}]^{5-}$ in 0.5 M H_2SO_4 at pH 0.33. There is no visible decomposition of the POM in this medium.

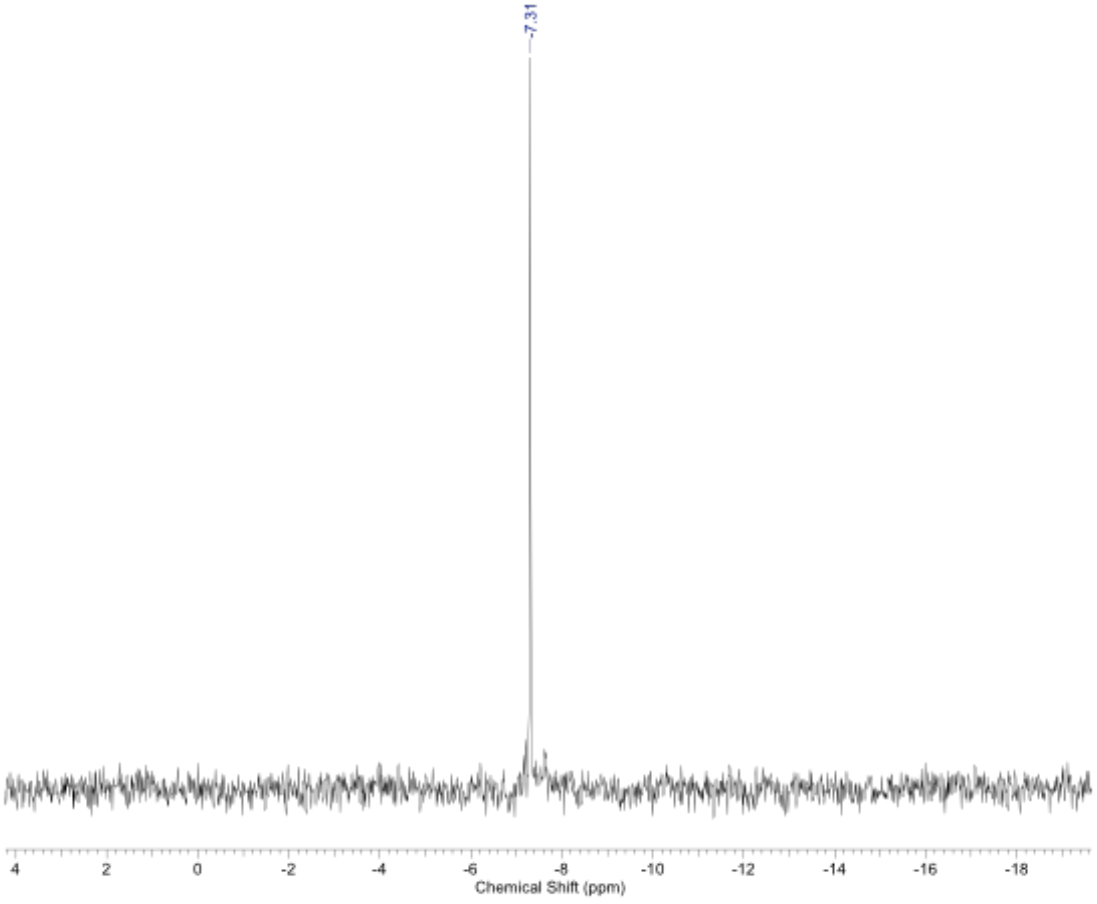

Figure 4.16 ^{31}P NMR Spectra of $[P_8W_{48}O_{184}]^{40-}$ in 0.5 M H_2SO_4 and D_2O (pH = 0.33).

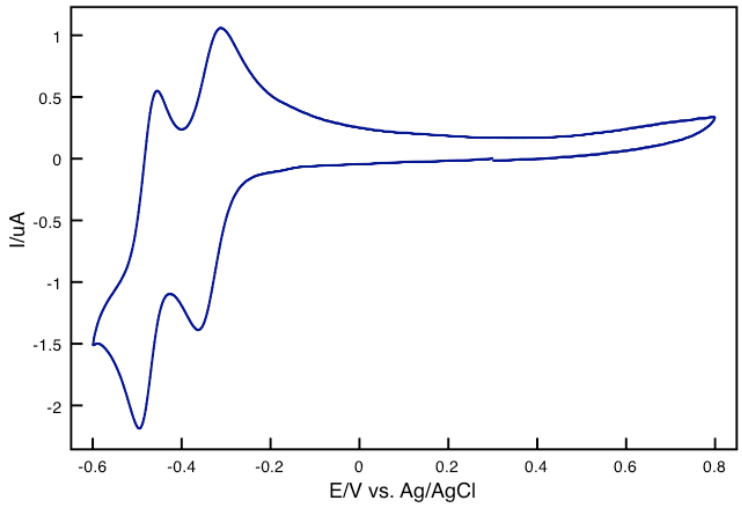

Figure 4.17. CV profile of $AlW_{12}O_{40}]^{5-}$ at pH = 0.33. Glassy carbon working electrode, platinum wire auxillary electrode, Ag/AgCl working electrode and scan rate of 10 $mV.s^{-1}$

4.3.6.1 Reduction of TcO_4^- using reduced $[AlW_{12}O_{40}]^{5-}$

Figure 4.18 shows the color changes Visible when a slight excess of clear colorless TcO_4^- is added to a reduced sample of blue $[AlW_{12}O_{40}]^{5-}$. Upon addition of the TcO_4^- the solution changes color from blue to slightly orange. The formation of the orange color provides evidence of TcO_4^- reduction, and the loss of blue color indicates re-oxidation of the POM. The resulting orange solution was characterized by both CV and UV-Vis.

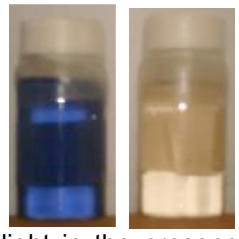

Figure 4.18. Upon exposure to sunlight in the presence of IPA the clear colorless solution of $[AlW_{12}O_{40}]^{5-}$ produces the characteristic blue solution as seen in the vial on the left. Upon addition of TcO_4^- the solution changed color from blue to a light orange as seen in the vial on the right.

Figure 4.19 compares the CV profiles of TcO_4^-, the blue solution of reduced $[AlW_{12}O_{40}]^{5-}$ and the orange solution of reduced $[AlW_{12}O_{40}]^{5-}$ plus TcO_4^-. The CV profile of the orange solution clearly shows the existence of a new species with a broad oxidation wave located between +900 mV and +1350 mV. The very sharp reduction wave (c.a. -300 mV) that corresponds to the broad oxidation is characteristic of hydrogen evolution, but it remains unclear what caused the catalysis of this reaction.

The reduction of TcO_4^- (as shown in the red trace) occurs at a more negative potential than where this very sharp peak appears and is followed by a symmetric and sharp re-oxidation wave that occurs at a more negative potential that the broad oxidation peak. This is indicative of the formation of a new species in the orange solution that is not TcO_4^-.

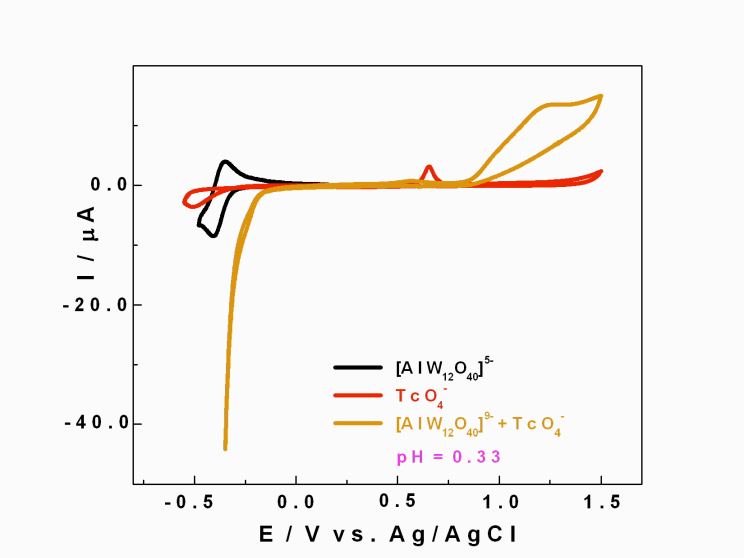

Figure 4.19. CV profiles of 10^{-4} M TcO_4^- (Red trace), 10^{-3} M $[AlW_{12}O_{40}]^{5-}$ (Black trace) and reduced $[AlW_{12}O_{40}]^{5-}$ plus TcO_4^- (orange trace). All in 0.5M H_2SO_4 at pH = 0.33 with a glassy carbon working electrode, a platinum wire auxillary electrode, a Ag/AgCl working electrode and scan rate of 10 $mV.s^{-1}$

The loss of the blue color in solution affirms the re-oxidation of the POM, which implies a transfer of electrons from the POM to Tc^{VII}. It is plausible then that either metallic Tc^{0} or colloidal $Tc^{IV}O_2$ particles have been produced, that these have in turn acted to catalyze the Hydrogen Evolution Reaction and are then re-oxidized on the glassy carbon electrode at very positive potentials. No evidence of particle formation is observed in the cell however, and further experimentation (such as TEM and Light scattering) is needed to verify this.

Figure 4.20 shows the UV data comparing TcO_4^-, $[AlW_{12}O_{40}]^{5-}$, reduced $[AlW_{12}O_{40}]^{5-}$ and reduced $[AlW_{12}O_{40}]^{5-}$ plus TcO_4^- . This data shows that the addition of TcO_4^- to the blue solution of reduced $[AlW_{12}O_{40}]^{5-}$ (orange trace) results in the appearance of a new and sharp absorption band at 494 nm (which does not match that of TcO_4^-, red trace). This is accompanied by the loss of the absorption band around 900 nm which is present in the UV profile of the reduced $[AlW_{12}O_{40}]^{5-}$ (blue trace). These UV profiles support the idea that the reduced POM donates electrons to Tc^{VII}. The Tc^{VII} is reduced and the POM is re-oxidized .

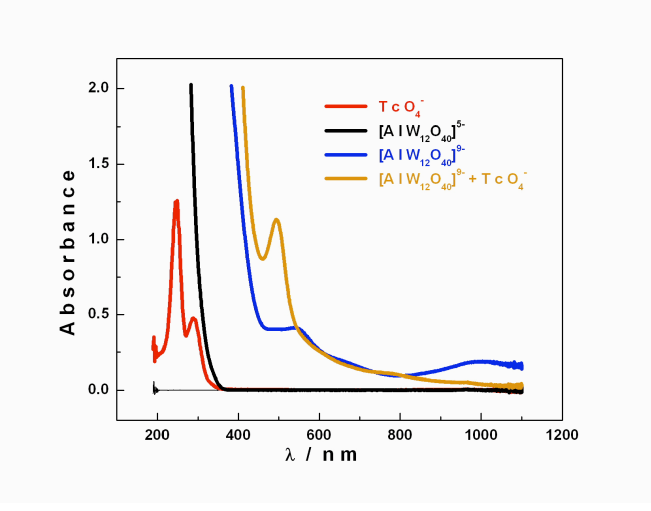

Figure 4.20 UV-Vis data comparing TcO_4^- (Red trace), $[AlW_{12}O_{40}]^{5-}$ (Black trace), reduced $[AlW_{12}O_{40}]^{5-}$ (blue trace) and reduced $[AlW_{12}O_{40}]^{5-}$ plus TcO_4^- (orange trace).

Notably the UV Absorbtion band of the resulting orange solution exhibits an absorbance band at 494 nm, which exactly matches to that of the $K_{7-n}H_n[Tc^{V}O(\alpha_2P_2W_{17}O_{61})]$ complex resulting from the reduction of TcO_4^- using reduced α_2-$[P_2W_{17}O_{61}]^{10-}$. In contrast to the CV data then, which indicates the possible formation of metallic Tc^0 or colloidal $Tc^{IV}O_2$ particles, this data implies the reduction of Tc (VII) to a low valent Tc species possibly in the +5 oxidation state, but needs to be further confirmed. The UV absorption bands for Tc(V) and Tc(IV) are too similar to allow for oxidation state verification by this technique.

Although the final oxidation state of the reduced Tc species remains ambiguous, the combination of the CV and UV results clearly indicate that reduction of the Tc(VII) in indeed occurring.

4.3.6.2 Reduction of TcO_4^- using reduced $[P_8W_{48}O_{184}]^{40-}$

The wheel shaped $[P_8W_{48}O_{184}]^{40-}$ POM can be reduced by up to 8 electrons and its structure offers multiple binding sites. This POM allows the opportunity for a molecule to both reduce and complex more than one Tc atom at a time, thus affording the possibility to overcome the 1:1 (POM to Tc) stoichiometric limitations observed for the $(\alpha_2P_2W_{17}O_{61})^{10-}$ system.

Figure 4.21 shows the color changes Visible when a slight excess of clear colorless TcO_4^- is added to a reduced sample of dark blue $[P_8W_{48}O_{184}]^{40-}$. Upon addition of the TcO_4^- the solution changes color from dark blue to red. The formation of the red color provides evidence of TcO_4^- reduction, and the loss of the dark blue color indicates re-oxidation of the POM. The resulting red solution was characterized by UV-Vis and ^{31}P

NMR. For ^{31}P NMR a new sample was prepared and characterized *in situ* (directly in a 5 mL NMR tube).

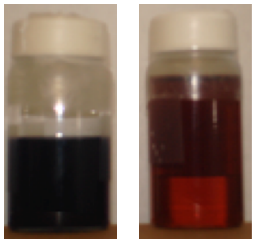

Figure 4.21. Upon exposure to sunlight in the presence of IPA the clear colorless solution of $[P_8W_{48}O_{184}]^{40-}$ produces the characteristic blue solution as seen in the vial on the left. Upon addition of TcO_4^- the solution changed color from blue to red as seen in the vial on the right.

Figure 4.22 shows the UV spectrum for the red solution of reduced $[P_8W_{48}O_{184}]^{40-}$ plus TcO_4^- . This data shows that the addition of TcO_4^- to the blue solution results in the appearance of a new absorption band at 494 nm with no evidence of the low energy blue band. This band at 495 nm matches to that of the orange $[AlW_{12}O_{40}]^{5-}$ solution as well as to the chemically synthesized $K_{7-n}H_n[Tc^VO(\alpha_2P_2W_{17}O_{61})]$ complex, once again pointing to a low valent Tc species.

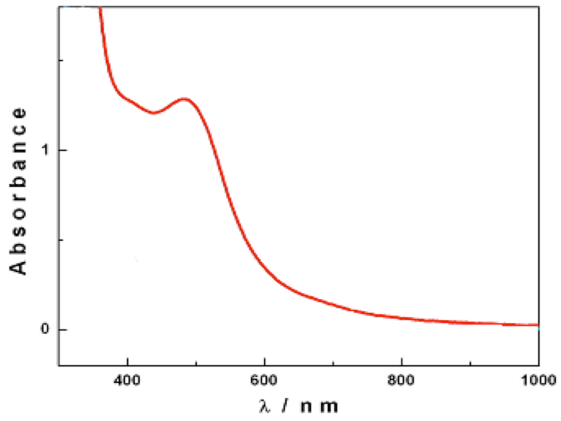

Figure 4.22 UV-Vis data for red solution of reduced $[P_8W_{48}O_{184}]^{40-}$ plus TcO_4^-.

Figure 4.23 shows the ^{31}P NMR of the resulting red solution (reduced $[P_8W_{48}O_{184}]^{40-}$ plus TcO_4^-). This spectrum shows 1 broad resonance between -7.2 and -7.39 ppm and a minor resonance at -0.31 ppm. The small peak at -0.31 ppm is indicative of the reduced form of the plenary α-$[P_2W_{18}O_{62}]^{6-}$ POM and is not unexpected under these highly acidic conditions.

The major resonance, although broader, matches to that of the oxidized form of $[P_8W_{48}O_{184}]^{40-}$ (at -7.31 ppm, see Figure 4.10). The broadness of this peak is most likely due to the presence of a small amount of the reduced $[P_8W_{48}O_{184}]^{40-}$ species, in which the added electrons are delocalized over the W atoms around the body of the wheel. A ^{31}P NMR spectrum showing this peak broadening for the reduced species can be found in the appendix. It might also be argued that the peak broadening is caused by the surface binding of a low valent Tc species (which would break the symmetry of the wheel structure), but further studies are needed to verify this assertion.

Although the ^{31}P NMR data does not show any direct evidence for complexation to Tc, the presence of largely re-oxidized $[P_8W_{48}O_{184}]^{40-}$, coupled to the formation of a red solution and the UV absorbance at 495 nm clearly indicate that the reduced POM is transferring electrons to Tc(VII) for reduction to a lower valent Tc species and the concomitant re-oxidation of the POM.

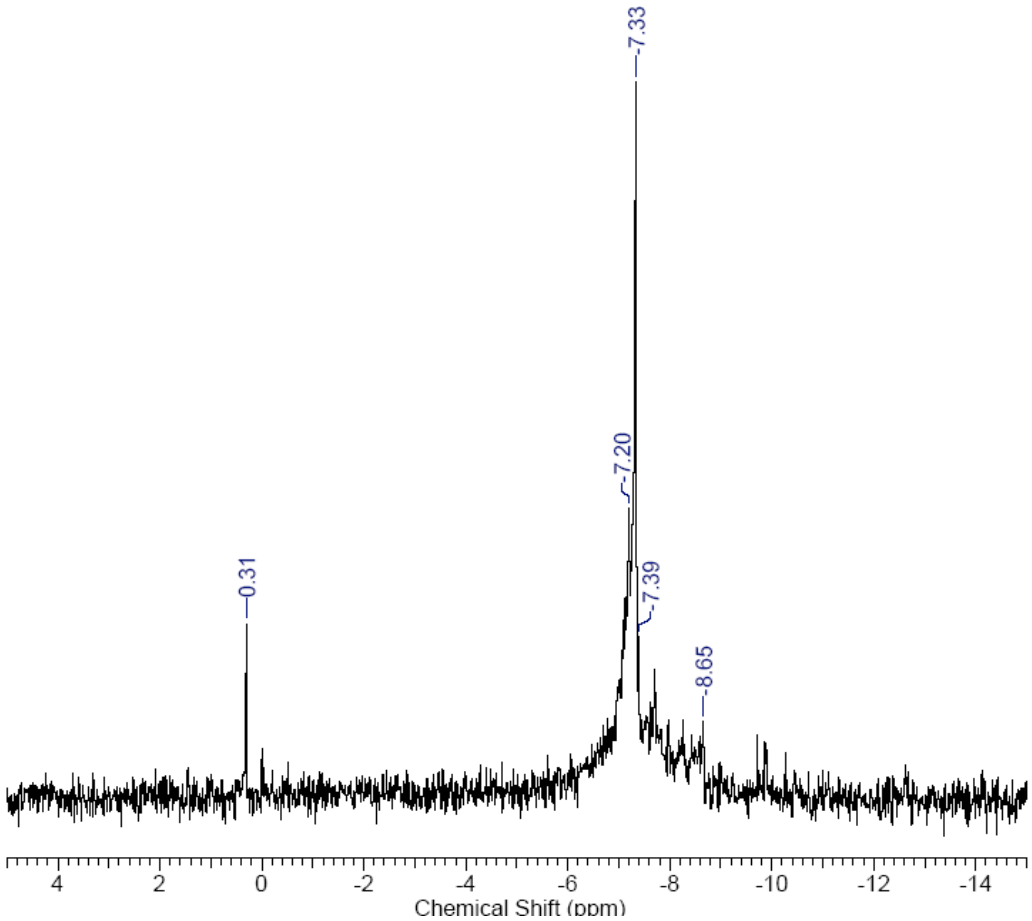

Figure 4.23. 31P NMR Spectra of $[P_8W_{48}O_{184}]^{40-}$ in 0.5 M H_2SO_4 and D_2O (pH = 0.33).

4.3.7 Photocatalytic Nature of the POMs

The mechanism proposed for the reduction of Tc(VII) by a photoreduced POM suggests that the POM is catalytic in nature. As a proof of principle, UV-Vis data was collected for the orange/red solutions of photoreduced POM plus TcO_4^- 1 week after reduction and then again 1 month after reduction. Table 4.4 shows these results, for reduced $(AlW_{12}O_{40})^{5-}$ plus TcO_4^-, reduced $(\alpha_2\text{-}P_2W_{17}O_{61})^{10-}$ plus TcO_4^- and reduced

$(P_8W_{48}O_{184})^{40-}$ plus TcO_4^-, along with a control sample (containing only TcO_4^- in a 30 % IPA solution).

There is a marked increase in the absorbance band at 494 nm (that of the reduced Tc species) for the data collected after 1 month as compared to that collected after 1 week. The increase in the absorbance band (due to the presence of more low valent Tc) is indicative of the continued reduction of Tc(VII), which in turn confirms the catalytic nature of the POM.

Compounds	TcO_4^- (control)	Reduced $(AlW_{12}O_{40})^{5-}$ plus TcO_4^-	Reduced $(\alpha_2\text{-}P_2W_{17}O_{61})^{10-}$ plus TcO_4^-	Reduced $(P_8W_{48}O_{184}]^{40-}$ plus TcO_4^-
	Pink	Orange	Orange	Dark Red
Absorbance at λ = 494 nm (After 1 week)	0	0.08	0.1	1.27
Absorbance at λ= 494 nm (After 1 month)	0.25	0.3915	0.492	>1 (Too large)

Table 4.4. UV-Vis data for reduced POMs plus TcO_4^- showing the catalytic nature of the POM.

4.4 Conclusion

The lacunary $(\alpha_2\text{-}P_2W_{17}O_{61})^{10-}$ Wells Dawson POM can be reduced both electrochemically and photolytically for the reduction of TcO_4^- to a low valent Tc(V) species. Upon reduction of Tc(VII) the $(\alpha_2\text{-}P_2W_{17}O_{61})^{10-}$ POM is re-oxidized and has been shown to successfully incorporate the resulting low valent ^{99}Tc(V) for formation of the $K_{7-n}H_n[Tc^VO(\alpha_2P_2W_{17}O_{61})]$ complex.

The $[AlW_{12}O_{40}]^{5-}$ Keggin and the Wheel shaped $[P_8W_{48}O_{184}]^{40-}$ POMs can be photolytically reduced for the reduction of TcO_4^- to a lower valent species. Although these systems have not been fully characterized, there is compelling evidence in both cases for the formation of a lower valent Tc species; which may be $^{99}Tc(IV)$ or $^{99}Tc(0)$ nanoparticles in the case of $[AlW_{12}O_{40}]^{5-}$.

The Wheel shaped $[P_8W_{48}O_{184}]^{40-}$ POM allows for the reduction and possible complexation of more than 1 Tc atom. This encourages the further expansion of this work to include the development of a viable nanomaterial for the reduction and complexation of the highly mobile TcO_4^- anion for its immobilization.

4.5 References

1. Lukens, W. W.; Shuh, D. K.; Schroeder, N. C.; Ashley, K. R., *Environ. Sci. Technol.* **2004,** *38*, 229-233.

2. Lukens, W. W.; Bucher, J. J.; Shuh, D. K.; Edelstein, N. M., *Environ. Sci. Technol.* **2005,** *39*, 8064-8070.

3. Lloyd, J. R.; Sole, V. A.; Van Praagh, C. V. G.; Lovley, D. R., *Appl. Environ. Microbiol.* **2000,** *66*, 3743-3749.

4. Burke, I. T.; Boothman, C.; Lloyd, J. R.; Mortimer, R. J. G.; Livens, F. R.; Morris, K., *Environ. Sci. Technol.* **2005,** *39*, 4109-4116.

5. Mandal, S.; Selvakannan, P. R.; Pasricha, R.; Sastry, M., *J. Amer. Chem. Soc.* **2003,** *125*, 8440-8441.

6. Geletii, Y. V.; Hill, C. L.; Bailey, A. J. H., K.I.; Atalla, R. H.; Weinstock, I. A., *Inorg. Chem.* **2005,** *44*, 8955-8966.

7. Altenau, J. J.; Pope, M. T.; Prados, R. A.; So, H., *Inorg. Chem.* **1977,** *14* (2), 417-421.

8. Pope, M. T.; Varga, G. M., *Inorg. Chem.* **1966,** *5* (7), 1249-1254.

9. Mandal, S.; Mandale, A. B.; Sastry, M., *J. Mater. Chem.* **2004,** *14*, 2868-2871.

10. Troupis, A.; Hiskia, A.; Papaconstantinou, E., *New J. Chem.* **2001,** *25*, 361-363.

11. Hiskia, A.; Troupis, A.; Papaconstantinou, E., *International Journal of Photoenergy* **2002,** *4*, 35-40.

12. Grika, E.; Troupis, A.; Hiskia, A.; Papaconstantinou, E., *Environ. Sci. Technol.* **2005,** *39*, 4242-4248.

13. DaVison, A.; Trop, H.; DePamphilis, B.; Jones, A., *Inorganic Synthesis* **1982,** *21*, 160.

14. Contant, R., *Inorg. Synth.* **1990,** *27*, 71-111.

15. Keita, B.; Girard, F.; Nadjo, L.; Contant, R.; Belghiche, R.; Abessi, M., *J. Electroanal. Chem.* **2001,** *508* (1-2), 70-80.

Chapter 5: An Introduction into the nature of Chemical Education Research.

5.1 Introduction

Chemical education research is the study and investigation of teaching and learning of chemistry and has long been the interest of academic chemists. Volume 1 of the Journal of Chemical Education was published in 1924. The articles published in the journal focused primarily on what was taught in the colleges and the nature of teaching and research filled the early pages. Clearly chemists were thinking about education; thinking about what was being done and what works in the classroom and lecture hall.

Sixty years after J. Chem. Ed. began publishing, the first symposium on research in chemical education was held at the American Chemical Society meeting in St. Louis.[1] This meeting marks the beginning of the modern era in chemical education research. An era in which the field began to mature, methodologies began to emerge, and chemists began to retool themselves as education researchers. Using this meeting as a benchmark, we can chronicle the growth in the field by briefly outlining the learning frameworks or models that underlie the chemical education research endeavor.

5.2 Early Framework

5.2.1 The Behaviorist Model

Prior to the 1984 ACS meeting the most commonly accepted model for teaching was based on the behaviorist perspective, which argues that because the human mind is inaccessible, the only way to observe learning is in terms of "the stimuli that impinge upon our senses and the observed responses to those stimuli." [2] Pavlov's conditioning of

dogs to salivate at the sound of a bell being rung is an exemplary example of the behaviorist design.

At the center of this behaviorist model is the assumption that because knowledge has an existence of it's own it can be "transferred intact from the mind of the teacher to the mind of the learner".[3] Chemistry teaching was synonymous with "telling is teaching",[4] and this assumption spurred chemical education researchers to focus their attentions on trying to find improved methods for getting knowledge into the heads of their students.

Skinners work with pigeons in the 1940's and his development of operant conditioning in the 1950s[5] spurred a movement towards the implementation of a variety of programmed learning activities that dominated throughout the 1960's and early 1970's.[2] The premise was that "programmed learning is better adapted to the presentation of subjective mater and that it holds the student's attention better." [6] Figure 5.1 shows an excerpt from a typical programmed chemistry text. These books were designed to combine the material presented in the text book with that presented in the study guide as an efficient method to train students to solve problems. The questions in such a text were specifically tailored to force students to make an explicit response, which would be followed by feedback, thereby guiding them to the correct response.[6]

To fully appreciate this paradigm however, one must step back and consider the historical perspective of the USA during this era. When the Soviet Union successfully launched Sputnik 1 (the first human-made robotic spacecraft to orbit earth) on October 4, 1957, the United States found themselves unprepared. In response, the U.S. government created The Advanced Research Projects Agency (giving rise to agencies such as

DARPA and NASA) and approved a phenomenal increase in the amount of spending on scientific research and education. At this same time the V.A. Bill was passed. This Bill offered free education to all returning war veterans from WW2. The combination of these events resulted in a huge influx of students at US Universities, and the programmed learning activities mentioned above provided a highly efficient means for educating the masses in a timely manner.

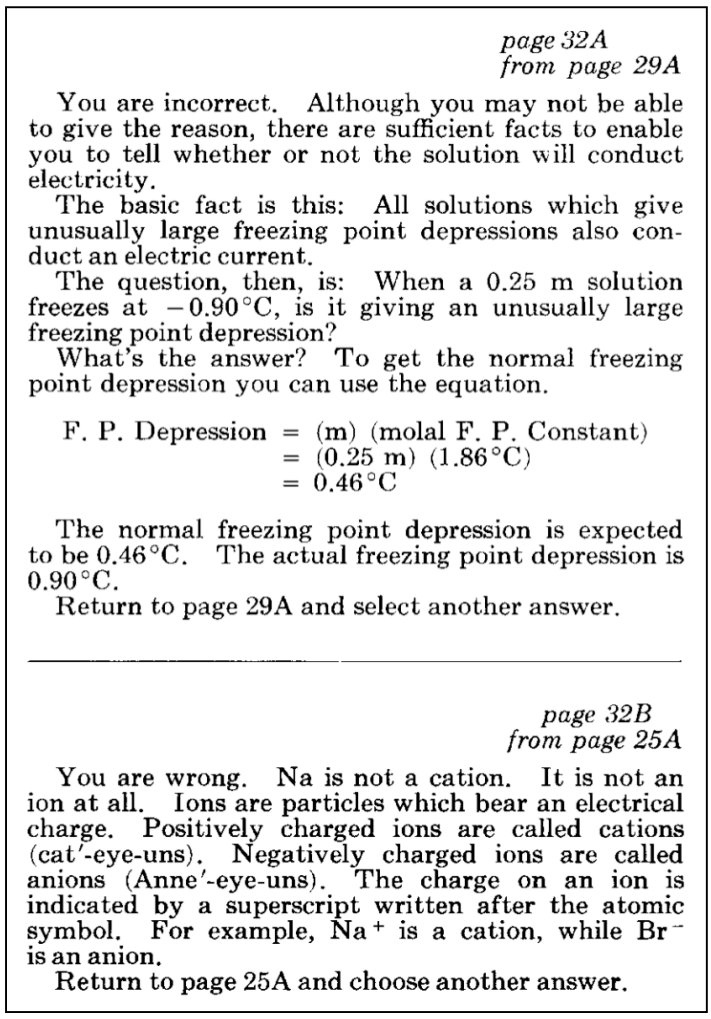

page 32A
from page 29A

You are incorrect. Although you may not be able to give the reason, there are sufficient facts to enable you to tell whether or not the solution will conduct electricity.

The basic fact is this: All solutions which give unusually large freezing point depressions also conduct an electric current.

The question, then, is: When a 0.25 m solution freezes at $-0.90\,^{\circ}C$, is it giving an unusually large freezing point depression?

What's the answer? To get the normal freezing point depression you can use the equation.

$$\begin{aligned} \text{F. P. Depression} &= (\text{m})\ (\text{molal F. P. Constant}) \\ &= (0.25\ \text{m})\ (1.86\,^{\circ}C) \\ &= 0.46\,^{\circ}C \end{aligned}$$

The normal freezing point depression is expected to be $0.46\,^{\circ}C$. The actual freezing point depression is $0.90\,^{\circ}C$.

Return to page 29A and select another answer.

---

page 32B
from page 25A

You are wrong. Na is not a cation. It is not an ion at all. Ions are particles which bear an electrical charge. Positively charged ions are called cations (cat′-eye-uns). Negatively charged ions are called anions (Anne′-eye-uns). The charge on an ion is indicated by a superscript written after the atomic symbol. For example, Na^{+} is a cation, while Br^{-} is an anion.

Return to page 25A and choose another answer.

Figure 5.1. An excerpt from the programmed chemistry text used by the United States Air Force Academy in 1963. [6]

At the forefront of behaviorism then, lay the exploration of so called *classroom conditioning* and its relation to a specified outcome, such as a correct answer, course grade or exam score.[7-10] The heart of research in chemical education then, lay simply with finding ways to *teach* chemistry more effectively.

5.2.2. What have we learned from this?

Although in the present day we may view this approach as being somewhat naive, from this work came some fundamental legacies that have proven crucial to paving the way to where we are today.[11] Among these are:

1) The knowledge of how to use language to teach, organize information, promote clear thinking and stimulate intellectual investigation.
2) The obligation to teach not our own perception of chemistry, but rather that which has been confirmed and accepted by the scientific community as a whole.
3) The incentive and know-how to do what it takes to reach our respective audience.
4) The aspiration to want to know the meaning of it all and to affirm the truth.

5.3 The Shift in Perspective

In the many years since the St. Louis symposium, the field of chemical education research has grown significantly. In fact there are now a number of U.S. institutions that offer a Ph.D. program in Chemical Education research.[12] Along with the expansion of the field, we have seen significant developments in both the complexity and types of questions being investigated, as well as in the methodology used for doing research in this area.

Most importantly, we as educators have come to realize that "teaching and learning are not synonymous: We can *teach*, and teach well, without having the students *learn*." [3] We have come to realize that students can be trained to provide reasonable responses without actually displaying any concrete understanding of the information they are parroting.[2] And hand in hand with this realization has come a gradual shift in the way we as chemical educators think about research in chemical education: the behaviorist-based paradigm has slowly given way to a philosophy based on information processing and constructivitst theories.[2, 7-10, 13]

5.4 Information processing

The theory of information processing suggests that "humans utilize several strategies to overcome limitations on *working memory"*,[2] which is thought to be that part of the brain where new and recalled information interact; the area where new information is linked to information already stored in our *long term memory.* When this happens the new information can be sequenced and made ready for a response to an external stimuli or packaged for storage. [14, 15] A simple cartoon demonstrating this phenomenon can be seen in Figure 5.2.

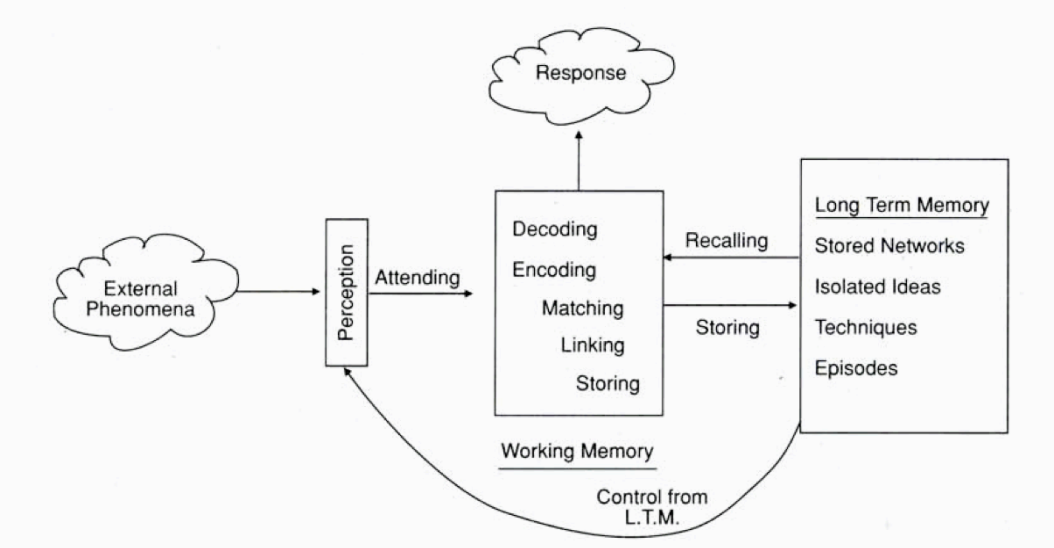

Figure 5.2. A simple version of the information processing theory. [15]

In 1983 Johnstone pointed out that that one of the major obstacles faced by students learning new material is their failed ability to package information into coherent chunks rather than trying to memorize all the pieces as separate facts.[14] When looking at the chemical structure of methyl propanoate (Figure 5.3) for example, most new organic chemistry students see 27 pieces of information (14 letters and 13 bonds). These students are processing the information as individual atoms arranged in an explicit sequence with either single or double bonds.

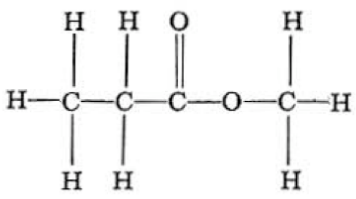

Figure 5.3. The chemical structure of methyl propanoate

Initially students are trying to memorize too many pieces of information, and it is only with time that they develop the cognitive skills necessary to package the information into "chunks". In this particular case those chunks would constitute a methyl group, a methylene group, a carbonyl group, an oxygen atom and a methyl group. As the students internalize these chunks they become further sorted and are arranged into a coherent single bit of information: a methyl propanoate molecule.[14]

5.5 The Constructivist Model

An appreciation for the effects of information processing has led most cognitive scientists today to accept a semi-constructivist model of knowledge. Constructivism is based largely on Piaget's model of intellectual development.[16] Piaget argued that knowledge is constructed in the mind of the learner as he or she attempts to organize his or her experiences in terms of some pre-existing mental structures or schemes.[3]

The implication of this is that knowledge grows inside the mind of the learner. [17] An individual perceives an environmental stimulus. This external signal is then interpreted in terms of some previously constructed pattern and modified for incorporation into the brain as new knowledge. All the information we process is added to our bank of knowledge and as this grows we build intelligence. The intelligence that we build is then subsequently used to process new information, which in turn adds to our intelligence. This process is summarized in Figure 5.4.

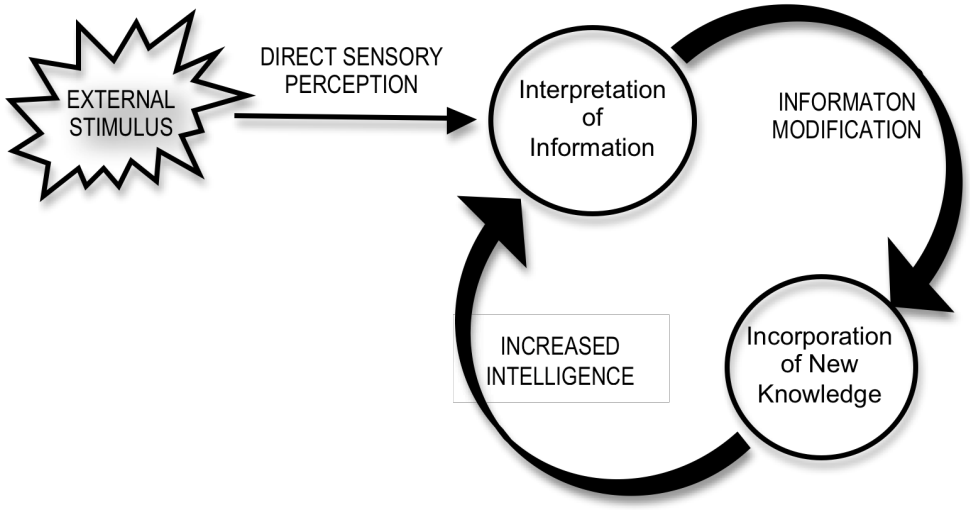

Figure 5.4. Schematic Representation of Constructivism

Constructivism then, shifts the attention away from what the teacher or program does and focuses on what goes on inside the mind of the student. It attempts to answer the question of *how* we come to know what we know, and was succinctly summarized by George Bodner who wrote: "This constructivist model can be summarized in a single statement: *Knowledge is constructed in the mind of the learner*." [3]

Arguably this statement is oversimplified, and some have pointed out that it seems to suggest that human idiosyncrasies may in some way be responsible for factual knowledge. Eric Sceri argues, "…the statement that '*knowledge is constructed'* is either simply incorrect or else so uncontroversial as to be completely redundant. If the author implies that human foibles determine whether or not the speed of light in a vacuum is either 3 or 4 or 5 x 10^8 m/s approximately, this is patently untrue." [18] The key to this misgiving lies in the explanation of the word knowledge. Perhaps a more prudent

approach would be to view knowledge as encompassing a body of information, rather than a series of undisputed facts. The process of learning then would be the organization of this body of information so that it makes sense and has the potential for later utility.

Regardless of the underlying cognitive theories, today's chemical educators feel comfortable with the fact that the information we teach our students is not simply transmitted to our students in the form that we *teach* it. Rather, the material is deconstructed and then methodically reformulated by our students while they attempt to find regularity and order as they *learn* it. In this way the responsibility for learning ultimately rests on the shoulders of the students, but the way the material is initially presented may significantly impact how it is segmented and later reconstructed. The main focus of chemical education research today then, has shifted towards teasing out those methods that will help our students *learn* more effectively.

To this end chemistry education research can be defined as "scholarship focused on understanding and improving chemistry learning",[2] and to realize this, we must examine variables related to both chemistry content, as well to the actions of our teachers and their students. Some resounding themes that have been at the forefront of our research are the following:

1) What do students and/or faculty believe makes chemistry difficult?
2) Can we predict which ideas will be more difficult?
3) Can we modify classroom instruction to make difficult ideas more accessible?
4) Which classroom methods are more effective?

5) Does satisfactory performance on a numerical problem indicate that a student has any conceptual understanding?

6) How do students learn?

7) Does co-operative learning improve student achievement?

8) Do gender and/or ethnicity have an impact on student learning?

Clearly these questions demonstrate an active response, by the scientific community, to the above-mentioned shift from behaviorism towards constructivism. This is not to say however, that investigations into more effective classroom practice have been abandoned. They have not. It is rather that the perspective from which we approach these types of studies has shifted. We have moved away from the simple short-term treatment vs. control group, and pre- vs. post-test designs towards trying to obtain more relevant information about cognitive learning.

5.6 The Nature of Knowledge in Chemical Education

In 1984 George Bodner introduced "constructivism" to chemists and precipitated a shift in thinking about chemistry education. Still trained as chemists, chemical educators began to focus scholarly efforts on student learning reflecting a shift from a purely behavioral or transmission perspective to an informational processing or constructivist perspective. However, chemical educators are neither philosophers nor psychologists (nor sociologists) and thus do not operate exclusively in any domain. In fact, one might argue that chemical educators are primarily pragmatists. While the focus of interest has shifted from what the teacher teaches to how the student learns, the

education researcher is still part of the long tradition of science education that emphasizes factual learning, conceptual understanding, and discovery. Striking a good balance that employs strategies *known to work* is the challenge.

The issue of "known to work" raises the nature of knowledge in chemical education. Chemists are trained to construct scientific knowledge and become acculturated, through their training, into the epistemology of science. Knowledge in chemical education fall more into the domain of social science. Research involving human subjects, central to the study of teaching and learning, is messy, complex, and contextual. Rarely can variables be isolated, rarely are controls easily available, and rarely can clear and unambiguous conclusions be drawn. Thus for the scientist, outcomes in education research can appear murky and ambiguous.

Epistemological differences between social science and science are reflected in the two broad methodologies used to conduct education research -- qualitative and quantitative. The choice of research methodology determines the types of research questions that can be addressed by the researcher similarly determines the meaning of knowledge. Chemical education researchers have come to recognize the value of both. As noted by Patton in his book *Qualitative Research and Evaluation methods, "*some questions lend themselves to quantitative techniques; others can only be answered using qualitative methods." He goes on to make an interesting and important distinction, being that quantitative research provides answers to questions of *more*, while qualitative research provides answers to questions of *better*.[19]

5.7 Quantitative Research Methods

For mainstream chemists quantitative research feels familiar in that it involves the same components that make-up traditional chemical research. It begins with a question or hypothesis, which is followed by research design, data collection, data evaluation and analysis, and finally an interpretation of the results.[20] This type of research is systematic, standardized and objective. It is deductive and aims to obtain reliable and reproducible quantitative measures to use as data for either answering a question or addressing a problem.

Quantitative research then, focuses on things that can be measured quantitatively using numbers and statistics. In chemical education research the main purpose of quantitative research is to "design and complete systematic, unbiased investigations of the relationship between some intellectual, psychosocial, or instructional variable (independent variable) and science proficiency (dependent variable)." [20]

5.7.1 Identification of Variables

To study the relationships between these variables one must first accurately identify the variables, which is strictly based on the underlying research question, and then determine how best to find the relationship between them. A common source of frustration in the identification of variables is the complication afforded by the human component of chemical education research. Human nature is by definition unpredictable, and from this it follows that human behavior may not be as well defined as that of chemical substances.

Another common constraint is the need to accommodate to another persons pre-existing class schedule, size and/or syllabus.[20] Although this does not directly impact the identification of a given set of variables in a particular study, it greatly influences the overall research design.

5.7.2 Statistical Correlation Methods

Once an appropriate set of variables has been identified and a legitimate set of numerical data collected, researchers perform a statistical analysis of the data in order to present their findings. Frequently researchers rely on statistical correlation methods to deduce the relationships between their variables. These correlation methods usually compare two or more groups of students and their respective pre-test/post-test performances.[20] A data analysis of this type relies heavily on the use of correlation coefficients and scatterplots, which are used to describe the direction and strength of any correlations.

It should be noted that the analysis of even simple correlation experiments can be complicated. An important distinction that must be made is the difference between correlation and causation. A strong correlation between variables does not necessarily provide any evidence that one variable is directly responsible for the behavior of the other. Another limitation of a correlation study is the size of the data set. A correlation observed for a subset of a given population will not necessarily hold true when expanded to the entire populace. Education research is replete with "contextual" problems – that is what works in one setting under one set of conditions may not transfer to another setting.

A typical example of a statistical correlation study would be the evaluation of student performance on a given exam (student grades); as was done by Robinson and Niaz to determine whether or not student achievement can be enhanced by interactive instruction even though less material was covered.[21] The data collected in this study however, focused entirely on students' test scores; that is to say whether or not students got more questions right, and failed to examine students real understanding of the material. Even though students got *more* questions right, did they understand the material any *better*?

5.7.3 The disconnect between More and Better

A clear example of the disconnect between more and better can be seen in the study by Treagust, Harrison and Vanville[22] who attempted to look at the effect of using analogies to teach students about optics. They too analyzed student exam scores, but found that there was no significant difference in the quantitative test scores for those students who had been taught with analogies as compared to those students who had not.

They then embarked upon a series of (qualitative) interviews and by this method they discovered that those students who had been taught with analogies displayed a deeper conceptual understanding of the material they had been taught. This conceptual understanding was not tested for on the traditional exam and thus the quantitative research experiment failed to realize it.

5.8 Qualitative Research Methods

Qualitative research attempts to address causality, to tease apart variables, and to build hypotheses. Classic qualitative methodologies include case studies, interviews, surveys and field observations. Qualitative research is not a methodology with which most traditional chemists feel comfortable. It is largely inductive, and in direct contrast to quantitative methods (that generate results based on observable data that can be expressed in numbers) qualitative techniques rely on the study of somewhat subjective data in the form of words (such as meaning, thinking and attitude).[23]

To this end Qualitative research sacrifices the objectivity that results from rigid statistically driven research in order to obtain a combination of flexibility, depth and detail.[1] This flexibility was eloquently captured by Lincoln and Guba who assert that "…the design of naturalistic inquiry… cannot be given in advance, it must emerge, develop, unfold." [24]

Qualitative research (in direct contrast to quantitative research) begins with the observance of a phenomenon. From this phenomenon the recognition of number of similarities and/or differences leads to the identification of a series of patterns. These patterns in turn lead to the development of a theory or hypothesis.[25] Qualitative research then, can be said to be inductive, hypothesis-*generating* research, rather than deductive, hypothesis-*testing* research.[26]

5.9 The need for Qualitative research methods

The principal driving force behind the need for qualitative methods in chemical education research is the afore-mentioned human component. When asking research

questions about personal cognition and meaning "then merely looking at quantified behavior is not a sufficient research design." [25] To attempt to obtain insight into the meanings that individuals inherently attach to their actions a move towards a more philosophical approach has been necessary. And accompanying this an unavoidable delve into the realms of anthropology and sociology, where qualitative research methods have been refined for the purposes of studying people, their cultures and interactions.

For the purpose of chemical education in-depth, open-ended interviews and "think-aloud" problem solving sessions along with personal field notes and reflective journals have become an integral part of data collection.[1] Interpretation of this type of data however can be difficult. Because of the nature of the research, data analysis often begins during data collection and most often the direction the research takes is directly influenced by the data interpretation. In qualitative research change must be anticipated and it is the flexibility that allows for this change that ultimately dictates the final outcome.[24]

5.10 A Contemporary Perspective

During the 1980's researchers in chemical education were involved in what was later termed the "paradigm wars".[27] During this period advocates from the traditional behaviorist (or quantitative) paradigm frequently clashed with those who had adopted the newly developing constructivist (or qualitative) approach. The main argument was that one had to choose between either strictly quantitative or strictly qualitative techniques and that the two methods could not be combined in a single study.[1]

This approach has since proven to be somewhat naïve, and in recent years we have bared witness to the publication of a variety of books that overtly describe a combination of quantitative and qualitative methods.[28, 29] I am of this frame of mind, and believe strongly in Patton's argument that quantitative and qualitative techniques "constitute alternative, but not mutually exclusive, strategies for research." [19]

It follows then, that a successful researcher in Chemical Education is one who recognizes the importance of both methodologies. In a Report by *The Taskforce on Chemical Education Research* it was written: "Research in chemistry education utilizes controlled experiments whenever possible, but may rely on observation in naturalistic settings when insufficient knowledge of the system or limitations on the ability to manipulate human being, is a factor." [30]

In accordance with the argument by Patton and that stated above, I believe that the fundamental means to an efficient Chemical Education research project lie with the attitude of the researcher; One must remain open-minded enough to determine the best available techniques to answer your chosen research question, flexible enough to allow for the integration of multiple research methods and adaptable enough to implement unforseen modifications to your initial research design.

Regardless of the methodology chosen however, any good research project should remain true to the following fundamental guidelines:[30]

1) The conclusions drawn from the research must be based on data.
2) The research must produce tangible results that have a relevant impact on the field of study.

5.11 The focus of this Thesis

This thesis includes the drafts of 2 papers (for submission to J.Chem Ed.) that broadly address questions of teaching and learning (in chemistry).

1. The Design of a Mercury Free Apparatus for teaching the Ideal Gas Law PV = nRT

Chapter 6 includes a draft of the paper: *A new mercury-free laboratory exercise for teaching the previously published Gas Module; physical behavior of gases and determination of the ideal gas law PV=nRT.* This paper focuses on the design of a mercury-free Laboratory apparatus for use in the teaching of Gas Laws. This Lab is part of an inquiry-based Gas Module for an introductory freshman chemistry course. The problem was approached strictly as the design of an apparatus by relying on the underlying chemical principles that would contribute to the functioning of the apparatus for a given purpose and under a given set of conditions.

2. An assessment of Chemistry 115 as a bridging course

Chapter 7 includes a draft of the paper: *CHEM 115 – A New Model for Under-prepared Chemistry Students*. This paper reports on the effectiveness of the Chem 115 preparatory course as a method of intervention for students who are failing the larger Chem102 lecture. The underlying research question was whether or not more students who take and pass Chem115 go on to re-take and pass Chem102 than students who have previously failed Chem102 and are attempting to retake the course without the Chem115 intervention. The Problem was approached as a quantitative examination comparing the performance of students (identified to be at-risk) with and without the preparatory course.

5.12 References

1. Bodner, G., M., *J. Chem. Educ.* **2004,** *81* (5), 618 - 625

2. Nurrenbern, S., C.; Dudley Herron, J., *J. Chem. Educ.* **1999,** *76* (10), 1354 - 1361

3. Bodner, G., M., *J. Chem. Educ.* **1986,** *63* (10), 873 - 878.

4. Spencer, J. N., *Chem. Educ.* **1999,** *76*, 566 - 569.

5. Skinner, B. F., *Harvard Educ. Rev* **1954,** *24*, 86 - 97.

6. Banks J., E., *J. Chem. Educ.* **1963,** *40* (1), 21 - 23.

7. lawrence, A. E., *J. Chem. Educ.* **1955,** *32*, 35.

8. Burkhalter, T. S., *J. Chem. Educ.* **1956,** *33*, 406.

9. Lander, A. J., *J. Chem. Educ.* **1965,** *42*, 231.

10. Stoppel, D. J., *J. Chem. Educ.* **1966,** *43*, 556.

11. Lippincott, T., W.; Bodner, G., M., *J. Chem. Educ.* **1984,** *61* (10), 843 - 844.

12. Mason, D., *J. Chem. Educ.* **2001,** *78*, 158 - 160

13. Von Glassersfeld, E., *The Impact of the Piagetian Theory on Educatio, Philosophy , and Psycology*. Murray, F. B. ed.; University Park Press: Baltimore, MD.: 1979.

14. Johnstone, A. H., *J. Chem. Educ.* **1983,** *60*, 968 - 971.

15. Johnstone, A. H., *J. Chem. Educ.* **1993,** *70* (9), 701 - 705

16. Resnick, L. B., *Scienc* **1983,** *220*, 477.

17. Dudley Herron, J., *J. Chem. Educ.* **1984,** *61* (10), 850 - 854

18. Scerri, E., R., *J Chem Educ.* **2003,** *80* (5), 468 - 474.

19. Patton, M. Q., *Qualitative research and Evaluation Methods*. 3rd ed.; Thousand Oaks, CA: Sage Publications:Thousand Oaks, CA: 2002.

20. Nurrenbern, S., C.; Robinson, W., R., *J. Chem. Educ.* **1994,** *71* (3), 181 - 183.

21. Robinson, W., R.; Niaz, M., *Internat. J. Science Educ.* **1991,** *13*, 203 - 215.

22. Treagust, D. F.; Harrison, A. G.; Venville, G. J., *Int. J. Sci. Educ.* **1996,** *18*, 213 - 229.

23. Schwandt, T. A., *Dictionary of Qualitative Inquiry*. 2nd ed.; Sage Publications: Thousand Oaks, CA: 2001.

24. Lincoln, Y. S.; Guba, E. G., *Naturalistic Inquiry*. Sage: Beverly Hills: 1985.

25. Phelps, A., J., *J. Chem. Educ.* **1994,** *71* (3), 191 - 194.

26. Glaser, B. G.; Strauss, A. L., *The Discovery of Grounded theory: Srategies for Qualitatiev Research.* Aldine: Chicago: 1967.

27. Gage, N. L., *Educational researcher* **1989,** *18* (7), 4 - 10.

28. Tashakkori, A.; Teddlie, C., *Mixed Methodology: Combining Qualitative and Quantitative approaches.* Sage Publications: Thousand Oaks, CA: 1998.

29. Tashakkori, A.; Teddlie, C., *Handbook of Mixed Methodds in Social and Behavioral Research.* 2003; Vol. Sage Publications: Thousand Oaks, C.A.

30. Bunce, D.; Gabel, D.; Dudley Herron, J.; Jones, L., *J. Chem. Educ.* **1994,** *71* (10), 850 - 852.

Chapter 6. The Design of a Mercury Free Apparatus for teaching the Ideal Gas Law PV = nRT

Draft of Paper for submission to J. Chem educ.

A new mercury-free laboratory exercise for teaching the previously published Gas Module; physical behavior of gases and determination of the ideal gas law PV=nRT

Donna McGregor, William V. Sweeney and Pamela Mills
Department of Chemistry, Hunter College, 695 Park Avenue, New York, NY 10065

6.1. Abstract

We have developed a new, mercury-free apparatus to measure the change in volume of a gas as a function of pressure at different temperatures. The apparatus is simpler than many found in the literature and can be used to study variations in Pressure (P), Volume (V), and Temperature (T).

6.2 Introduction

In September 2000 we published in this journal[1] an integrated, inquiry-based, classroom/laboratory unit that focuses on the physical behavior of gases and the "discovery" of the ideal gas law. The unit was designed for incoming freshman and requires an apparatus that can collect *both* Boyle's law data as well as the temperature dependence of the PV data. Our original apparatus used a capillary tube that is sealed at one end and contains a fixed volume of air that is trapped beneath a small plug of mercury (see Figure 6.1)[1,2].

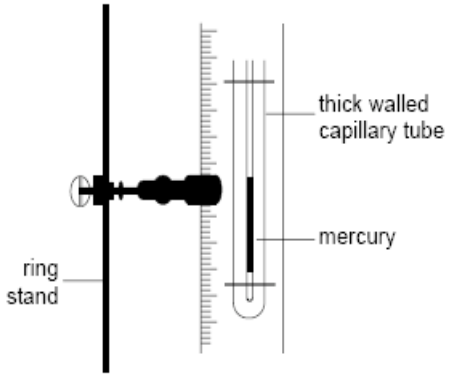

Figure 6.1. Schematic diagram of the experimental apparatus used in the original model to measure the volume of a gas as a function of pressure. A thick-walled capillary tube, sealed at one end, contained a small volume of mercury over a trapped volume of air. The capillary tube is attached to a half-meter stick with millimeter markings. The pressure of the trapped volume of air is varied by rotating the extension clamp that holds the meter stick.

The force that the mercury plug applies on the trapped air column can be changed as the angle of tilt of the capillary tube is varied.[1-4] Now, however, the use of mercury in student laboratories is generally considered a safety hazard. Indeed, as of September 2004 (according to the Environmental Conservation law, Article 27, Title 21), the use of elemental mercury is no longer allowed in New York City schools.[5,6] Thus it became necessary for us to seek an alternate experimental apparatus.

We require an apparatus that would allow Boyle's law PV data to be acquired different temperatures. Further, at least at one temperature the collected data must be of sufficient accuracy to observe the non-linearity in a plot of pressure vs. volume. We were unable to find an appropriate mercury-free experimental approach from the literature that satisfied our criteria. We did find numerous experimental methods for the measurement of changes in volumes as a function of pressure (to determine Boyles Law); data were collected using cylinders with moving pistons[7, 8] and syringe pump type devices.[9-13] A range of approaches were found for measuring pressure (fixed volume) or volume (fixed

pressure) as a function of temperature, including a U-tube apparatus,[13] an experimental design consisting of a graduated cylinder inverted in a beaker of water[14], and a commercial device from Vernier[15]. None of these designs could be readily adapted to our experiment.

6.3 Apparatus Design and Discussion

We developed an apparatus that is composed of two standard 50mL glass burettes whose tips are connected using a 7 feet length of 3/8" diameter clear plastic vacuum tubing (see Figure 6.2). To create the trapped air column the burettes are attached to a ring stand and placed at equal heights on the laboratory bench. 200mL of water, which is poured into the top of one of the burettes and allowed to flow through the tubing into the second burette, is then permitted to reach a state of equilibrium between the two vessels. The state of equilibrium is reached at the point when the water level in the first burette is equal to that in the second burette. Once this equilibrium is reached a rubber stopper is secured in the top of one of the burettes thereby trapping a fixed volume of air in its headspace, while leaving the water in the other burette exposed to the atmosphere (see Figure 6.2). At this point the pressure of the trapped air column is equal to the atmospheric pressure.

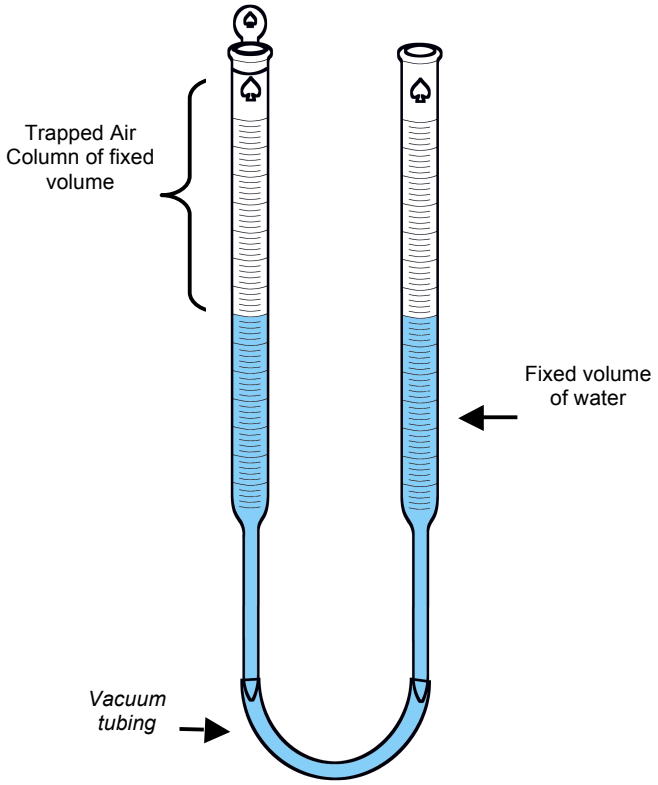

Figure 6.2. Schematic representation of the experimental apparatus used to measure the volume of a gas as a function of pressure; two standard 50mL glass burettes connected by a fixed length of clear vacuum tubing. The burette on the left is sealed with a stopper and a predetermined amount of water is poured into the open burette. This gives rise to a fixed volume of air being trapped in the headspace of the sealed burette. The pressure of the trapped volume of air is varied by creating a height differential between the two water levels. In this representation the water in the system is at equilibrium and the applied pressure on the air column is due only to the force exerted by the atmospheric pressure.

Pascal's Principle states that any pressure applied to a fluid is transmitted without change. If the liquid columns in the two burettes are at equilibrium (i.e., not moving), then the pressure exerted by the trapped air on the water must be equal to the sum of the atmospheric pressure and the height differential between the two water levels (see Figure 6.3). An important consideration here is the units of pressure, where the height differential will be measured in cm of water (H_2O) and the atmospheric pressure is given

in cm of mercury (Hg). The density of mercury (d = 13.6g/mL) can be easily used to convert between pressure units of cm Hg and cm H_2O. In other words,

$$P_{\text{trapped air}} = P_{\text{atm}}(\rho Hg/\rho H_2O) + (Y_1 - Y_2). \qquad \text{(eq. 6.1)}$$

This analysis ignores the effect of water vapor pressure on the trapped air. Including this important factor leads to

$$P_{\text{trappedair}} = P_{\text{atmosphere}}(\rho Hg/\rho H_2O) + (Y_1 - Y_2) + P_{H2O}(\rho Hg/\rho H_2O) \qquad \text{(eq. 6.2)}$$

Where $P_{\text{trapped air}}$ is the pressure of the trapped air column, $P_{\text{atmosphere}}$ is the pressure of the atmosphere, $(Y_1 - Y_2)$ is the hydrostatic pressure (Figure 6.3), and P_{H2O} is the vapor pressure of water. P_{H2O} values can be obtained from tabulated values found in a range of sources, such as the CRC Handbook of Chemistry and Physics.

The pressure of the trapped air can be altered by raising or lowering one of the burettes in relation to the other. If students raise the open burette, the water level in the open burette will fall, which results in a rise in the level of the water in the sealed burette. This creates a positive change in pressure on the trapped air column, which is reflected by a decrease in its total volume. Alternately students can raise the sealed burette containing the trapped air column. In this case the pressure on the trapped air column will decrease, and its volume will consequently grow larger.

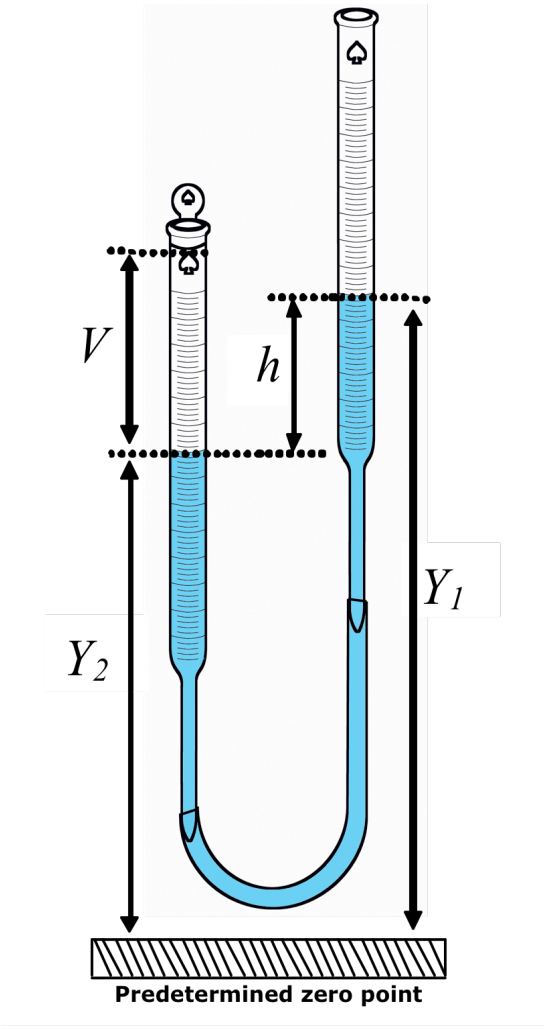

Figure 6.3. Schematic representation of the apparatus when there is a positive pressure being applied to the gas in the trapped air column; L represents the length o the air column, h represents the vertical height difference between the water levels in each burette and Y1 and Y2 represent the vertical heights of each water level relative to a pre-determined zero point.

In the lab students will record the volume of the trapped air column (V), as well as the vertical heights (Y_1 and Y_2) of the water-levels in each burette relative to a pre-determined (and arbitrary) zero point such as the floor or the top of the lab bench (see Figure 6.3). The values for V are read directly from the burette and then added to the already measured fixed volume of the burette that is above its graduations. The vertical

height difference (h, where $h = Y_1 - Y_2$) between the water levels in each burette reflects the hydrostatic force on the air column due to the water column. This force is related to the total pressure ($P_{trapped\ air}$) of the gas in the trapped air column by equation 6.2 above.

To obtain a large enough range of data a maximum *h* value of approximately 130cm must be reached in both the positive and negative pressure directions. To achieve this, the vacuum tubing must be at least 7 feet long. A representative set of data, collected at room temperature, can be seen in Table 6.1.

Y_1 (cm)	Y_2 (cm)	*h* (cm)	V (mL)	$P_{trapped\ air}$ (cm H_2O)
172.2	43.6	128.6	28.05	1168.32
136.9	71.1	65.8	29.6	1105.52
0.1	0	0.1	31.7	1039.82
2.1	63.1	-61	33.9	978.72
44.3	169.4	-125.1	36.5	914.62

Table 6.1. Representative set of height and volume data collected at room temperature, including the calculated total pressure on the trapped air column $P_{trapped\ air} = P_{atm}(\rho Hg/\rho H_2O) + (Y_1 - Y_2) - P_{H2O}(\rho Hg/\rho H_2O)$

The plot of pressure vs. volume using the data from Table 1 produces a downward curve (see Figure 6.4). The curvature is slight but observable. One objective of the Gas Module is to have students discern the difference between a graph with curvature and a linear graph. Thus any apparatus chosen must produce data that enables visualization of the curvature. Using the above apparatus we were able to observe both the curvature in the PV data and the linearity in the P vs 1/V plot (see Figure 6.5).

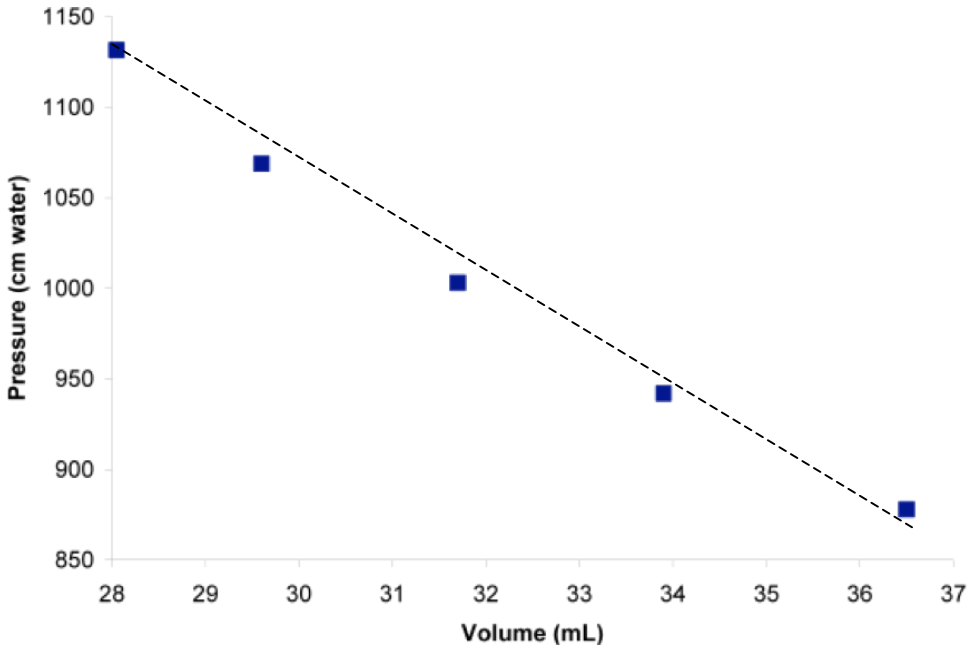

Figure 6.4. Representative data correlating the Volume (V) of the gas in the air column with the total applied pressure ($P_{trapped\ air}$) at room temperature. The dotted line (representing what would be a linear regression) clearly shows the curvature of the data points.

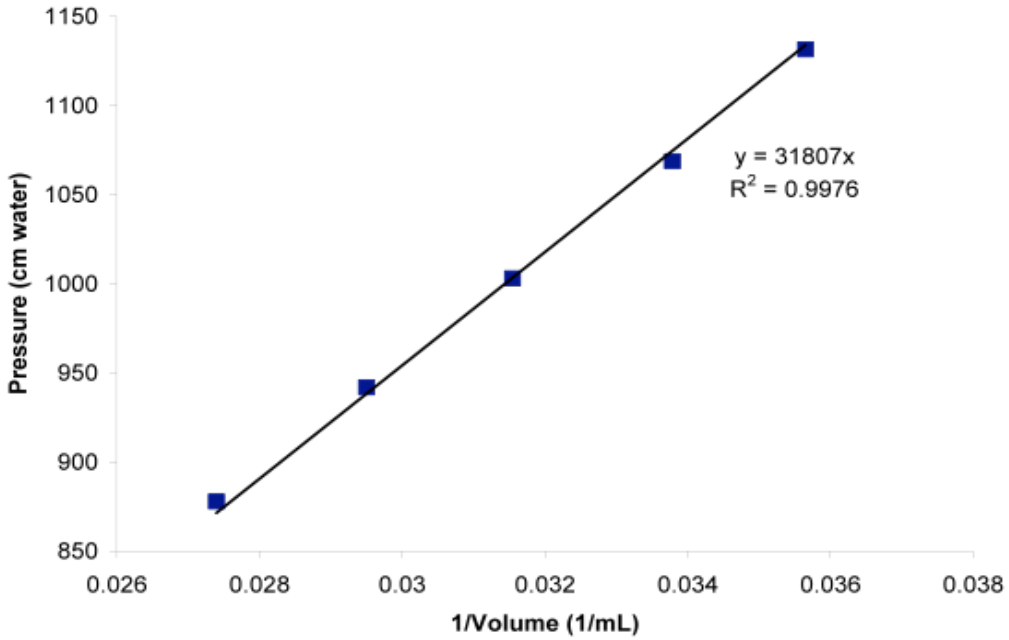

Figure 6.5. Representative linear data correlating the volume (V) of the gas in the air column with the total applied pressure ($P_{trapped\ air}$) at room temperature. The solid line represents the best linear fit.

From the above data it is clear that our apparatus satisfies the Boyle's law criterion, but the apparatus must also be able to acquire good PV data at a range of temperatures. The second phase of the Gas Module requires students to observe changes in the PV plots as a function of temperature.

In the freshman laboratory we have observed a diverse number of protocols over the past ten years that students perform to achieve variations in temperature; among them the use of cold or hot packs attached to the portion of the burette that houses the trapped air column, or alternately ice baths for low temperature data and hair dryers for high temperature data. In the representative data shown here, a ziploc bag filled with ice water (attached to the portion of the burette that contained the air column) was used to collect cold temperature data (5°C) and a hairdryer (set on medium heat), positioned to blow hot air into a large plastic bag that covered the entire sealed burette, was used to collect hot temperature data (57°C). We have measured the PV curves at different temperatures and produced the graphs in Figure 6.6.

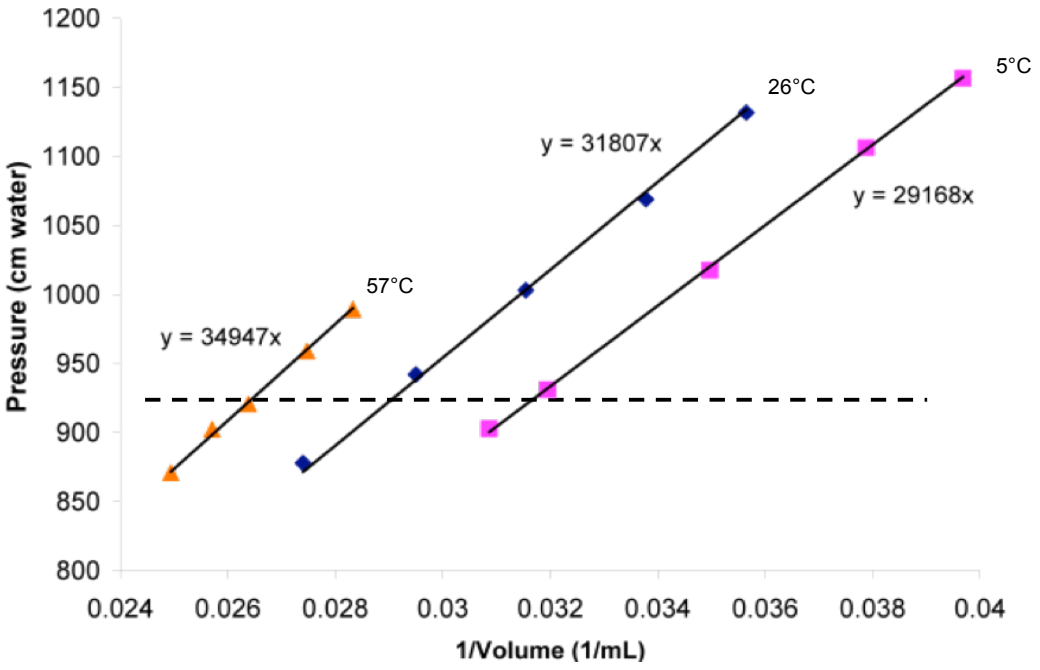

Figure 6.6. Representative linear data correlating the volume (V) of the gas in the air column with the total applied pressure ($P_{trapped\ air}$) at 3 temperature values (5, 26 and 57 ºC). The solid lines represent the best linear fit. The dotted line represents a fixed pressure value of 925cm water to extract reciprocal length data.

Because the apparatus is "self-assembled" and pressure is dependent on the number of moles of gas in the air column, any variations in the assembly of the experimental apparatus will result in inconsistent pressure values for the temperature trials. The apparatus thus needs to be re-constructed by the students at the beginning of each lab period to re-collect the room temperature data. This is important to ensure that all the temperature dependent data can be accurately compared when combined on a single plot.

To derive the ideal gas law (constant n) students must collapse all their data into a single line by plotting Pressure vs Temperature/Volume. A graph of the "hybrid variable" (T/V) using the Kelvin temperature scale is shown in Figure 6.7.

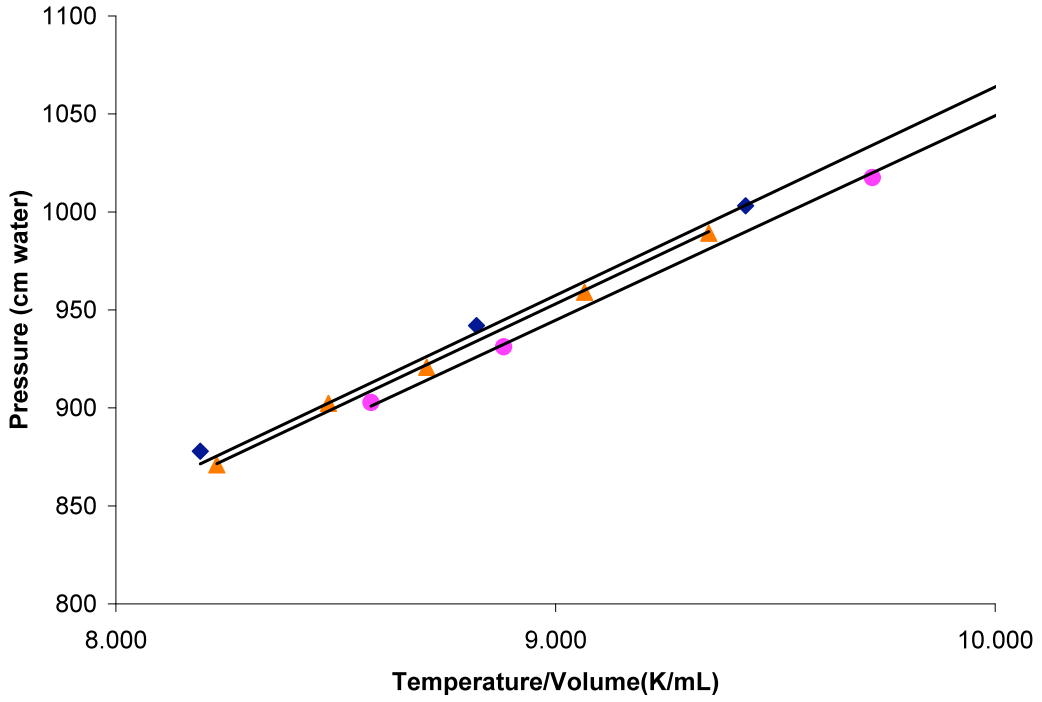

Figure 6.7. Representative linear data correlating the Volume of the gas in the air column with the total applied pressure at 3 temperature values, and plotted using the "hybrid variable" temperature/Volume. The solid lines represent the best linear fit. Using Kelvin as the units of temperature.

The final portion of the laboratory exercise is to establish the existence of absolute zero. To introduce this concept students plot the Temperature of the trapped air column as a function of Volume at several fixed pressures (see Figure 6.8). This data is not measured experimentally, but rather it is extracted from their Pressure vs. 1/Volume plots; a horizontal line (corresponding to a fixed pressure) is drawn across the graph and at the point at which it intersects with the trendline for each individual temperature

dependent plot, a vertical line (which corresponds to the reciprocal of the corresponding volume) is drawn (see Figure 6.6). While this is the conceptual representation of how values of volume as a function of temperature are obtained at constant pressure, in fact values of V and T are obtained from the equations of the fitted lines from P vs. 1/V plots.

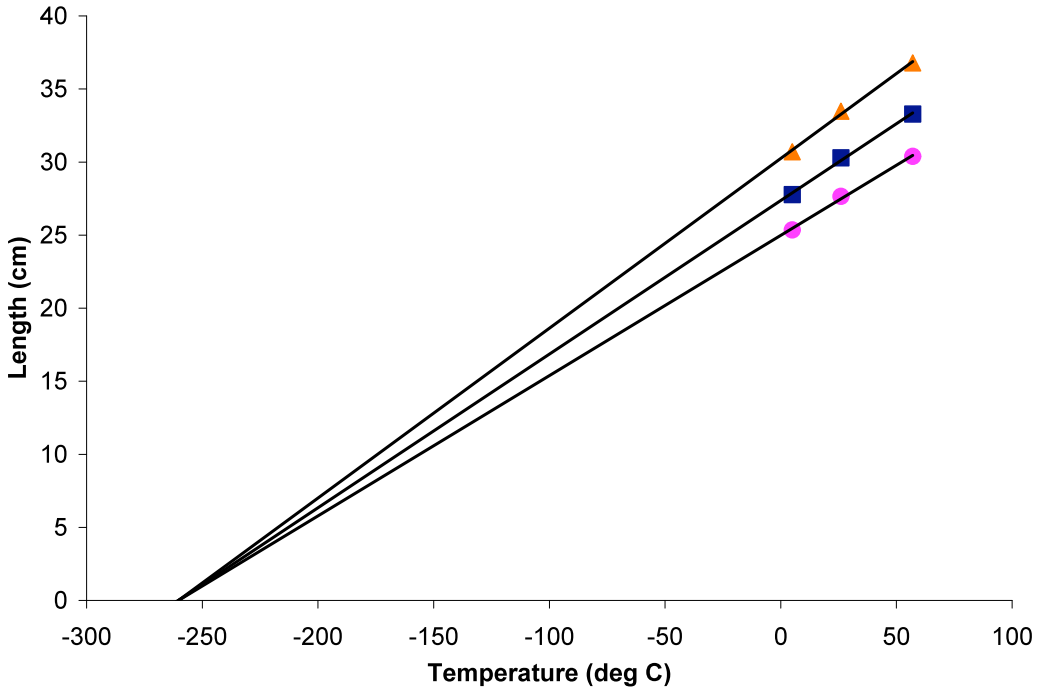

Figure 6.8. Representative linear data correlating the length (L) of the gas in the air column with the Temperature at 3 fixed pressures (950, 1050 and 1150 cm H_2O). The solid lines represent the best fit linear regression for each set of data. Backwards extrapolation of the linear regression to cross the x axis yields a reasonably good value for absolute zero (-273° C).

When this extracted volume is plotted as a function of the temperature an accurate set of student data will yield a reasonable value for absolute zero (-273°C or 0K). The data collected by this apparatus and represented here was of high quality and yielded an extrapolated absolute zero value of 13.752K, and a comprehensive set of student data

(collected by a class of first semester freshman) resulted in relatively good values for absolute zero, with some as precise as 4.5K.

6.4 Conclusion

As can be seen from the representative data here, this new experimental apparatus allows us to successfully collect pressure and length data (at various temperatures) using a simple and safe (mercury free) experimental set-up that yields remarkably good results. The apparatus is of general utility and can be used for many types of gas law experiments. Our need for a single, mercury-free apparatus that can be used to collect high quality P, V, and T data places an extra demand on the quality of the apparatus – one that was met by this device.

6.5 References:

1. Mills, Pamela A.; Sweeney, William V. *J. Chem. Educ*. **2000**, 77, 9, 1161
2. Domin, D. *J. Chem. Educ.* **1999**, 76, 543-547
3. Breck, W. G.; Holmes, F. W. *J. Chem. Educ*. **1967**, 44, 293
4. Hermens, R. A. *J. Chem. Educ*. **1983**, 60, 764
5. http://www.dec.ny.gov/chemical/285.html
6. http://law.justia.com/newyork/codes/environmental-conservation/env027-2107_27-2107.html
7. http://www.practicalphysics.org/go/Experiment_380.html
8. http://www.physics.umd.edu/lecdem/services/demos/demosi3/i3-41.htm
9. http://www.bradley.edu/las/phy/laboratories/110lab2002/boyle's/boyles_law_syringe.htm
10. http://sciencekit.com/low-cost-boyleandrsquo%3Bs-law-apparatus/p/IG0023590/
11. Lewis, Don, L. *J. Chem. Educ*. **1997**, 74, 2, 209
12. Deal, Walter, J. *J. Chem. Educ*. **1975**, 52, 6, 405
13. Ivanov, Dragia T. *Physics Education*. **2007**, 42, 2, 193
14. Kim, Myung-Hoon; Kim, Michelle, S.; Ly, Suw-Young. *J. Chem. Educ*. **2001**, 78, 2, 238
15. Bopegedera, A. M. R. P. *J. Chem. Educ*. **2007**, 84, 3, 465
16. CRC Handbook of Chemistry and Physics,

Chapter 7. An assessment of Chemistry 115 as a bridging course

Draft of Paper for submission to J. Chem educ.

CHEM 115 – A New Model for Under-prepared Chemistry Students

Donna McGregor, Pamela Mills and William V. Sweeney
Department of Chemistry, Hunter College, 695 Park Avenue, New York, NY 10065

7.1 Abstract

In this paper, we report on a novel and effective diagnostic procedure to identify students at-risk (potential failures) in the first semester General Chemistry course. Students who are identified as at-risk are placed into a newly created, preparatory chemistry course. We report on the assessment of the effectiveness of the preparatory course by comparing the performance of at-risk students with and without the preparatory course. We find that although this combination of identification and support for at-risk students has increased the probability of student success, it has not led to a significant number of additional successful science majors.

7.2 Introduction

Diagnostic placement exams have long been a staple of higher education, particularly in specific, highly sequenced, disciplines (such as mathematics or language). Unlike mathematics or language, the first course in a majors-based chemistry sequence (General Chemistry I) does not build on any prior knowledge. In this regard General Chemistry is conceptually different from, for example, calculus, which does build on the student's understanding of mathematical principles such as algebra. On the other hand,

chemistry educators have long recognized that the pacing and demands of the General Chemistry course poses a particular challenge for students who have never taken a chemistry course in high school. Many institutions, particularly large public institutions, have thus created an introductory or preparatory chemistry course for students who did not have a high school course. As such, the preparatory chemistry course is not viewed as a remedial, i.e. non-college, level course.[†]

Once institutions create alternative courses or sequences, the challenge becomes placing students into the appropriate course. The earliest editions of the *Journal of Chemical Education* contain articles that address this issue.[1, 2] There are two fundamental concerns: 1) placing students into an appropriate course and 2) assessing the effectiveness of the preparatory course.

It has become very clear that no diagnostic exam can predict accurately a student's performance in General Chemistry. On the other hand, there are metrics that can predict, with some accuracy, performance at the extreme – either failing or high levels of success.[3] Student motivation plays a significant role in student success and cannot be assessed accurately by a diagnostic metric. As a consequence, institutions have focused on identifying students not likely to succeed in General Chemistry. Commercial diagnostic exams (the Toledo CPE, the California Chemistry Diagnostic Test) as well as exams developed locally have been used to identify these students. The best reported accuracies of these exams is 70-80%. [4]

[†] The language describing chemistry courses can be confusing. There are often three types of introductory courses: General Chemistry, the year-long sequence for majors (Chem 102-105 at HC), a health science sequence that includes a one-semester overview of principles and a one-semester overview of organic chemistry (Chem 100 and Chem 120 at HC), and an "introductory" or "preparatory" course (Chem 115). The preparatory course and the health science course are fundamentally different courses with different learning outcomes and goals. In this report, the majors sequence will be called "General Chemistry" and the preparatory course will be called "Preparatory Chemistry." The health science (or nursing) sequence is not part of this discussion.

Until recently, Hunter College had no preparatory chemistry course[‡]. Seven years ago (in the Fall 2002), the department sought to institute such a course and began the process by looking at diagnostic exams. None of the diagnostic exams employed (the California Chemistry Diagnostic Test as well as locally constructed ones) achieved the 70-80% accuracy with the Hunter student population. It should be noted however, that we did not disaggregate our student population according to various demographic factors and thus do not know if the diagnostic measures would be accurate predictors for particular cohorts within our population. We surmise that the "motivation" factor is considerable at Hunter given the enormous diversity of the student population.

In this paper, we report on the department's novel and effective diagnostic procedure to identify students at-risk (potential failures) in the first semester General Chemistry course. Students who are identified as at-risk are placed into a newly created, preparatory chemistry course. We report on the assessment of the effectiveness of the preparatory course by comparing the performance of at-risk students with and without the preparatory course.

[‡] It is important to note that many universities have a Chem 115-type course. Comparable courses at other universities include:
Chem 101 at University of Illinois Chicago
Chem 103 at University of Maryland*
Chem 1A at University of California Berkeley*
Chem 115 at California State University, Fullerton

(*These institutions have two general chemistry sequences -- one for majors and one for non-majors. This is the first course in the non-majors sequence)

7.3 Results and Discussion

Early Identification of Student Readiness in General Chemistry

Institutions that have a multi-tiered approach to first year chemistry often use a placement exam as well as indicators from high school courses and SAT scores. For examples, some courses will only admit students with an AP course score of 3-5. All other students begin with the preparatory course. Some schools have written placement exams that are administered on the first day of class. Most institutions use the California Chemistry Diagnostic Test, published by the American Chemical Society's Division of Education. There is a robust literature on the validity of the exam. [5, 6]

The most common application of the diagnostic exam is the use of a cutoff score for placement into a particular course. Recently, a modification of the cutoff score model has been proposed. Legg, *et. al* argue that the test should be used for advisement purposes and a probability factor should be given to the student.[7] Using a logistic regression model, the probability of success in the course, based on the diagnostic test, is extremely accurate.

We have found that, while the academic literature on placement testing is interesting, its applicability to our student population is limited. Firstly, the administration of the California Chemistry Diagnostic Test correlated poorly with student success in one of our larger Chem 102 sections. Secondly, the use of the test as an advisement tool will fair poorly. Students at Hunter College rarely opt for the more appropriate course despite statistic proof of their impending failure.

Thus we have developed another diagnostic model -- the first exam in the Chem 102 course. Students are told on the first day of Chem 102 that the first exam will act as a

diagnostic exam. Students who fall below a certain cutoff value will be required to transfer to Chem 115 -- a course offered at the same time and with the same number of credits. To assess the accuracy of the first exam to predict failure in General Chemistry five sections of general chemistry were analyzed. Student performance on the first exam was correlated with student's grades in the course. The five sections numbered 391 students and were taught by five different instructors with significantly different pedagogical styles. The class size varied from under 40 to over 100.

The students' performances on the first exam was grouped into standard deviation categories according to:

< 1s bel:	Student scores fell 1 standard deviation below the mean
< ½ s bel:	Student scores fell ½ standard deviation below the mean
bel avg:	Student scores fell below the mean
0 - ½ s:	Student scores fell between the average and ½ standard deviation above the mean
½ - 1 a:	Student scores fell between ½ and 1 standard deviation above average
> 1s a:	Student scores were 1 standard deviation or more above average.

Student performances are shown in Table 1. In Table 1, the percentages reported are the percentages of students in the given category. For example, 90.22% of the students who scores 1 standard deviation between the mean received a grade of F. Each column's percentages should add to 100%.

Grade	< 1s bel	< ½ s b	below avg	0 - ½ s a	0 - 1 s a	> 1s a
f	90.22%	84.21%	75.22%	37.50%	19.86%	2.06%
d	7.61%	10.53%	10.43%	8.93%	12.06%	1.03%
c	1.09%	3.95%	8.70%	50.00%	31.91%	9.28%
b	1.09%	1.32%	5.22%	3.57%	29.79%	35.05%
a	0.00%	0.00%	0.43%	0.00%	6.38%	52.58%

Table 7.1 Correlation of Student Performance on Exam 1 with Final grade

The results in table 1 are striking. Only 2% of the students who scored 1 standard deviation below average passed the course with a grade of C or better. This corresponds to 2 students from the five sections. The statistics do not get much better for the other categories below the mean. Only 5% of the students who scored ½ standard deviation below the mean passed with a C or better. This corresponds to 8 students. It is particularly striking that only 14% of the students who score *anywhere* below average pass the course with a C or better.

The scores on the first test are a significant predictor of success in Chem 102. In fact it is a *rare* student who goes on to pass the course after a poor showing on the first exam.

Based on these data, the chemistry department selects a score usually between ½ and 1 standard deviation below the mean as the cutoff for transferring students to Chem 115. Constraints, such as the room size, limit the number of students we can transfer.

It should be noted that students who are required to transfer to Chem 115 generally oppose the transfer. This opposition continues despite the statistical evidence of their probable failure. Clearly, allowing students to transfer based on "advice" would be a failed enterprise. In Spring 2004 for example, five students complained so persistently and loudly that the chemistry advisor allowed them to remain in Chem 102. All five students failed the course.

Chem 115 -- The Effectiveness of the Intervention

The effectiveness of the Chem 115 intervention was assessed by first constructing a baseline cohort. This cohort is composed of students in the day Chem 102 classes who failed the Chem 102 class for the first time. These students took Chem 102 when the Chem 115 intervention was not available. Thus the baseline group is almost identical to, although slightly better than, the Chem 115 group because we are not isolating just the students who did poorly on the first exam. The baseline cohort is therefore students who need the intervention (Chem 115) but for whom the intervention is not available.

For ease of analysis, we choose the Fall 1999 and Spring 2003 semesters and constructed the baseline cohort from these students. We then compare the behaviors of this cohort with those enrolled in Chem 115 regarding

1) the percentage of students who return to Chem 102

2) the percentage of students who pass Chem 102

3) the percentage of students who continue onto Chem 104 and/or Chem 222.

Baseline Cohort

Metric	Fall 99	Spring 2003
Number of day students who failed Chem 102 for the first time	56	53
Number of students repeating Chem 102	20	14
Number of students who passed Chem 102 on second try	4	0
Percent success of repeaters	20%	0
Average GPA of passed courses	1.5	

Table 7.2 Baseline Cohort Data: Profile of students failing Chem 102 in Fall 1999 and Spring 2003 semester

109 students failed Chem 102 for the first time in the Fall 1999 and Spring 2003 semesters. Of these students, 34 repeated Chem 102 by the Fall 2004 semester. Of the 34 students, 4 students passed Chem 102 on their second try. The percent success of the baseline cohort is 12%. These students are successful with an average GPA of 1.50.

Chem 115 Cohorts

Comparison data is generated for the Chem 115 students. Since Chem 115 was first offered in Fall 2002, students have had less time to repeat Chem 102 than the Fall 1999 cohort. Despite this, the Chem 115 cohort is vastly more successful than the Chem 102 repeaters.

Metric	Fa02	Fa03	Sp04	Fa04	Sp05	Sp06	Fa06	Fa07
Number of students enrolled in Chem 115	88	78	65	109	77	49	21	40
Number of students passing Chem 115	79	69	38	78	55	33	8	34
Number of students repeating Chem 102	67	52	30	63	50	25	12	32
Number of students who passed Chem 102	54	19	15	28	37	19	8	25
Percent success	81%	38%	50%	45%	74%	76%	67%	78%
Average GPA of passed courses	2.40	1.91	2.07					

Table 7.3. Chem 115 Cohort Data: Profile of students failing Chem 102

7.4 Conclusions

The identification of at-risk students and the intervention (Chem 115) exceed all reported success on preparatory chemistry courses. The identification of the at-risk student based on the first exam is a stunningly accurate predictor of subsequent failure in the course. Depending upon the choice of cut-off, the first exam can predict failure with a 98% accuracy. No diagnostic tool has ever reported an accuracy of this caliber.

The intervention designed (Chem 115) is an exceedingly better tool than having students repeat the General Chemistry course after experiencing a failure. Students who are placed into Chem 115 and then return to the General Chemistry sequence do not obtain outstanding grades. This raises an important research question as to how students can acquire the skills necessary to succeed well above average in a General Chemistry

class. Clearly at-risk students do not acquire sufficient skills in one semester. However, these students do benefit in other ways from the Chem 115 experience. They do not have a failing grade on their transcript, they have a successful experience in a science course, and they do pass General Chemistry at a significantly higher rate than those students with no preparatory course.

The procedure we use to identify and intervene with at-risk students is an alternative to the traditional diagnostic exam approach. The institution must participate in the process by assisting with room assignments and with registration procedures. Students cannot adjust their schedule one month into the semester. Thus there has to be a seamless transition from the Chem 102 class to the Chem 115 class. This is best achieved by having a room and class offered at the same time as the original Chem 102 class.

It should be noted that the students in Chem 115 were identified as the weakest performing students on the first exam. Students scoring below average but not 1 standard deviation below average may also benefit from an intervention. However, room size limitations prevents us from offering Chem 115 to these higher performing students. It is also possible that the nature of the intervention is and should be different depending upon the student's performance on the first exam. Fine tuning the Chem 115 class to match expectations and maximum resources is an ongoing effort at Hunter College.

7.5 References

1. Scofield, M.B. *J. Chem. Educ.* ***1927,*** 4, 1168-1175.
2. Smith, O.M.; Trimble, H.M. *J. Chem. Educ.* (1929) 6, 93-97.
3. McFate, C.; Olmsted III, J. (1999) *J. Chem. Educ.* **76**, 562-565.
4. Bentley, Andrea B.; Gellene, Gregory I., (2005) *J. Chem. Educ.* 82, 125-130.
5. Russell, A.A. (1994) *J. Chem. Educ.* **71,** 314-317.
6. Hovey, N.W.; Krohn, A. (1958) *J. Chem. Educ.* **35**, 507-509.
7. Legg, Margaret J.; Legg, Jason C.; Greenbowe, Thomas J. (2001) *J. Chem. Educ.* 78, 1117.

Bibliography of References

Chapter 1

1. Jurisson, S. S.; Lydon, J. D., *Chem. Rev.* **1999,** *99*, 2205-2218.

2. Committee on the Review of the Hanford Sites environmental Remediation Science and Technology Plan. Board on radioactive waste Management, National Research Council.Sciene and Technology for Environmental Cleanup at Hanford. National Acedemy Press, Washington D.C. : 2001.

3. *Summary of the Hanford Site Environmental Report for the Calender year 2007.*; PNNL-17603-SUM; Pacific Northwest National Laboratory, Richland, washington: Sept 2008.

4. Van Ostenberg, D. O.; Trapp, H. D.; Lam, D. J., *Phys. Rev.* **1962,** *126*.

5. Kessler, K. G.; Trees, R. E., *Phys. Rev.* **1953,** *92*.

6. Schwochau, K., *Angew. Chem.* **1964,** *76*.

7. Boyd, G., *J. Chem. Educ.* **1959,** *36*, 3.

8. Cobble, J. W., *J. Chem. Phys.* **1953,** *21*.

9. Mendeleev, D. I., *Liebigs Ann. Chem, Suppl.* **1872,** *8*, 133-229.

10. Perrier, C.; Segre, E., *J. Chem. Phys.* **1937,** *5*, 712 - 716.

11. Perrier, C.; Segre, E., *Nature (London)* **1937,** *140*, 193 - 194.

12. Moore, C. E., *Science* **1951,** *114*, 59 - 61.

13. Miller, F. J.; Zittel, H. E., *Analyt. Chem.* **1963,** *35*.

14. Merrill, P. W., *Astrophys. J.* **1952,** *116*, 21 - 26.

15. Merrill, P. W., *Science* **1952,** *115*, 484.

16. Merrill, P. W., *Publ. Astron. Soc. Pac.* **1956,** *68*, 70 - 71.

17. Kenna, B. T.; Kuroda, P. K., *J. Inorg. Nucl. Chem.* **1961,** *23*, 142 - 144.

18. Kenna, B. T.; Kuroda, P. K., *J. Inorg. Nucl. Chem.* **1964,** *26*, 493 - 499.

19. Lukens, W. W.; Shuh, D. K.; Schroeder, N. C.; Ashley, K. R., *Environ. Sci. Technol.* **2004,** *38*, 229-233.

20. Lukens, W. W.; Bucher, J. J.; Shuh, D. K.; Edelstein, N. M., *Environ. Sci. Technol.* **2005,** *39*, 8064-8070.

21. French, M. A.; Hao, Z.; Pates, J. M.; Bryan, S. E.; Wilson, R. C., *Anal. Chem.* **2005,** *77*, 135.

22. Lloyd, J. R.; Sole, V. A.; Van Praagh, C. V. G.; Lovley, D. R., *Appl. Environ. Microbiol.* **2000,** *66*, 3743-3749.

23. Wildung, R. E.; Gorby, Y. A.; Krupka, K. M.; Hess, N. J.; Li, S. W.; Plymale, A. E.; McKinley, J. P.; Fredrickson, J. K., *Appl. Environ. Microbiol.* **2000,** *66* (6), 2451-2460.

24. Torstenfeld, B., *Technetium in the Geological Environment, A literature survey*. 1981.

25. Chen, J.; Boerrigter, H.; Veldkamp, A., *Radiochim. Acta* **2001,** *89*.

26. Burke, I. T.; Boothman, C.; Lloyd, J. R.; Mortimer, R. J. G.; Livens, F. R.; Morris, K., *Environ. Sci. Technol.* **2005,** *39*, 4109-4116.

27. DiPrete, D. P.; DiPrete, C. C.; Sigg, A., *Journal of radioanal. and nuclear chemistry* **2005,** *263*.

28. Egorov, O., B.; O'Hara, M., J.; Grate, J., W., *Anal. Chem. 76*.

29. Wakoff, B.; Nagy, K., L., *Environ. Sci. Technol.* **2004,** *38*.

30. Golchert, N. W.; Sedlet, J., *Anal. Chem.* **1969,** *41*, 669 - 671.

31. Gawenis, J., A.; Kauffman, J., F.; Jurisson, S., S, *Anal. Chem.* **2001,** *73* (9).

32. Cobble, J. W.; Boyd, G. E.; Smith, W. T.; Nelson, C. M.; Parker, G. W., *J. Amer. Chem. Soc.* **1952,** *74*, 1852.

33. Burgeson, I. E.; Deschane, J. R.; Blanchard, J. D. L., *Separation Science and Technology* **2005,** *40*, 201 - 223.

34. King, W. D.; Hassan, N. M.; McCabe, D. J.; Hamm, L. L.; Johnson, M. E., *Separation Science and Technology* **2003,** *38*, 3093 - 3114.

35. Gu, B. H.; Brown, G. M.; Bonnesen, P. V.; Liang, L. Y.; Moyer, B. A.; Ober, R.; Alexandratos, S. D., *Environ. Sci. Technol.* **2000,** *34*, 1075 - 1080.

36. Wildung, R. E.; Li, S. W.; Murray, C. J.; Krupka, K. M.; Xie, Y.; Hess, N. J.; Roden, E. E., *FEMS Microbiology Ecology* **2004,** *49*, 151-162.

37. Daqing, C.; Eriksen, T. E., *Environ. Sci. Technol.* **1996,** *30*.

38. Magirius, S.; Carnall, W. T.; Kim, J. I., *Radiochim. Acta* **1985,** *38*, 29-32.

39. Lieser, K. H.; Coetzee, P. P.; Foerster, M., *Radiochim. Acta* **1985,** *38*, 33-35.

40. Hill, C., *Chem. Rev.* **1998,** *98*, 1-3.

41. Gouzerh, P.; Proust, A., *Chem Rev* **1998,** *98*, 327 - 357.

42. Day, V. W.; Klemperer, W. G., *Science* **1985,** *228*, 533-541.

43. Leclerc-Laronze, N., M. ; Haouas, M.; Marrot, J.; Taulelle, F.; Herve, G., *Angew. Chem. Int. Ed.* **2006,** *45* (1), 139-142.

44. Fang, X.; Hill, C. L., *Angew. Chem. Int. Ed.* **2007,** *46*, 3877-3880.

45. Day, V. W.; Klemperer, W. G.; Schwartz, C.; Wang, R.-C., Molecular Models of early transition metal oxides: polyoxoanions as organic functional groups. In *Surface Organometallic Chemistry: Molecular Approaches to Surface Catalysis*, Kluwer Academic Publishers: New York, 1988; p 173.

46. Long, D.-L.; Burkholder, E.; Cronin, L., *Chem. Soc. Rev.* **2007,** *36*, 105-121.

47. Saito, A.; Choppin, G. R., *Inorg. Chem.* **1991,** *30* (24), 4563-4566.

48. Saito, A.; Tomari, H.; Choppin, G. R., *Inorganica Chimica Acta* **1997,** *258*, 145-153.

49. Luo, Q.; Howell, R. C.; Bartis, J.; Dankova, M.; Horrocks, W. D., Jr.; Rheingold, A. L.; Francesconi, L. C., *Inorg. Chem.* **2002,** *41*, 6112-6117.

50. Luo, Q.; Howell, R. C.; Dankova, M.; Bartis, J.; Williams, C. W.; Horrocks, W. D., Jr.; Young, J., V.G.; Rheingold, A. L.; Francesconi, L. C.; Antonio, M. R., *Inorg. Chem.* **2001,** *40*, 1894-1901.

51. Bartis, J.; Dankova, M.; Lessmann, J. J.; Luo, Q.-H.; Horrocks, W. D., Jr.; Francesconi, L. C., *Inorganic Chemistry* **1999,** *38*, 1042-1053.

52. Ciabrini, J.-P.; Contant, R., *J. Chem. Research (S) 1993, 391* **1993**, 2720-2744.

53. Contant, R.; Ciabrini, J.-P., *J. Chem. Research (S) 1982, 50-51* **1982,** *1982*, 641-660.

54. Contant, R.; Rocchiccioli-Deltcheff, C.; Fournier, M.; Thouvenot, R., *Calloids and Surfaces A: Physicochemical and Engineering Aspects* **1993,** *72*, 301-306.

55. Contant, R.; Abbessi, M.; Canny, J.; Belhouari, A.; Keita, B.; Nadjo, L., *Inorg. Chem.* **1997,** *36*, 4961-4967.

56. Contant, R.; Herve, G., *Reviews in Inorganic Chemistry* **2002,** *22* (2), 63-111.

57. Keita, B.; Girard, F.; Nadjo, L.; Contant, R.; Canny, J.; Richet, M., *Journ. of Electroanal. Chem.* **1999,** *478*, 76-82.

58. Harmalker, S. P.; Leparulo, M. A.; Pope, M. T., *J. Amer. Chem. Soc.* **1983,** *105*, 4286-4292.

59. Leparulo-Loftus, M. A.; Pope, M. T., *Inorg. Chem.* **1987,** *26*, 2112-2120.

60. Sadakane, M.; Dickman, M. H.; Pope, M. T., *Inorg. Chem.* **2001,** *40* (12), 2715-2719.

61. Sadakane, M.; Ostuni, A.; Pope, M. T., *J. Chem. Soc. Dalton Trans.* **2002**, 63-67.

62. Abbessi, M.; Contant, R.; Thouvenot, R.; Herve, G., *Inorg. Chem.* **1991,** *30*, 1695-1702.

63. Zhang, C.; Howell, R. C.; Fieselmann, H. L.; Todaro, L.; Francesconi, L. C., *Inorg. Chem.* **2005,** *44*, 3569-3578.

64. Boglio, C.; Lenoble, G.; Duhayon, C.; Hasenknopf, B.; Thouvenot, R.; Zhang, C.; Howell, R.; Burton-Pye, B.; Francesconi, L. C.; Lacote, E.; Thorimbert, S.; Malacria, M.; Afonso, C.; Tabet, J.-C., *Inorg Chem* **2006,** *45* (3), 1389-1398.

65. Keita, B.; Lu, Y. W.; Nadjo, L.; Contant, R., *Electrochemistry Communications* **2000,** *2*, 720-726.

66. Kozik, M.; Hammer, C. F.; Baker, L. C. W., *J. Am. Chem. Soc.* **1986,** *108*, 2748-2749.

67. Kozik, M.; Baker, L. C. W., *J. Am. Chem. Soc.* **1990,** *112*, 7604-7611.

68. Acerete, R.; Hammer, C. F.; Baker, L. C. W., *Journ. Amer. Chem. Soc.* **1982,** *104*, 5384-5390.

69. Ciabrini, J. P.; Contant, R.; Fruchart, J. M., *Polyhedron* **1983,** *2* (11), 1229-33.

70. Lopez, X.; Bo, C.; Poblet, J. M., *J. Am. Chem. Soc.* **2002,** *124*, 12574-12582.

71. Keita, B.; Levy, B.; Nadjo, L.; Contant, R., *New. J. Chem.* **2002,** *26*, 1314-1319.

72. Contant, R.; Richet, M.; Lu, Y. W.; Keita, B.; Nadjo, L., *Eur. J. Inorg. Chem.* **2002**, 2587-2593.

73. Mandal, S.; Selvakannan, P. R.; Pasricha, R.; Sastry, M., *J. Amer. Chem. Soc.* **2003,** *125*, 8440-8441.

74. Geletii, Y. V.; Hill, C. L.; Bailey, A. J. H., K.I.; Atalla, R. H.; Weinstock, I. A., *Inorg. Chem.* **2005,** *44*, 8955-8966.

75. Altenau, J. J.; Pope, M. T.; Prados, R. A.; So, H., *Inorg. Chem.* **1977,** *14* (2), 417-421.

76. Pope, M. T.; Varga, G. M., *Inorg. Chem.* **1966,** *5* (7), 1249-1254.

77. Mandal, S.; Mandale, A. B.; Sastry, M., *J. Mater. Chem.* **2004,** *14*, 2868-2871.

78. Troupis, A.; Hiskia, A.; Papaconstantinou, E., *New J. Chem.* **2001,** *25*, 361-363.

79. Hiskia, A.; Troupis, A.; Papaconstantinou, E., *International Journal of Photoenergy* **2002,** *4*, 35-40.

80. Grika, E.; Troupis, A.; Hiskia, A.; Papaconstantinou, E., *Environ. Sci. Technol.* **2005,** *39*, 4242-4248.

Chapter 2

1. Zhang, C.; Howell, R. C.; Luo, Q.; Fieselmann, H. L.; Todaro, L.; Francesconi, L. C., *Inorg. Chem.* **2005,** *44*, 3569-3578.

2. Boglio, C.; Lenoble, G.; Duhayon, C.; Hasenknopf, B.; Thouvenot, R.; Zhang, C.; Howell, R.; Burton-Pye, B. P.; Francesconi, L. C.; Lacote, E.; Thorimbert, S.; Malacria, M.; Afonso, C.; Tabet, J.-C., *Inorg Chem* **2006,** *45* (3), 1389-1398.

3. Davison, A.; Trop, H.; DePamphilis, B.; Jones, A., *Inorganic Synthesis* **1982,** *21*, 160.

4. Ciabrini, J.-P.; Contant, R., *J. Chem. Research (S) 1993, 391* **1993**, 2720-2744.

5. Contant, R., *Inorg. Synth.* **1990,** *27*, 71-111.

6. Bartis, J.; Dankova, M.; Blumenstein, M.; Francesconi, L. C., *Journal of Alloys and Compunds* **1997,** *249*, 56-68.

7. Keita, B.; Girard, F.; Nadjo, L.; Contant, R.; Belghiche, R.; Abessi, M., *J. Electroanal. Chem.* **2001,** *508* (1-2), 70-80.

8. Contant, R.; Ciabrini, J.-P., *J. Chem. Res. (S) 1977, 222* **1977,** *M*, 2601-2617.

9. Contant, R.; Ciabrini, J.-P., *J. Chem. Research (S) 1982, 50-51* **1982,** *1982*, 641-660.

10. Davison, A.; DePamphilis, B. V.; Jones, A. G.; Franklin, K. L.; Lock, C. J. L., *Inorg. Chim. Acta* **1987,** *128* (2), 161-167.

11. Venturelli, A.; Nilges, M. J.; Smirnov, A.; Belford, R. L.; Francesconi, L. C., *J. Chem. Soc., Dalton Trans.* **1999**, 301-310.

12. Ortega, F.; Pope, M. T., *Inorg. Chem.* **1984,** *23*, 3292-3297.

13. Finke, R. G.; Rapko, B.; Saxton, R. J.; Domaille, P. J., *J. Am. Chem. Soc.* **1986,** *108*, 2947-2960.

14. Finke, R. G.; Droege, M. W.; Domaille, P. J., *Inorg. Chem.* **1987,** *26*, 3886-3896.

15. Finke, R. G.; Lyon, D. K.; Nomiya, K.; Sur, S.; Mizuno, N., *Inorg. Chem.* **1990,** *29* (10), 1784-1787.

16. Bartis, J.; Kunina, Y.; Blumenstein, M.; Francesconi, L. C., *Inorg. Chem.* **1996,** *35* (5), 1497-1501.

17. Jorris, T. L.; Kozik, M.; Casan-Pastor, N.; Domaille, P. J.; Finke, R. G.; Miller, W. K.; Baker, L. C. W., *J. Am. Chem. Soc.* **1987,** *109*, 7402-7408.

18. Sadakane, M.; Dickman, M. H.; Pope, M. T., *Inorg. Chem.* **2001,** *40* (12), 2715-2719.

19. Sadakane, M.; Ostuni, A.; Pope, M. T., *J. Chem. Soc. Dalton Trans.* **2002**, 63-67.

20. Zhang, C.; Howell, R. C.; Fieselmann, H. L.; Todaro, L.; Francesconi, L. C., *Inorg. Chem.* **2005,** *44*, 3569-3578.

21. Boglio, C.; Lenoble, G.; Duhayon, C.; Hasenknopf, B.; Thouvenot, R.; Zhang, C.; Howell, R. C.; Burton-Pye, B. P.; Francesconi, L. C.; Lacote, E.; Thorimbert, S.; Malacria, M.; Afonso, C.; Tabet, J.-C., *Inorg. Chem.* **2006,** *45* (3), 1389-1398.

22. Bartis, J.; Sukal, s.; Dankova, M.; Kraft, E.; Kronzon, R.; Blumenstein, M.; Francesconi, L. C., *J. Chem. Soc., Dalton Trans* **1997**, 1937-1944.

23. Bartis, J.; Dankova, M.; Lessmann, J. J.; Luo, Q.-H.; Horrocks, W. D., Jr.; Francesconi, L. C., *Inorganic Chemistry* **1999,** *38*, 1042-1053.

24. Salmonte, J. L.; Pope, M. T., *Canadian Journal of Chemistry* **2001,** *79* (5/6), 802-808.

25. Howell, R. C.; Perez, F. G.; Jain, S.; Horrocks, W. D., Jr.; Rheingold, A. L.; Francesconi, L. C., *Angew. Chem. Int. Ed.* **2001,** *40*, 4301-4304.

26. Zhang, C.; Howell, R.; Scotland, K. B.; Perez, F. G.; Todaro, L.; Francesconi, L. C., *Inorg Chem* **2004,** *43*, 7691-7701.

27. Zhang, C.; Bensaid, L.; McGregor, D.; Fang, X.; Howell, R. C.; Burton-Pye, B.; Luo, Q.; Todaro, L.; Francesconi, L. C., *J. Cluster Sci.* **2006,** *17*, 389-426.

28. Acerete, R.; Hammer, C. F.; Baker, L. C. W., *Journ. Amer. Chem. Soc.* **1982,** *104*, 5384-5390.

29. Keita, B.; Girard, F.; Nadjo, L.; Contant, R.; Canny, J.; Richet, M., *Journ. of Electroanal. Chem.* **1999,** *478*, 76-82.

30. Contant, R.; Richet, M.; Lu, Y. W.; Keita, B.; Nadjo, L., *Eur. J. Inorg. Chem.* **2002**, 2587-2593.

31. Keita, B.; Levy, B.; Nadjo, L.; Contant, R., *New. J. Chem.* **2002,** *26*, 1314-1319.

32. Keita, B.; Belhouari, A.; Nadjo, L.; Contant, R., *J. Electroanal. Chem.* **1998,** *442*, 49-57.

33. Contant, R.; Abbessi, M.; Canny, J.; Belhouari, A.; Keita, B.; Nadjo, L., *Inorg. Chem.* **1997,** *36*, 4961-4967.

34. Contant, R.; Herve, G., *Reviews in Inorganic Chemistry* **2002,** *22* (2), 63-111.

35. Keita, B.; Lu, Y. W.; Nadjo, L.; Contant, R., *Electrochemistry Communications* **2000,** *2*, 720-726.

36. Kozik, M.; Baker, L. C. W., *J. Am. Chem. Soc.* **1990,** *112*, 7604-7611.

37. Kozik, M.; Hammer, C. F.; Baker, L. C. W., *J. Am. Chem. Soc.* **1986,** *108*, 2748-2749.

38. Ciabrini, J. P.; Contant, R.; Fruchart, J. M., *Polyhedron* **1983,** *2* (11), 1229-33.

39. Lopez, X.; Bo, C.; Poblet, J. M., *J. Amer. Chem. Soc.* **2002,** *124*, 12574-12582.

40. Lopez, X.; Bo, C.; Poblet, J. M., *J. Am. Chem. Soc.* **2002,** *124*, 12574-12582.

Chapter 3

1. Lyon, D. K.; Miller, W. K.; Novet, T.; Domaille, P. J.; Evitt, E.; Johnson, D. C.; Finke, R. G., *J. Amer. Chem. Soc.* **1991,** *113*, 7209-7221.

2. Davison, A.; Trop, H.; DePamphilis, B.; Jones, A., *Inorganic Synthesis* **1982,** *21*, 160.

3. Ciabrini, J.-P.; Contant, R., *J. Chem. Research (S) 1993, 391* **1993**, 2720-2744.

4. Contant, R., *Inorg. Synth.* **1990,** *27*, 71-111.

5. Bartis, J.; Dankova, M.; Blumenstein, M.; Francesconi, L. C., *Journal of Alloys and Compunds* **1997,** *249*, 56-68.

6. Graham, C. R.; Ott, L. S.; Finke, R. G., *Langmuir* **2009,** *25*, 1327 - 1336.

7. Venturelli, A.; Nilges, M. J.; Smirnov, A.; Belford, R. L.; Francesconi, L. C., *J. Chem. Soc., Dalton Trans.* **1999**, 301-310.

8. Finke, R. G.; Rapko, B.; Saxton, R. J.; Domaille, P. J., *J. Am. Chem. Soc.* **1986,** *108*, 2947-2960.

9. Finke, R. G.; Droege, M. W.; Domaille, P. J., *Inorg. Chem.* **1987,** *26*, 3886-3896.

10. Finke, R. G.; Lyon, D. K.; Nomiya, K.; Sur, S.; Mizuno, N., *Inorg. Chem.* **1990,** *29* (10), 1784-1787.

11. Jorris, T. L.; Kozik, M.; Casan-Pastor, N.; Domaille, P. J.; Finke, R. G.; Miller, W. K.; Baker, L. C. W., *J. Am. Chem. Soc.* **1987,** *109*, 7402-7408.

12. Bartis, J.; Kunina, Y.; Blumenstein, M.; Francesconi, L. C., *Inorg. Chem.* **1996,** *35* (5), 1497-1501.

13. Sadakane, M.; Dickman, M. H.; Pope, M. T., *Inorg. Chem.* **2001,** *40* (12), 2715-2719.

14. Sadakane, M.; Ostuni, A.; Pope, M. T., *J. Chem. Soc. Dalton Trans.* **2002**, 63-67.

15. Salmonte, J. L.; Pope, M. T., *Canadian Journal of Chemistry* **2001,** *79* (5/6), 802-808.

16. Bartis, J.; Sukal, s.; Dankova, M.; Kraft, E.; Kronzon, R.; Blumenstein, M.; Francesconi, L. C., *J. Chem. Soc., Dalton Trans* **1997**, 1937-1944.

17. Bartis, J.; Dankova, M.; Lessmann, J. J.; Luo, Q.-H.; Horrocks, W. D., Jr.; Francesconi, L. C., *Inorganic Chemistry* **1999,** *38*, 1042-1053.

18. Boglio, C.; Lenoble, G.; Duhayon, C.; Hasenknopf, B.; Thouvenot, R.; Zhang, C.; Howell, R. C.; Burton-Pye, B. P.; Francesconi, L. C.; Lacote, E.; Thorimbert, S.; Malacria, M.; Afonso, C.; Tabet, J.-C., *Inorg. Chem.* **2006,** *45* (3), 1389-1398.

19. Howell, R. C.; Perez, F. G.; Jain, S.; Horrocks, W. D., Jr.; Rheingold, A. L.; Francesconi, L. C., *Angew. Chem. Int. Ed.* **2001,** *40*, 4301-4304.

20. Zhang, C.; Howell, R. C.; Scotland, K. B.; Perez, F. G.; Todaro, L.; Francesconi, L. C., *Inorg. Chem.* **2004,** *43*, 7691-7701.

21. Zhang, C.; Howell, R. C.; Luo, Q.; Fieselmann, H. L.; Todaro, L.; Francesconi, L. C., *Inorg. Chem.* **2005,** *44*, 3569-3578.

22. Zhang, C.; Bensaid, L.; McGregor, D.; Fang, X.; Howell, R. C.; Burton-Pye, B.; Luo; Q.; Todaro, L.; Francesconi, L. C., *Journal of Cluster Science* **2006,** *17*, 389-426.

23. Keita, B.; Girard, F.; Nadjo, L.; Contant, R.; Canny, J.; Richet, M., *Journ. of Electroanal. Chem.* **1999,** *478*, 76-82.

24. Contant, R.; Richet, M.; Lu, Y. W.; Keita, B.; Nadjo, L., *Eur. J. Inorg. Chem.* **2002**, 2587-2593.

Chapter 4

1. Lukens, W. W.; Shuh, D. K.; Schroeder, N. C.; Ashley, K. R., *Environ. Sci. Technol.* **2004,** *38*, 229-233.

2. Lukens, W. W.; Bucher, J. J.; Shuh, D. K.; Edelstein, N. M., *Environ. Sci. Technol.* **2005,** *39*, 8064-8070.

3. Lloyd, J. R.; Sole, V. A.; Van Praagh, C. V. G.; Lovley, D. R., *Appl. Environ. Microbiol.* **2000,** *66*, 3743-3749.

4. Burke, I. T.; Boothman, C.; Lloyd, J. R.; Mortimer, R. J. G.; Livens, F. R.; Morris, K., *Environ. Sci. Technol.* **2005,** *39*, 4109-4116.

5. Mandal, S.; Selvakannan, P. R.; Pasricha, R.; Sastry, M., *J. Amer. Chem. Soc.* **2003,** *125*, 8440-8441.

6. Geletii, Y. V.; Hill, C. L.; Bailey, A. J. H., K.I.; Atalla, R. H.; Weinstock, I. A., *Inorg. Chem.* **2005,** *44*, 8955-8966.

7. Altenau, J. J.; Pope, M. T.; Prados, R. A.; So, H., *Inorg. Chem.* **1977,** *14* (2), 417-421.

8. Pope, M. T.; Varga, G. M., *Inorg. Chem.* **1966,** *5* (7), 1249-1254.

9. Mandal, S.; Mandale, A. B.; Sastry, M., *J. Mater. Chem.* **2004,** *14*, 2868-2871.

10. Troupis, A.; Hiskia, A.; Papaconstantinou, E., *New J. Chem.* **2001,** *25*, 361-363.

11. Hiskia, A.; Troupis, A.; Papaconstantinou, E., *International Journal of Photoenergy* **2002,** *4*, 35-40.

12. Grika, E.; Troupis, A.; Hiskia, A.; Papaconstantinou, E., *Environ. Sci. Technol.* **2005,** *39*, 4242-4248.

13. Davison, A.; Trop, H.; DePamphilis, B.; Jones, A., *Inorganic Synthesis* **1982,** *21*, 160.

14. Contant, R., *Inorg. Synth.* **1990,** *27*, 71-111.

15. Keita, B.; Girard, F.; Nadjo, L.; Contant, R.; Belghiche, R.; Abessi, M., *J. Electroanal. Chem.* **2001,** *508* (1-2), 70-80.

Chapter 5

1. Bodner, G., M., *J. Chem. Educ.* **2004,** *81* (5), 618 - 625

2. Nurrenbern, S., C.; Dudley Herron, J., *J. Chem. Educ.* **1999,** *76* (10), 1354 - 1361

3. Bodner, G., M., *J. Chem. Educ.* **1986,** *63* (10), 873 - 878.

4. Spencer, J. N., *Chem. Educ.* **1999,** *76*, 566 - 569.

5. Skinner, B. F., *Harvard Educ. Rev* **1954,** *24*, 86 - 97.

6. Banks J., E., *J. Chem. Educ.* **1963,** *40* (1), 21 - 23.

7. lawrence, A. E., *J. Chem. Educ.* **1955,** *32*, 35.

8. Burkhalter, T. S., *J. Chem. Educ.* **1956,** *33*, 406.

9. Lander, A. J., *J. Chem. Educ.* **1965,** *42*, 231.

10. Stoppel, D. J., *J. Chem. Educ.* **1966,** *43*, 556.

11. Lippincott, T., W.; Bodner, G., M., *J. Chem. Educ.* **1984,** *61* (10), 843 - 844.

12. Mason, D., *J. Chem. Educ.* **2001,** *78*, 158 - 160

13. Von Glassersfeld, E., *The Impact of the Piagetian Theory on Educatio, Philosophy , and Psycology*. Murray, F. B. ed.; University Park Press: Baltimore, MD.: 1979.

14. Johnstone, A. H., *J. Chem. Educ.* **1983,** *60*, 968 - 971.

15. Johnstone, A. H., *J. Chem. Educ.* **1993,** *70* (9), 701 - 705

16. Resnick, L. B., *Scienc* **1983,** *220*, 477.

17. Dudley Herron, J., *J. Chem. Educ.* **1984,** *61* (10), 850 - 854

18. Scerri, E., R., *J Chem Educ.* **2003,** *80* (5), 468 - 474.

19. Patton, M. Q., *Qualitative research and Evaluation Methods*. 3rd ed.; Thousand Oaks, CA: Sage Publications:Thousand Oaks, CA: 2002.

20. Nurrenbern, S., C.; Robinson, W., R., *J. Chem. Educ.* **1994,** *71* (3), 181 - 183.

21. Robinson, W., R.; Niaz, M., *Internat. J. Science Educ.* **1991,** *13*, 203 - 215.

22. Treagust, D. F.; Harrison, A. G.; Venville, G. J., *Int. J. Sci. Educ.* **1996,** *18*, 213 - 229.

23. Schwandt, T. A., *Dictionary of Qualitative Inquiry*. 2nd ed.; Sage Publications: Thousand Oaks, CA: 2001.

24. Lincoln, Y. S.; Guba, E. G., *Naturalistic Inquiry*. Sage: Beverly Hills: 1985.

25. Phelps, A., J., *J. Chem. Educ.* **1994,** *71* (3), 191 - 194.

26. Glaser, B. G.; Strauss, A. L., *The Discovery of Grounded theory: Srategies for Qualitatiev Research.* Aldine: Chicago: 1967.

27. Gage, N. L., *Educational researcher* **1989,** *18* (7), 4 - 10.

28. Tashakkori, A.; Teddlie, C., *Mixed Methodology: Combining Qualitative and Quantitative approaches.* Sage Publications: Thousand Oaks, CA: 1998.

29. Tashakkori, A.; Teddlie, C., *Handbook of Mixed Methodds in Social and Behavioral Research.* 2003; Vol. Sage Publications: Thousand Oaks, C.A.

30. Bunce, D.; Gabel, D.; Dudley Herron, J.; Jones, L., *J. Chem. Educ.* **1994,** *71* (10), 850 - 852.

Chapter 6

1. Mills, Pamela A.; Sweeney, William V. *J. Chem. Educ*. **2000**, 77, 9, 1161
2. Domin, D. *J. Chem. Educ.* **1999**, 76, 543-547
3. Breck, W. G.; Holmes, F. W. *J. Chem. Educ*. **1967**, 44, 293
4. Hermens, R. A. *J. Chem. Educ*. **1983**, 60, 764
5. http://www.dec.ny.gov/chemical/285.html
6. http://law.justia.com/newyork/codes/environmental-conservation/env027-2107_27-2107.html
7. http://www.practicalphysics.org/go/Experiment_380.html
8. http://www.physics.umd.edu/lecdem/services/demos/demosi3/i3-41.htm
9. http://www.bradley.edu/las/phy/laboratories/110lab2002/boyle's/boyles_law_syringe.htm
10. http://sciencekit.com/low-cost-boyleandrsquo%3Bs-law-apparatus/p/IG0023590/
11. Lewis, Don, L. *J. Chem. Educ*. **1997**, 74, 2, 209
12. Deal, Walter, J. *J. Chem. Educ*. **1975**, 52, 6, 405
13. Ivanov, Dragia T. *Physics Education*. **2007**, 42, 2, 193
14. Kim, Myung-Hoon; Kim, Michelle, S.; Ly, Suw-Young. *J. Chem. Educ*. **2001**, 78, 2, 238
15. Bopegedera, A. M. R. P. *J. Chem. Educ*. **2007**, 84, 3, 465
16. CRC Handbook of Chemistry and Physics,

Chapter 7

1. Scofield, M.B. *J. Chem. Educ.* ***1927,*** 4, 1168-1175.

2. Smith, O.M.; Trimble, H.M. *J. Chem. Educ.* (1929) 6, 93-97.

3. McFate, C.; Olmsted III, J. (1999) *J. Chem. Educ.* **76**, 562-565.

4. Bentley, Andrea B.; Gellene, Gregory I., (2005) *J. Chem. Educ.* 82, 125-130.

5. Russell, A.A. (1994) *J. Chem. Educ.* **71,** 314-317.

6. Hovey, N.W.; Krohn, A. (1958) *J. Chem. Educ.* **35**, 507-509.

7. Legg, Margaret J.; Legg, Jason C.; Greenbowe, Thomas J. (2001) *J. Chem. Educ.* 78, 1117.

Appendix

A1. CV data comparing α_1-$[P_2W_{17}O_{61}]^{10-}$ (solid line) and $K_{7-n}H_n[Tc^VO(\alpha_1P_2W_{17}O_{61})]$

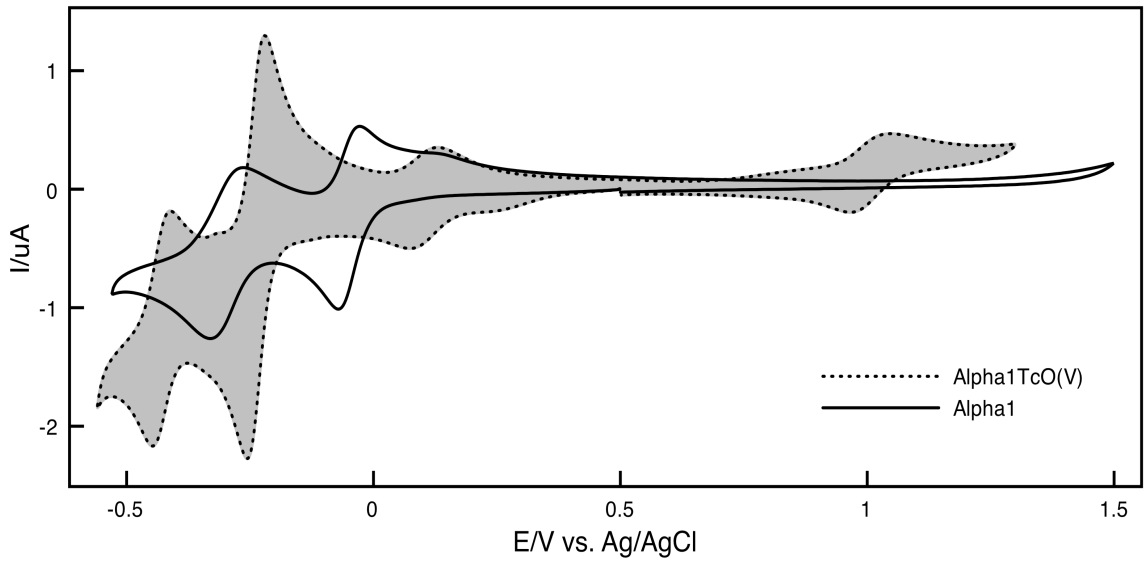

Figure A1.1. CV of α_1-$[P_2W_{17}O_{61}]^{10-}$ (solid line) and $K_{7-n}H_n[Tc^VO(\alpha_1P_2W_{17}O_{61})]$ (dotted line) in 0.5 M Na_2SO_4 at pH 0. Working electrode, glassy carbon, auxiliary electrode platinum wire and reference electrode, Ag/AgCl. Scan rate 10mV/s.

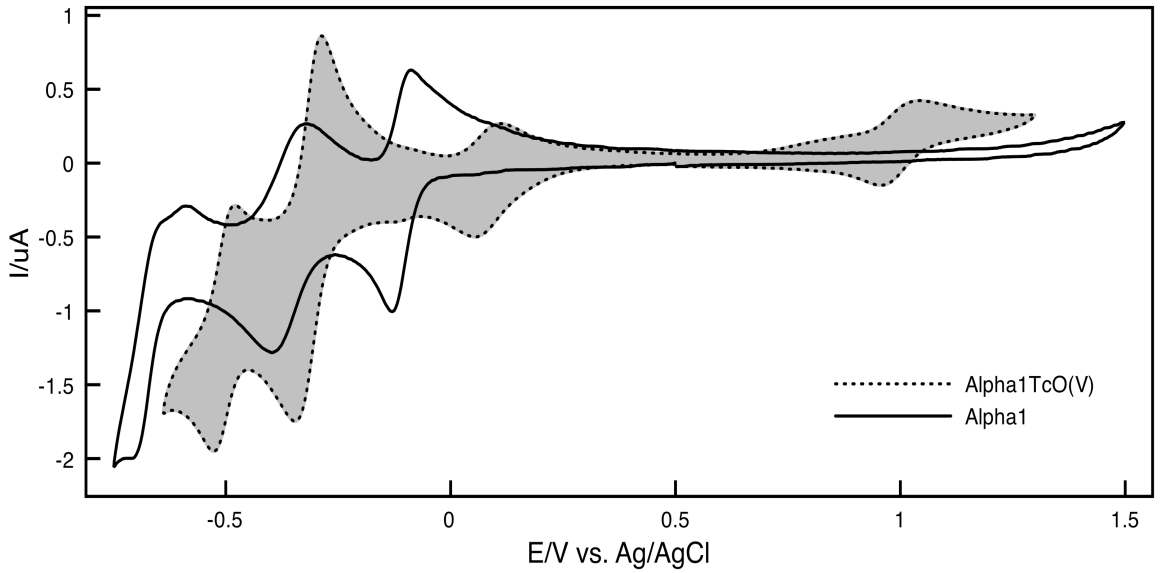

Figure A1.2. CV of α_1-$[P_2W_{17}O_{61}]^{10-}$ (solid line) and $K_{7-n}H_n[Tc^VO(\alpha_1P_2W_{17}O_{61})]$ (dotted line) in 0.5 M Na_2SO_4 at pH 1. Working electrode, glassy carbon, auxiliary electrode platinum wire and reference electrode, Ag/AgCl. Scan rate 10mV/s.

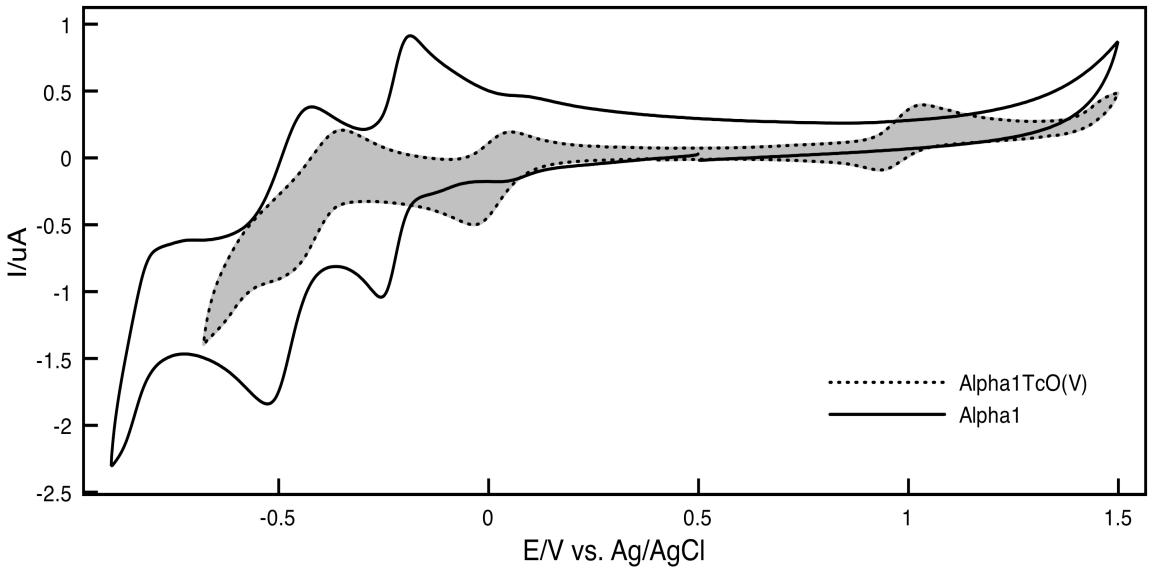

Figure A1.3. CV of α_1-$[P_2W_{17}O_{61}]^{10-}$ (solid line) and $K_{7-n}H_n[Tc^VO(\alpha_1P_2W_{17}O_{61})]$ (dotted line) in 0.5 M Na_2SO_4 at pH 3. Working electrode, glassy carbon, auxiliary electrode platinum wire and reference electrode, Ag/AgCl. Scan rate 10mV/s.

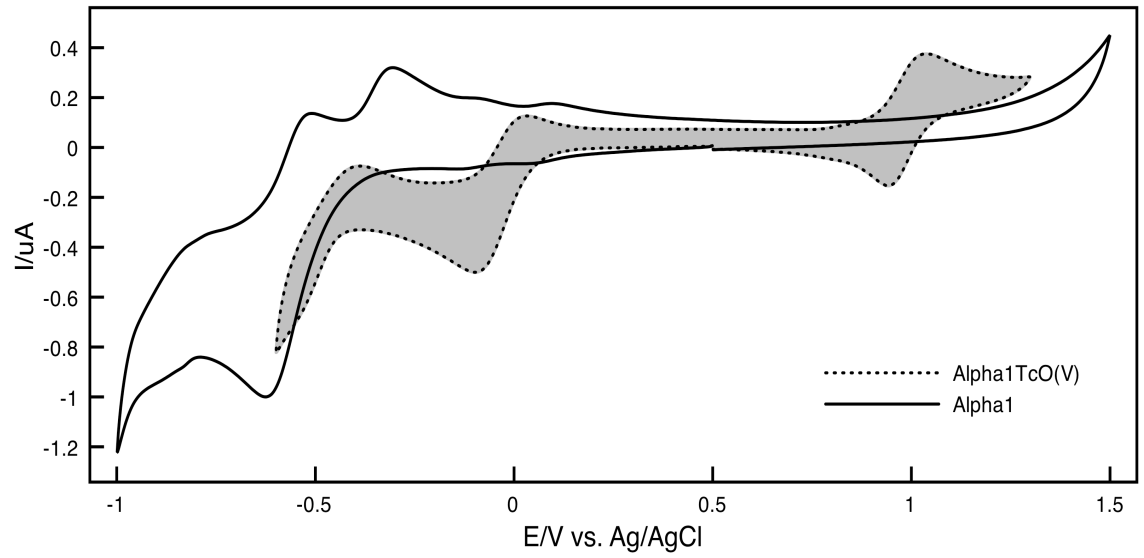

Figure A1.4. CV of α_1-$[P_2W_{17}O_{61}]^{10-}$ (solid line) and $K_{7-n}H_n[Tc^VO(\alpha_1P_2W_{17}O_{61})]$ (dotted line) in 0.5 M Na_2SO_4 at pH 5. Working electrode, glassy carbon, auxiliary electrode platinum wire and reference electrode, Ag/AgCl. Scan rate 10mV/s.

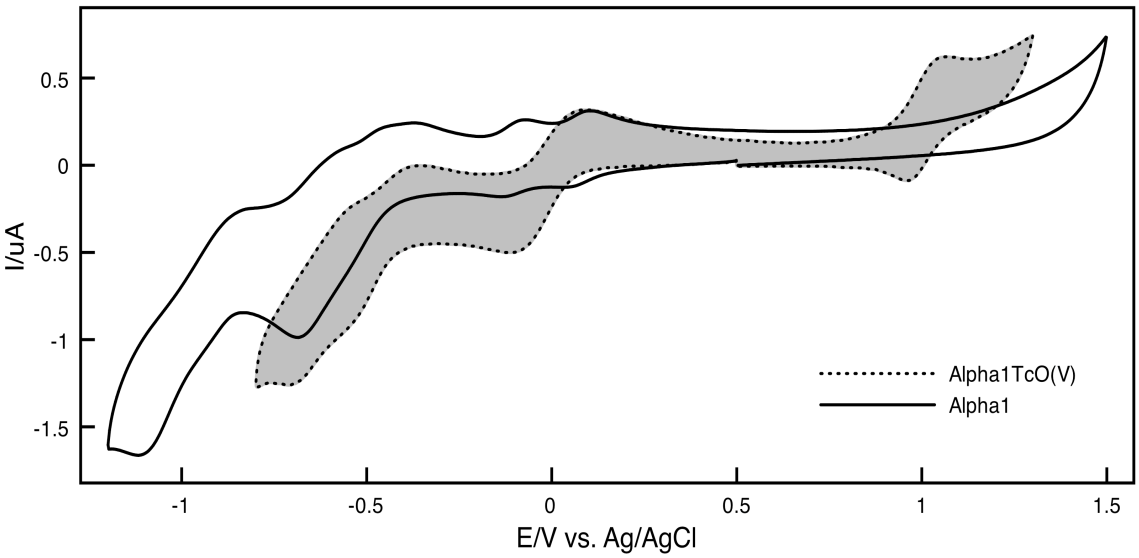

Figure A1.5. CV of α_1-$[P_2W_{17}O_{61}]^{10-}$ (solid line) and $K_{7-n}H_n[Tc^VO(\alpha_1P_2W_{17}O_{61})]$ (dotted line) in 0.5 M Na_2SO_4 at pH 7. Working electrode, glassy carbon, auxiliary electrode platinum wire and reference electrode, Ag/AgCl. Scan rate 10mV/s.

A2. Deconvoluted CV data for $K_{7-n}H_n[Tc^VO(\alpha_1P_2W_{17}O_{61})]$

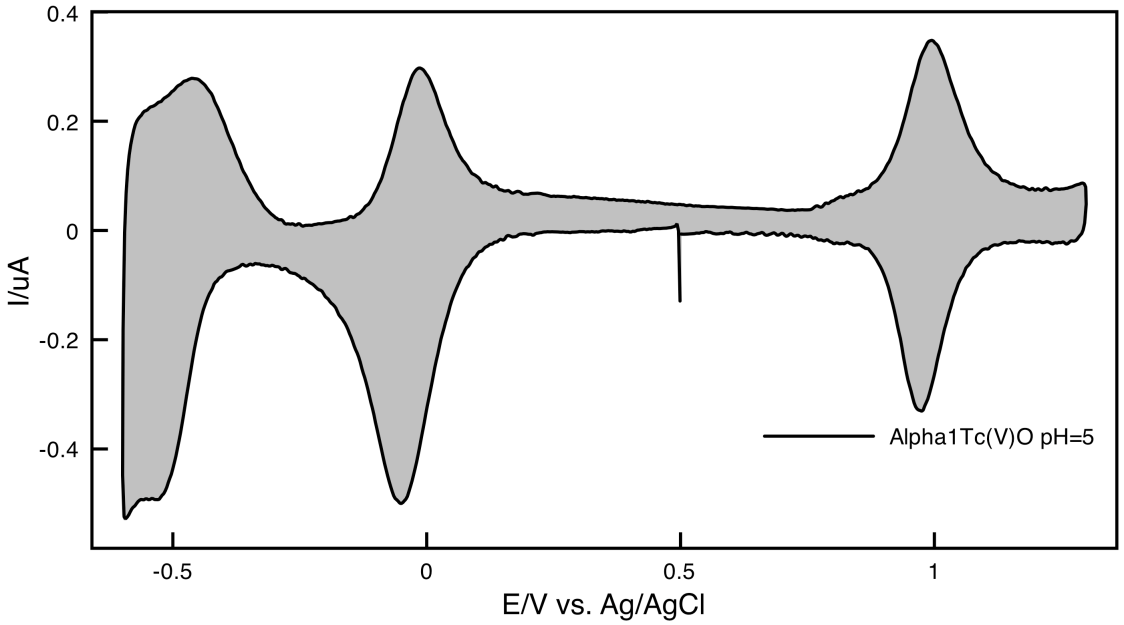

Figure A2.1. Deconvoluted CV of $K_{7-n}H_n[Tc^VO(\alpha_1P_2W_{17}O_{61})]$ in 0.5 M Na_2SO_4 at pH 5. Working electrode, glassy carbon, auxiliary electrode platinum wire and reference electrode, Ag/AgCl. Scan rate 10mV/s.

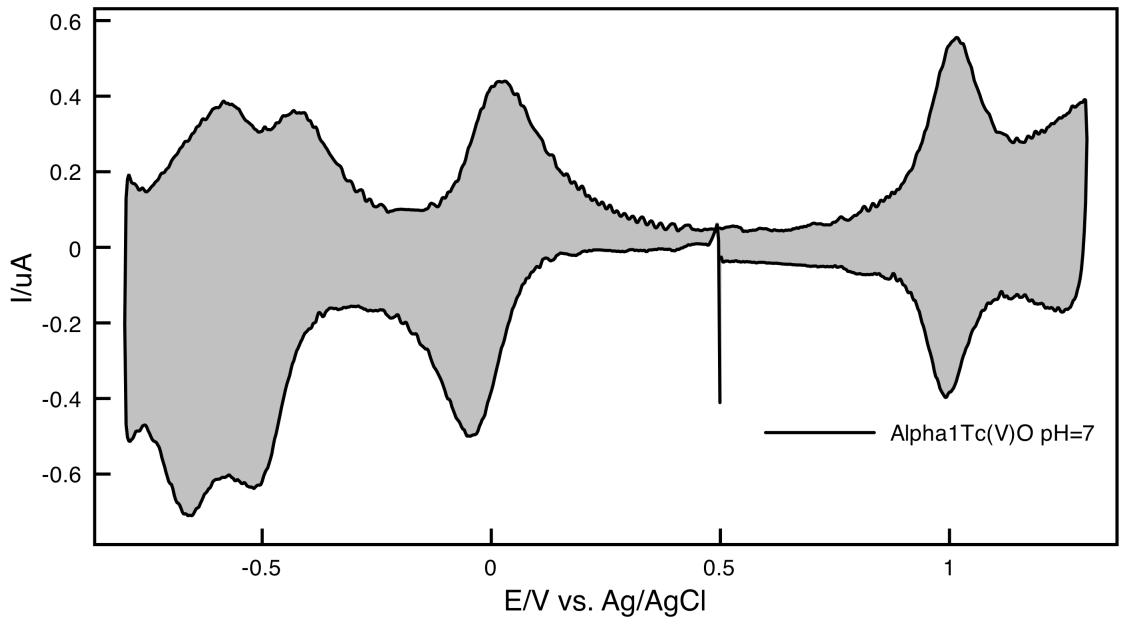

Figure A2.2. Deconvoluted CV of $K_{7-n}H_n[Tc^{V}O(\alpha_1P_2W_{17}O_{61})]$ in 0.5 M Na_2SO_4 at pH 7. Working electrode, glassy carbon, auxiliary electrode platinum wire and reference electrode, Ag/AgCl. Scan rate 10mV/s.

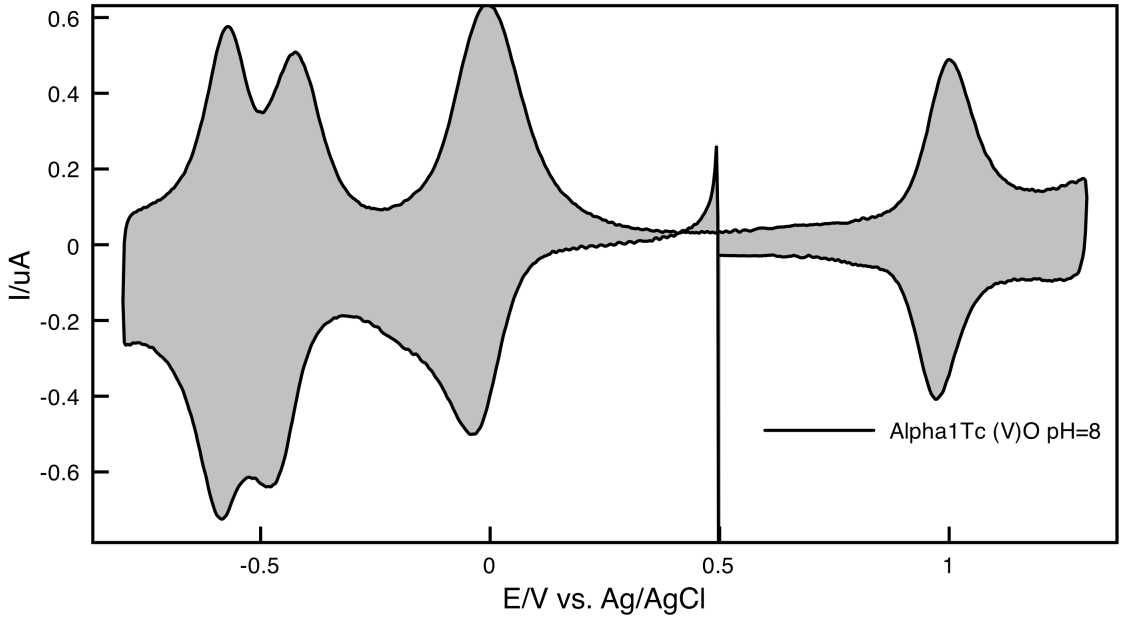

Figure A2.3. Deconvoluted CV of $K_{7-n}H_n[Tc^{V}O(\alpha_1P_2W_{17}O_{61})]$ in 0.5 M Na_2SO_4 at pH 7. Working electrode, glassy carbon, auxiliary electrode platinum wire and reference electrode, Ag/AgCl. Scan rate 10mV/s.

A3. CV data comparing α_2-$[P_2W_{17}O_{61}]^{10-}$ (solid line) and $K_{7-n}H_n[Tc^VO(\alpha_2P_2W_{17}O_{61})]$

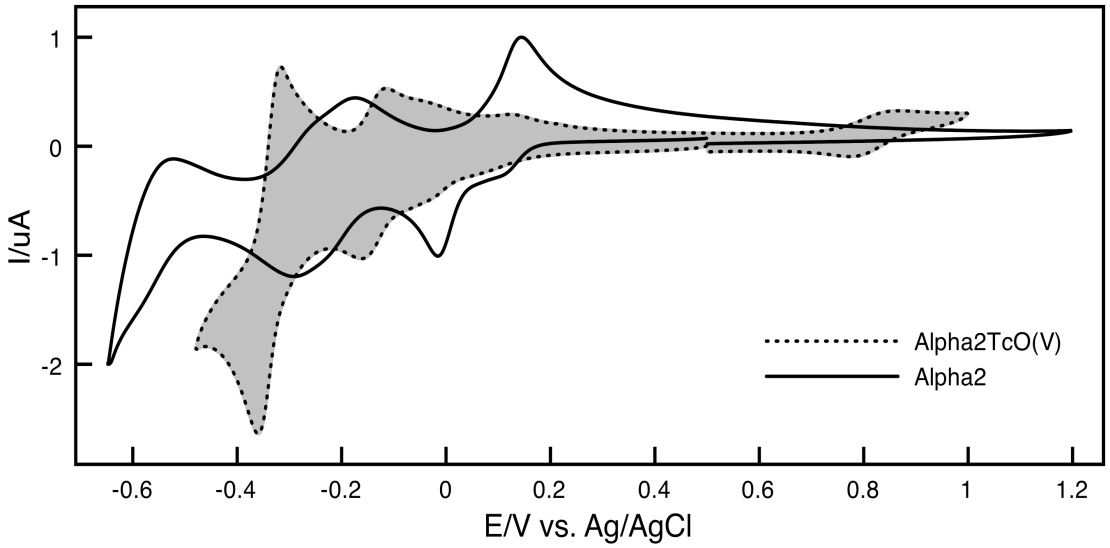

Figure A3.1 CV of α_2-$[P_2W_{17}O_{61}]^{10-}$ (solid line) and $K_{7-n}H_n[Tc^VO(\alpha_2P_2W_{17}O_{61})]$ (dotted line) in 0.5 M Na_2SO_4 at pH 0. Working electrode, glassy carbon, auxiliary electrode platinum wire and reference electrode, Ag/AgCl. Scan rate 10mV/s.

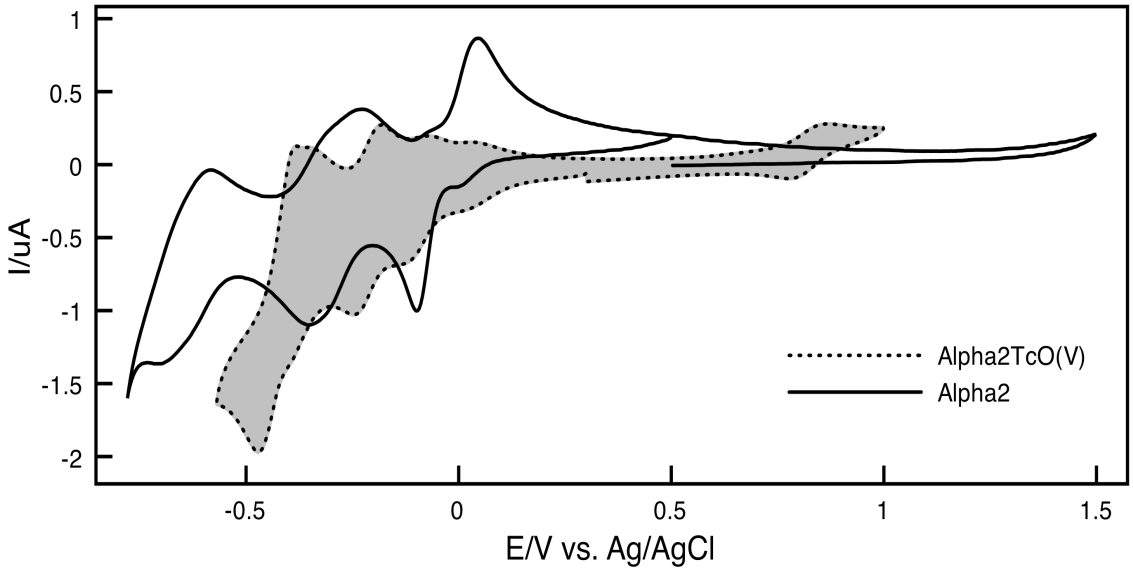

Figure A3.2. CV of α_2-$[P_2W_{17}O_{61}]^{10-}$ (solid line) and $K_{7-n}H_n[Tc^VO(\alpha_2P_2W_{17}O_{61})]$ (dotted line) in 0.5 M Na_2SO_4 at pH 1. Working electrode, glassy carbon, auxiliary electrode platinum wire and reference electrode, Ag/AgCl. Scan rate 10mV/s.

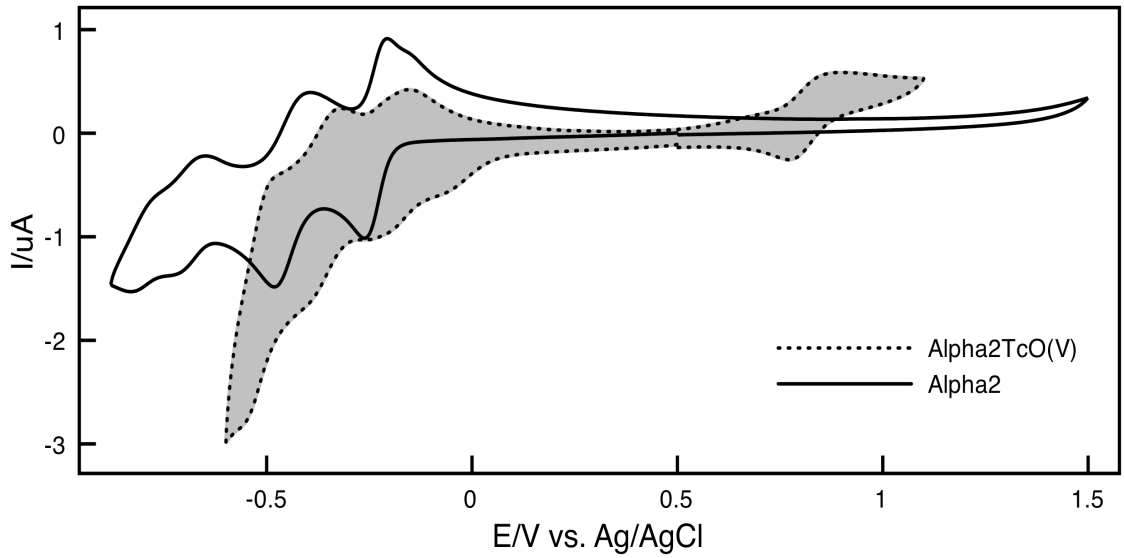

Figure A3.3. CV of α_2-$[P_2W_{17}O_{61}]^{10-}$ (solid line) and $K_{7-n}H_n[Tc^VO(\alpha_2P_2W_{17}O_{61})]$ (dotted line) in 0.5 M Na_2SO_4 at pH 3. Working electrode, glassy carbon, auxiliary electrode platinum wire and reference electrode, Ag/AgCl. Scan rate 10mV/s.

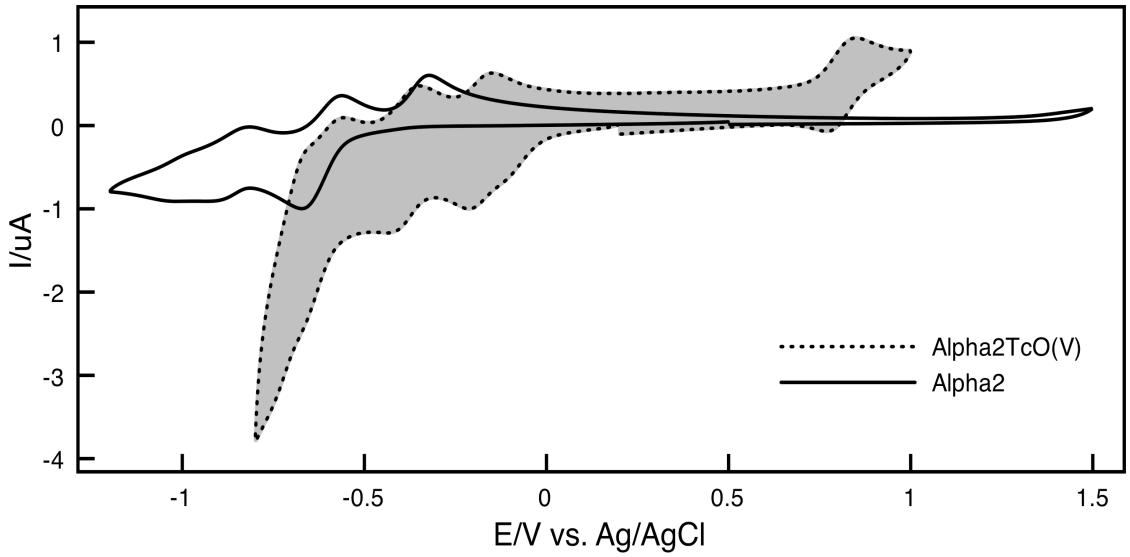

Figure A3.4. CV of α_2-$[P_2W_{17}O_{61}]^{10-}$ (solid line) and $K_{7-n}H_n[Tc^VO(\alpha_2P_2W_{17}O_{61})]$ (dotted line) in 0.5 M Na_2SO_4 at pH 5. Working electrode, glassy carbon, auxiliary electrode platinum wire and reference electrode, Ag/AgCl. Scan rate 10mV/s.

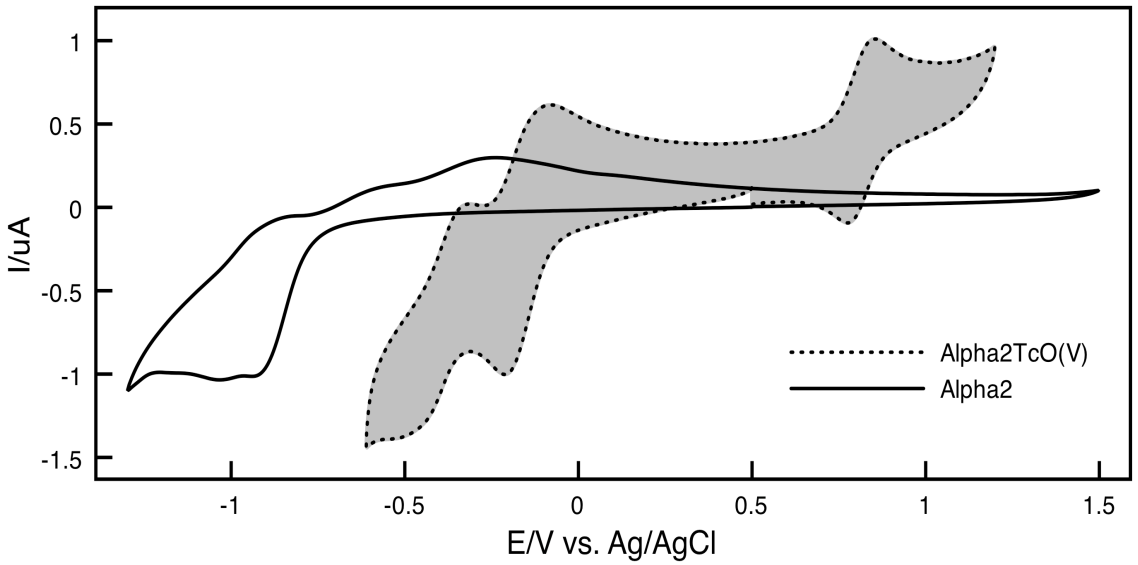

Figure A3.5. CV of α_2-$[P_2W_{17}O_{61}]^{10-}$ (solid line) and $K_{7-n}H_n[Tc^VO(\alpha_2P_2W_{17}O_{61})]$ (dotted line) in 0.5 M Na_2SO_4 at pH 7. Working electrode, glassy carbon, auxiliary electrode platinum wire and reference electrode, Ag/AgCl. Scan rate 10mV/s.

A4. Deconvoluted CV data for $K_{7-n}H_n[Tc^VO(\alpha_2P_2W_{17}O_{61})]$

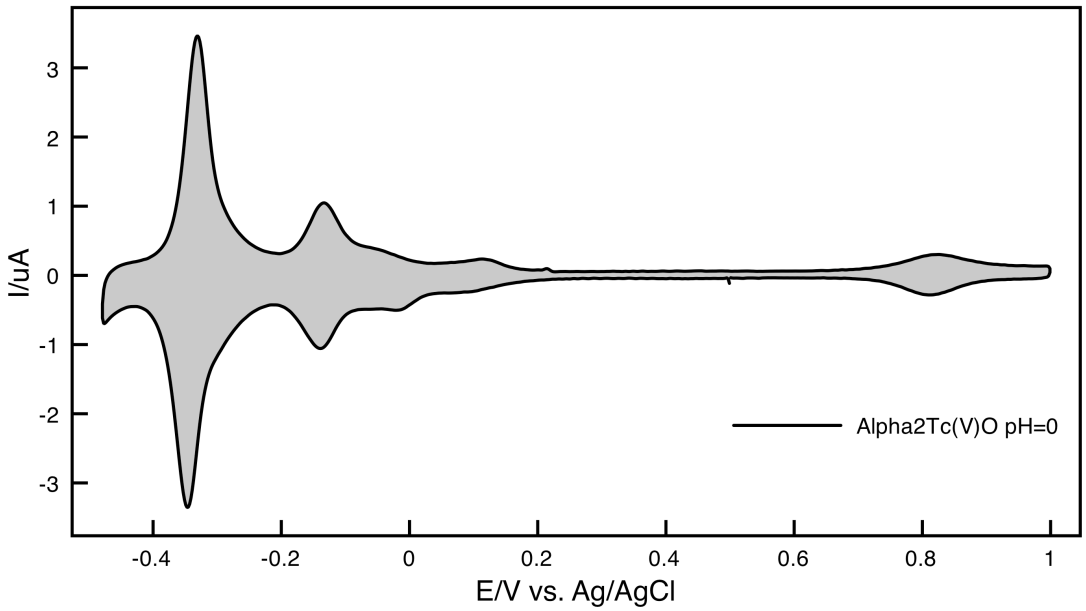

Figure A4.1. Deconvoluted CV of $K_{7-n}H_n[Tc^VO(\alpha_2P_2W_{17}O_{61})]$ in 0.5 M Na_2SO_4 at pH 0. Working electrode, glassy carbon, auxiliary electrode platinum wire and reference electrode, Ag/AgCl. Scan rate 10mV/s.

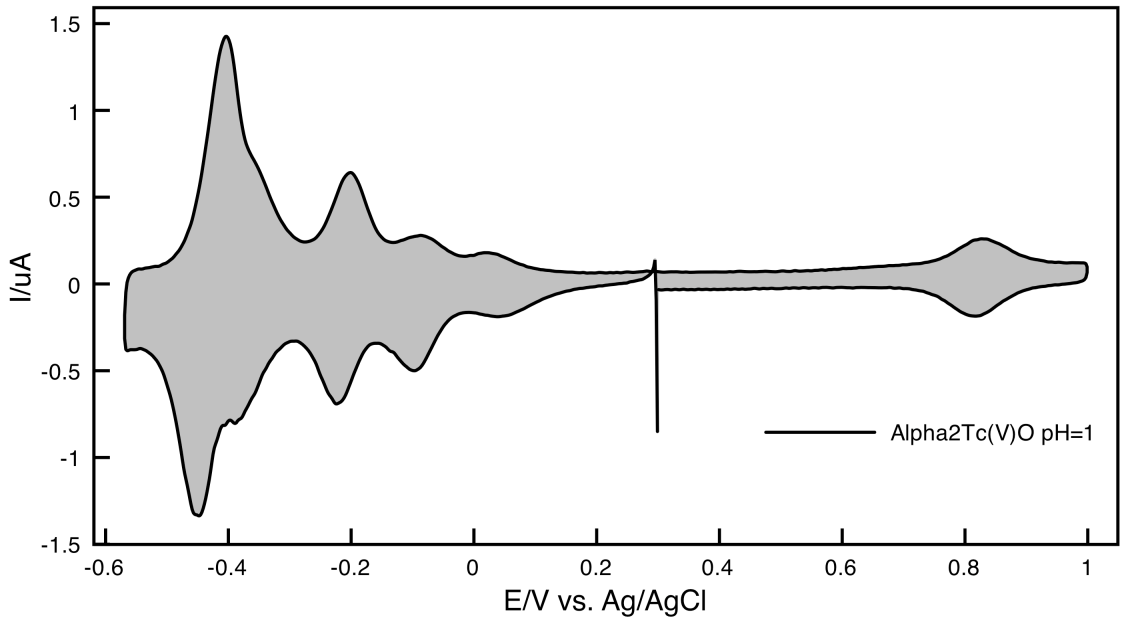

Figure A4.2. Deconvoluted CV of $K_{7-n}H_n[Tc^{V}O(\alpha_2P_2W_{17}O_{61})]$ in 0.5 M Na_2SO_4 at pH 1. Working electrode, glassy carbon, auxiliary electrode platinum wire and reference electrode, Ag/AgCl. Scan rate 10mV/s.

A5. ^{31}P NMR spectrum of a blue solution of reduced $[P_8W_{48}O_{184}]^{40-}$